Characterising the Role of Pin Movement on Infection in External Fracture Fixation

Mr Blake McCall

Doctor of Philosophy

Aston University

June 2019

Aston University

Characterising the Role of Pin Movement on Infection in External Fixation

Blake Declan McCall
Doctor of Philosophy, June 2019

Thesis Summary

External fixation is an essential surgical technique for treating trauma, limb lengthening and deformity correction, however pin-site infection and pin loosening are significant challenges that still need to be overcome. Throughout the clinical literature there is anecdotal evidence which highlights a relationship between excessive movement at the soft tissue pin-site interface and an increased risk of pin-site infection. However the mechanisms by which pin movement may influence pin-site infection and wound healing are poorly understood. Therefore the aim of this doctoral research was to develop and test an in vitro skin equivalent pin-site model to understand and study the role of pin movement on the development of infection and wound healing in external fixation.

Three studies were carried out to: first investigate bacterial attachment on pins using the novel pin machine to simulate pin movement in a bacterial culture (*Staphylococcus aureus* and *Staphylococcus epidermidis*) and using our optimised bacterial detachment method; a scratch assay with a fibroblast wound model when exposed to mono-species and multi-species bacterial conditioned media (*Staphylococcus aureus* and *Staphylococcus epidermidis*); a human skin-equivalent pin-site model using the novel pin machine and using ELISAs to study pro-inflammatory markers in the media (IL-1α, IL-8, TNF-α).

No significant increase in bacterial attachment was observed when movement was applied to pins submerged in a bacterial culture, highlighting the fact that pin-site infection is a multi-factor problem involving bacterial colonisation, wound healing of the skin and mechanics of the pin itself. An increase in IL-1α and IL-8 expression was observed when a pin was implanted and left static compared to control ($p<0.05$), which increased further when movement was applied to the pin ($p<0.05$), confirming that pin movement has a negative effect on the wound healing of soft tissue around the pin-site. When studying the effect of bacteria on the wound healing in vitro, planktonic and biofilm equivalents of *S. aureus* and *S. epidermidis* reduced the rate of migration compared to control ($p<0.05$). However the most significant impact on wound healing was observed for a planktonic multi-culture of both species, indicating a possible increased virulence of multi-species *Staphylococci* compared to single species infections.

This work highlights the importance of studying multi-species environments in vitro to better understand infection development at pin sites or other wound sites. This research has also confirmed that pin movement is an important factor in maintaining sterile pin-sites however the pin-site skin-equivalent model developed can potentially be used to evaluate the efficacy of pin movement restriction treatments such as wound dressings. The implications of evaluating these clinical interventions for more effective treatments and a reduction in antibiotic use, which helps to tackle the growing global challenge of antimicrobial resistance.

Key Words: External Fixation, Pin-Site Infection, Biofilm, Wound Healing, Percutaneous Implants

Acknowledgements

I would like to express my appreciation to my supervisor Dr Sarah Junaid. You have been an important mentor and friend throughout my PhD. I would like to thank you for advice and encouragement throughout my research and for supporting me in the decision to pursue research projects in fields outside of my previous mechanical engineering education.

I would also like to thank associate supervisor Dr Kate Sugden although my research drifted from your field of expertise during the last two years of my PhD, your support throughout my project has still been very much appreciated. Also I would like to thank Dr Karan Rana, having you to fire questions, and finding necessary equipment for me at short notice saved many of my experiments from failure.

I would also like to thank my colleague Pranav Bathrinarayanan, your guidance during my first year of my PhD was very much appreciated and the interesting conversations you occasionally sparked gave us both a much need distraction from our research.

Finally I would like to thank my brother Adam McCall and especially my parents, Jane and Mark McCall. The love and support you have given me over the years has not gone unappreciated. Although you may not have been able to provide technical advice for my research, I know you would have if you could! The support and encouragement you have given me other the last three years both financial and emotional have been significant in me completing my PhD.

Contents

List of Abbreviations

(AMR)	Antimicrobial Resistance
(BCM)	Biofilm Conditioned Media
(CFU)	Colony Forming Unit
(DMEM)	Dulbecco's Modified Eagle Medium
(ECM)	Extracellular Matrix
(ELISA)	Enzyme Linked Immunosorbent Assay
(FGM)	Fibroblast Growth Medium
(H&E)	Hematoxylin and Eosin
(HDF)	Human Dermal Fibroblasts
(IL-1α)	Interleukin 1 alpha
(IL-8)	Interleukin 8
(KGM)	Keratinocyte Growth Medium
(LVDT)	Linear Variable Differential Transformer
(MEM)	Minimal Essential Medium
(MOI)	Multiplicity of Infection
(MRSA)	Methicillin Resistant Staphylococcus Aureus
(NHEK)	Normal Human Epidermal Keratinocytes
(OD600)	Optical Density 600 nm
(OTR)	Oxygen Transfer Ratio
(PBS)	Phosphate Buffered Saline
(PCM)	Planktonic Conditioned Media
(PMMA)	Polymethylmethacrylate
(RPM)	Revolutions per Minute
(*S. aureus*)	Staphylococci Aureus
(*S. epidermidis*)	Staphylococci Epidermidis
(SEM)	Scanning Electron Microscopy
(STA)	Soft Tissue Artefact
(TNF-α)	Tumour Necrosis Factor Alpha
(TNS)	Trypsin Neutralising Solution

List of Tables and Figures

Chapter 1: Introduction

1.0 Introduction

External fracture fixation devices have evolved from being a last resort treatment to a valuable technique for limb lengthening and reconstruction. However complications are still common, in particular pin loosening and pin-site infection. In order to better understand the mechanisms that lead to these complications a brief insight into the mechanics of external fixation, the pathology of infection and would healing, as well as the physiology of skin is presented in this chapter.

1.1 History of external fixation

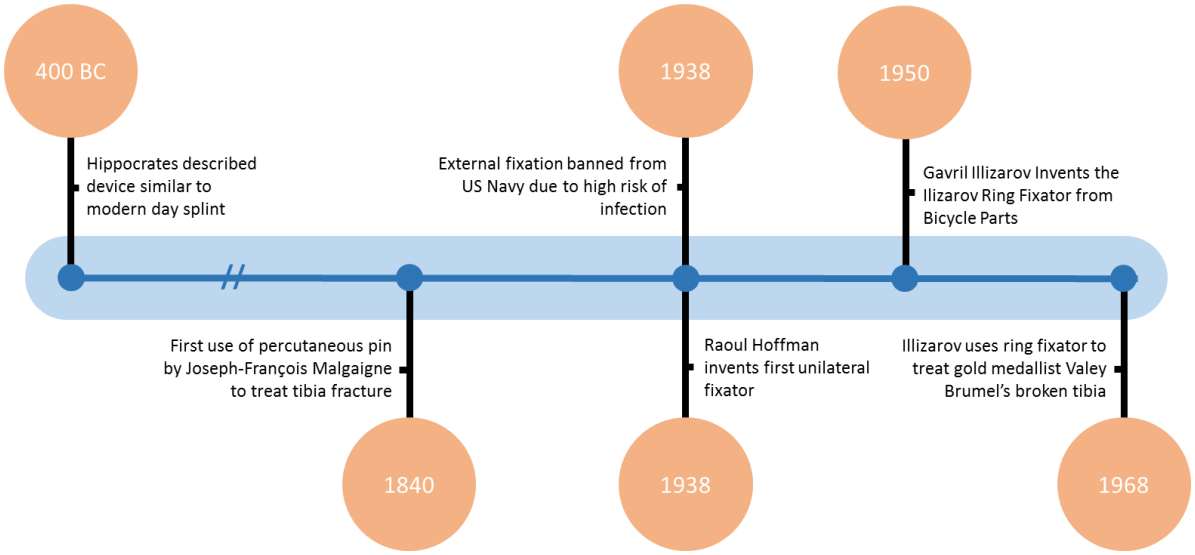

Figure 1.1: Timeline illustrating the history of external fixation. The first primitive external fixator was proposed by Hippocrates in 400 BC, it wasn't until over 2000 years later when the modern day ring and unilateral fixators were invented

The idea of using an external construct to support a fracture during healing was first proposed by Hippocrates as early as 400 BC (Seligson *et al*, 2011). Hippocrates described a device, similar to a modern day splint but made from Egyptian leather rings, connected by four wooden rods from a cornel tree. Little advancement was made towards modern day fixators for several thousand years, until 1840 AD, when Joseph-François Malgaigne was credited with the first use of a percutaneous pin for the treatment of a tibia fracture (Seligson *et al*, 2011). Historically external fixation has been associated

with a high risk of infection and mechanical instability. However this is mainly due to inexperienced surgeons operating in non-sterile environments, which is why it has become a more favourable fixation option over the last century due to advances in our understanding of pathology and microbiology *(figure 1.1)*. Eventually the problem reached such an extent that the US military banned the use of external fixation during the World War 2 (Bibbo *et al*, 2010). In 1938, Raoul Hoffmann realised major improvements were essential to make the external fixator more clinically relevant, leading him to design the first modern day unilateral fixator (*figure 1.2b).* Finally in the 1950's Gavrill Ilizarov invented the ring fixator *(figure 1.2c)*, initially made from bicycle parts. He gained fame for his fixator design in 1968, when he successfully treated the broken tibia of successful gold medallist high jumper Valey Brumel (Spiegelberg *et al*, 2010). The Ilizarov fixator's versatility has made it one of the most recognisable external fixator designs which is still being used today for treating open fractures, deformity correction and limb lengthening procedures.

1.2 Mechanics of external fixation devices

There are many different types of fixators, the most common being the Ilizarov ring fixator and the Hoffman unilateral fixator. Another common fixator is the hybrid fixator which is most similar to the Ilizarov ring fixator but instead uses a combination of both fixator wires and half-pins to position the bone fragments. This following chapter briefly describes the design and mechanics behind unilateral fixators with a more in-depth analysis of ring fixators, which will be the primary focus of this review.

1.2.1 Unilateral fixators

Unilateral fixators, such as the Hoffman fixator, are oriented across a single plane on the longitudinal axis of the bone, with all pins located on one side *(figure 1.2b).* They allow the limb to remain functional by providing support and stability to the bone (Behrens *et al*, 1986). Since the pins themselves are only fixed at one end, they experience cantilever bending when subject to axial loading (Paley *et al*, 1990), therefore the mechanics of unilateral fixators varies considerably to that of ring fixators. The stability

of all unilateral frames is dependent upon several factors, including the number of pins used, the thickness of the pins and the distance between the frame and the bone (Fragomen *et al*, 2007). Calhoun *et al* investigated the stiffness of different wire and half-pin systems and found that compared to ring fixators, which have high axial stiffness, half-pin systems possess higher bending and torsional stiffness (Calhoun *et al*, 1992).

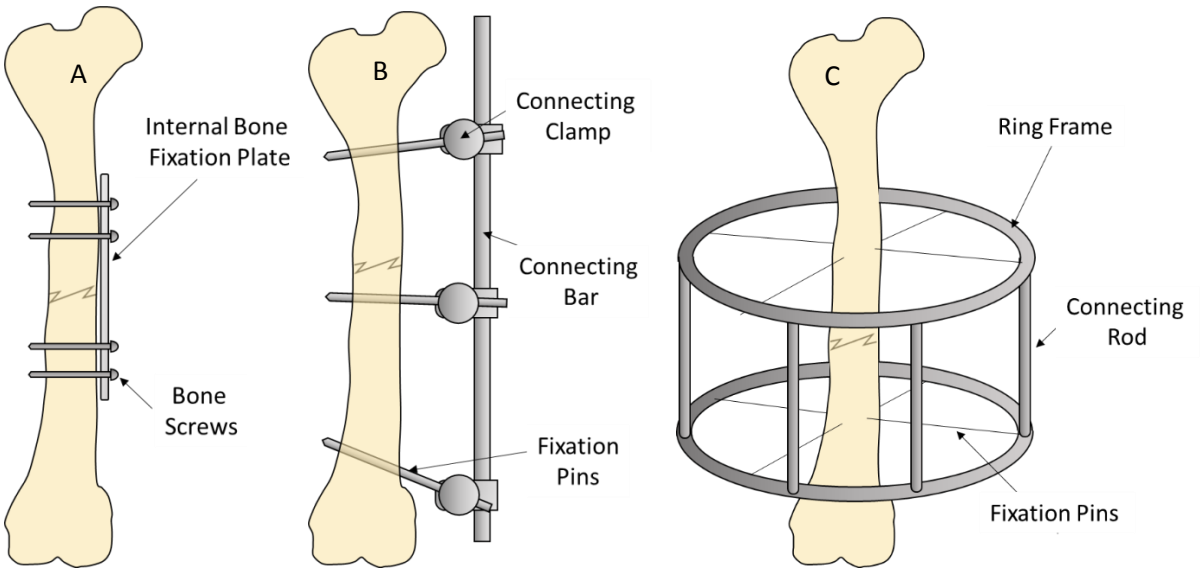

Figure 1.2: A diagram to illustrate the design of various fracture fixation devices. (A) Illustrates an internal fixation plate with bone screws. (B) Illustrates a unilateral fixation device. (C) Illustrates a external ring fixator. Important characteristics between the unilateral compared to ring fixators included thicker fixation pins and the orientation of fixation pins to one side of the bone meaning the pins undergo cantilever bending during mechanical loading of the frame

1.2.2 Ring fixators

Ring fixators, such as the Ilizarov external fixator, use smaller diameter tensioned wires, rather than the large pins used in unilateral fixators. It would easily be assumed that smaller diameter wires would offer less stability than the large diameter pins used in unilateral fixators, however the ability to tension the wires means a tensioned 1.6 mm thick wire, loaded in 3 point bending, offers stiffness equivalent to a 4 mm fixation pin in cantilever bending (Lewis *et al*, 1998). Although this means the pin-site

wounds are much smaller than with unilateral fixators, there are two pin-sites per wire as the wire itself protrudes from both sides of the bone (Davies *et al*, 2005) *(figure 1.2c).*

1.2.3 Ring diameter & material

The diameter of the fixator ring directly influences the length of the fixation wire, therefore it is recommended that the smallest diameter ring is used in order to maximise stability (Lewis *et al*, 1998). In Ilizarovs original paper detailing the design of his ring fixator, it is recommended that the smallest ring possible is used, leaving a minimum of 2 cm distance between the skin and ring to allow for tissue swelling and pin-site care (Ilizarov, 1992). Over the years, the most common material for the manufacture of the rings has been stainless steel, yet aluminium and carbon composites are increasingly being used (Lewis *et al*, 1998). The benefits of Ilizarov rings composed of aluminium or carbon composite compared to traditional steel frames are that they have a much higher strength-to-weight ratio as well as being more radiolucent than their stainless steel counterparts, allowing for clearer x-ray imaging. A further benefit of using carbon composite rings is that the plastic deformation that is exhibited by stainless steel at high loads is avoided (Nele *et al*, 1994). Kummer *et al* showed that aluminium rings performed as well as stainless steel in axial, torsional and bending stiffness while carbon composite rings performed 5% better in bending and axial stiffness but showed a decrease in rigidity (Kummer, 1990).

1.2.3.1 Wire thickness, tension & orientation

The most commonly used fixation wires in external ring fixators range from 1.5 mm to 2 mm in diameter (Lewis *et al*, 1998). A single tensioned 1.8 mm diameter fixation wire is around 50% stiffer than an equally tensioned 1.5 mm wire (Kummer, 1990), as strength and stiffness of a fixation wire increases proportionally to the diameter of the wire squared (Fleming *et al*, 1989). Additionally the number of wires used in the fixator also has an effect upon the stiffness of the system since the axial and torsional stiffness is proportional to the total number of wires, regardless of the number of rings

used (Fleming *et al*, 1989). Applying an axial tensile force to the wire during assembly, and then tightening the cannulated bolt while this force is maintained, creates a fixed tension across the wire. Wire tension improves the overall rigidity of the system as well as increasing axial stiffness (Lewis *et al*, 1998), the wires also exhibit a self-stiffening effect due to tension, whereby the stiffness of the wire increases with increased deflection (Aronson *et al*, 1992). However Gasser *et al* showed that increasing the wire tension of a 1.8 mm fixation wire from 60 N to 120 N only resulted in an increase in axial stiffness of 10% (Gasser *et al*, 1990). Thus it is important that the tension does not exceed 50% of the yield strength to minimise the risk of wire breakage or plastic deformation (Lewis *et al*, 1998) as well as mechanical slip between the wire and fixation bolt, which is the most common cause of loss of tension (Aronson *et al*, 1992).

1.2.4 Comparing infection rates in unilateral, ring and hybrid fixators

In an attempt to compare the infection rates of different external fixation devices in order to identify which design is the least susceptible to infection, Parameswaran *et al* studied the infection rates in 285 fractures over a four year period (Parameswaran *et al*, 2003). Of these 285 fractures, 77 were treated with ring fixators, 178 with unilateral fixators and 30 with hybrid fixators. Parameswaran found that hybrid fixators had a similar risk of infection as that of unilateral fixators with infection rates of 12.9 % and 20 % respectively. Although these results for hybrid and unilateral fixators were not significantly different from each other, the number of infections in the ring fixator group was significantly lower, with an infection rate of just 3.8 % ($p < 0.04$). Another study, conducted by Antoci *et al*, found similar results (Antoci *et al*, 2008). Of a total of 88 patients treated for tibia and femoral limb lengthening, Antoci found that half-pins, used in unilateral and hybrid fixators, had an infection rate of 78 %, which was significantly higher than the 33 % infection rate of fixator wires. Upon further investigation Antoci noticed that 100 % of the half-pins used in unilateral fixators became infected, while half-pins used in hybrid fixators had a lower infection rate of 78 %. Since both devices use the same pin type, the discrepancy in infection rates is most likely due to the mechanics of the fixator itself, perhaps hybrid

fixators help prevent excess pin movement compared to unilateral fixators leading to a reduction in infection rates.

1.3 Complications with external fracture fixation

External fixators have numerous benefits for the fixation of fractures or limb lengthening in comparison to other methods available. Compared to alternative internal fixation devices such as orthopaedic plates and screws or intramedullary nails, the benefits of external fixation are numerous. By using minimally invasive, percutaneous pins, surgeons are able to orient the frames to treat a diverse range of fractures, optimising the stability of the system and minimising tissue dissection (Fragomen *et al*, 2007). In spite of these benefits, having multiple wires passing through the skin, muscle and bone and out the other side can lead to a multitude of other complications. These range from limb mal-alignment, fracture non-union, pin loosening and pin-site infections, which can delay healing by 7 weeks or more (Richardson *et al*, 1992). The most common and severe of these complications being the latter two, of which pin-site infections are the focus of this review.

1.3.1 Pin-Site infection

A pin-site wound is essentially an open door for bacteria from the skin and outside environment to enter to host and disrupt the host's immune system. Allowing the infectious bacteria direct access to soft tissue and bone along the pin-tract. This has resulted in high incidences of pin-site infection, with infection rates reported in literature ranging from 4.5 % to 100 % (Antoci *et al*, 2008; Garfin *et al*, 1986; Mahan *et al*, 1991; Parameswaran *et al*, 2003). There are many physical factors which may have an effect upon the likelihood of infection occurring, such as the type of fixator design used, the pin-site care procedure given and the pin material. However it is important to consider that this variation in reported infection rates may be due to the lack of consensus among surgeons in determining the point at which a wound has become infected.

1.3.2 Pin loosening

Pin-site loosening occurs gradually over time, as mechanical loading on the fixator repeatedly stresses the pin-bone interface, the interface can begin to deteriorate (Saithna, 2010). Once a pin becomes loose, the fixator loses stability, and an unstable fixator creates an unsuitable environment for optimal bone healing (Parameswaran *et al*, 2003). There also appears to be a synergistic relationship between pin-site loosening and infection, in that pin-loosening often leads to infection and vice versa (Ferreira *et al*, 2012) although the causative factor of this relationship is still under debate and not clearly understood. Older patients as well as those suffering from diseases such as osteoporosis and osteomalacia are the most at risk of pin loosening, since both suffer from a deterioration of the bones mechanical properties (Donaldson *et al*, 2012).

1.4 Pathology of Infection

Infection is a serious risk throughout all medical disciplines. In 2013, The European Centre for Disease Prevention conducted a study into infection rates of 1181 long term care facilities in 17 different European countries. The results showed that the prevalence of health-care associated infections is around 3.4%, estimating that around 4.2 million people suffered from infections in 2013 alone (ECDC, 2014). The increased use of medical implants throughout medicine has resulted in an increase of implant related infections, whereby biofilms adhere to the surface of the implant creating multi-species bacterial colonies which have a high resistance to antimicrobial therapy. This resistance to antimicrobial therapy means larger doses of antibiotics are required to treat the infections, contributing to the 40% increase in antibiotic use worldwide between 2000 and 2010 (O'Neill, 2017). This increase in antibiotic consumption has been a large contributor to the emergence of antimicrobial resistant (AMR) bacteria, a recent review commissioned by the UK predicts that AMR will be the leading cause of death by 2050 with an estimated 10 million deaths per year costing up to 100 trillion USD (O'Neill, 2017). Therefore a strong understanding of the characteristics of the pathogens causing these infections, as well as methods of minimizing the colonization of these pathogens is essential in

order for biomedical engineers to develop optimal performance implants which effectively reduce these high rates of infection.

1.4.1 Process of infection

Infection represents an imbalance between the amount of bacterial present and the host's ability to defend itself. Therefore, if the host immune system is weakened, the combination of bacterial species is correct or the number of bacteria present is just right, infection will occur (Sussman *et al*, 2011). In the case of wounds, exposed subcutaneous tissue provides a suitable surface for a large variety of micro-organisms to contaminate and colonize (Bowler *et al*, 2001). In which case, the wound healing process will be halted until the infection has been dealt with (Mulder, 2002), the presence of just four or more different species of bacteria in a wound has been associated with delayed healing (Bowler, 2003). Therefore it is important to understand the stages of infection, in order to make predictions about the behavior of infectious pathogens, which may help in the development of medical devices designed to reduce the risk of infection.

1.4.2 Types of infectious bacteria

A healthy human is host to more bacteria than there are cells in their body. It is estimated that as many as 10^{14} bacteria can be found both inside and outside of the body, such as on the skin or within the intestinal tract (Varki, 2009). Many species of bacteria colonize the skin, for example *Staphylococcus* genus such as *Staphylococcus aureus (S. aureus)* and *Staphylococcus epidermidis (S. epidermidis)* as well as, *Streptococcus* and *Propionibacterium* genus can regularly be found on the outside of skin, ranging in numbers from a few hundred, to several thousand per cm^2 in moister areas, such as the groin or armpit (Mims *et al*, 1993). When a wound is created in the dermis, aerobic and anaerobic bacteria begin to colonize the wound, most of the infectious bacteria that colonises the wound is often found in surrounding skin, the oral cavity and gut, or from the surrounding environment (Bowler *et al*, 2001). The vast majority of skin and soft tissue infections are caused by *S. aureus*, *S. epidermidis* and *β-haemolytic streptococci* (Dryden, 2010), however *Pseudomonas aeruginosa*, *Escherichia coli*,

Klebsiella, *eterobacter*, *enterococcus* and *beta-hemolyic styreptocci* have also been identified as primary causes of delayed healing and infection (Mangram *et al*, 1999). The bacteria most commonly found colonising external fixator pins differs from the bacteria which is usually associated with other internal medical devices such as hip and knee prosthesis. In 1991, Mahan *et al* studied a total of 214 external fixator pins in 42 patients (Mahan *et al*, 1991). Of these 214 pin-sites, 74.8% were tested positive for bacteria. The most predominant organism cultured from these infected pin-sites was *S. epidermidis* with 90.6% of pins testing positive, while 37.5% of pins tested positive for *S. aureus* and 9.4% tested positive for *Escherichia coli*.

1.4.2.1 *Staphylococcus aureus*

In 1884, Friedrich Rosenbach first isolated the pathogen Staphylococcus aureus. He named the species after the Latin word Aurus, meaning golden, due to the bacteria's golden colour during culture, caused by the carotenoid pigments (Rosenbach, 1884). *S. aureus* is found naturally on the skin, however it only colonises a certain percentage of healthy adults (van Belkum, 2006). Around 20% of the population are frequent carriers of *S. aureus*, 60% of the population carry the bacteria intermittently and approximately 20% of the population never carry it at all (Kluytmans *et al*, 1997). The reasons why *S. aureus* only colonises a certain percentage of the population is unknown, but may involve undiscovered host factors (Romeo, 2008). Interestingly enough, Wertheim *et al* found that *S. aureus* carriers have 3 x higher risk of developing a nosocomial *S. aureus* infection (Wertheim *et al*, 2004). However these carriers of *S. aureus* are actually 24% less likely to die from the infection, indicating a possible improved immune reaction due to regularly carrying the bacterium. The skin and mucous membranes are excellent barriers against *S. aureus*, however when either of them is breached due to the presence of a pin-site, *S. aureus* can infect the underlying soft tissue creating an abscess or lesion (Elek, 1956).

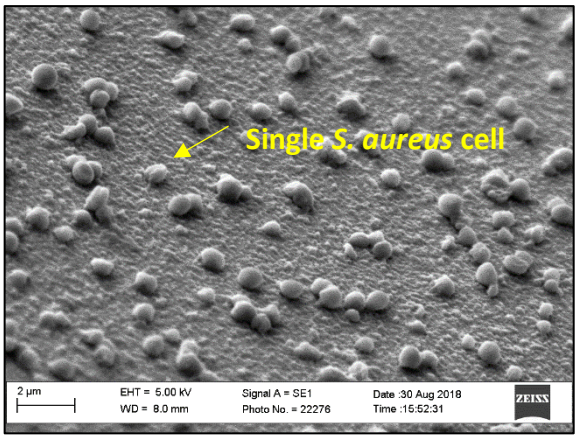

Figure 1.3: Scanning electron microscopy image of *Staphylococcus aureus* adhered to stainless steel fixation pins. Individual *S. aureus* cells up to 1 µm in diameter can be seen dispersed evenly across surface of the fixation pin with no clear formation of extracellular matrix (Scale Bar 2 µm).

1.4.2.2 *Staphylococcus epidermidis*

The word Staphylococcus stems from the Greek word Staphylo, meaning grapes. In 1881, Alexander Ogston first coined the term staphylococcus to describe the grape like clusters of bacteria formed by the genus of bacteria. *S. epidermidis* in particular is one most abundant bacteria found within the human skin flora, with high colonisation in the armpit, head and nostrils (Kloos *et al*, 1975). Since *S. epidermidis* is so abundant on the human skin, it is not surprising that it would be found in external fixator pin-sites. This large abundance has led *S. epidermidis* to be the most frequent cause of infections originating in hospitals, with infection rates around the same as its more well-known cousin *S. aureus* (NNIS, 2004). Most notably *S. epidermidis* is a common source of infection due to implanted medical devices, most likely due to the high probability of the implant devices becoming contaminated by touching the surface of the skin during implantation (Uckay *et al*, 2009). While these infections rarely develop into life threatening conditions such as sepsis, their frequency and difficultly to treat makes them a serious problem to public health (Otto, 2009). Compared to its cousin bacteria *S. aureus*, *S. epidermidis* does not produce many tissue-damaging toxins (Otto, 2009), instead, the success of *S. epidermidis* in causing infection is attributed to its ability to form a resistant biofilm.

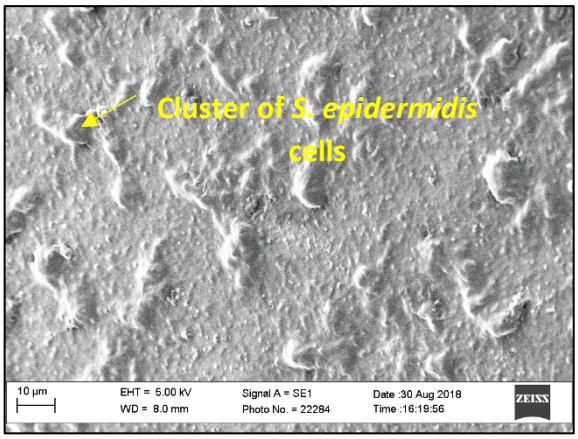

Figure 1.4: Scanning electron microscopy image of *Staphylococcus epidermidis* adhered to stainless steel fixation pins – Clusters of *S. epidermidis* cell can be seen with a diameter of around 10 µm. Extracellular matrix can be distinctly seen covering the clusters of cells (Scale bar = 10 µm)

1.4.3 Planktonic bacteria and biofilms

Bacteria can exist in both planktonic and biofilm states, with biofilms being predominant in the healthcare environment (Percival *et al*, 2014). As a result biofilms are associated with around 65% of human infections worldwide (Potera, 1999). It has been shown that once a biofilm has developed it can delay wound healing (Zhao *et al*, 2010), however the mechanisms of delayed wound healing due to biofilms are poorly understood. When bacteria go from a planktonic state to a biofilm state the bacteria secrete quorum sensing molecules which allow the biofilm to change its phenotype, gene expression and protein production (Dotsch *et al*, 2012; Sauer *et al*, 2002). These changes give the biofilms unique characteristics, including increased resistance to antibiotics and host immune responses (Costerton *et al*, 1999). Brözel *et al* monitored changes in global gene expression patterns in attached *Pseudomonas aeruginosa* cells and found more than 11 proteins whose levels were altered during various stages of attachment (Brözel *et al*, 1995). Similarly, Secor et al analysed the extracellular proteins of *S. aureus* biofilm conditioned media (BCM) and planktonic conditioned media (PCM) using mass spectrometry and 1D gel electrophoresis. The total protein concentrations of BCM and PCM were found to be similar, but BCM clearly contained more features. On the other hand several glycolytic enzymes were found to be present in PCM and not in BCM which supports the idea that metabolic

processes vary between planktonic and biofilm cultures and that those different metabolic states may have a large impact on the pathogenic effects of *S. aureus* (Secor *et al*, 2011). Cytokine production is also significantly different between cells in their planktonic form and their biofilm equivalent. Kirker *et al* demonstrated that PCM induced more interleukin-6, interleukin-8, vascular endothelial growth factor, transforming growth factor-β1, heparin-bound epidermal growth factor, matrix metalloproteinase-1, and metalloproteinase-3 production in fibroblasts compared to the BCM, while BCM induced more tumor-necrosis factor-α production (Kirker *et al*, 2012). Since higher cytokine levels indicate delayed wound healing, which is also associated with biofilm formation, it is unexpected that fibroblasts grown in PCM would express greater levels of cytokine production, as this would indicate that planktonic *S. aureus* produces more toxins that its biofilm counterpart, however this is not seen clinically, since the majority of human infections resulting from biofilm formation.

1.4.4 Characteristics of biofilms

Biofilms are an ancient mode of survival for bacteria in hostile environments (Gupta *et al*, 2016) which appears in the fossil record as early as 3.25 billion years ago (Hall-Stoodley *et al*, 2004). The first study of biofilms began when Anton Van Leeuwenhoek analysed plaque scrapped from his own teeth in the 17th century (Percival *et al*, 2014). Since then biofilms have been extensively studied but they still propose a high threat due to their autoimmune properties and antibiotic resistance. By organising into groups, and living within a self-produced extracellular polymeric substance, composed mainly of polysaccharides and proteins, bacteria are able to protect themselves from host immune responses and antibiotics (Hurlow *et al*, 2015). For this type of bacteria colonisation, the surfaces of implanted medical devices, such as external fixator pin sites, are the ideal environment for biofilms to develop.

1.4.5 Stages of biofilm formation

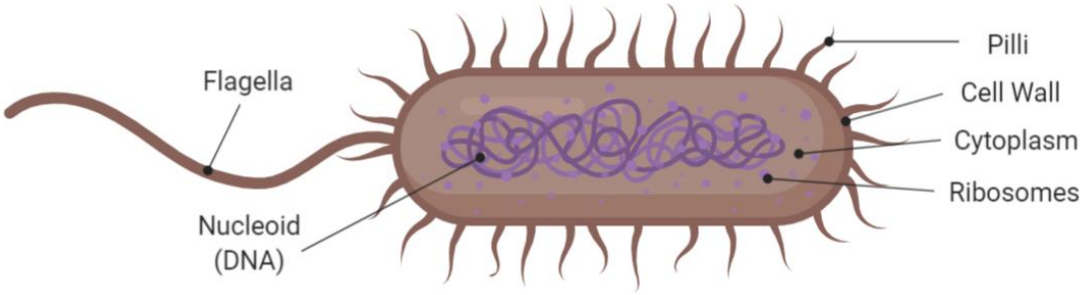

Figure 1.5: Diagram of typical bacteria cell structure. Pilli and flagella are used by the bacteria to adhere to the surface during the initial stages of biofilm formation

Biofilm formation can be categorized into 5 distinct stages known as: contamination, colonization, critical colonization, local infection and systemic infection *(figure 1.6).* Contamination and colonisation involve free-moving planktonic bacteria invading the host and adhering to the surface of the target body, either by physical forces or by the use of the bacteria's pili and flagella *(figure 1.5)* (Marić *et al*, 2007). Some of these cells are then immobilized and become irreversibly adhered to the surface as the attractive forces become greater than the repulsive forces (Garrett *et al*, 2008). If the wound reaches critical colonization, bacteria will begin to communicate with each other through auto-inducer signals inducing the secretion of an extracellular polysaccharide substance which stabilises the biofilm, consequently wound healing will be be delayed causing abnormal granulation tissue, yet often typical signs of infection will not be present (Healy *et al*, 2006). If the infection is not treated during critical colonization, local infection can occur. It is generally agreed that local infection is defined as when bacterial numbers reach 10^5 cells per gram of tissue or one milliliter of exudate, this causes the bacteria to overwhelm host defenses and proliferate uncontrollably (Bowler, 2003) causing the biofilm to grow to a thickness of around 100 µm (Gupta *et al*, 2016). Classical signs of local infection include redness and warmth of the wound as well as swelling and pain in the host (Healy *et al*, 2006). If a local infection is left untreated the bacteria may begin to spread around the body and colonize new surfaces, new saccharolytic enzymes start to breakdown the stabilizing polysaccharides within the matrix, allowing

the bacteria on top of the biofilm to be released in order to find new surfaces to colonize (Gupta *et al*, 2016). Thus it is important that clinicians are able to accurately identify biofilm formation as well as pathogen species in order to treat the infection so it does not develop into a more serious life-threatening condition such as systemic or bone infection (osteomyelitis) which may lead to multi-organ failure and death (Healy *et al*, 2006)

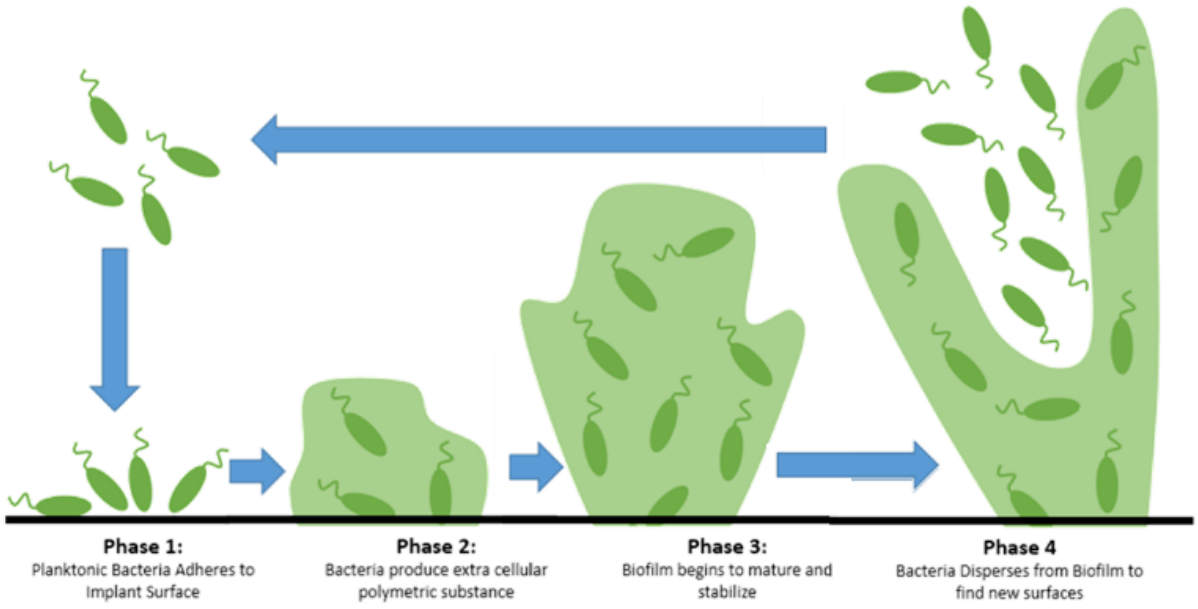

Figure 1.6: Diagram illustrating the main phases of biofilm formation. Phase 4 describes how the outer layers of a mature biofilm revert to a planktonic stage in order to locate new surfaces to colonise

1.4.6 Classifying biofilms

As mentioned in *section 1.4.2*, the organisms commonly associated with bacterial infection on fixator pins, such as *S. aureus*, can also be found harmlessly colonising the surface of the skin. Therefore, wound cultures do not provide conclusive evidence of infection, as the swabs may become contaminated by the bacteria harmlessly colonising the surface of the skin and doesn't necessarily indicate pin-site infection. To combat this, most authors have suggested that pin-site infection can be diagnosed when local signs of infection are present, rather than relying on laboratory tests (Schalamon *et al*, 2007). This has led to a disagreement among clinicians in determining at what point infection has occurred, which may play a significant role in the large discontinuity in infection rates seen in literature.

Several papers have attempted to develop classification systems for pin-site infection in external fixators, the most cited of which is the Checketts-Otterburn classification system *(table 1.1)* (Checketts *et al*, 2000). Checketts *et al* classified pin-site infection into two groups, minor infection, grades 1 – 3, and major infection, where treatment involves the removal of the pin, graded 4 – 6. The major downfall of the Checketts system is that it is reliant on qualitative observational data, which leads to discrepancies between clinicians. These discrepancies make it difficult to compare studies in a systematic review, in order to compare the effectiveness of various treatments on reducing infection. Another classification system for pin-site infection, proposed by Saleh *et al*, described a simpler grading system which focuses on the response of the infection to various treatments rather than on the symptoms of infection (Saleh *et al*, 1992). This provides little benefit in preventing serious infection, as it is not until basic treatments have failed that the clinician knows the severity of the infection, at which point the infection may have begun to spread.

Table 1.2: Checketts-Otterburn classification of pin-site infections – Adapted from (Shirai *et al*, 2009)

Grade	Classification	Characteristics	Treatment
1	Minor Infection:	1. Slight Redness 2. Little Discharge	Improve pin-site care
2	Minor Infection	1. Redness of skin 2. Discharge 3. pain and tenderness of soft tissue	Oral antibiotics
3	Minor Infection	1. No improvement with antibiotics	Infected pins removed
4	Major infection	1. Severe soft tissue infection of several pins 2. Possible pin loosening	External fixation abandoned
5	Major infection	1. Infection may involve bone 2. Visible on radiographs	External fixation abandoned
6	Major infection	1. Occurs after frame removal 2. Discharge at intervals 3. Radiographs show new bone formation and sometimes sequestra	Curettage of the pin tracks

1.4.7 Multicellular biofilms

Bacteria rarely exist in a single species planktonic forms as they have been commonly studied in the laboratory. Instead most bacteria exist as part of complex poly-microbial biofilm communities attached to host and implant surfaces. Molecular analysis of 2963 patients with chronic wounds found that chronic wounds are regularly colonised by between 2 and 5 different bacterial species (Wolcott *et al*, 2016). *S. aureus* in particular has been identified by several studies as one of the main co-infecting microbes in patients with poly-microbial infections (Finelli *et al*, 2008). The interactions between bacteria in these poly-microbial environments can be either competitive or cooperative, with both types of interactions often leading to the development of more-persistent *S. aureus* strains with increased virulence and antibiotic resistance (Nair *et al*, 2014). Cooperative interactions involving *S. aureus* have been identified with *Canadida albicans* (Adam *et al*, 2002), *Enterococcus faecalis* (Ray *et al*, 2003) and *Haemophilus influenzae* (Margolis *et al*, 2010). On the other hand competitive interactions have been observed between *S. aureus* and many other bacteria, including *Pseudomonas aeruginosa* (Margolis *et al*, 2010) and *S. epidermidis* (Frank *et al*, 2010). For example, several studies have shown an adverse relationship between *S. aureus* and *S. epidermidis* since the presence of *S. epidermidis* in the nasal cavities, has been reported to correlate with the absence of *S. aureus* (Frank *et al*, 2010). However, just because these interactions are competitive does not mean that these organisms completely inhibit the colonization of *S. aureus*; rather, *S. aureus* employs numerous defence strategies for its survival, counterattacking the competing bacteria for survival in the same environment. For example, through a process called horizontal gene transfer, *S. aureus*, which primarily colonises the nose can acquire a single gene from *S. epidermidis*, a commensal skin coloniser, in order to change its phenotype to be able to withstand the harsh conditions associated with residing on skin (Planet *et al*, 2013). Both *S. aureus* and *S. epidermidis* are opportunistic and nosocomial pathogens, however unlike *S. aureus*, which causes severe acute infections, *S. epidermidis* frequently causes chronic infections and has a greater capacity to attach to the indwelling medical devices and

form biofilms (Nair *et al*, 2014). This greater capacity at forming biofilms is largely due to its production of an extracellular matrix, in particular the serine protease. This biofilm-destroying factor has been shown to disrupt even pre-formed *S. aureus* biofilms, including those formed by methicillin-resistant *S. aureus* (MRSA). The serine protease also increases *S. aureus* susceptibility to human β-defensin 2, an antimicrobial peptide released during inflammation of the nasal cavity which usually has low bactericidal activity against gram-positive bacteria such as *S. aureus*. This shows that *S. epidermidis* may act synergistically with the immune system responses in order to eliminate *S. aureus* from the nasal cavity (Iwase *et al*, 2010). It is clear that the interactions between bacteria in multispecies infections is complex, resulting in changes to the physiology of bacteria compared to its single species isolates as well as changes to the host immune response, both of which are not fully understood. Therefore it is important to consider both bacteria together when studying *Staphylococci* infections rather than only studying single species cultures which is most often found in the in vitro literature.

1.4.8 Effect of shear on bacterial attachment and biofilm formation

Several studies have been conducted investigating the effect of shear stress on bacterial adhesion and biofilm formation which has led many researchers to identify that the biofilm formation strongly depends hydrodynamic forces, such as shear wall stress (Fonseca *et al*, 2007; Liu *et al*, 2002; Park *et al*, 2011). A low wall shear stress may limit the forces on the bacteria which may cause detachment, therefore promoting bacterial adhesion. While a high wall stress stress is likely to overwhelm the attachment forces of the bacteria and therefore prevent long-lasting bacteria adhesion. However high wall shear stress increases the mixing efficiency and convective transport of the bacteria which may actually promote microbial adhesion, as it increases the access of bacteria to the colonising surface (Saur *et al*, 2017). For example, *Pseudomonas aeruginosa* create more long lasting adhesion events to surfaces under shear stress, even though their probability of sticking is reduced. Additionally, bacteria attaching under identical flow conditions are more likely to detach when shear is suddenly decreased, which shows that individual cells dynamically respond to shear rate variations, modifying their

adhesion state (Lecuyer *et al*, 2011). In order to measure the effect of shear on bacterial attachment, many methods have been adopted, the most common of which is the use of microfluidic channels. Park *et al* measured the attachment of bacteria in a microfluidic channel at various flow rates and showed that that relationship between biofilm formation and shear stress is strongly linked, as physical stresses activate or deactivate their corresponding metabolism and relevant response (Park *et al*, 2011). They found that at a high flow rate of 0.1 µL / min and above, cells are easily detached from the surface as initial attachment is relatively weak and reversible. However at a low flow rate of around 0.04 – 0.05 µL / min biofilm coverage in the microchannel is also reduced which implies that low flow rate could not provide the relevant environment for bacterial attachment. They attributed this to a problem to a lack of nutrient and oxygen delivery at low flow rates, which leads to a deficiency in both nutrient and oxygen which are essential to bacterial growth and biofilm formation. Another study used a method of placing glass beads into the culture medium which was then aliquoted into the wells of a microtiter plate and incubated in an orbital shaker order to generate hydrodynamic forces (Fonseca *et al*, 2007). It was hypothesised that these conditions would increase aeration (Duetz *et al*, 2001; Ramsey *et al*, 2004; Stepanovic *et al*, 2001) and create shear forces that are similar to those created in flow cells. Using this dynamic model it was possible to detect changes in morphology that may influence attachment and biofilm formation abilities under the influence of shear stress. Fonseca *et al* highlighted that although planktonic culture density at 1 h was significantly higher under dynamic conditions, the adhesion values were significantly lower with the exception of the control. These studies highlight the fact that the relationship between bacterial attachment and shear stress is a non-linear one, in that bacteria may favour a higher shear stress environment for the formation of biofilms but if these stress are too great it may lead to detachment of bacteria when the shear forces begin to exceed the adhesion forces between bacteria and the surface.

1.4.9 Antibiotic resistance

The most common method of treating an infection is by the use of antibiotics such as methicillin, derived from the penicillium fungi. Between 2011 and 2014 the consumption of antibiotics in the UK rose by around 6.5% to a total of 1.2 million doses being taken daily (Espaur, 2015). This high rate of antibiotic consumption has led to the emergence of antibiotic resistant strains of bacteria, such as MRSA, which was first identified by Patricia Jevons in 1961 (Jevons, 1961). From just 1999 to 2005 the estimated number of MRSA-related hospitalisation in the US more than doubled from 127,036 to 278,203 and as a result over 6,600 deaths occurred due to MRSA in 2005 alone (Klein *et al*, 2007). By 2050 deaths due to antimicrobial resistance is expected to reach 10 million worldwide, surpassing deaths by cancer and diabetes combined *(figure 1.7).* Biofilms themselves also have their own methods of defending against antibiotics. The extracellular polymeric substance produced by bacteria in a biofilm slows the diffusion of antibiotics throughout the biofilm, preventing the antibiotics reaching the bacteria forming the first few layers (Crossley *et al*, 2009). Mature biofilms, older than 7 days, have shown resistance to antibiotic doses 500 – 5000 times the concentrations required to kill free floating planktonic bacteria of the same species (Khoury *et al*, 1992). This dramatic increase in hospital admissions related to antibiotic resistant strains of bacteria as well as the ability of bacteria to defend itself against antibiotic treatments puts emphasis on the fact that more effort should be given to the early identification and prevention of infection, rather than simply treating them with antibiotics as they appear.

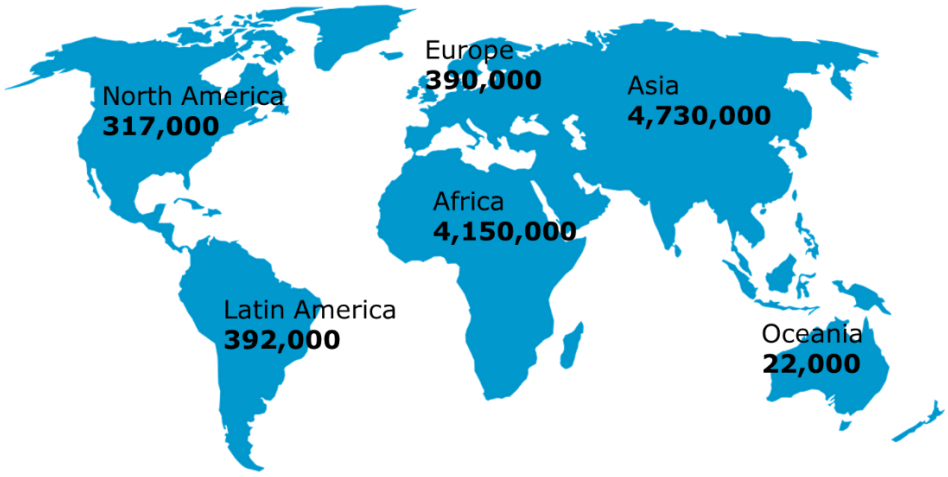

Figure 1.7: Deaths attributed to antimicrobial resistance every Year by 2050 (WHO). It is estimated that there are currently 700,00 deaths per year due to antimicrobial resistance which is expected to reach 10 million worldwide by 2050, surpassing deaths by cancer and diabetes combined.

1.5 Wound healing

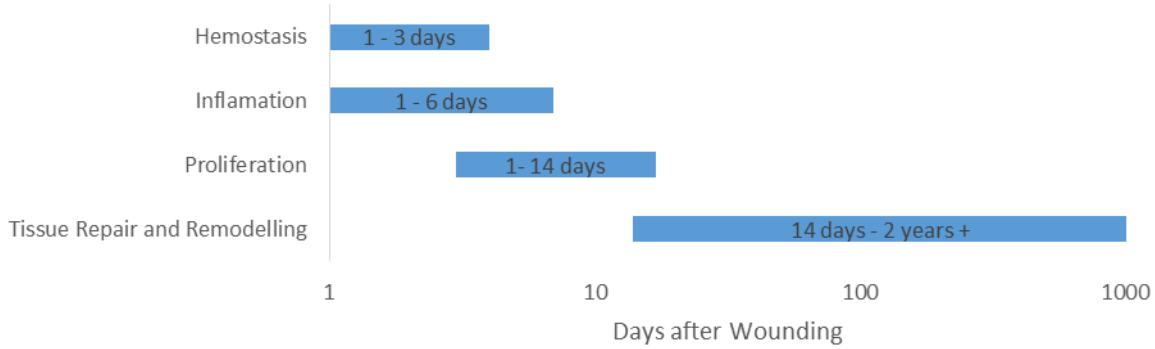

Figure 1.8: Gantt chart to illustrate the timescale on which each stage of wound healing occurs. Haemostasis, inflammation and proliferation often occur simultaneously and once tissue repair may continue for years after injury, as is seen with the slow healing of scar tissue

When skin becomes damaged and a wound results, the barrier between the inside body and the external environment becomes broken, providing a doorway for infectious bacteria to enter the host. If the wound is superficial in that the dermis has not been penetrated, tissue regeneration occurs, whereby epithelial cells will regenerate identical cells and function is quickly restored. However, if the wound penetrates deeper into the dermis, hair and sweat glands as well as nerve and blood vessels can become damaged, requiring the process of tissue repair. Tissue repair is often described in four

separate stages, haemostasis, inflammation, proliferation and maturation, but in reality they form a continuous process, often dubbed the 'healing cascade' *(figure 1.8)* (Flanagan, 2013).

1.5.1 Stages of wound healing

Haemostasis occurs immediately after injury, it is the first reaction of the body is to control bleeding and prevent any micro-organisms penetrating the wound (Mulder, 2002). When blood comes in contact with the collagen in the damaged blood vessels, blood platelets are activated. The endothelial surfaces of the blood vessels become rougher, making it easier for platelets to cling to each other and form a platelet plug (Mulder, 2002). Fibrinogen protein is converted into the protein fibrin which forms a clot, sealing the damaged blood vessels in order to prevent further blood loss. The platelets then begin to shrink which draws the wound edges together to allow for repair (Mulder, 2002). Platelets are not only essential in forming a clot at a wound site, they also produce multiple growth factors and cytokines which help to regulate to healing process (Harper *et al*, 2014). Inflammation also occurs immediately after injury but usually lasts around 4 to 6 days (Hess, 2008). Since the body's main defence from outside micro-organisms is breeched by the wound, the key aim of inflammation is to prevent infection (Harper *et al*, 2014). Inflammation is characterised by a host of cells such as white blood cells and macrophages flooding the wound site (Hess, 2013) and can usually be identified by changes in colour of the surrounding skin, increased temperature, swelling, increased pain or loss of function (Sussman *et al*, 2007). The increase in permeability of the surrounding vasculature results in 'leaky' vessels, allowing cells to flood the site. Around 24 to 48 hours after injury the leukocytes, particularly neutrophils, are at peak numbers in the wound and begin to destroy foreign bacteria and necrotic host tissue (Baranoski *et al*, 2008). This is achieved either through a process called phagocytosis, whereby the bacteria is ingested by the neutrophils, or they can de-granulate, releasing a variety of substances toxic to the bacteria (Harper *et al*, 2014). The proliferation phase is a complex process which incorporates angiogenesis, the formation of granulation tissue, collagen deposition and epithelialization (Harper *et al*, 2014). Proliferation usually begins around 3 days after injury and can

lasts several weeks (Baranoski *et al*, 2008). The initial damage to blood vessels and resulting platelet plug causes the centre of the wound to be fairly avascular, the process of angiogenesis then develops a network of capillaries from the offshoots of healthy blood vessels (Harper *et al*, 2014). Granulation tissue forms, which contains a mixture of cells and proteins, such as fibroblasts, stimulating the production of collagen, giving the tissue its tensile strength and structure (Hess, 2013). The final stage of the proliferation stage is epithelialization. This is the process whereby epithelial cells grow into the wound from surrounding healthy tissue, the cells then contact similar cells from the edges of the wound and begin to seal the wound (Huether *et al*, 2012). Tissue remodelling and maturation begins several weeks post injury but can continue for several years, involving scar formation and scar remodelling (Teller *et al*, 2009). Within 3 weeks the tensile strength of the scar is approximately 20% that of normal skin, as healing continues the scar will reach a maximum of 70% - 80% the tensile strength of normal skin (Baranoski *et al*, 2008).

1.5.2 Biomarkers for wound healing

A biomarker is an objectively quantifiable substance that can be used as an indicator of a normal physiological function, or a pharmacologic response to a therapeutic intervention, in order to better predict healing outcomes, monitor disease progression and measure response to treatment (Lindley *et al*, 2016). Biomarkers can be categorized as predictive or diagnostic, based on the type of information they provide. Predictive biomarkers can be used to predict outcomes or determine whether a patient will benefit from a given treatment, while diagnostic biomarkers can be utilized to identify the presence of factors that have the potential to influence the clinical outcome. Histology, in conjunction with other molecular markers, has long been established as a diagnostic approach for many diseases, including vasculitis, kidney disease and transplant rejection as well as its most well-known application in cancer and pre-cancerous lesions (Kallenberg, 2015; Yang *et al*, 2012). Researchers have identified several of the cellular events associated with wound healing, platelets, neutrophils, macrophages, and epidermal cells such as fibroblasts and keratinocytes are primary

contributors to the wound healing process (Shah *et al*, 2012). They release Inflammatory cytokines, in particular Interleukins 1 alpha (IL.-1α) and Interleukins 6 (IL-6) and tumour necrosis factor alpha (TNF-α), which are upregulated during the inflammatory phase in order to act as signalling molecules between cells to initiate various wound healing process such as cellular growth, proliferation, differentiation and reepithelialisation (Werner *et al*, 2003). Consequently cytokine levels, especially levels of IL-1α, IL-6 and TNF-α have been found to be significantly higher in non-healing wounds compared to that of healing wounds and may also serve as prognostic biomarkers for healing outcomes (Lindley *et al*, 2016). Trengrove *et al* found that concentrations of IL-1α were almost 3.5 x greater in non-healing chronic leg ulcers compared to that of healing wounds (Trengove *et al*, 2000). Biedler *et al* also reported similar findings for Il-8 (Beidler *et al*, 2009), however Beidler stated that the large variation in levels between subjects, possibly due to a variation in immune response and skin physiology, makes it difficult to use as a marker for wound healing in vivo (Gohel *et al*, 2008).

1.6 Physiology of human skin

Human skin is often dubbed "the largest organ of the body" but this is not entirely true. If surface area is to be considered, the gas exchanging surface of the lung's airways is estimated to be almost 70 m^2 while the skins surface area of a 70 kg man is only 1.7 m^2 (Sontheimer, 2014). Despite this, the importance of the skin for human survival cannot be understated. The main function of the skin is to provide an effective barrier between the inside of the body and the outside world in order to defend against foreign organisms (Proksch *et al*, 2008). Human skin is composed of two layers, which together are called the cutis. The outer-most layer of skin is called the epidermis, while the bottom layer is called the dermis. The following section of this review attempts to categorize the composition of these skin layers, detailing key features and identifying important cells, in order to provide sufficient understanding to investigate wound healing and infection further.

1.6.1 Epidermis

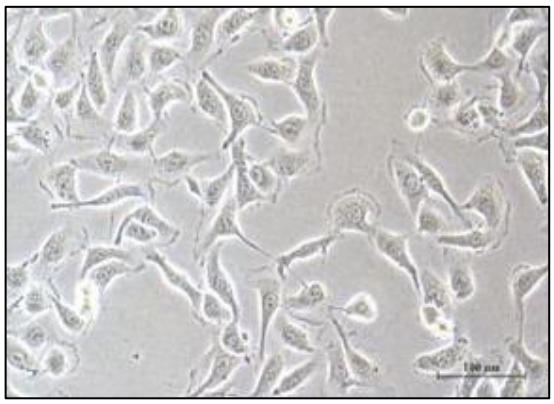

Figure 1.9: In vitro culture of human epidermal keratinocytes. Keratinocytes constitute 90% of the cells found within the epidermis. Scale bar 100 µm. (Adapted from (Nayak *et al*, 2013) Available via License CC BY 4.0)

The epidermis is the outer most layer of skin, 'epi' in Greek meaning 'on' or 'upon' and dermis meaning 'skin'. Over 90% of the epidermis is composed of keratinocyte cells *(figure 1.9)* (Freinkel *et al*, 2001), which have very strong desmosomes resulting in a very dense structure, with less than 2% of the total epidermal volume being intercellular space (Silver *et al*, 2003). The remaining 10% of the epidermis contains a combination of melanocyte cells, which produce a pigment called melanin, Langerhans cells, which are macrophages only found in the epidermis, and Merkel cells, which are associated with sensory nerve endings (Colville *et al*, 2009). Although the epidermis is only around 80 microns thick, it contains four sublayers, known as the stratum basalis, the stratum spinosum, the stratum granulosum and the stratum corneum (Orgill *et al*, 2009). Throughout these layers the keratinocytes differentiate to become more mature and accumulate keratin as they move outwards through the layers so that cells in the stratum corneum are fully keratinised to form a dead and hardened impermeable surface.

1.6.2 Dermis

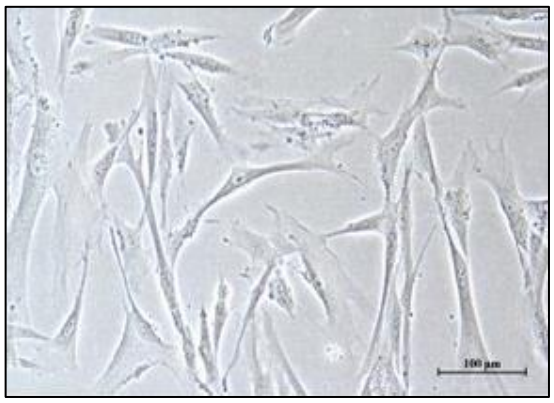

Figure 1.10: In vitro culture of human dermal fibroblasts. Fibroblasts are the most common cells found in the connective tissue of animals. Scale bar 100 µm. (Adapted from (Nayak *et al*, 2013) Available via License CC BY 4.0)

Below the epidermis is the dermal layer, which has a total thickness of around 1 or 2 mm (Orgill *et al*, 2009) accounting for 75% of the skins dry weight (Freinkel *et al*, 2001) and is separated from the epidermis by the basement membrane. The dermis is made up of fibres of connective tissue that run in all directions, composed of elastin and collagen *(figure 1.10).* The collagen fibres provide most of the mechanical strength to the skin, while the elastin fibre provides the recoil strength (Scanlon *et al*, 2006). A study conducted by Dennis Orgill in 1983 found that the tensile strength of the dermis can range anywhere 3.4 – 68.9 MPa (Orgill, 1983). The dermis consists of two layers, the upper layer is called the papillary layer and the lower layer is called the reticular layer. The papillary layer is composed of loose connective tissue which adheres to the basement membrane of the epidermis (Paulson, 2014). Dermal papillae are found in the papillary layer, within which are looping blood vessels that provide nutrition to the epidermis as well as removing waste products and controlling temperature (Phillip Cochran, 2010). The reticular layer is thicker than the papillary layer, containing various amounts of fat, as well as coarse collagen fibre, oriented parallel to the skin surface (Paulson, 2014). Since the dermis provides a large contribution towards the mechanical properties of skin as a whole and collagen and elastin make up the majority of the proteins found throughout the dermis, these proteins have a large influence on the mechanical properties of the dermis itself, therefore we have describe the physiology of these proteins in more detail below

1.6.2.1 Collagen

Collagen is the protein which is responsible for skin firmness (Kielty *et al*, 2002). It is the main component of the skin, contributing to around 77% of the skins fat-free dry weight (Finlay, 1969). In total there are at least 16 different types of collagen, however, types I, II and III make up around 80-90% of all the collagen in the body (Cicchi *et al*, 2010). In a relaxed position, collagen fibers are arranged in a disorganized fashion (Hussain *et al*, 2013) with individual collagen fibers ranging from 50 – 200 nm in length (Pawlaczyk *et al*, 2013). However, when the skin is stretched, these collagen fibers begin to align parallel to each other (Hussain *et al*, 2013), forming bundles of collagen with diameters ranging between 0.5 – 3 mm (Pawlaczyk *et al*, 2013). Mechanically, collagen has a high tensile strength as well as high stiffness but lacks extensibility, this means collagen is the main component contributing to the structure of the skin but does not provide much in terms of recoil ability (Goldsmith *et al*, 2012). Under a tensile load, collagen and elastin fibres are considered to be linear elastic, yet the stress strain curve for skin as a whole is non-linear (Bark *et al*, 2009)

1.6.2.2 Elastin

Elastin is the protein which provides elasticity to all layers of the skin (Kielty *et al*, 2002). Elastin is the second main component of the dermis next to collagen, although it contributes just 4% to the skins overall fat-free dry weight (Hussain *et al*, 2013). Elastin fibres are significantly thinner and more convoluted than collagen fibres (Xu *et al*, 2008), as well as being much less stiff than collagen, resulting in elastin having almost no contribution towards the tensile strength of skin (Goldsmith *et al*, 2012). However, this low stiffness means elastin has a long-range elasticity, showing full recovery when strains greater than 100% are applied (Hendriks, 2005). Through an intimate relationship with collagen, thick horizontal elastin fibres at the reticular layer, and perpendicular elastin fibres at the papillary layer (Pawlaczyk *et al*, 2013) ensure collagen returns to its disorganised structure at rest (Goldsmith *et al*, 2012) resulting in a full recovery of skin tissue shape following regular skin deformations (Geerligs, 2009). However, if the deformation is great enough, elastic fibres can fragment, which often results in a loss of recoil of the skin (Goldsmith *et al*, 2012)

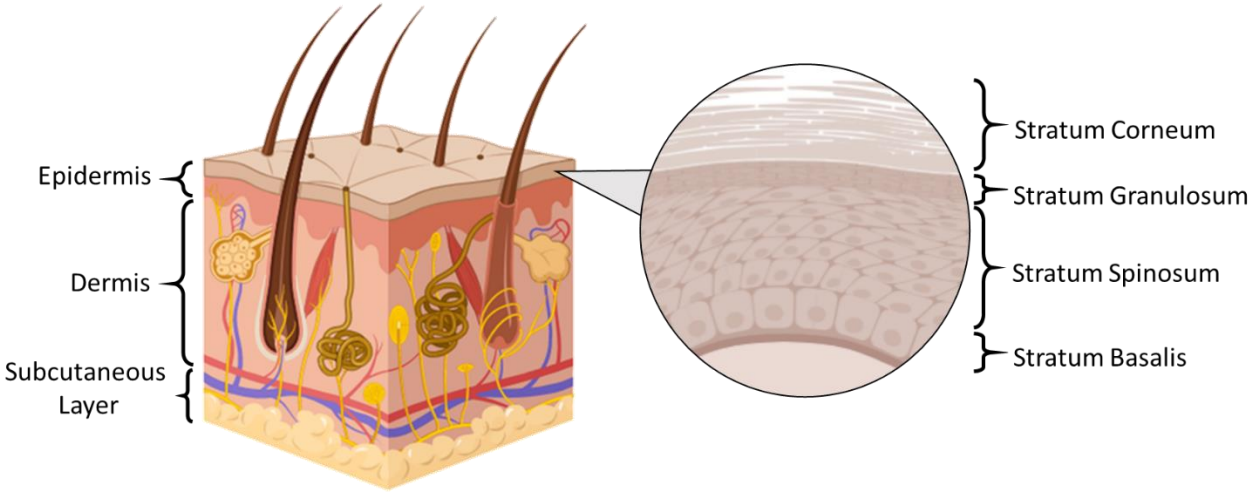

Figure 1.11: Diagram to describe the structure of human. (Left) illustrates the overall structure of the skin containing hair follicles, sweat glands and blood vessels. (Right) Details the differentiation of the keratinocytes throughout each layer of the epidermis.

1.6.3 Role of epidermal cells and wound healing

Fibroblasts and keratinocytes are the main cells found throughout the dermal and epidermal layers, and as a result play a crucial role in the wound healing process (Tracy *et al*, 2016; Wojtowicz *et al*, 2014). Shortly after a wound is made in the dermis, fibroblasts migrate to the wound area and proliferate, initiating the repair phase of wound healing. They synthesize growth factors and extracellular matrix (ECM) molecules, including collagen and fibronectin, which form wound granulation tissue and provide structural integrity to the wound (Clark, 1989). Similarly in the presence of a wound, keratinocytes migrate to the wound site and respond to inflammatory signals to eliminate infection and complete the process of reepithelialisation (Singer *et al*, 1999). Therefore, in acute healthy wounds, fibroblasts show more activity and respond well to growth factors, whereas in chronic wounds, fibroblasts respond poorly to growth factors requiring higher doses to initiate the same response (Loot *et al*, 2002). What is more proteolytic activity is increased which leads to the destruction of the extracellular matrix (Shah *et al*, 2012). Similarly secretions from healthy wounds stimulate DNA synthesis in in vitro fibroblast cultures (Katz *et al*, 1991), while secretions from chronic, non-healing wounds inhibit the same fibroblasts in vitro (Mendez *et al*, 1999). Since fibroblast activity is governed in response to inflammatory markers such as growth factors and cytokines, and fibroblasts

response to these inflammatory markers is reduced in chronic wounds, one would expect cytokine production to be elevated in chronic wounds when fibroblasts are non-responsive. This was indeed shown by Trengove *et al* who reported that levels of the pro-inflammatory cytokines IL-1α and TNF-α were higher in non-healing wounds compared to healing wounds, which then began to fall significantly when healing was initiated (Trengove *et al*, 2000). It is clear that fibroblast and keratinocyte activity plays a key role in the wound healing process, therefore initial adhesion and proliferation of fibroblasts are essential to the integration of soft tissue around external fixation pins in order to produce a healthy pin-site. Enhancing fibroblast adhesion and proliferation, through biocompatible pin materials or improved pin-site wound care may be the most effective approach at minimising complications in external fixation.

Chapter 2: Literature Review

2.0 Introduction

A pin-site wound, created by the entry point of the fixator wire into the skin surface, is essentially an open door for bacteria to enter the host, disrupting the host's immune system and allowing access to soft tissue and bone beneath the skin surface. This has resulted in high incidences of pin-site infection, with infection rates reported in the literature ranging from 4.5% to 100% (Antoci *et al*, 2008; Garfin *et al*, 1986; Mahan *et al*, 1991; Parameswaran *et al*, 2003). A comparison between healthy and infected pin-site wounds can be seen in *figure 2.1*. Another major complication is pin-loosening, whereby mechanical loading on the fixator repeatedly stresses the pin-bone interface, causing the interface to deteriorate (Saithna, 2010). Once a pin becomes loose, the fixator loses stability, and an unstable fixator creates an unsuitable environment for optimal bone healing (Parameswaran *et al*, 2003). Many researchers have commented on the apparent converse relationship between pin-site loosening and infection, whereby a pin that has become loose often results in infection and vice versa (Ferreira *et al*, 2012; Parameswaran *et al*, 2003). Significant effort has been made intraoperatively and postoperatively to prevent the occurrence of pin-site infections, however pin-site infections are often difficult to diagnose and once infection has developed the most common method of treatment, bar removing the pin itself, is through administering antibiotic treatments. The current high rate of antibiotic consumption has led to the emergence of antibiotic resistant strains of bacteria, such as methicillin resistant S*taphylococcus aureus* (MRSA). The emergence of antibiotic resistant strains of bacteria has put emphasis on the fact that more research must be conducted to identify the major factors which cause these infections to develop, and engineer methods of infection prevention, rather than simply treating the infections with antibiotics as they occur.

The aims of the following literature review are:

1. Understand the relationship between wound healing and infection in external fixation
2. Understand the role mechanical movement has on wound healing and infection
3. Highlight current methods of preventing pin-site complications and identify gaps in the literature

Figure 2.1: Images illustrating healthy and infected pin-site wounds. A good pin-site (left) is not painful and has little redness and swelling. A poor pin-site (middle) may be painful and show redness as well as exudate oozing from the wound. An infected pin site (right) is noticeably painful, red and swollen and lots of exudate present

2.1 Relationship between wound healing and infection in external fixation

Once bacteria are able to colonise the pin-site wound, the surface of external fixator pins provide the ideal environment for bacteria to attach and form biofilms. A mature biofilm then requires concentrations of antibiotics 500 – 5000 x of that needed to kill planktonic bacteria of the same species (Khoury *et al*, 1992). If a local infection is left untreated it may migrate along the pin-tract and infect the underlying muscle and bone, causing a potentially life-threatening systemic infection (Healy *et al*, 2006). When studying the antimicrobial ability of silver coated external fixation pins, Collinge *et al* observed that there was a strong collation between pin motion and infection, with 88% of infected pins experienced motion, while motion was only noticeable in 56% of uninfected pins (Collinge *et al*, 1994). Therefore it is not only important to understand the mechanisms of infection, but also how the hosts immune system responds to the presence of a pin-site wound and what factors affect the rate of pin-site healing. In external fixation, a pin site wound can be said to have similar characteristics to a chronic wound which also contains a foreign body. Since the presence of a fixation pin prevents the wound from fully closing, the intention of wound care should not be closure of the wound but instead to facilitate rapid healing of skin around the pin in order to create a bone-pin interface that is sealed from the external environment, much like how a pierced ear heals (Ferreira *et al*, 2012).

2.1.1 Foreign body immune reaction

The presence of a fixation pin in a wound, initiates a foreign body immune reaction. For small debris such as dead cells and dirt, macrophages engulf and breakdown the debris through a process called phagocytosis. However, if the foreign body is too large to be engulfed, such as a fixator pin, the macrophages begin to fuse together, forming much larger multi-nucleated foreign body cells (Jay *et al*, 2010). These foreign body giant cells are usually found along the pin-skin interface, encapsulating the implant in a firm collagen shell, which effectively isolates it from the host tissue (Brodbeck *et al*, 2009). This provides a barrier to bacteria and a mechanical lock of the tissue with the implant, limiting micro-motion between the implant and tissue which could weaken the attachment (Isackson *et al*, 2011). However, an adequate and long lasting seal rarely forms due to the low level shear forces and stress concentrations at the skin interface, creating avulsions which often lead to the seal repeated breaking and preventing the collagen shell from fully maturing (Holt *et al*, 2008). When studying percutaneous devices, Von Recum *et al* found that the thickness of this shell is dependent upon the magnitude of mechanical stresses across the pin-skin interface (von Recum, 1984). However, the cellular composition of the shell itself is dependent upon the bio-compatibility of the implant, with very compatible materials, such as carbon, resulting in a thin fibrous capsule often without any inflammatory cells present (von Recum, 1984).

2.2 Mechanical movement between pin and skin in external fixation

Throughout the literature it is clear that many clinicians acknowledge that there is a relationship between the relative movement between the soft tissue and pin and an increased risk of infection in external fixation (Bibbo *et al*, 2010; Browner *et al*, 2014; Canale *et al*, 2012; Ferreira *et al*, 2012; Holmes *et al*, 2005; Santy *et al*, 2009; Santy *et al*, 2015) however there is a very limited number of studies that have investigated the effect of skin movement around external fixator pins. This relationship may be due to movement continuously disrupting the fibrous collagen shell, which forms around the fixator

pin as a foreign body immune response, to be repeated broken before it is fully mature. By repeatedly breaking this shell and disrupting any additional skin growth around the pin, the body fails to isolate the pin from the host tissue, leaving the pin tract open for infectious bacteria, which regularly colonize the surface of the skin, to be able to enter the host. Collinge *et al* observed a correlation between pin motion and infection, with 28 of 32 (88%) of pins experiencing motion becoming infected while only 9 of 16 (56%) unaffected pins had motion (Collinge *et al*, 1994). As far as the microenvironment of the pinhole is concerned, it makes little difference whether the pin is moving with respect to the tissue or the tissue is sliding back and forth along the pin e.g. muscle contractions (Browner *et al*, 2014). The effect is the same, which is relative motion between soft tissues and a contaminated foreign body (Browner *et al*, 2014). Therefore, in order to better understand the movement experienced by the skin and at the pin-site three modes of movement have been hypothesis *(figure 2.2)*. The following section explores these modes of movement in order to understand their mechanisms and hypothesize how they may influence the rate of pin-site infection.

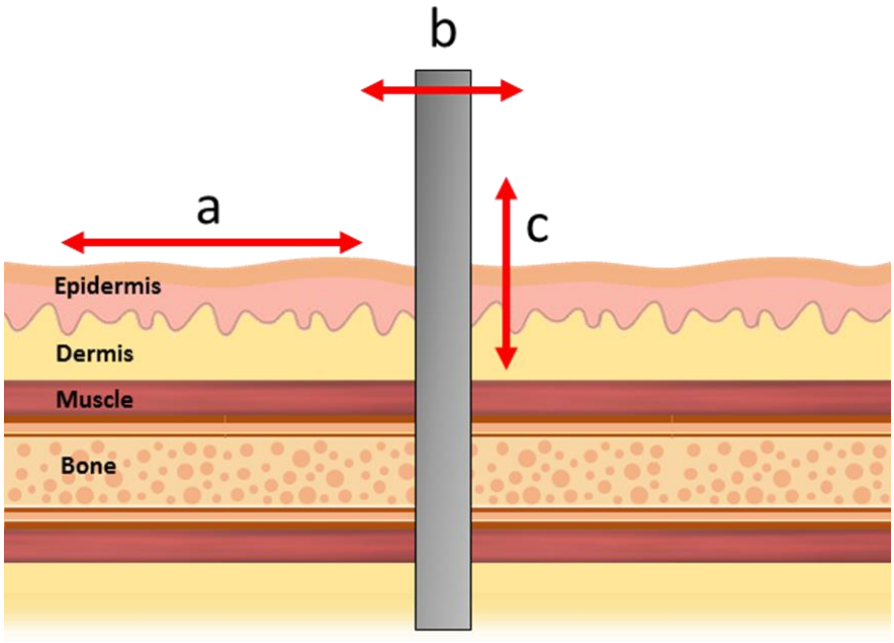

Figure 2.2: Diagram to illustrate the components of a pin-site. Two modes of relative movement between the pin and skin interface has been hypothesised by the other of this review. (a) Changes in skin strain as a result of skin tension. (b) Deflection of pin due to patient activity. (c) Shearing along pin due to muscle contraction

2.2.1 Modes of movement

The load bearing properties of external fixator's means patients are often able to walk on the fracture, applying their full weight, permitting micro-motion across the fracture, which is known to stimulate osteogenesis (De Bastiani *et al*, 2012) and improve the rate of healing (Fragomen *et al*, 2007). This allows for joint motion exercises to be performed in order to improve healing of the fracture, and even mobilisation of the patients with full weight bearing, as recommended by Ilizarov himself (Gessmann *et al*, 2011). As a result of this patient activity three significant translations at the pin skin interface have been hypothesis (*figure 2.2)*. Firstly changes in the orientation of the natural tension of skin are restricted by the presence of the pin, causing a change in strain across the skin at the pin-site (a). Secondly as the patient applies weight to the fixation frame, significant forces are translated to the fixation pins, causing a deflection to a occur (b). Lastly since the pin is rigidly fixed to the underlying bone it moves in unison with the skeletal structure which does not necessarily translate to movements across the skin surface, causing additional strain across the pin-site. It is also possible that this is further enhanced by the the expansion and contraction of muscles as the patient moves their limb causing the volume of the lower limb to change, thus resulting in the skin sliding axially along the pin, generating shearing forces along the pin tract (*c)*.

2.2.1.1 Natural skin tension

In 1861 the Austrian anatomist Karl Langer observed that by puncturing the skin of a cadaver in multiple locations and joining the major axis of the wounds, the contour lines of the natural tension of the skin could be mapped (Gallagher *et al*, 2012). Over 150 years since skin tension was first observed, these Langer Lines of tension are still used throughout medical and cosmetic surgery. It is now known that skin extensibility and skin tension at the edge of the wound are major influences in how a wound will heal. An increase in tension across a surgical wound increases the tissue pressure, which reduces micro perfusion and limits the availability of oxygen to the wound (Anaya *et al*, 2006). Oxygen deprived tissue then results in a prolonged inflammation phase and delayed healing, increasing the risk of

infection (Huether *et al*, 2012). A study conducted in 1978 by Sommerland *et al*, compared the effects of tension on four wound closure techniques (Sommerlad *et al*, 1978). When there was little tension across the wound, the weak collagen bonds managed to withstand the forces and remain aligned along the wound, producing a narrow scar. However, when the tension was great enough to overcome the collagen bonds, the longitudinal fibres separate when the sutures were removed, causing collagen fibres to be arranged in a disorganised fashion, therefore producing a less sightly scar (Sommerlad *et al*, 1978). If it is assumed that the quality of scar formation correlates to the quality of wound healing, then Sommerland's research demonstrates that minimising the tension across the pin-site will result in improved healing around the pin-site and therefore a reduced risk of infection. In a paper which investigated the effect of daily and weekly pin-site care on infection rates, Camathias *et al* concluded that:

> *"Skin tension at the time of insertion is in our opinion one of the most important factors in producing sterile pin sites" (Camathias et al, 2012)*

Therefore it is important that surgeons familiarize themselves with the natural tension of the skin, in order to position pins in areas of low tension to avoid any unnecessary increased risk of infection.

2.2.1.2 Human gait cycle

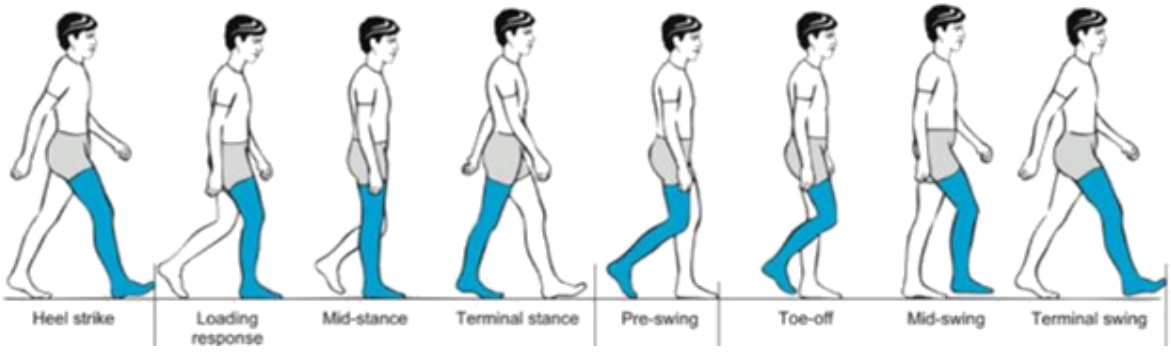

Figure 2.3: Diagram illustrating the human gait cycle. Image obtained from (Diyana Nordin *et al*, 2018) Available via license: CC BY 4.0

Patient activity has been identified as a primary source of relative movement between the pin and skin, therefore the frequency of pin movement is likely to correspond to the frequency of the human gait cycle. Gait cycle is the time period during walking between one foot contacting the ground and to that same foot contacting the ground again *(figure 2.3).* The average duration of one gait cycle of men ranges from 0.98 to 1.07 seconds (Murray *et al*, 1964), resulting in a walking frequency of approximately 60 steps a minute or 1 Hz.

2.2.1.3 Soft tissue artefact

Skin movement across external fixation pin-sites is difficult to determine as external fixation pins have interfaces at both the skeletal bone and soft tissue. There is often a discrepancy between skeletal movement and soft tissue translations, known as the soft tissue artefact (STA). In addition, the pins inserted through the skin will likely restrict skin movement, therefore the skin around the pin site is subject to changes in strain. Many attempts have been made at categorising these artefacts by using surface markers along with fluoroscopy (Cappello *et al*, 2005; Cappozzo *et al*, 1995; Fuller *et al*, 1997; Holden *et al*, 1997), invasive pins such as intra-cortical pins (Cole *et al*, 1993; Fuller *et al*, 1997; Lafortune *et al*, 1992; Reinschmidt *et al*, 1997), percutaneous trackers (Holden *et al*, 1997; Manal *et al*, 2000) and external fixators (Alexander *et al*, 2001; Cappello *et al*, 1997; Cappozzo *et al*, 1996). The large variation in measurement techniques, different joint locations and small sample sizes throughout the literature means the reported values of STA vary significantly. As a result of these studies have identified that the magnitude of STA is dependent upon the physical characteristics of the subjects (Holden *et al*, 1997), the location of the markers (Schwartz *et al*, 2004) and the variety of tasks being performed (Fuller *et al*, 1997), meaning STA values are repeatable within the same subject, but not among multiple subjects. Despite this several studies have observed a greater magnitude of STA in the shank compared to that of the thigh (Leardini *et al*, 2005; Peters *et al*, 2010; Stagni *et al*, 2005) with many studies showing that skin mounted markers can exhibit displacements relative to the underlying bone of anywhere between 0.7 mm and 10.9 mm (Gao *et al*, 2008; Garling *et al*, 2007). The large

discrepancy between measured values of soft tissue artefact across the tibia is most likely due to the large range of variables used throughout studies with little correlation between measurement technique and subject activity in each study. Therefore, obtaining a definitive value for the soft tissue artefact across the shank is unachievable, as the value will vary significantly between patients.

2.3 Preventing infection and improving wound healing in external fixation

The previous sections of this review highlighted the issue that bacterial adhesion and biofilm formation to external fixation pins may result in decreased antibiotic sensitivity (Qu *et al*, 2014), and that relative movement between the pin and skin may play a significant role in increasing the risk of infection occurring. The following section discusses the many engineering and clinic methods that have been adopted in an attempt to produce better healing around the pin and minimise the infection rate, including surgical techniques and post-operative pin-site care, the use of antimicrobial solutions as well as a redesign of the pin itself.

2.3.1 Pin-site care

Pin-site care refers to the treatment of pin-sites both intraoperatively and postoperatively to reduce the incidence of infection in external fixation. Currently there is no agreement among clinicians regarding the most effective method of pin-site care. The five main areas of controversy regarding pin-site care are as follows:

1. The frequency of care
2. The Use of Antimicrobial Solutions
3. The removal of pin-site crusts
4. The use of topical ointments
5. The use of dressings

In 2010, the royal College of Nursing Society funded a project which was aimed at gathering a consensus regarding pin-site care from specialist practitioners working in the field of limb

reconstruction and external fixation (Timms *et al*, 2013). From this consensuses it was found that the majority of specialist practitioners agree on several key aspects of pin-site care, including the use of chlorhexidine for cleaning the pin-site, and sterile non-shed dressing wrapped so that compression is applied to the pin-site. One of the most commonly referenced pin site care protocols in the literature is the Russian protocol of pin site care, developed by the 'Ilizarov Scientific Centre for Restorative Orthopaedics' (Kofman *et al*, 2012). The Russian protocol advises a non-touch method during pin insertion in order to minimise bacterial contamination while also utilising pulse drilling to reduce heat-induced tissue necrosis. Following surgery, pin-sites should be cleaned daily for the first 3 days with 70% ethanol, followed by weekly dressing changes until the fixator is removed. In 2005, Davies *et al* studied the effectiveness of the Russian protocol against regular local custom care (Davies *et al*, 2005). A total of 120 patients were studied, 74 of which received the Russian protocol pin-site care while the remaining 46 received local custom care. Davies found that the patients which were treated with the Russian protocol had a 37% lower proportion of infected pin-sites. It was also observed that there was a 50% chance of infection after 24 days for local custom pin-site care but this increased to 92 days when the Russian protocol was used. However the large number of variables between pin-site care methods make it difficult to systematically review these pin-site care protocols, therefore more detailed clinical research and basic scientific research is required so that the effectiveness of each treatment can be measured individually in order to develop an optimal pin-site care protocol.

2.3.2 Compressive dressings

When investigating pin-site care protocols, many clinician's recommend methods of care that are aimed at reducing the skin movement around the pins. Clinicians often utilise compressive dressings such clips, syringe bungs (Canale *et al*, 2012) or tightly wrapped gauze (Browner *et al*, 2014). These stoppers help to maintain slight pressure on the pin dressing and minimize the pin-skin interface motion which is a prelude to pin site infection (Canale *et al*, 2012). The difficulty with compression dressings is knowing how much compression is beneficial as too much compression may lead to

adverse effects, such as pressure ulcers or skin necrosis (Timms *et al*, 2013). Since patients are usually required to clean and dress the pin-sites themselves it is often difficult to ensure that the correct amount of compression is being applied. In a consensus conducted by the Royal College of Nursing there was agreement (96.7%) that compression should be applied around the pin or wire immediately post-operatively, as well as agreement (86.7%) that any dressing should be pushed down with a bung or clip. It was also agreed that any compression should be light compression (90%) although the meaning of light compression needs defining further. There was agreement that the compression should be maintained throughout the treatment (70%) with less agreement (53.3%) that compression should be applied for 48 h post-operatively – possibly reflecting a view that compression should, in fact, be maintained for longer than this as reflected in the previous statement. (Timms *et al*, 2013). It is clear that these dressings likely prevent some degree of skin movement but the relationship between compression dressings and reduced infection rates has not been scientifically proven. It must also be considered that many of these compressive dressings' devices cannot be replaced until the fixator is removed, consequently this creates a potential breeding ground for infectious bacteria.

2.3.3 Pin placement

Although optimal pin placement along the mid-shaft of the tibia has not been defined, many studies have identified areas of the lower limb where pin placement should be avoided due to a high risk of complications. Surgeons are often advised to place skin incisions so that they avoid areas of high skin tension (Ferreira *et al*, 2012) and muscle transfixion (Browner *et al*, 2014) as well as avoiding placing pins in the proximity of joints (Lowery *et al*, 2015; Stevens *et al*, 1995) as several studies have identified a correlation between pins which penetrate the joint capsule and a greater susceptibility to septic arthritis (Hutson *et al*, 1998; Lowery *et al*, 2015; Stevens *et al*, 1995). As a result clinicians now suggest a distance of at least 14 mm from the joint capsule in order to avoid capsular penetration (DeCoster *et al*, 2004; Reid *et al*, 2001). The effect that pin placement near joints has on the risk of infection can be seen in a study conducted by Hove *et al* (Hove *et al*, 1997). Hove investigated the differences between

static and dynamic fixation of the wrist and found that 15 of their patients (43%) in the dynamic fixator group developed pin-site infections, but only 4 (11%) developed infection in the static fixator group. They attributed this difference in infection rates to the motion allowed by the dynamic fixator, which permitted movement between the skin and pin, and appeared to increase skin irritation around the wrist and lead to higher infection rates.

2.3.4 Pin material

Steel has been used for the manufacture of medical implants for over a century, beginning when Lane first introduced his metal plate for bone fracture fixation in 1895 (Lane, 1895). Today the most frequently used metal for medical applications is 316L stainless steel, however titanium is becoming increasingly common due to its superior strength-to-weight ratio and Young's moduli which more closely resemble that of bone. There are several factors which determine the biocompatibility of a metal, one of the most important factors is the ability of the metal to resist corrosion from bodily fluids. Titanium's corrosion resistance is due to the 3 – 10 nm thick oxide layer which forms on its surface when exposed to oxygen (Raikar *et al*, 1995), while stainless steel implants are known to initiate a foreign body reaction, causing the formation of a fibrous capsule, enclosing the implant in a liquid filled void (Gristina, 1987). While the choice of material may be a crucial factor in determining the outcome of a large load bearing, long life-expectancy implant such as a joint replacement prosthesis, for a low load bearing, temporary implant such as an external fixator pins, the differences are less noticeable. DeJong *et al*, conducted a study testing the antimicrobial efficiency of various external fixator pins in a goat model and found a 100% infection rate in both stainless steel and titanium pins (DeJong *et al*, 2001). The largest reduction in infection rates in external fixation was achieved not by changing the pin material but instead when a pin coating such as hydroxyapatite and nitric oxide was applied, this way the superior mechanical properties of stainless steel could be retained while at the same time utilising the antimicrobial properties of these coatings.

2.3.5 Pin coatings

2.3.5.1 Hydroxyapatite coated external fixation pins

Hydroxyapatite (HA) is a crystalline molecule composed of both calcium and phosphate (Jennison *et al*, 2014) and is the most abundant mineral found in human bone (Geesink *et al*, 1988). Consequently by coating external fixation pins in HA, a very strong fixation between the implant and bone is formed (Geesink *et al*, 1988). Moroni *et al* studied the extraction torque of uncoated, HA-coated and titanium-coated pins (Moroni *et al*, 2002). Moroni recognised that the torque required to extract the HA pins was 13 times higher than that of the uncoated pins, and 2 times higher than that of the titanium pins. On the other hand, DeJong *et al* studied both stainless steel and titanium pins, with and without a hydroxyapatite/chlorhexidine coating (DeJong *et al*, 2001). After contaminating the pins with a *S. aureus* and implanting them into goats, DeJong observed that 100% of the uncoated pins developed infection, while only 12.5% of the coated pins were colonized by bacteria and just 4.2% became infected. These studies provide strong evidence that coating fixator pins in HA improves both bone fixation and anti-bacteria properties, further supporting the hypothesis that pin loosing and pin-site infection are closely connected.

2.3.5.2 Nitric oxide coated external fixation pins

Nitric Oxide (NO) is a chemical compound that plays a central role in the natural immune systems response to infection (Holt *et al*, 2011). It has been shown that NO plays a key role in bone tissue engineering and fracture healing, with studies suggesting NO production is increased within the first 2 weeks of fracture healing (Keskin *et al*, 2007). Furthermore studies have shown that NO significantly reduces fibrogen-mediated adhesion of both Gram-negative and Gram-positive bacteria, in particular *S. aureus*, *S. epidermidis* and *E. coli* (Charville *et al*, 2008). While the primary goal is prevention of bacteria adhesion and biofilm formation, NO has also shown to greatly enhance the efficiency of antimicrobial compounds in the removal of pre-existing mature biofilms containing *P. aeruginosa*

(Barraud *et al*, 2006). The evidence suggests that NO may offer an alternative to conventional antibiotics, with another benefit being its short half-life, allowing it to be administered locally, avoiding the systemic side effects of conventional antibiotics (Oda *et al*, 1997)

2.3.5.3 Silver-coated external fixation pins

The antimicrobial properties of silver have been utilized to limit microbial colonization in a wide number of clinical applications. Silver has been commonly used to coat catheters in order to slow down biofilm development and can also be found in hygiene products such as face creams and water filtration cartridges. However recently the effectiveness of silver's antimicrobial properties is under debate. In 1994 Colligne *et al* demonstrated a reduction of infection rates of external fixation pin tracts in six sheep inoculated with *S. aureus* of 22% when applying a silver coating to the pins (Collinge *et al*, 1994). This was further supported by Wassall *et al*, when they showed that silver-coated pins could reduce the adhesion of *E. coli*, *P. aeruginosa* and two strains of *S. aureus* (Wassall *et al*, 1997). However, in 2006 Coester *et al* performed an in-vivo study of 19 patients with silver and stainless pin and found no significant difference between infection rates and removal torque of both pins types (Coester *et al*, 2006). While silver antimicrobial properties are still under debate, the toxicity of silver at high levels is clear. Braydich-Stolle *et al* assessed the nano-toxicity of silver against mouse stem cells (Braydich-Stolle *et al*, 2005). It was observed that nanoparticles between 5 µg / ml and 10 µg / ml induced necrosis. Since silver use is severely limited by the toxicity of silver ions to humans, nano-technology has been used to develop silver particles between 1 and 100 nm diameter, with large surface areas, known as silver-nanoparticles. Silver-nanoparticles allow implants to be completely coated with only small amounts of silver, limiting the potential risks of toxicity (Chaloupka *et al*, 2010). Therefore there may be a potential use silver-nanoparticles in the coating of external fixation pins to utilise the antimicrobial properties of silver while minimising the toxic effects.

2.3.5.4 Pin surface topography

Surface topography is an important characteristic in medical implants as it directly influences the development of the collagen shell. For example, smooth breast implants may result in a layer of macrophages just one or two cells thick, which allows the implants to move within the soft tissue making it difficult for any soft tissue seal to form (Picha *et al*, 1996). On the other hand implants with greater surface area, such as fabrics or porous materials, will have a much higher ratio of macrophages and foreign body giant cells (Ratner *et al*, 2012). Von Recum theorized that material pore size is a major influence on forming an adequate seal around the pin (von Recum, 1984), stating that if the pore size is greater than 40 µm then the implant has a much larger surface area and therefore tissue is able to grow into the pores, improving the soft tissue seal and therefore creating a barrier to infection. Isackson *et al* investigated this hypothesis on percutaneous implants in rabbit models and found that smooth surface implants had a 7-fold increased risk of infection compared to their porous counterparts (Isackson *et al*, 2011). This has now been implemented clinically in amputation prosthesis, by creating micro-machined grooves (Chehroudi *et al*, 2002; Pendegrass *et al*, 2006), pits (Chehroudi *et al*, 2002) and porous surfaces (Isackson *et al*, 2011), which result in increased cell attachment. This approach could be utilised in external fixation, however engineering a porous pin while maintaining the mechanical strength to withstand the bending forces generated across the fixation pins my prove challenging.

2.3.5.5 Antimicrobial-release coated pins

Significant research has been done into the coating of implant surfaces with materials which slowly release anti-microbial solutions directly to the implant site. Polymers such as PMMA impregnated with antibiotics (Gollwitzer *et al*, 2003; Voos *et al*, 1999) and Sol-gel coatings (Mahltig *et al*, 2004) have been extensively studied. Conventional use of systemic antibiotics have several drawbacks including kidney and liver complications as a result of systemic toxicity, poor penetration into the target sight and need for hospitalized monitoring (Price *et al*, 1996). Therefore the administration of antibiotics by a local

delivery device addresses the major disadvantages of the systemic approach by maintaining a high local antibiotic concentration for an extended duration of release without the issue of systemic toxicity (Gristina, 1987; Zalavras *et al*, 2004). The effectiveness of such devices is dependent on the rate and manner in which the drug is released. If the drug is released quickly, the entire drug could be released before the infection combatted, on the other hand if the release is delayed, infection may set in further, thus making it difficult to manage the wound (Zilberman *et al*, 2008). The most extensively studied and earliest commercially available slow release coatings was developed in 1970 according to Buchholz and Engelbrecht's innovative idea of releasing antibiotics from polymethylmethacrylate (PMMA) bone cement (Buchholz *et al*, 1970). However there were several drawbacks to this method, firstly PMMA only allows a small fraction of the antibiotic to diffuse through its pores and secondly PMMA is non-degradable and therefore when failure occurs surgery is required to remove the PMMA to allow new bone to regenerate (Zilberman *et al*, 2008). Another more promising development is micron-thin films known as sol-gels, which can be coated on surfaces impregnated with drugs in order to control the local delivery of these drugs. These silica sol-gel films adhere to metallic surfaces well and exhibit excellent mechanical properties, making them ideal for coating the surface of medical implants such as external fixation pins. Adams *et al* demonstrated that Sol-gel coated titanium alloy rods significantly inhibited *S. aureus* viability and growth both in vitro and in vivo, decreasing the final microbial numbers by more than four orders of magnitude (Adams *et al*, 2009). Sol-gels can be shaped into granules, powder, thin films or microspheres which each provide different release kinetics. For implants in particular a glass like film can be applied to the implant surface, these films produce a slow and controlled release of the impregnated substance which occurs at room temperature and does not interfere with the activity of the drug (Adams *et al*, 2009). In conclusion these impregnating these sol-gel coatings with antibiotics provide a promising method for treatment of pin-site infection without the drawbacks of systemic antibiotic therapy. Additionally impregnating the sol-gels with antimicrobial materials, such as silver nano-particles has shown to prevent the formation of biofilms (Babapour *et*

al, 2011) therefore this method may potentially be used for preventing infection occurring in external fixation rather than the treatment of infection once if occurs.

2.3.5.6 Bioelectric effect

For several decades low voltage electric currents have been investigated for their ability to disrupt bacteria adherent to implant surfaces. Studies have shown that when an electrical current is applied to a stainless steel implant infected with *S. aureus* and *S. epidermidis*, the current was able to enhance detachment of the biofilm (Del Pozo *et al*, 2009; Ercan *et al*, 2011; Van der Borden *et al*, 2005). It was previously thought that the application of an electrical current acts synergistically with antimicrobial agents rather than working independently to dislodge bacteria (Khoury *et al*, 1992). However, Pozo *et al*, showed that electrical currents of 20 - 2000 μA effectively reduced the bacterial biofilm formation on Teflon coupons in the absence of any antimicrobial agents (Del Pozo *et al*, 2009). Since the adhesion of bacteria to an implant surface is mediated by attractive Lifshitz-Van der Waals forces, acid–base interactions and electrostatic forces (Hermansson, 1999) and all naturally occurring surfaces, including those of bacterial cells, are generally negatively charged, these electrostatic forces between bacteria and a biomaterials surface are repulsive (Jucker *et al*, 1996). Consequently by applying an electrical current, these repulsive forces can be increased, causing the bonding of the bacterial to the implant surface to decrease (Ueshima *et al*, 2002). Furthermore the low-voltage electric currents have also been used for the treatment of bone non-union as bone cells proliferate when subject to electrical stimulation (Brighton *et al*, 2001). Therefore there may be potential for electrical currents to be used in external fracture fixation to not only prevent biofilm formation, which should in turn reduce infection rates, but also increase the rate of healing for severe fractures and non-unions.

2.4 Discussion

Complications with external fixation reported in the literature, such as pin loosening or pin-site infection are common, with infection rates reported in the literature ranging from 4.5% to 100% (Antoci *et al*, 2008; Garfin *et al*, 1986; Mahan *et al*, 1991; Parameswaran *et al*, 2003). A review of the literature has identified that there is an inverse relationship between wound healing and infection in external fixation. In summary, if the wound healing process is impaired, the wound is kept open for a longer period, allowing infectious bacteria a greater opportunity to enter the host and cause infection. Conversely, if a wound becomes infected, the wound healing process is often halted until the infection has been combated. Therefore, in order to reduce the rate of infection in external fixation, attention should be paid not only to preventing infectious bacteria from entering the host, but also to produce adequate healing around the pin, which means the development of a collagen shell around the pin, isolating it from the host.

Current attempts at improving the healing around the pin-site, include pin-site care protocols and re-engineered pin materials. However, these protocols often include several treatments administered simultaneously, making it difficult to systematically assess the effectiveness of each treatment and alternative pin materials such as titanium, seem to have no effect upon infection rates, possibly due to the relatively short time the pin is in situ compared to other implants such as joint replacement.

A significant amount of the work regarding external fixation complications has been on characterising the pin-bone interface (Churches *et al*, 1985; Hyldahl *et al*, 1991; Moroni *et al*, 2002; Pettine *et al*, 1993; Saithna, 2010), which has led to successful innovation in pin coatings, such as hydroxyapatite and nitric oxide coatings, contributing towards reducing pin-loosening complications. However there has been little to no research into the pin-skin interface, which is surprising considering the large number of researchers that have acknowledged the relationship between soft tissue movement and an increased risk of infection (Bibbo *et al*, 2010; Browner *et al*, 2014; Canale *et al*, 2012; Ferreira *et al*, 2012; Holmes *et al*, 2005; Santy *et al*, 2009). Despite the lack of empirical evidence, many surgeons

and clinicians have attempted to prevent excessive skin movement around the pins by avoiding pin placement in areas of high skin tension or through areas with thick layers of soft tissue, as well as using compressive dressings, such as bungs, clips and gauze dressing in order to apply pressure to the pin-site (Browner *et al*, 2014). According to clinicians, these stoppers help to maintain slight pressure on the pin dressing and minimize the pin-skin interface motion which is a prelude to pin site infection (Canale *et al*, 2012). However, research conducted to study the efficacy of these treatments and the degree to which compression is beneficial in minimising skin movement and reducing infection is non-existent. Therefore there is an opportunity to investigate the efficacy of these treatments and the degree to which they are beneficial, as it is known that a high degree of pressure can lead to delayed healing and even pressure sores, and the dressings themselves may provide an additional surface for bacteria to colonise.

Research into the natural tensions of skin and the soft tissue artefacts have identified that there are significant translations of the skin over the tibia during patient activity, therefore it is hypothesised that these skin translations cause the collagen shell around the pin to repeatedly break, preventing an adequate seal against bacteria from developing. Which then allows commensal bacteria such as *Staphylococci aureus* and *Staphylococci epidermidis* to infect the exposed soft tissue. Since the pin-tract provides a direct route from the skin surface to the deeper subcutaneous tissue and bone, if not treated early, these superficial pin-site infections may develop, migrating along the pin-tract to cause more serious Osteomyelitis or Sepsis. Much of what we know about the factors affecting pin-site infections are empirically derived, with the majority of the non-clinical research adopting animal models, therefore much like the clinical studies on pin-site infection, the complexity of interactions due to the physiology of animal models, makes it difficult to interpret the results.

In conclusion there is a large gap in the literature regarding this relationship between skin movement, tissue growth and pin-site infection, therefore there is an opportunity to conduct fundamental basic science research to understand how the movement of the skin around the pin or the movement of the

pin itself effects the pathophysiology of infectious bacteria. By developing an accurate in vitro model of the pin-site scenario, the effect that pin movement frequency, duration and magnitude has on the wound healing properties and bacteria adhesion can be investigated in order to gather a stronger understanding of the interactions between the skin and pin of both in the presence of infection.

2.5 Research plan

2.5.1 Research question

Does relative movement between the pin and skin influence the bacterial attachment and wound healing around the pin in external fracture fixation?

2.5.2 Aim

The aim of this doctoral research was to characterise the effect of pin movement on pin-site infection through in vitro models which replicate the infected pin-site scenario. From these models the effect that frequency, duration and magnitude of relative movement generated between the pin and skin has on the wound healing and bacteria adhesion could be studied.

2.5.3 Hypothesis

Similar to how a high degree of tension across a regular wound influences the rate of healing, producing less than optimal scarring (Sommerlad *et al*, 1978), it is hypothesised that mechanical tension and shearing across the skin, caused by the relative movement at the pin-skin interface, will increase the rate of high-adherent bacterial attachment to the pin and/or negatively influence wound healing at the pin-site.

2.5.4 Key objectives

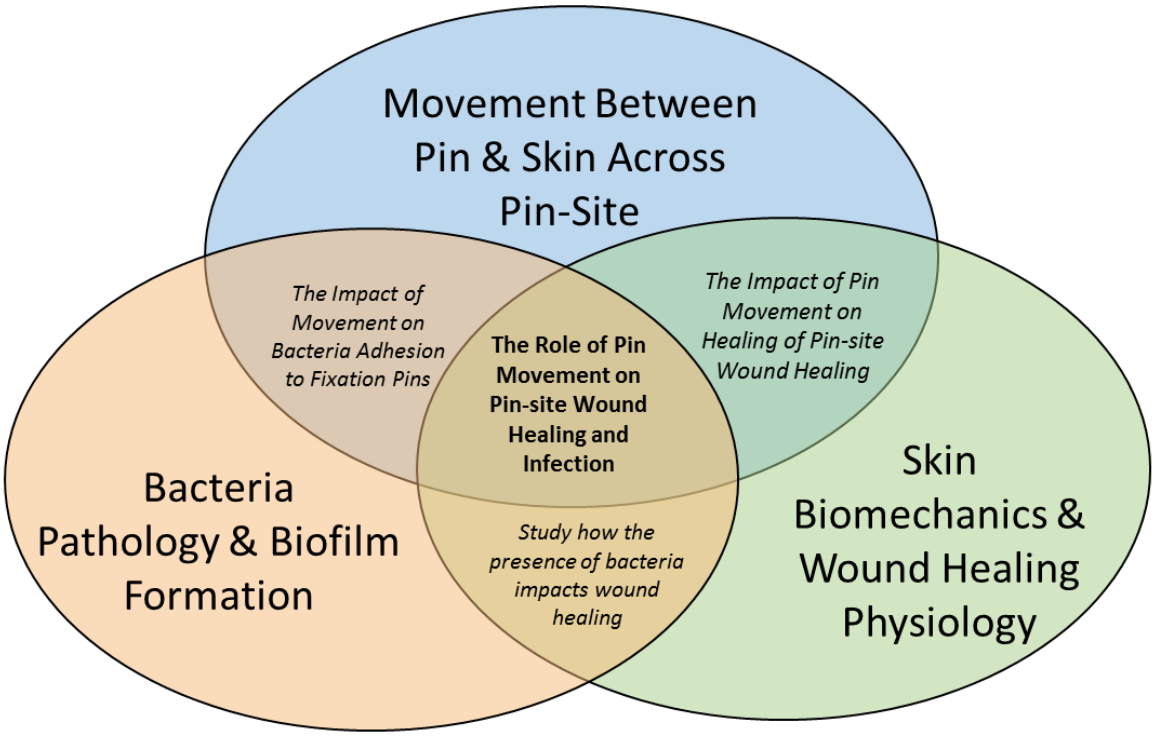

Figure 2.4: Venn diagram describing the three main factors in pin-site infection – The following research aims to investigate the relationship between each factor in order to characterise the role of movement on the development of infection in external fixation

In order characterise the pin-site scenario for study, the pin-site scenario was simplified to three main components, the pin itself, the soft tissue and the infectious bacteria *(figure 2.4)*. Before a model of the complete pin-site is developed, the interactions between each component was studied individually. For example, the effect of movement on bacterial adhesion to fixation pins without the inclusion of soft tissue, or the effect of movement on wound healing of the skin model without bacteria present. Each of these interactions form a chapter of the following thesis, which, due to the multidisciplinary nature of the project each have their own introductory and methodology sections.

The following key objectives were proposed:

1. Design and develop a pin machine to replicate external fixation pin movement in vitro
2. Characterise the effect of movement on biofilm formation to external fixation pins
3. Investigate the effect that bacteria often isolated from pin-site wounds in biofilm and planktonic form have on the rate of wound healing
4. Investigate the effect that movement of a fixation pin has on the wound healing properties of a human skin equivalent

2.5.5 Scope

The scope of this research was confined to understanding what effect relative movement between the pin and skin has on the pin-site produced by the use of external fracture fixation treatment. External fixators are most commonly used to treat fractures of superficial bones such as the tibia and the most common fixator currently in use today is the Ilizarov ring fixator which utilises 1.5 mm to 2 mm fixation pins. However, the relevance of the findings from this study will also extend too many other percutaneous devices which involve a skin-implant interface and are at risk of infection, such as dental implants, catheters, and limb prosthesis anchors.

2.5.6 Ethical considerations

For this PhD research project, ethical approval will not be required. The ethical considerations have previously been met by establishing standard operating procedures for the cell lines and bacterial cultures that will be used throughout the project. The remit and use of these cell lines and bacterial cultures will not change from work already carried out in the tissue laboratories. Human Tissue act training was conducted through the school of life and health sciences at Aston University in order to culture primary human epidermal cells at passage 2 and below

Chapter 3: Design and Development of a Machine to Replicate Pin Movement in Vitro

3.1 Introduction

Based upon anecdotal evidence presented throughout the literature it has been hypothesized that movement between the pin and skin in an external fixation pin-site wound is a major factor in determining whether pin-site infection will occur (Bibbo *et al*, 2010; Browner *et al*, 2014; Canale *et al*, 2012; Ferreira *et al*, 2012; Holmes *et al*, 2005; Kazmers *et al*, 2016; Santy *et al*, 2009), currently research to investigate this relationship on a more fundamental level is non-existent. Studies which have investigated the soft tissue interface of transcutaneous implants such as external fixation pins have often used animal models or clinical studies and have focused mainly on pin coating materials (Adams *et al*, 2009). Not only are these animal models often physiologically inaccurate, there are inherent difficulties in studying pin movement using an animal model, as controlling the animals movement would be very challenging and potentially unethical. Therefore in order to understand this relationship in more detail a 'pin machine' was developed, to be used in conjunction with human skin equivalent models and bacterial cultures, which replicates the mechanics of pin movement seen in vivo. This pin-site model will allow for the role of pin movement on external fixation pin-sites to be investigated as well as the impact movement has on the formation of biofilms and the quality of wound healing around the pin. In order for the pin machine to be physiologically relevant to in vivo external fracture fixation, several parameters must be controlled. Firstly the magnitude of displacement generated by the pin machine should be similar to the magnitudes of pin-skin movement seen across the pin-site in clinical settings, additionally the frequency which the movement is applied should fall within frequency with which the patient loads the fixator and finally the distance between the rigid pin fixture at the base of the machine and the surface of the human skin equivalent should match the soft tissue thickness between the bone and skin surface across the tibia. The following sections review the literature in these areas in order to determine suitable, physiologically relevant values for these parameters.

3.1.1 Magnitude of movement across the pin-site

In the previous chapter it was briefly discussed how the relative movement between the pin and skin is governed by the natural skin tension and its variation due to patient activity, and soft tissue artefacts (STA). In order to better understand the magnitude of STA experienced in the lower limb, a systematic review of the literature was conducted. For each study reviewed, the location of the markers, along with the measurement technique and type of activity performed by the subject were noted, as they were described by the author. From the systematic review *(table 3.1)* it is clear that the measured values of STA vary significantly between studies as a result of the variations in measurement technique and patient activity in each study. Since soft tissue artefact is a result of the disparity between translations on the skin surface in respect to the underlying skeletal structure, comparing STA measurements from the patients gait cycle to that of as step-up task is not possible as biomechanical properties, such as knee flexion angle, are significantly different between both tasks, resulting in a disparity between measured STA's. Similarly the measurement technique will have an effect upon the measured STA as the degree of accuracy in measurements obtained from fluoroscopy (Stagni *et al*, 2005) compared to a more basic set-up using a motion capture camera system with percutaneous skeletal markers will be significantly different. Therefore a definitive value for STA across the shank, applicable to all subjects, would be unachievable, as the magnitude of STA is dependent upon the physical characteristics of the subjects (Holden *et al*, 1997), the location of the markers (Schwartz *et al*, 2004) and the variety of tasks being performed (Fuller *et al*, 1997), meaning STA values are repeatable within the same subject, but not among multiple subjects. In spite of this we have used the data collect to define a range of displacement that the pin must move. The maximum measured value of STA was 10.9 mm while the minimum was 0.7 mm which gives average value between the studies of 5.9 mm ± 3.40 mm.

Table 3.1: Systematic review of studies investigating the soft tissue artefact across the shank

- Adapted from Peters et al. (Peters *et al*, 2010)

Location	Maximum Translations (mm)	Subject Activity	Measurement Technique	Reference
Tibia Diaphysis	2.7	Knee Flexion Angle 0-70°	X-ray radiography with Attachment System	(Südhoff *et al*, 2007)
Tibia	0.7 – 4	Gait Cycle	Intercortical bone pins on cadaver	(Gao *et al*, 2008)
Frontal border of tibia	8.3	Step-Up Task	Fluoroscopy with plate mounted markers	(Gao *et al*, 2008)
Frontal border of tibia	10.9	Step-Up Task	Fluoroscopy with strap mounted markers	(Garling *et al*, 2007)
Proximal tibia	7.1, 3.7 and 2.1 (X, Y, Z)	Natural Cadence walking	Percutaneous skeletal trackers	(Manal *et al*, 2003)
Shank	3.9, 4.7, 6.0 (X, Y, Z)	Sit to Stand	Fluoroscopy and Stereo-photogrammetry	(Stagni *et al*, 2005)
Shank	9.8, 10, 8.7 (X, Y, Z)	Hip Extension	Fluoroscopy and Stereo-photogrammetry	(Stagni *et al*, 2005)

3.1.2 Frequency of movement across the pin-site

The load bearing properties of an external fixator means patients are often able to walk on the fracture, applying their full weight to the fractured limb. This permits micro-motion across the fracture, which is known to stimulate osteogenesis (De Bastiani *et al*, 2012) and improve the rate of healing (Fragomen *et al*, 2007). The average duration of one gait cycle of of an adult male ranges from 0.98 to 1.07 seconds (Murray *et al*, 1964) resulting in a walking frequency of approximately 60 steps a minute or 1 Hz. Therefore the pin machine was designed to generate pin movement at a frequency 1 Hz similar to that of a human gait cycle, in order to simulate a patient walking on the fixator.

3.1.3 Thickness of soft tissue around fixation pins

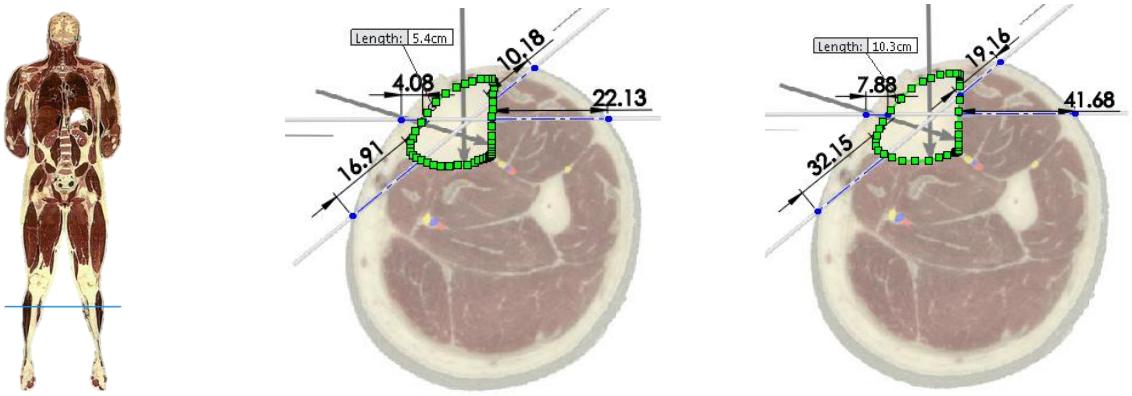

Figure 3.1: Measurements of soft tissue thickness around pins. Minimum (left) and maximum (right) tibia shaft circumerences adapted from Nayagam et al. (Nayagam, 2007)

In order to simulate the fixture of the pin inside the bone the pin will be rigidly fixed to the base of the pin machine and a displacement applied to the opposite end of the pin, causing the pin to experience cantilever bending. Although it has previously been identified that unilateral fixators experience cantilever bending while ring fixators are subjected to three point bending *(section 1.2),* the diameter of wire used in our machine is applicable to ring fixator wires. Consequently a simplified model of the ring fixator pin-site has been proposed by modelling half of the ring fixator pin, from the rigid bone fixture, through the soft tissue and cutaneous layers and out to the fixation frame. Therefore the distance between the rigid pin fixture at the base of the machine and the pin-skin interface should be relevant to the thickness of soft tissue between the bone and skin surface in humans. Since the tibia bone is not central to the calf, and fixator wires are not usually located in uniform positions in the leg, therefore the radius of the calf does not accurately represent the thickness of the soft tissue. A study conducted by Nayagam *et al*, used cross-sectional, anatomic images, obtained from the visual human project, to help describe to surgeons the ideal pin placement when fitting external fixators (Nayagam, 2007). Since these images are cross sections of a human male cadaver, the anatomy is scaled proportionally, and can therefore be used to make various approximate measurements regarding the

thickness of soft tissue around the pins. A separate study by Gupta *et al*, recorded anatomical measurements of dry tibia bones originating from a south Indian population and found the circumference of the tibia at its mid-shaft ranged from 5.40 mm to 10.30 mm (Gupta *et al*, 2015). By applying these measurements to the pin placement diagram, the diagrams can be accurately scaled and direct measurements can be taken from the diagrams to measure the thickness of soft tissue around the pins *(figure 3.1).* The thickness of soft tissue along the pin tracts varied from 4.08 mm to 41.68 mm with an average of 19.27 mm, therefore when designing the pin machine the distance between the skin equivalent and base of the pin machine should lie within this range in order to maintain physiological relevance of the model.

From this literature search we have identified a range of values for STA across the shank, the frequency of the human gait and anatomical soft tissue thicknesses across around the tibia, therefore the aim of this chapter is to utilise these measurements in order to design and develop a physiologically relevant pin-machine to apply mechanical loading to either an external fixation pin inserted into either a human skin equivalent model or bacterial suspension, to create an in vitro model in order to study the effect of pin movement on wound healing and infection in external fixation.

3.1.4 Aims and objectives

The aim of the work presented in this chapter was to describe the development an in vitro model which accurately represents the pin-site wound scenario in order to study the effect of various factors contributing towards pin-site infection, such as pin movement, pin-site care dressings and topical ointments. In order to achieve this aim there are several design objectives listed below which must be satisfied.

3.1.4.1 Design objectives

1. Develop a mechanical loading system which is physiologically relevant by generating a deflection across the skin surface in the range of 0.7 mm to 10.8 mm with a frequency of 1 Hz

2. Develop a well system which can maintain a sterile environment while supporting both skin equivalent models grown on trans-well inserts at an air-liquid interface, as well as bacterial suspensions

3.1.4.2 Design requirements

1. Suitable to fit in an incubator therefore must be compact, moisture resistant and temperature resilient

2. It should be possible to sterilise the entire machine before each experiment

3. Must hold enough media and have battery power to support air-liquid interface for 72 hours with the ability to easily aliquot samples from the media

4. Must be physiologically relevant – Generate pin deflections expected clinically, should be anatomically accurate

3.3 Design and development of a pin movement system

3.3.1 Design requirements

1. Generate deflections of the pin across the skin surface in the range of 0.7 mm to 10.8 mm
2. Apply a deflection to the skin at a frequency of 1 Hz
3. Fit in incubator and run for 72 hours uninterrupted in a 37 °C and 5% CO_2 environment
4. Must have significant driving force to bend pins

The initial pin machine concept adopted the use of an eccentric CAM system *(figure 3.2),* which was developed with an undergraduate student as part of his final year project *(Figure 3.3)*. The displacement of the pin was determined by the distance between the centre of the cam and the offset hole, therefore the magnitude of pin movement could be varied by changing CAM designs. The student designed the CAM system to use a 6 volt brushed DC geared motor with an output speed of 230 rpm (RS Components) which was then reduced to 1 Hz (60 RPM) by using the pulse width modulation capabilities of an Arduino microcontroller. However reducing the speed of the motor also reduced the torque and therefore a complex set of interchangeable gears and motors would be required in order to adjust the speed of the motor while maintaining significant torque. This led to a change in the design, which utilised a linear actuator (Actuonix, UK) to provide the displacement required via digital controls using a microcontroller (Arduino UNO, Arduino cc, USA).

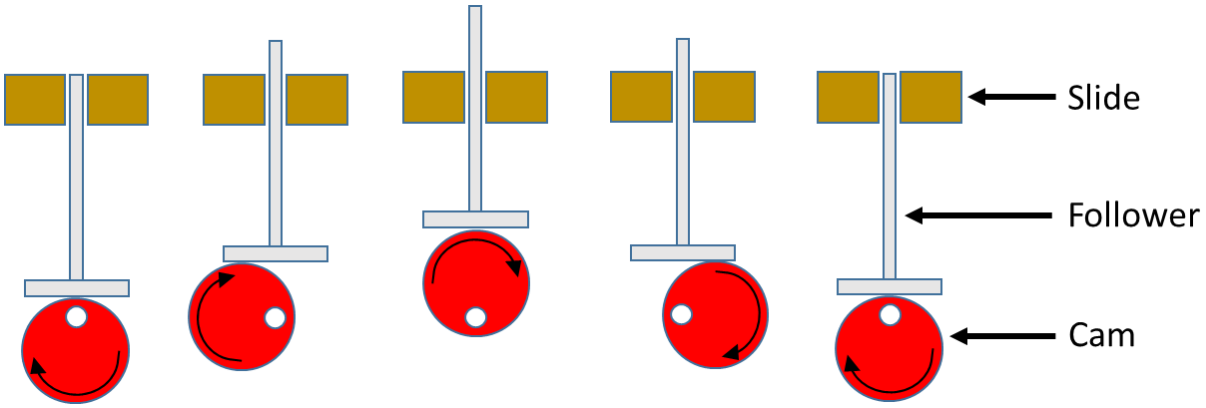

Figure 3.2: Diagram to illustrate the mechanics behind the eccentric cam. A cam is attached to a motor by a hole which is offset from the centre of the cam. As the motor rotates the cam is causes the follower to rise and fall along a sinusoidal wave, the magnitude of which is determined by the offset distance of the centre of rotation form the true centre of the cam. The rise and falling of the cam pushes the follower which is able to slide freely, thus converting rotation of the motor to a linear motion.

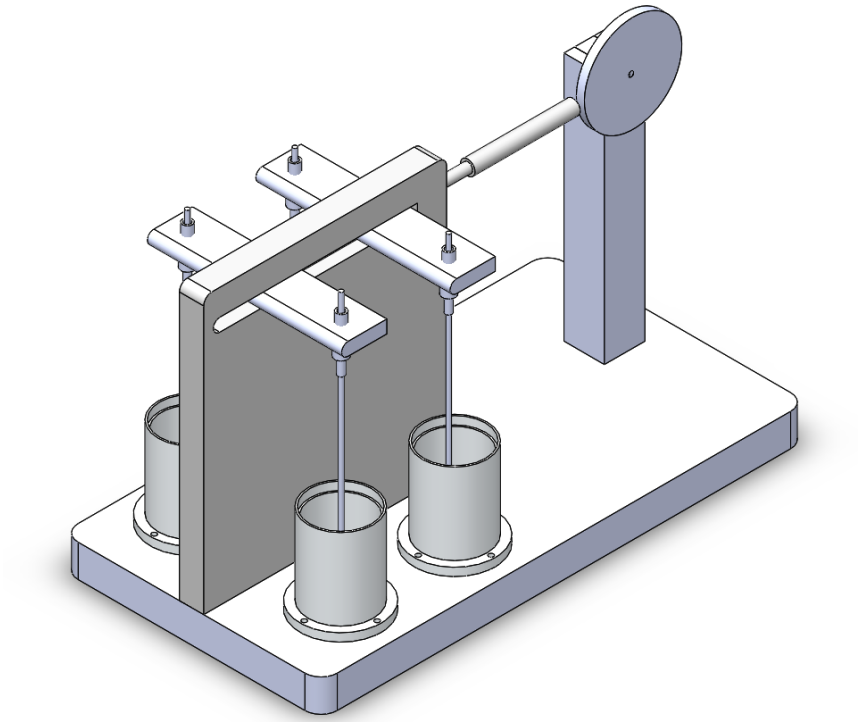

Figure 3.3: Design concept for pin machine proposed by undergraduate student. The four pin design using two arm bars was retained in the final design. However several changes were made in the final design to better satisfy the design requirements listed in *section 3.3.1*

3.3.2 Final pin machine design

The final pin design retained several characteristics of the final year student's prototype including the use of a shaft and two sliding arms to translate the linear movement to all 4 pins, however several distinct changes were made. Firstly the machine was made wider, and a second upright support was added to improve the stability of the machine and reduce any losses throughout the system. Second the shaft was redesigned to include ridges which better support the arm bars and a slide was added to the top of the upright supports to allow access to grub screws *(figure 3.5)*, which not only prevented slippage of the arm bars but also allowed for easy disassembly for cleaning and sterilisation. Finally oilite bearings were added at the interface between the upright supports and the arm shafts in order to reduce the friction between both components and therefore improve the sliding mechanism.

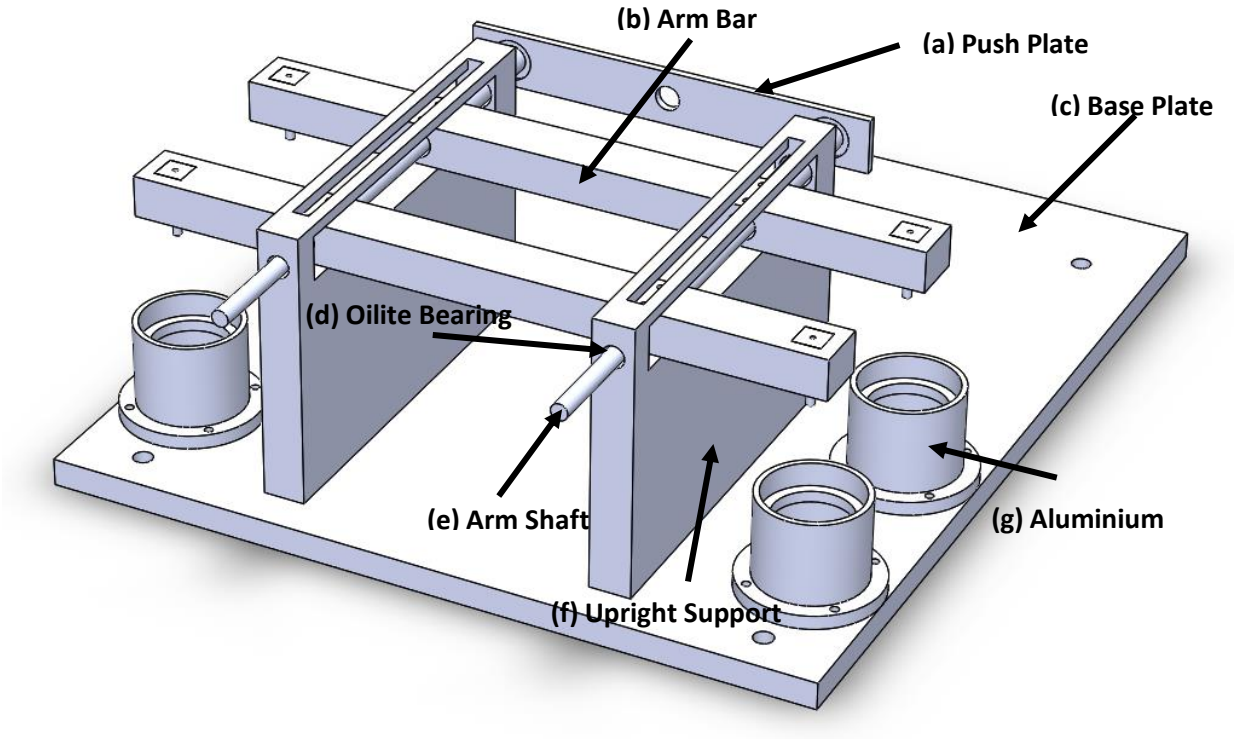

Figure 3.4: Drawing of final pin machine design with main components annotated.
(For working drawings see appendices *section 9.1*)

a. Push Plate – Connects to mechanisms providing linear displacement
b. Arm Bar – Distributes displacement to all four pins attached to either end of bars
c. Base Plate – Supports the attachment for all other components and bolts to incubator tray
d. Oilite Bearings – Self-lubricating bearings provide a smooth sliding motion
e. Arm Shafts - Change in diameter along the shaft helps to position arm bars correctly
f. Upright supports – Slot in top allows access to grub screws securing arm bars
g. Aluminium wells – Support the addition of transwell inserts

3.3.3 Key features

3.3.3.1 Sliding mechanism

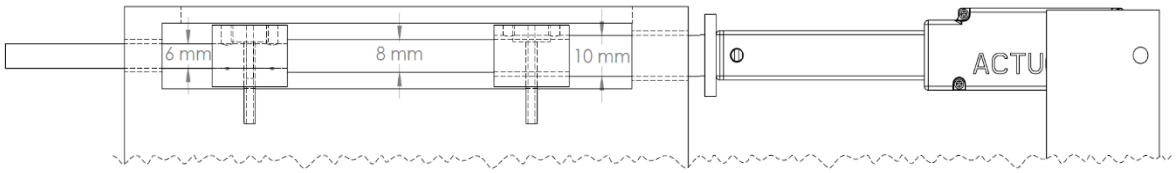

Figure 3.5: Close up of the pin arm and shaft mechanism. The shaft is machined to change in diameter from 6 mm to 8 mm and finally 10 mm. This creates a 2 mm lip which the Pin Bar can sit against and be fastening with grub screws to prevent the pin arm from sliding backwards during its operation. An Oilite bearing with internal diameter 6 mm was used at the front of the shaft and a 10 mm internal diameter iolite bearing was used at the back to allow the shaft to slide freely with minimal friction.

3.3.3.2 Human skin equivalent pin-site system

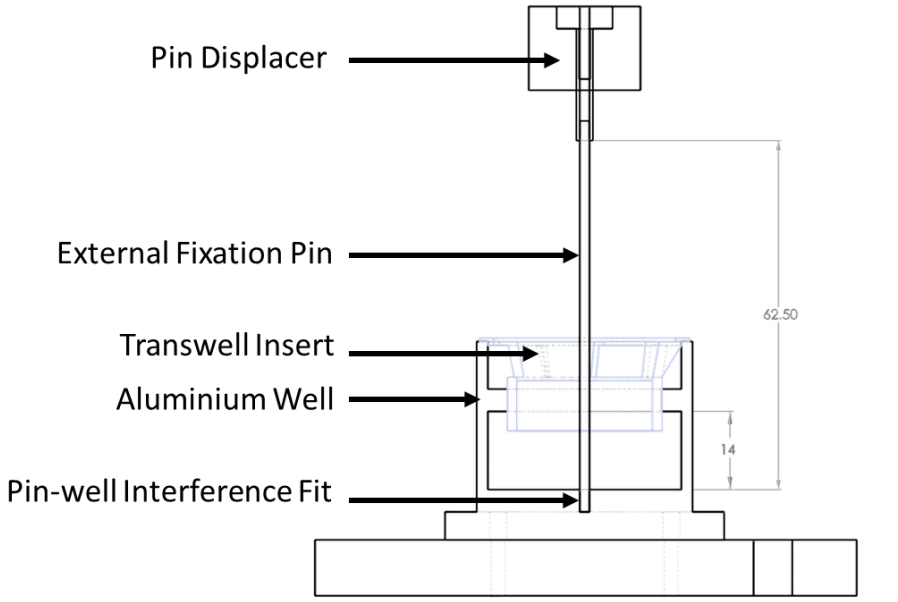

Figure 3.6: Diagram to illustrate how the pin machine and aluminium well fit together. Measurements of the pin length (62.50 mm) and distance from base to skin surface (14 mm) are shown

3.3.4 Linear actuator selection & set-up

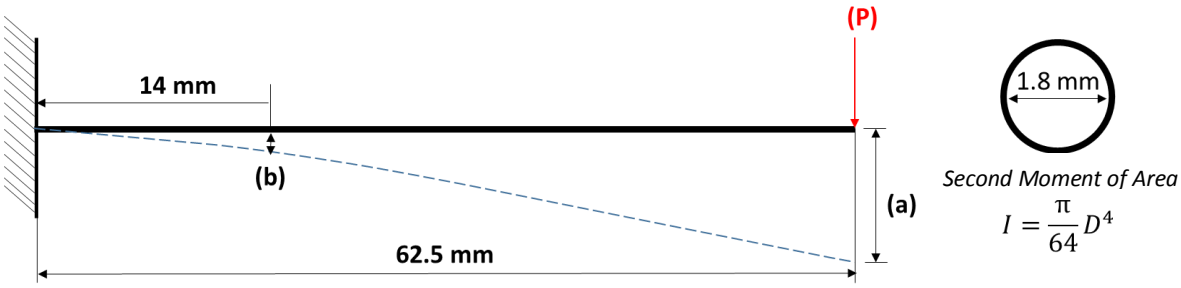

Figure 3.7: Cantilever bending diagram to illustrate how the pin machine will bend the pin. (P) is the force applied via the linear actuator to the end of the pin which has a total length of 62.5 mm. (a) is the deflection at the end of the pin as a result of the force applied by the linear actuator and (b) is the deflection at the surface of the skin at a distance of 14 mm from the base of the pin

3.3.4.1 Pin deflection calculations

Table 3.2: Mechanical Propteries for 316L - Fixation pins were purchased from OrthoFIx, USA for use in the pin movement studies. The pins were 1.8 mm in diameter fabricated from 316 L stainless steel.

Variable	Symbol	Value	Units
Diameter of Wire	D	1.8	mm
Second moment of area	I	0.515299735	mm^4
Young's Modulus	E	205	GPa
Density	ρ	8000	kg/m^3

In order to calculate the actual pin length required to achieve the desired deflection in the range of 0.7 mm to 10.7 mm across the skin interface, the pin is modelled as a a cantilever beam *(figure 3.7).* It was previously discussed that the distance from the base of the pin machine to the surface of the skin should represent the thickness of soft tissue between the skin and bone surface and therefore should be between 4.08 mm to 41.68 mm. For the aluminium well design described previously this distance was 14 mm, which fits within the desired range and close to the calculated average of 19.27 mm. The pin length of 62.5 mm was retained from the undergraduate students design. By calculating the moment of inertia of the 1.8 mm diameter fixation pins and using the mechanical properties of the pins described in *table 3.2* it was possible to calculate the maximum pin deflection as well as the pin deflection at the skin pin site *(table 3.3).* These results were then plotted onto a graph in order to

visualise the maximum pin deflection required by the linear actuator in order to generate a given deflection across the skin surface *(figure 3.8).*

Table 3.3: Calculated max deflection of pin and deflection across skin for a given force – Max deflection was calculated using $\delta_{max} = \frac{PL^3}{3EI}$ and deflection at the skin was calculated using $y = \frac{Px^2}{6EI}(3l - x)$ where x is distance between the skin interface and the rigid fixture at end of pin. (Calculated results are presented in graphical format in figure 3.9)

Force (N)	Max Deflection (mm)	Deflection at Skin (mm)
1	0.77	0.05368
5	3.85	0.268399
10	7.71	0.536798
20	15.42	1.073596
50	38.54	2.683989
100	77.08	5.367978

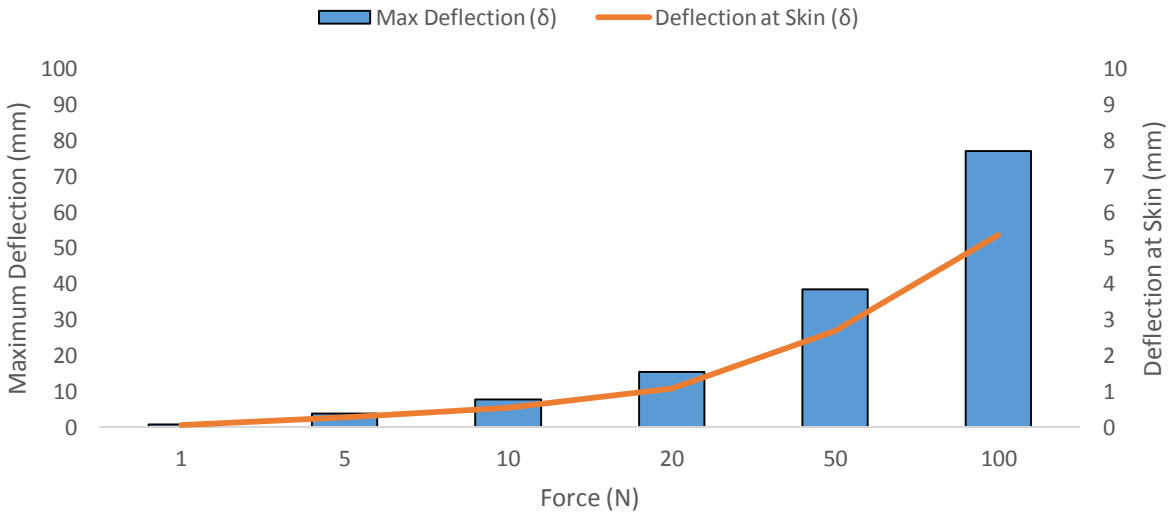

Figure 3.8: Graph illustrating deflection of pin and deflection across skin surface as a result of a given force. Primary y-axis shows maximum deflection of pin as a result of the force from linear actuator. Secondary axis shows the calculated deflection across the skin for a given force

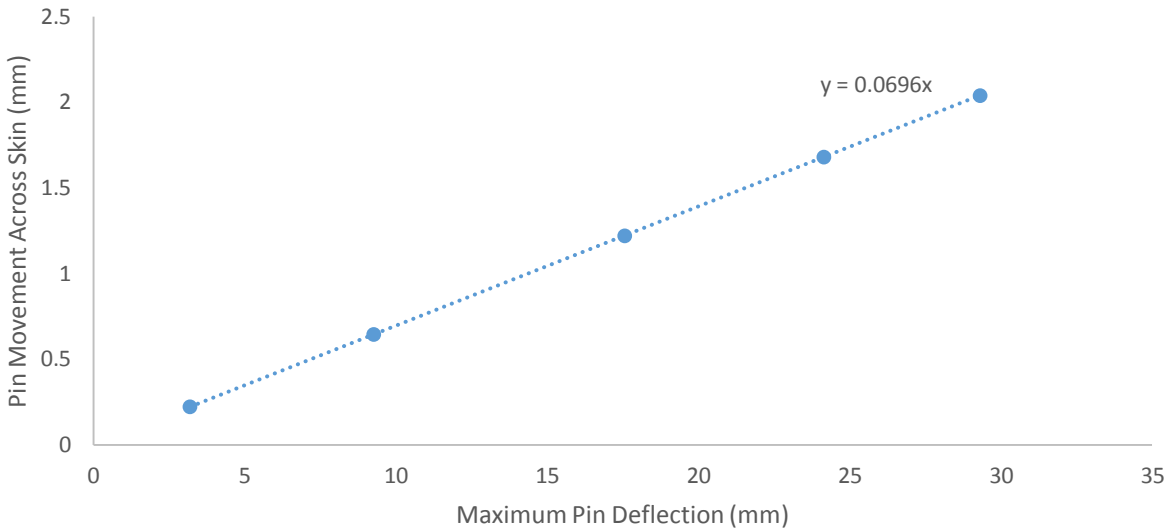

Figure 3.9: Pin movement at skin Interface against maximum deflection of pin. Equation of graph reads y = 0.0696x therefore pin movement at the skin interface can be calculated from maximum deflection by multiplying by 0.0696

3.3.4.2 Actuator selection

Table 3.4: Table showing max force and max speed for each gear ratio for the L16-R linear actuator - (table adapted from Actuonix.co.uk)

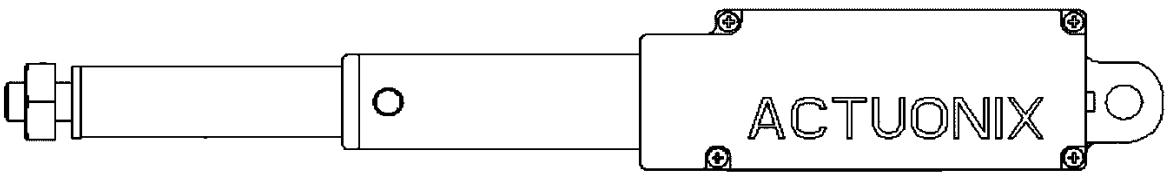

Figure 3.10: Diagram of Actonix© Linear Actuator

Gearing Options	**63:1**
Peak Power Point	75 N @ 10 mm/s
Peak Efficiency Point	38 N @ 15 mm/s
Max Speed (no load)	20 mm/s
Max Force (lifted)	100 N
Back Drive Force	46 N
Stroke Options	**100 mm**
Mass	74 g
Repeatability	0.4 mm
Operating Temperature	-10 °C to +50°C

In order to achieve a 15.42 mm deflection at the top of the pin, a 20 N force is required which results in a 1.07 mm deflection across the pin-skin interface, which is within the 0.7 mm – 10.7 mm range

obtained from the literature. If all four pins are attached to the pin machine, each pin will require 20 N to bend, therefore the required force exerted on the pins to generate 15.42 mm of deflection will be 80 N. Therefore the linear actuator with a 63:1 gearing ratio was selected for our application as it has the ability to generate forces within the required range while also having a velocity high enough to run at 1 Hz up to a maximum displacement of around 10 mm. All actuator models are capable of running at -10 °C to 50 °C therefore the incubator temperature of 37 °C should not have an effect upon the performance of the actuator *(table 3.4).*

3.3.5 Linear actuator set-up and optimisation

The linear actuator is operated by an Arduino microcontroller (Arduino UNO, Arduino cc, USA), which can be programmed (C++ coding) to allow for adjustment of stroke length and add time delays. The circuit diagram and coding for the microcontroller has been illustrated in figure 3.11.

3.3.5.1 Microcontroller circuit and code

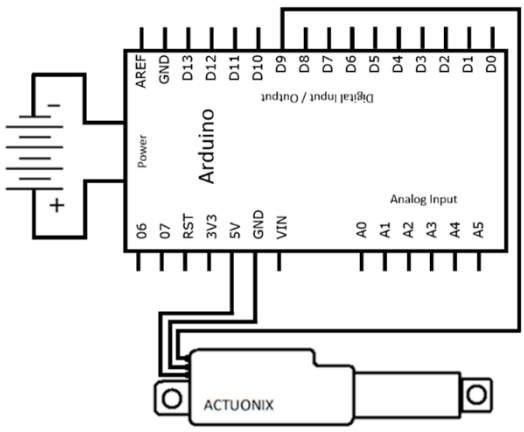


```
#include <Servo.h>

Servo myservo;


int pos = 0;                              // Variable to store the servo position
int a=10;                                 // Duration of outward stroke
int b=10;                                 // Duration of inward Stroke

void setup() {
  myservo.attach(9);                      // Actuator is connected at Digital Input 9
}

void loop() {
  for (pos = 180; pos <= 0; pos += 1) {   // Position from 0 degrees to 180 degrees
    // in steps of 1 degree
    myservo.write(pos);                   // tell servo to go to position in variable
    delay(a);                             // Delay until stroke direction change
  }
  for (pos = 180; pos >= 0; pos -= 1) {
    myservo.write(pos);
    delay(b);                             // Delay until loop is repeated
  }
}
```

Figure 3.11: Schematic diagram of microcontroller wiring and coding.

(Left) Circuit consisting of the linear actuator connects to digital input/output port. Arduino is connected to a 5 volt external power study

(Right) The code is designed so that it always performs at maximum stroke speed. In order to adjust the distance that the actuator arm travels, the delays times are adjusted. For example is the delay time is 10 milliseconds, the actuator will extend its arm at full speed for 10 milliseconds at which point it will change direction and begin the inward stroke. Therefore, by increasing the delay time, the distance the arm travels will increase, likewise if the delay is decreased the distance will decrease

3.3.5.2 Validation of pin machine movement

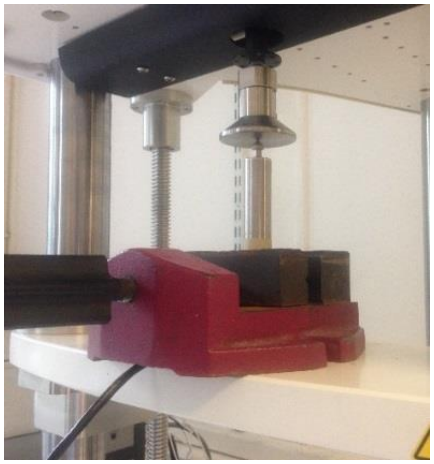

Figure 3.12: Image of linear actuator set-up in Electroforce machine for calibration

In order to determine whether the linear actuator is performing at the desired magnitude and frequency a validation study was conducted. A linear voltage differential transducer (LVDT) was used to validate the pin movement. Since the LVDT records the change in voltage produced when its piston is depressed, a calibration process had be to undertaken to identify the scale factor required to translate the measurements from voltage to displacement. An ElectroForce Universal testing machine (ElectroForce 3230, TA Instruments, Delaware, USA), which is known to have very high accuracy and precision, was used to apply a known displacement to the LVDT so that the voltage for that displacement could be recorded *(Figure 3.12).* The displacement was tested at 0.2 mm increments from 0 – 5 mm with each increment being held for a duration of 5 seconds and using a sampling rate of 10 Hz.

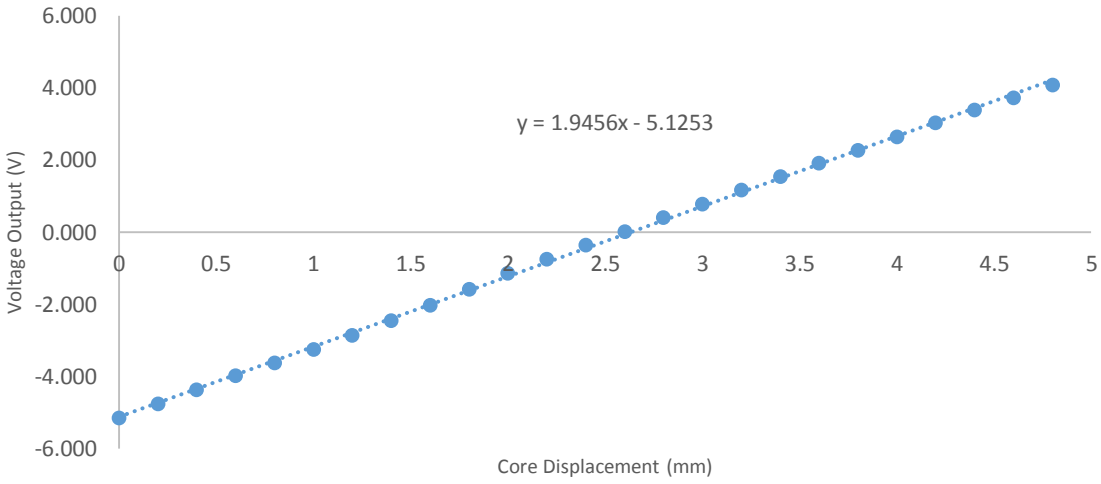

Figure 3.13: Plot of core displacement against LVDT voltage output with gradient labelled. Equation of the linear trend line can be used to translate between voltage and displacement in millimetres

The voltage output for each increment was plotted against the core displacement *(figure 3.13).* The scale factor was derived using a linear line of best fit showing the relation to be y = 1.9456x – 5.1253. This conversion relationship was used in Labview to collect LVDT displacement data of the pin machine actuator motion.

3.3.5.3 Validation results

The linear actuator works at a maximum speed of 20 mm/s, therefore if the stroke length is increased, the frequency that the actuator moves is decreased as it takes longer for the actuator to perform one cycle with a 10 mm stroke length compared to one cycle of a 1 mm stroke length. In order to control the stroke lengths of the actuator the time duration of the outstroke and instroke was adjusted. A graph was then plotted from the frequency and magnitude of pin movement for a number of time delays from 2 – 20 ms. By measuring the amplitude and frequency of various delay times and plotting them on a graph of amplitude against frequency we can determine the required time delay to achieve the desired pin defection of 15 mm which would result in a pin movement at the skin interface of around 1 mm at a frequency of 1 Hz *(figure 3.14).* Additionally a plot of code delay time against maximum deflection was plotted *(figure 3.15)* to order to determine the time delay required to achieve a desired magnitude of pin deflection.

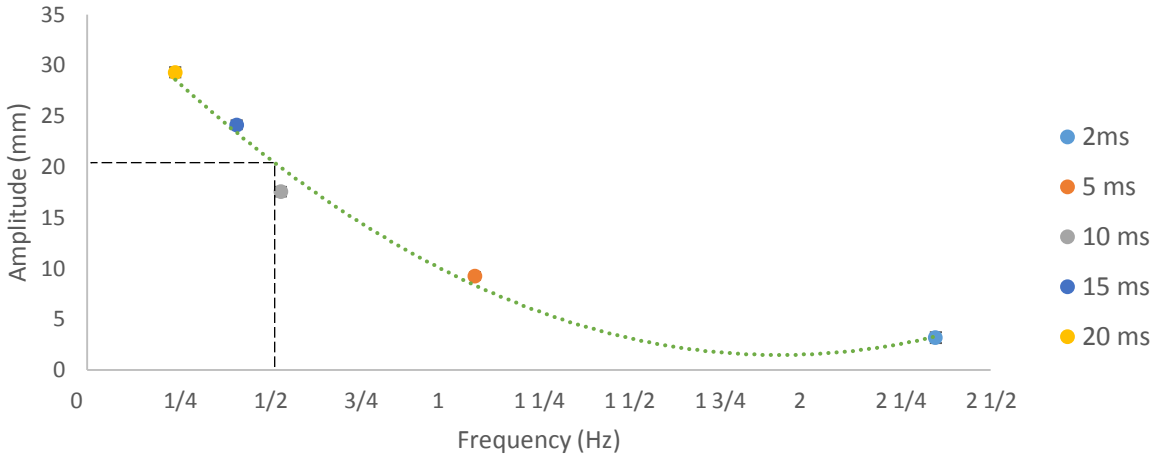

Figure 3.14: Graph of stroke freuqency of linear actuator against pin deflection for a range of time delays from 2 – 20 ms

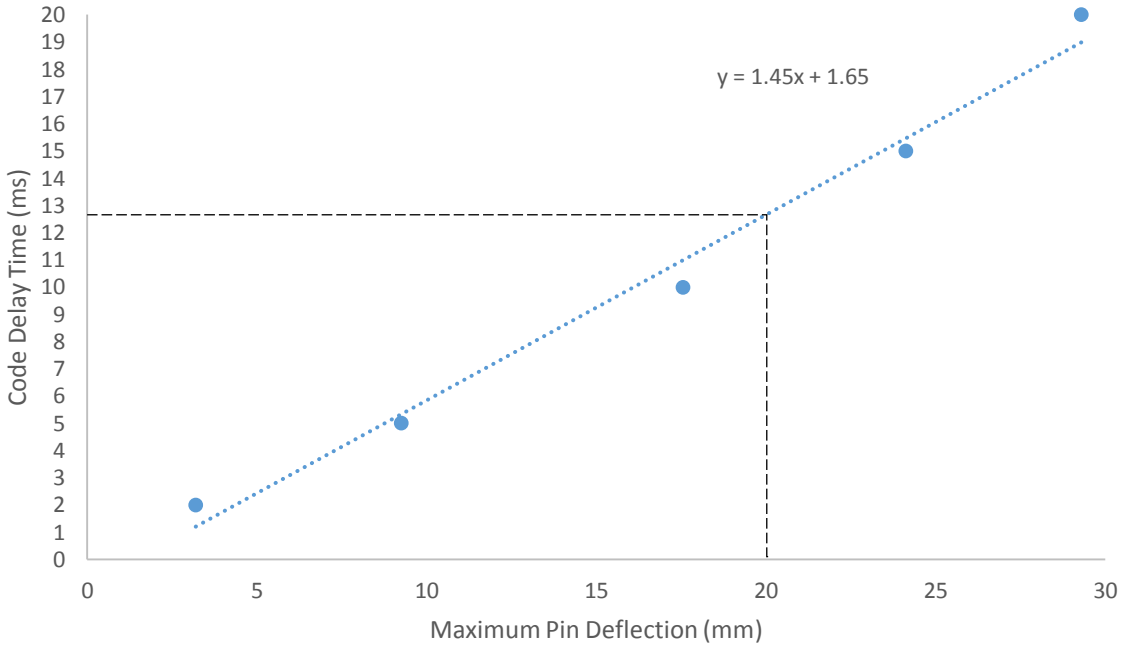

Figure 3.15 Graph code time delay against maximum pin deflection. At as frequency of 1 Hz the maximum pin deflection is between 15 – 20 mm, therefore a code delay time of 13 ms was required for a pin deflection of 20mm at a frequency of 1 Hz

3.4 Design and development of an aluminium well to support a transwell insert

For the well component of the pin machine there are several design requirements which must be met. For each requirement 3 possible design concepts have been proposed which have then been analysed using a decision matrix in order to select the most suitable design which best solves the design requirements. Each design was also scored on its ease of use, manufacture cost and manufacture complexity in order to minimise the time and cost of producing the pin machine, therefore making the pin-machine more accessible to other labs with minimal fabrication facilities.

3.4.1 Design requirements

1. Must represent underlying soft tissue thickness - Base to skin surface should 19.27 mm ± 5 mm
2. Must support a 6-well transwell insert securely with no movement while still allowing the transwell insert to be removed for sampling
3. External fixation pin should be mounted rigidly to the base of the well to represent the pin-bone interface and generate pin bending
4. Must mount directly to the base of the pin machine while being able to remove for cleaning and sterilisation

3.4.2 Design concepts

For each design requirements of the aluminium well several design concepts were developed (figure 3.16 – 3.19) which were later systematically compared in order to select the most suitable design for the pin machine.

3.4.2.1 Anatomically relevant membrane-to-base height

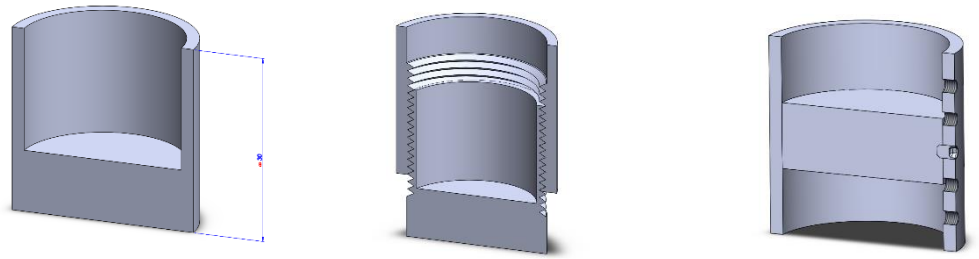

Figure 3.16: Fixed head device (a) two part screw height adjustment (b) Multi-level grub screw height adjustment (c)

3.4.2.2 Clamp insert securely

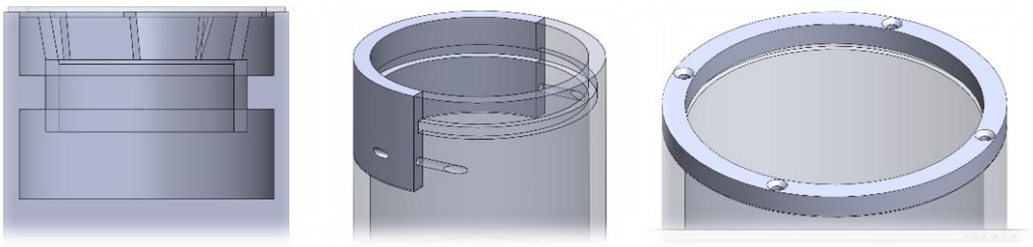

Figure 3.17: Tight fit around transwell (a) removable side piece (b) screw tightened ring (c)

3.4.2.3 Rigid fixture of pin to base

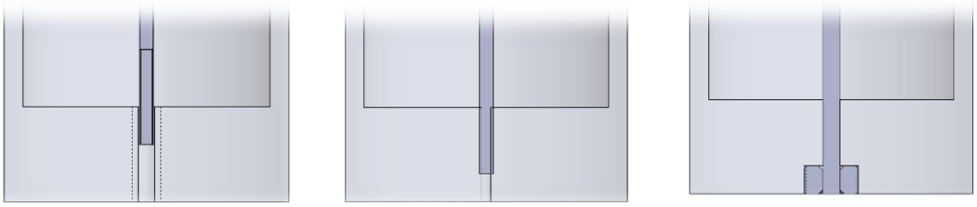

Figure 3.18: Tapped and threaded pin (a) interference fit pin (b) bolted pin with nut (c)

3.4.2.4 Fixture to Base Plate

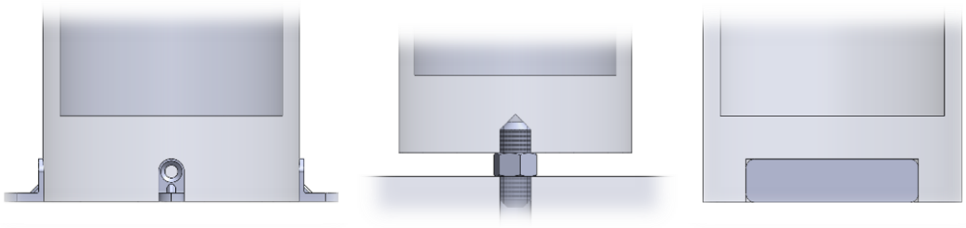

Figure 3.19: Single bolt threaded to base (a) magnet of bottom of well (b) lip with screw holes around base (c)

3.4.3 Decision matrix

In order to systematically compare each design concept by their ability to satisfy the design requirements a decision matrix was used. Each design was compared by how well they satisfy the design requirement, the ease of use and the complexity and cost of manufacture, these criteria were given a weighting of 1-5 with a higher weighting indicating a more important criteria. Similarly each design was then given a rating of 1 – 5, 1 being low and 5 being high satisfaction for each criteria. The individual ratings multiplied by the weighting of each criteria then gives a numerical value for how well the design meets the requirements with the lower values being the most suitable design.

Table 3.4: Decision matrix to evaluate the ability of each aluminium well design concept to satisfy the design requirements

		Satisfy requirement		**Ease of use**		**Complexity of manufacture**		**Cost of manufacture**		
	Weighting	5		4		3		2		
Design Requirement	**Design Concept**	**Score**	**Total**	**Score**	**Total**	**Score**	**Total**	**Score**	**Total**	**Sum**
Pin-bone to pin-skin distance	Fixed height device	3	15	5	20	4	12	4	8	63
	Two part screw adjustment	5	25	3	12	1	3	1	2	50
	Grub screw height adjustment	4	20	2	8	2	6	2	4	44
Mount transwell insert securely	Tight fit around transwell	4	20	5	20	5	15	5	10	84
	Removable side piece	4	20	3	12	2	6	2	4	53
	Screw tightened ring	4	20	3	12	3	9	2	4	57
Rigid fixture of pin to base	Tapped and threaded pin	5	25	2	8	2	6	3	6	57
	Interference fit pin	4	20	5	20	5	15	5	10	84
	Bolted pin with nut	5	25	2	8	3	9	3	6	61
Mount of well to base of machine	Single bolt threaded to base plate	4	20	4	16	3	9	3	6	65
	Magnet on bottom of well	3	15	5	20	4	12	2	4	65
	Lip with screw hole around base	5	25	3	12	3	9	5	10	72

3.4.4 Final design

The outcome of the decision matrix was used to develop the final design of the aluminium well. In order to maintain a sterile environment for the skin model or bacterial culture during experimentation, Opsite (Smith & Nephew) was placed over the opening of the well. Additionally a pneumatic valve and stopcock was added in order to allow for sampling of the media contained within the well without disruption to the culture, which could introduce contaminates.

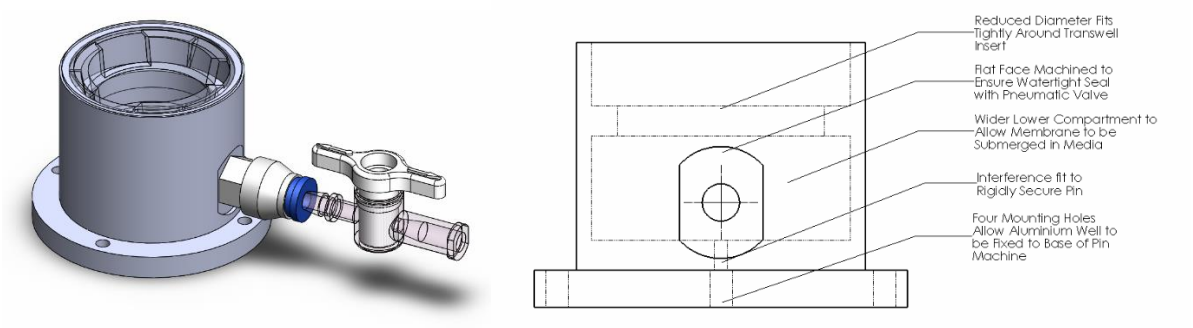

Figure 3.20: Description of key features of aluminium well design (working drawings can be found in the Appendices *section 9.1*)

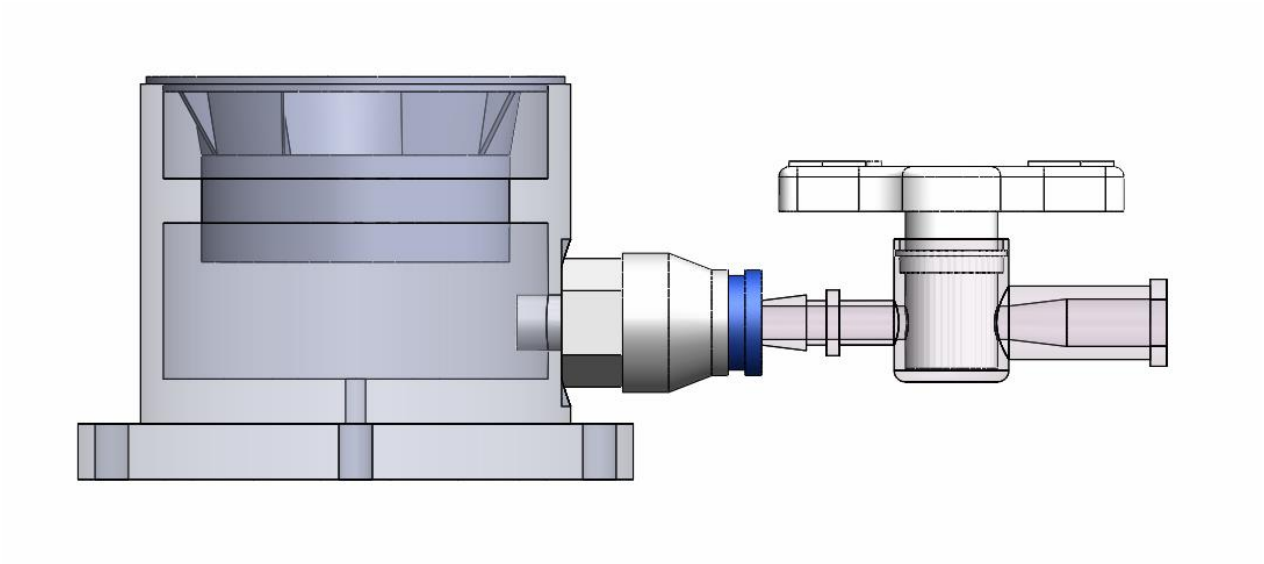

Figure 3.21: Image of tray design with trans-well plate fitted

3.5 Discussion

The aim of the current chapter was to develop a physiologically relevant in vitro pin machine to replicate relative pin movement between the pin and skin as seen in vivo. This was achieved by designing the machine to meet several anatomical criteria, such as the soft tissue thickness between the bone and skin interfaces as well as generating movements in the frequency range of the human gait cycle and magnitudes that lie within measured STA values across the shank. The machine was then validated by measuring the pin displacement and frequency using a calibrated LVDT and comparing the measured values to those calculated.

The previous chapter highlighted the fact that pin-site infection has a converse relationship with wound healing, such that a slow healing pin-site has a greater risk of infection and vice versa. Therefore the pin machine was designed to study not only wound healing, by having the ability to incorporate a skin sample such as a human skin equivalent grown on a transwell membrane, but also the ability to be used as a culture vessel for bacterial suspensions in order to investigate the effect of pin movement on bacterial attachment to fixation pins.

Existing research into pin-site infection has often utilises animal models, however intrinsic differences in the skin physiology and wound healing response of these animals means any findings from these studies may not be applicable to human pin-site infection. Additionally clinical research into pin-site infection is often difficult to interpret as variations in pin-site care and patient physiology make it difficult to determine the efficacy of an individual treatment. The pin machine described in this chapter offers a novel in-vitro model to study pin-site infection. By minimising the number of variables in system the effect of pin movement on bacterial colonisation and soft tissue wound healing as well as the ability of various treatments in preventing pin-site infection can be carefully assessed.

Chapter 4: The Effect of Movement on the Formation of *Staphylocci epidermidis* Biofilm to External Fixation Pins

4.0 Introduction

Pin-site infection is a common complication in external fracture fixation treatment, with infection rates reported in the literature ranging from 4.5% to 100% (Antoci *et al*, 2008; DeJong *et al*, 2001; Garfin *et al*, 1986; Mahan *et al*, 1991; Parameswaran *et al*, 2003). One explanation for these high infection rates is that implant surfaces, such as fixation pins, are highly susceptible to colonisation by bacteria, as their surfaces provide an ideal environment for bacterial attachment and subsequent biofilm formation. Once contained within a biofilm, resistance to the host immune response or antibiotic treatment is significantly increased, resulting in additional healthcare costs, complications linked to antimicrobial resistance (AMR) and decreased patient wellbeing. The ability of these bacteria to form multi-layered biofilm containing a matrix of extracellular polymeric substances (An *et al*, 2000), increases their resistance to antibiotics by as much as 5000 times the concentrations required to kill free floating planktonic bacteria of the same species (Khoury *et al*, 1992) making treatment of these infections a major challenge for clinicians. Due to the emergence of antibiotic resistant bacteria as a result of the over prescription of antibiotics (Llor *et al*, 2014), treating these infections with antibiotics is unsustainable. Instead, more attention should be given to researching methods of infection prevention, so that our dependency on antibiotics is reduced.

Another factor that has been mentioned anecdotally throughout the literature, is that excessive movement between the pin and skin across the pin site, correlates to an increase in the rates of pin-site infection (Bibbo *et al*, 2010; Browner *et al*, 2014; Canale *et al*, 2012; Ferreira *et al*, 2012; Holmes *et al*, 2005; Kazmers *et al*, 2016; Santy *et al*, 2009), however this has not been thoroughly investigated on a fundamental level. Patient activity generates mechanical movement of the pins via the fixation frame, as well as changes in tension across the skin and volumetric changes of the limb as the muscles contract and relax. It is likely that this relative movement generates shear forces between the bacteria and pin surface. Several studies have been conducted investigating the effect of shear stress on bacterial adhesion and biofilm formation which has led many researchers to identify that the biofilm

formation is strongly influenced by hydrodynamic forces such as shear wall stress (Fonseca *et al*, 2007; Liu *et al*, 2002; Park *et al*, 2011). A low wall shear stress may limit the forces on the bacteria which may cause detachment, therefore promoting bacterial adhesion. While a high wall stress stress is likely to overwhelm the attachment forces of the bacteria and therefore prevent long-lasting bacteria adhesion. However a high wall shear stress increases the mixing efficiency and convective transport of the bacteria which may actually promote microbial adhesion, as it increases the access of bacteria to the colonising surface (Saur *et al*, 2017). For example, *Pseudomonas aeruginosa* has been shown to create more long lasting adhesion events to surfaces under shear stress, even though their probability of sticking is reduced. Additionally, bacteria attaching under identical flow conditions are more likely to detach when shear is suddenly decreased, which shows that individual cells dynamically respond to shear rate variations, modifying their adhesion state (Lecuyer *et al*, 2011). Although microfluidic chambers appear to be the optimal method for studying bacterial adhesion under shear, due to their ability to control flow rate precisely, these devices are not designed to incorporate a second substrate such as an external fixation pin for bacterial to adhere to, therefore the Fonseca *et al* method of utilising an orbital shaker to generate hydrodynamic forces was adopted and modified for our study (Fonseca *et al*, 2007).

Colony forming unit (CFU) plate counts are the most common method for quantifying the number of bacteria in a sample, however the bacteria must first be dislodged from the surface of the pins and suspended in a buffer solution in order to perform a CFU count. There are many protocols described in the literature regarding the removal and measurement of adherent bacteria with various degrees of accuracy, such as glass-bead vortexing, shockwave treatment, electric-current and chemical-treatment, although sonication and vortexing has been shown to increase the number of bacteria isolated from retrieved joint implants whilst limiting damage to the bacteria compared to other methods (Nguyen *et al*, 2002; Andrej Trampuz *et al*, 2007; Tunney *et al*, 1998). Trampuz *et al*, reported that sample cultures obtained by the sonication of explanted hip and knee prostheses was approximately 18 % more sensitive than conventional culture of excising periprosthetic tissue among

patients undergoing hip or knee revision or resection arthroplasty (Andrej Trampuz *et al*, 2007). However the duration of sonication times required to dislodge all high-adherent bacteria reported in the literature ranged from as little as 1 minute to up to 30 minutes (Goldman *et al*, 1996; A. Trampuz *et al*, 2007; van de Belt *et al*, 2001) despite the fact that long durations of sonication have been used to induce cell disintegration by disrupting the cell membrane, leading to a decrease in bacterial viability (Kobayashi *et al*, 2007). Moreover, bacteria may be present on the surface of the pin but not highly adherent to the surface and not contained within the biofilm, therefore these bacteria must be removed before sonication to ensure that only measurements of highly adherent bacteria are made. A validation study is needed in order develop a method of washing low adherent bacteria from the surface of the pins and to determine the frequency and duration of the ultrasonic treatment required to be high enough so that all bacteria are detached from the pin surface, but also low enough not to cause noticeable damage to the bacteria.

4.1 Aims and hypothesis

The primary aim of this chapter was to investigate the role of movement on the attachment of bacteria to the surface of fixation pins. Movement was applied passively through shaking of the bacterial culture during incubation and directly by applying movement to the pin submerged in a static bacterial culture, in order to generate shear forces between the bacteria and pin surface. To achieve this a secondary aim to develop and validate a method for the removal and measurement of both high and low adherent bacteria attached to the surface of the pin was proposed.

The hypothesis for this study were as follows:

1 The rate of bacterial attachment to the surface of fixation pin samples will increase with increasing shaking frequency during incubation

2 The rate of bacterial attachment to the surface of fixation pin samples will increase with increasing magnitude of pin movement applied directly to the pin sample via the ‘pin machine’

4.2 Methods

4.2.1 Microorganisms

The biofilm-forming *Staphylococcus epidermidis* RP62A (*S. epidermidis*) was used throughout this study to investigate the mode of biofilm formation on external fixation pins. The bacteria was stored on MicroBank beads (Pro-lab Diagnostics, Neston, UK) at -80 °C prior to the study. When required, the isolates were revived and cultured onto CM0003 nutrient agar (Oxoid Ltd, UK) and then incubated at 37 °C and 5% CO_2 for 24 hours before being transferred to storage at 4 °C. In order to reduce the risk of contamination and maintain cell viability, co-cultures of the bacteria were made on a weekly basis. For each co-culture a streak plate was made in order to isolate individual colonies, so that homogenous starter cultures could be produced.

4.2.2 External fixation pin samples

Surgical-grade external fracture fixation pins, manufactured from 316L stainless steel with a diameter of 1.8 mm was purchased from Orthofix UK (Orthofix Ltd, HQ city, Country). The pins were cut using a circular saw into samples of length 25 mm ± 0.1 mm for the shaking frequency studies and 100 mm ± 1 mm for the pin machine studies, the small tolerance required of the 25 mm pin samples ensured that there was a maximum variance in total surface area between the pins of ≤ 0.75 %. Since the ends of the pins are generally not exposed to bacteria in a clinical setting, it was important that the properties of the pin ends did not significantly affect the results of the study. This meant ensuring the surface roughness of the pin ends was equal or less than that of the main body of the pin, to ensure large amounts of bacteria did not adhere to the pin ends. To achieve this, the pin ends were polished following the cutting process, using silicon carbide polishing wheels with increasing coarseness ranging from 180 up to 1200 grit *(figure 4.1).* The pins were then viewed under a microscope at 100 x magnification so that the topography of the main body could be compared to that of the pin ends. Qualitative microscopic analysis allowed us to visually compare scratches on the main body to those on the pin ends. Quantitate measurements using a surface profilometer (Talysurf 4, Taylor Hobson)

found the average roughness (R_a) values of the main body of the pin samples to be 0.15 µm ± 0.03 *(table 4.1)* ensuring good precision among samples, however the limitations of the equipment meant we were unable to measure the surface roughness of the pin ends. Prior to their use in the bacterial attachment studies, the pins were autoclaved using high-pressure saturated steam at 121 °C for 1 hour.

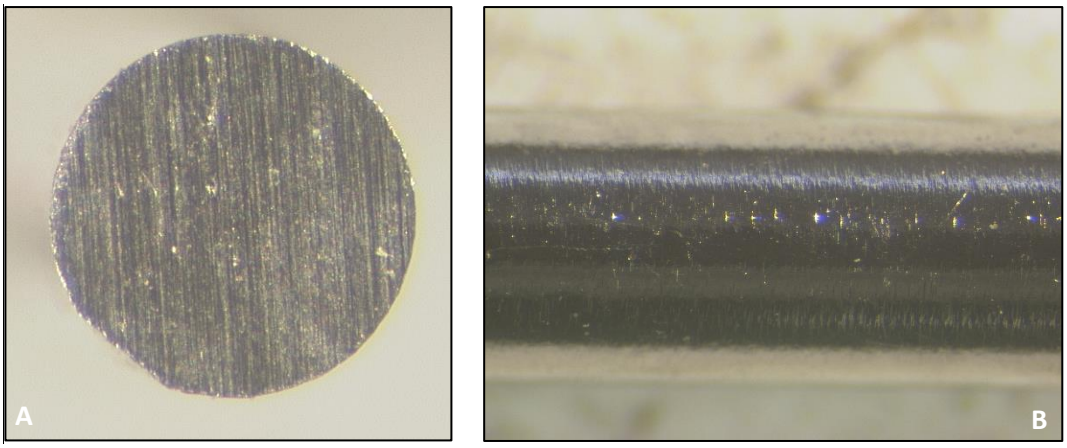

Figure 4.1: Quantification of pin surface roughness. Images of Pin end (A) and Pin Main Body (B) under Optical Microscope at 10x magnification

Table 4.1: Surface roughness results for pin main body

	Arithmetical Mean Deviation (Ra) (µm)	RMS (R_q) (µm)	Max Peak Height (R_p) (µm)	Max Valley Depth (R_v) (µm)	Mean Peak to Peak (R_{tm}) (µm)
Pin 1	0.12	0.15	0.57	0.77	0.78
Pin 2	0.15	0.19	0.41	0.73	0.9
Pin 3	0.17	0.21	0.48	0.94	1.09
Average	0.15	0.18	0.49	0.81	0.92
Standard Deviation	0.025	0.031	0.080	0.112	0.156

4.2.3 Pin mount device

A pin mount device was fabricated in order to fix the pin upright in the universal tube so that it resisted the fluid motion of the bacterial culture during shaking thereby increasing the shear forces generated between the bacteria and pin surface. There were two key design objectives for the pin mount, the first was to achieve a clearance fit inside a 25 mL centrifuge tube so that the mounts could be removed to be cleaned and re-sterilised. The second objective was to achieve a clearance fit around the centre

pin hole, so the pin could be easily removed to study bacterial attachment. After optimising the design a total of 12 pin mounts were machined from aluminium using a CNC lathe.

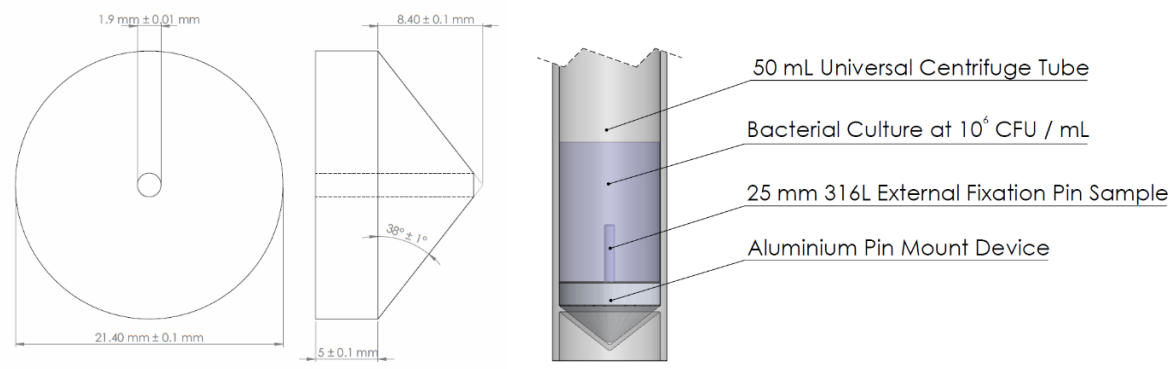

Figure 4.2: Technical drawing of pin mount device – Drawing of mount device (left) along with a diagram Illustrating how the pin mount device fits into the universal centrifuge tube so that the pin can be surported virtucally upright

4.2.4 Starter cultures

In order to prepare starter cultures for each study, 10 mL of nutrient broth (Oxoid Ltd) was inoculated with 1 single colony of *Staphylococcus epidermidis*. This inoculum was incubated for 6 – 12 hours at 37 °C with 5% CO_2 at 180 revolutions per minute (RPM). Following this incubation period the optical density was measured and compared to the standard growth curve *(figure 4.6)* in order to determine the concentration of viable bacteria in each culture and to ensure the culture is in the logarithmic phase of its growth. Once the bacterial suspension had reached the logarithmic phase, the cultures were diluted using nutrient broth to achieve a final working concentration of 10^6 CFU / mL.

4.2.4.1 Biofilm formation

The time allowed for biofilm formation varies considerably throughout the literature with many studies incubating samples anywhere from a few hours up to 46 hours. However, most researchers opt for an incubation period of around 24 hours (Christensen *et al*, 1987; Olson *et al*, 1988; Tollefson *et al*, 1987; van der Borden *et al*, 2004). Therefore, in order to grow biofilm onto the surface of the pin samples, the pins were added to the diluted starter cultures which were then incubated for a further 24 hours.

Scanning electron microscopy was performed on the pin samples to confirm the formation of biofilm *(section 4.3.6).*

4.2.4.2 Standard growth curve

Performing a growth curve study was needed to identify the duration of incubation required until the bacteria begins to enter the log and stationary phases of their growth whereby the growth of bacteria is optimal and less susceptible to contamination. A correlation curve was carried out between optical density and colony forming units per millimetre (CFU / mL) to determine the bacterial concentration of a culture. The growth curve study was performed by inoculating 1 colony of *Staphylococcus epidermidis* into 10 ml of nutrient broth. At each time point (0, 1, 2, 3, 4, 5, 6, 7, 8, 24, 48 and 72 hours) the optical density of the inoculum was measured using a spectrophotometer set to 600 nm which had been calibrated using a broth blank. For each time point the CFU / mL of the cell suspension was measured by performing a range of serial dilutions from 10^1 to 10^6 and inoculating an aliquot of these dilutions onto nutrient agar (Oxoid Ltd, UK) after which the plates were incubated at 37 °C and 5% CO_2 for 24 hours. Once visible colonies had formed on agar, the number of colonies were counted and the number of CFU per mL of bacterial suspension was calculated. To account for human and rounding errors any CFU plates with less than 25 or greater than 250 colonies were disregarded for all studies. *Figure 4.6* shows the fluctuation of bacterial viability in CFU / mL of *Staphylococcus epidermidis* over 72 hours. From the distribution of the curve it is easy to identify each stage of the growth cycle. For the first 3 – 4 hours of incubation following inoculation the bacteria remains in the lag phase, from 4 - 5 hours the bacteria is in the log phase where bacterial growth is exponential, the bacteria then enters the stationary phase between 10 - 24 hours whereby there is no longer enough nutrients to sustaining proliferation, and finally after 24 hours the death phase occurs as nutrients are too depleted to sustain existing bacteria. *Figure 4.7* shows a plot of optical density against CFU / mL over a 24 hour period. From these data points a linear trend line can be plotted, the equation of which can be used to convert between optical density measurements and CFU / mL. It was found that by multiplying the optical

density of a sample by 5 x 10^7 a close approximate to the number of CFU contained within 1 mL of the sample could be calculated.

4.2.5 Optimising high and low adherent bacteria removal

4.2.5.1 Removing low-adherent bacteria

After incubation of the pin samples in the bacterial culture, bacteria are present of the surface of the pins which are not strongly adhered to the pin and therefore not contained within the biofilm, but instead reside in water droplets on the surface of the sample and therefore must be removed so that only highly adherent bacteria contained within the biofilm could be measured. This was done by performing a number of rinses of the pin in sterile phosphate buffered saline (PBS) (Oxoid Ltd, UK). A validation study was performed in order to determine the number of rinses required to effectively remove all of the low-adherent bacteria. Each rinse step involved using sterile forceps to dunk the pin a total of 5 times into a universal containing 10 mL of PBS, the sample was then transferred to another universal of PBS and the sample was dunked again 5 times, this was repeated with ten universals for a total of ten rinses. After all 10 individual rinse steps had been performed with each sample, an aliquot of 100 µL from each rinse solution was taken and a number of serials dilutions from 10^{-1} to 10^{-6} were performed. These dilutions were then plated onto nutrient agar and incubated for 24 hours at 37 °C with 5 % CO_2, after which the number of colony forming units on each nutrient agar plate could be counted allowing for the total number of viable bacteria in each rinse solution to be measured. This was repeated a total of 3 times (n = 3) to determine to optimal number of wash cycled required to ensure the majority of the low adherent bacteria had been removed.

4.2.5.2 Removing high-adherent bacteria

Following the rinse cycles for removing low adherent bacteria, the samples underwent a second stage of processing to dislodge the bacteria contained within the biofilm, which we have called high-adherent bacteria *(figure 4.3).* For our study a sonication bath was used which had a fixed frequency

of 35 kHz (RK-100; Sonorex, Bandelin), therefore a time dependant verification study was performed in order to determine the length of sonication time required to dislodge the cells from the biofilm before a significant decrease in bacterial viability occurs. After performing the low-adherence rinse process the pin samples were placed in a 2 mL Eppendorf tube containing 2 mL of PBS so that the samples were fully submerged. The tubes were then placed in the sonication bath using a floating tube rack in order to control the position of the tube within the bath. The pins samples were then sonicated for 1, 2, 3, 4, 5, and 10 minutes and at each time point were vortexed for 5 seconds to ensure the bacteria were evenly distributed before an aliquot of 100 µL was inoculated onto nutrient agar.

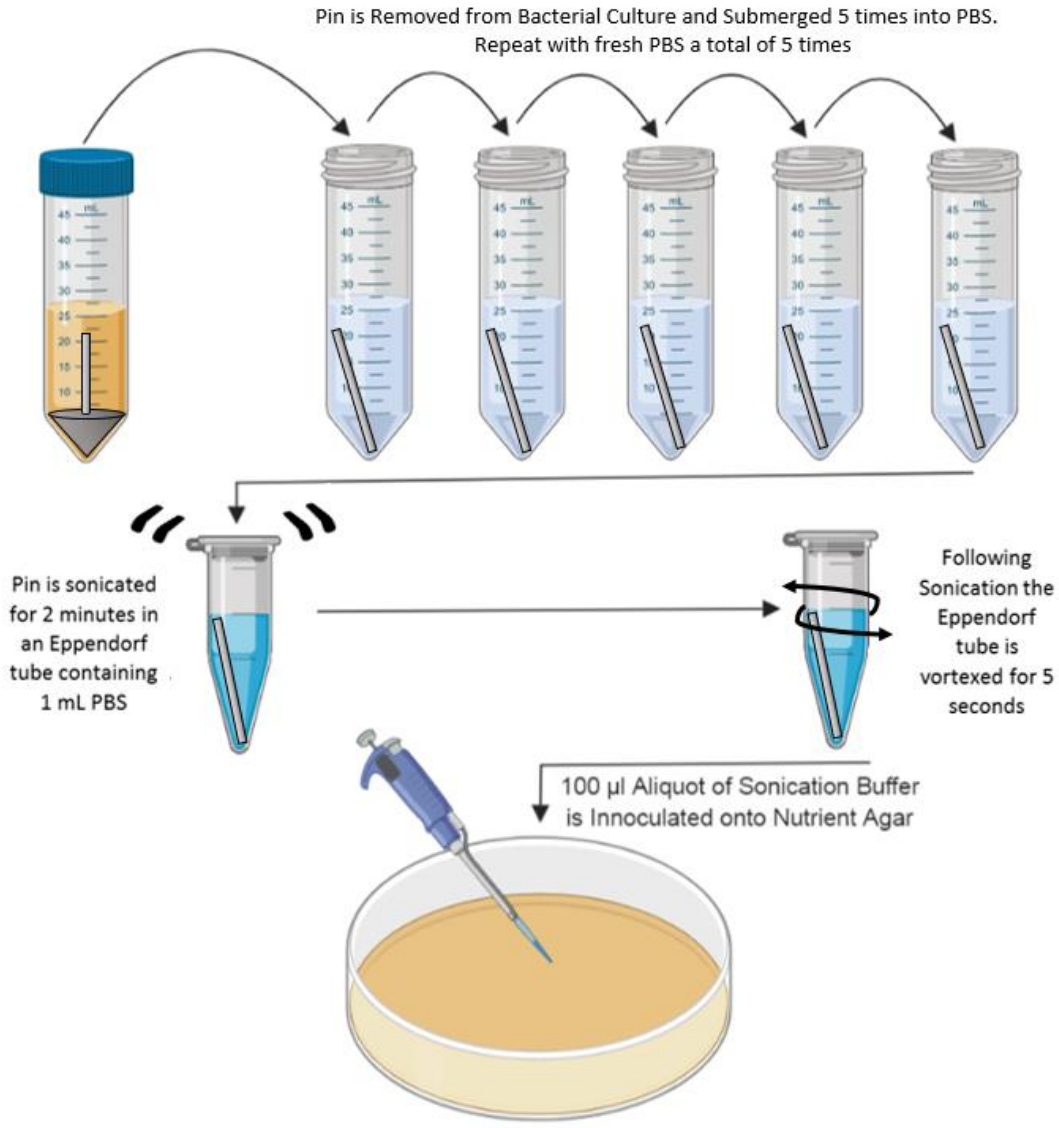

Figure 4.3: Diagram illustrating the method employed to removing low and high adherent bacteria from the surface of the pin samples

4.2.6 Measuring the effect of shaking frequency on bacteria attachment

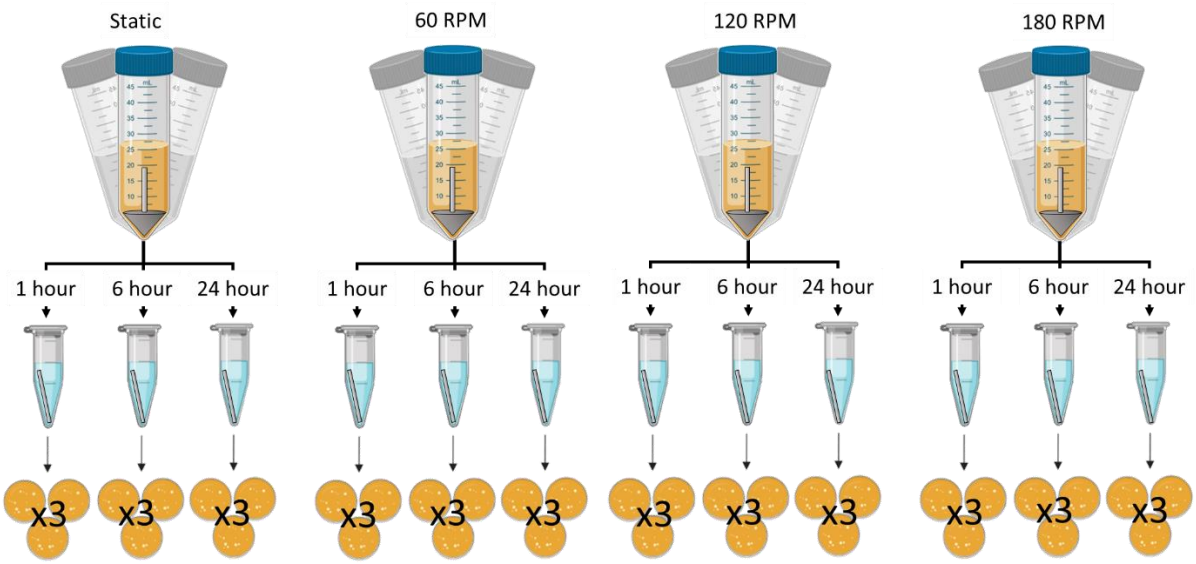

Figure 4.4: Diagram Illustrating the method developed for measuring the rate of bacterial attatchment under a range of different incubation shaking frequencies. Serial dilutions of the sonication buffer were performed before aliquotting onto agar plates to ensure CFU counts were within the exceptable range.

After sterilisation each pin and mount was placed in the bottom of a 25 mL universal tube containing 10 mL of starter culture. These universal tubes were then incubated at 37 °C and 5% CO_2 for 1, 6 and 24 hours while being to subjected to movement generated by the shaking frequency with an amplitude of 20 mm (0, 60, 120 and 180 RPM). At each time point the universal tube was removed from the incubator, the pin removed, and rinsed 5 times and then sonicated for 2 minutes and vortexed for 5 seconds in accordance to the protocols described previously. Following the removal of the high adherent bacteria, a 100 µL aliquot of the PBS sonication buffer solution was taken and a number of serial dilutions performed, which were then inoculated onto nutrient agar in triplicates. Plate counts were performed and the study was repeated on separate days a total of 3 times (n=3).

4.2.7 Scanning electron microscopy

In order to develop a better understanding of how the microorganisms interact with the fixation pin and how the biofilms form on the surface of the pins, biofilms of *S. epidermidis* and *S. aureus* were grown on fixation pin samples and imaged using scanning electron microscopy (SEM). Pin samples

were added to a 50 mL universal containing 10 mL of *S. epidermidis* or *S. aureus* grown in nutrient broth. These were incubated for 24 hours at 37 °C and 180 RPM after which the broth was aspirated and replaced with fresh broth, this was repeated 3 times for a total of 72 hours after which the pin samples were removed and washed in PBS three times. During which time a solution of 6 % (v/v) paraformaldehyde was made by mixing 600 µL of paraformaldehyde with 9.4 mL of PBS, ensuring the pH was 7.0. After rinsing, the pins were then added to the 6 % paraformaldehyde fixative for 30 minutes. Once the pin samples had been fixed they were then dehydrated by submerging the pin samples in ethanol solutions of increasing concentration ranging from 20 % ethanol, to 30 %, 40 %, 50 %, 60 %, 70 %, 80 %, 90 % and 100 % ethanol, after which the samples were critically dried by immersion in HDMS which was left to completely evaporate from the sample.

4.2.8 Measuring the effect of direct pin movement on bacterial attachment

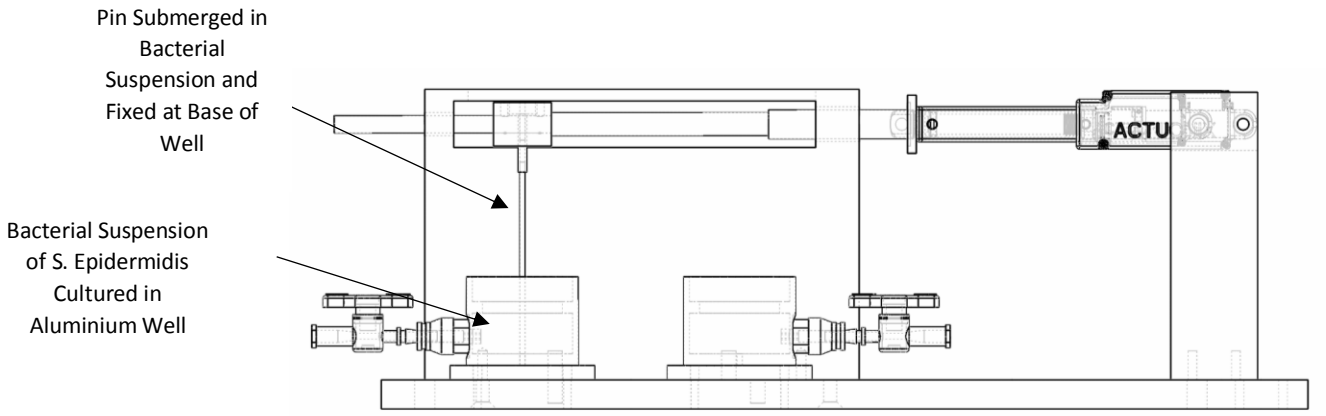

Figure 4.5: Diagram to illustrate the experimental set-up for measuring the effect movement of a fixation pin has on the attatchment of bacteria to said fixation pin

From *figure 4.10* we can see that after 24 hours the static culture had approximately 10,000 attached bacteria, which is at the low end of the detection range for accurate CFU counts. Since all bacteria cultures remained static during the pin machine study, it was decided that the starter cultures should be incubated until they reach an optical density at 600 nm of 1.0 (5 x 10^7 CFU / mL) in order to ensure

that the concentration of viable bacteria was great enough to develop biofilms on the pin samples. Each aluminium well was then filled with 15 mL of starter culture and covered in a layer of Opsite (Smith & Nephew, USA) to prevent contamination of the broth. A 100 mm sterile pin sample was then pierced through the Opsite and pushed into the hole at the base of the well. Three of these pin-bacteria samples were then connected to the pin machine in order to apply mechanic movement to the pin, while 3 were left unconnected so that the pin remained static, acting as a control group. Two degrees of movement were studied, a small deflection of 10 mm at a speed of 1 Hz in order to represent the frequency of a regular human gait, and a large deflection of 20 mm at a frequency of 0.5 Hz to reflect the amplitude of the orbital shaker used in the previous study *(section 4.2.6).* The linear actuator was then set to run the appropriate pin movement and the whole pin machine was placed into an incubator at 37 °C and 5 % CO_2 for 24 hours. After 24 hours the pins were carefully removed from the pin machine ensuring not to touch the section of pin which was submerged in bacterial culture in order to avoid dislodging any adherent bacteria. Each pin was then placed into individual 15 mL centrifuge tubes of which 2 mL of PBS was then added so that the area of pin with bacterial attachment was fully submerged. In order to dislodge the bacteria adhered to the pin, the wash and sonication protocol described previously was used, whereby each centrifuge tube was sonicated for 2 minutes followed by 5 seconds of vortexing to distribute the bacteria throughout the PBS so that serial dilutions could be performed and CFU counts measured. Each pin sample was plated out in triplicates and the experiment was repeated 3 times on separate days (n=3).

4.2.8 Statistical tests

The data collected throughout this study was analysed for statistical significance using a two tailed, unpaired Student's t-test when comparing the difference between two group means. When comparing groups split on two independent variables a two-way analysis of variance was used. A p-value of <0.05 was considered statistically significant.

4.3 Results

4.3.1 Growth curves

A growth curve of *S. epidermidis* over a 72 hour period has been presented in *figure 4.6*. The curve indicates that between 2 and 10 hours after inoculation the bacteria is in the exponential phase whereby the bacteria are dividing by binary fission and therefore doubling in numbers after each generation. After 10 hours the culture enters the stationary phase where proliferation slows down due to a lack of nutrients and a build-up of toxins. After 24 hours the bacteria is in the death phase whereby nutrients in the broth are depleted and waste products increase resulting in cell death. A plot of CFU against optical density at 600 nm is presented in *figure 4.7*, the equation of the trend line can be used to estimate the number of viable bacteria in a sample from the optical density reading in order to determine the cell density of the broth without requiring the time consuming CFU counts to be performed.

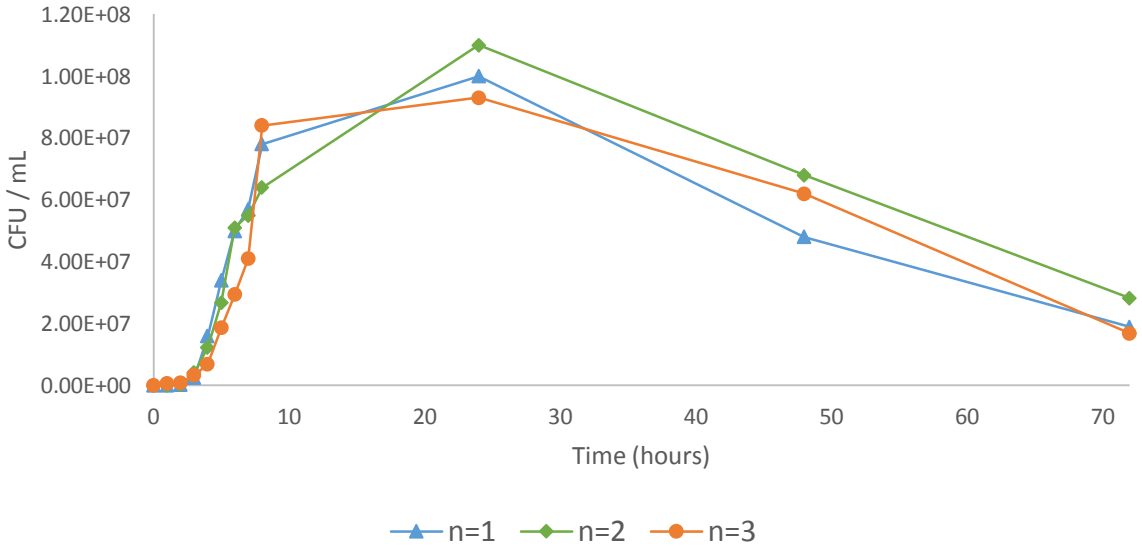

Figure 4.6: Plot of optical density against time for a *S. epidermidis* culture over a 72 hour period. From 1 to 2 hours the bacteria is in the lag phase of growth, 2 – 10 hours is the exponential phase, 10- 24 is the stationary phase after which the bacteria enters the death phase until all nutrients are depleted from the medium.

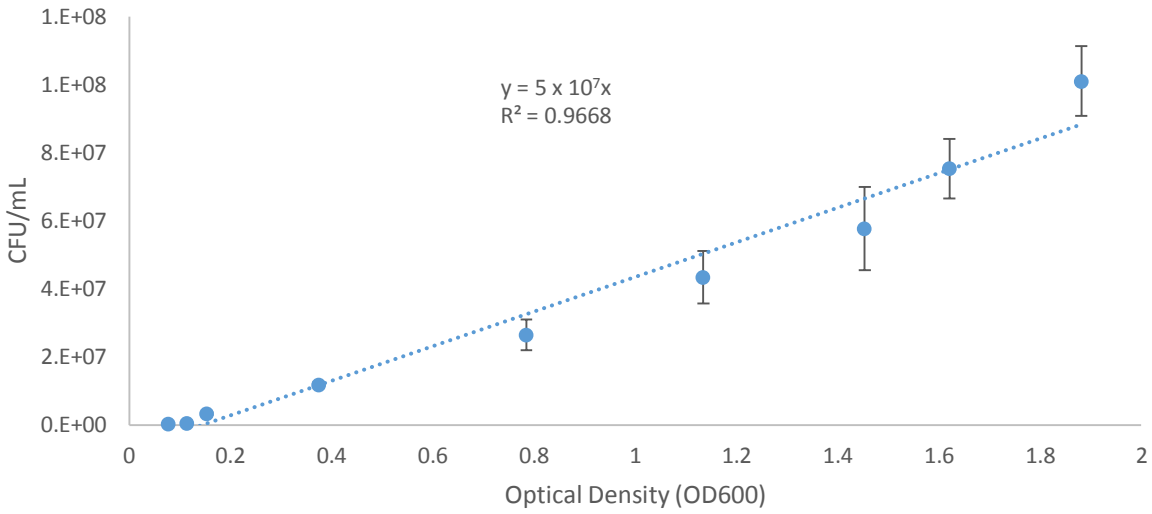

Figure 4.7: Plot of CFU / mL against optical density for *Staphylococcus epidermidis* over a 24 hour period – The equation of the linear trend line ($y = 5 \times 10^7 - 6 \times 10^6$) can be used to calculate estimates of CFU / mL from optical density. Error Bars Represent the Standard Deviation from the mean (n=3)

4.3.2 Low adherent bacteria validation results

A validation study was performed to determine the optimum number of wash cycles required to remove the majority of low adherent bacteria from the surface of the pin samples. *Figure 4.8* shows the CFU / mL of each rinse solution on a logarithmic scale. It is clear that the majority of the low adherent bacteria is removed during the first five rinses after which the graph begins to converge towards 10^3 CFU / mL. On average, 96.7 % of low adherent bacteria was removed after the first rinse, followed by another 85.5 % after the second rinse. By the fifth rinse, the concentration of viable bacteria in the rinse solution had fallen by over 99.8 %. Following the 5th rinse the graph levels out as the bacteria count no longer falls, indicating that the majority of the low adherent bacteria has been removed. Therefore 5 rinses were used for the remainder of the study when removing low-adherent bacteria.

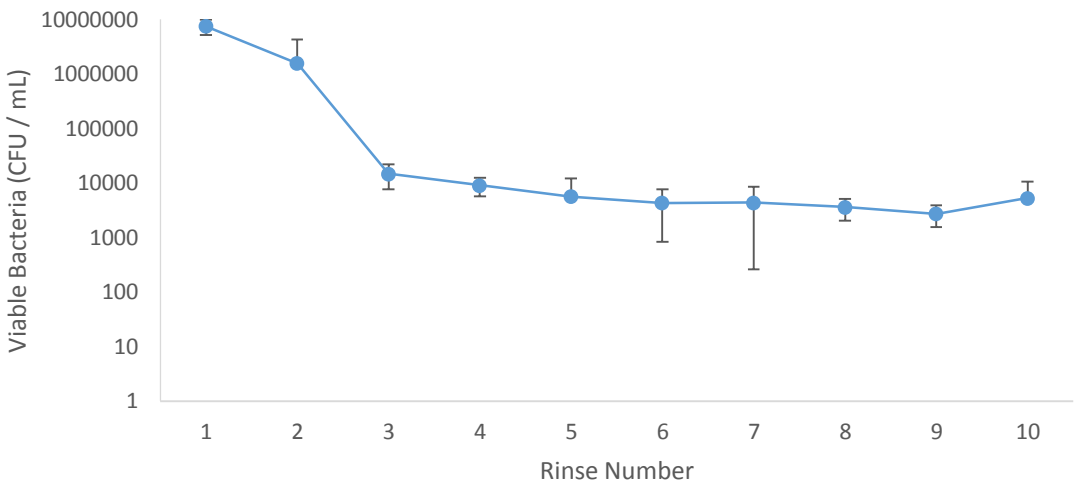

Figure 4.8: Total number of colony forming unit's measured in wash buffer up to 10 washes. From 1 to 4 washes low adherent bacteria was still present on the surface of the pins, the curve begins to converge after 4 washes indicating the vast majority of the low adherent bacteria had been washed away. Error bars represent the standard deviation between results (n=3).

4.3.3 High adherent bacteria validation results

A second validation study was performed to determine the optimum sonication time required to dislodge highly adherent *S. epidermidis* bacteria for counting, without inducing cell lysis. The results seen in *figure 4.9* show that on average the number of viable bacteria released from the pin surface into the sonication buffer increased 3-fold from 5 x 10^2 to 1.52 x 10^3 CFU / mL when the sonication time was increased from one to two minutes. After two minutes of the concentration of viable bacteria in the sonication buffer was at its highest (1.52 x 10^3), after which the number of viable bacteria measured began to fall, indicating possible cell disintegration. From this study it is clear that 2 minutes is the optimal duration of sonication in order to dislodge the majority of the *S. epidermidis* cells highly adherent to the surface of the pin sample, after which cell density beings be decrease indicating possible cell death. Therefore for the remainder of this study a sonication time of 2 minutes was used to effectively remove all high adherent *S. epidermdis* from the pins in order to perform CFU counts.

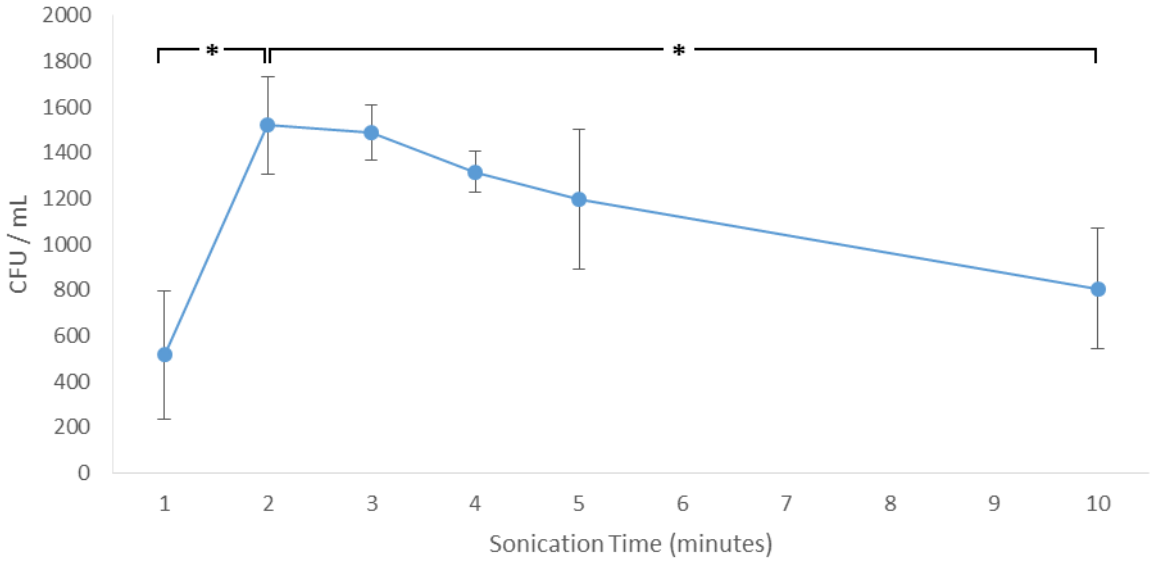

Figure 4.9: Highly adherent bacteria dislodged from pin surface for sonication duration up to ten minutes. The number of bacteria dislodged increased significantly when sonication time was increased from 1 to 2 minutes, however this began to decrease when sonication time was increased from 2 minutes. After 10 minutes the number of dislodged bacteria was significantly lower than at 2 minutes. * Indicates a significant difference of $p<0.05$. Error bars represent the standard deviation from the mean (n=3)

4.3.4 The effect of shaking frequency on bacterial adhesion to external fixation pins

4.3.4.1 Bacterial adhesion to pin surface

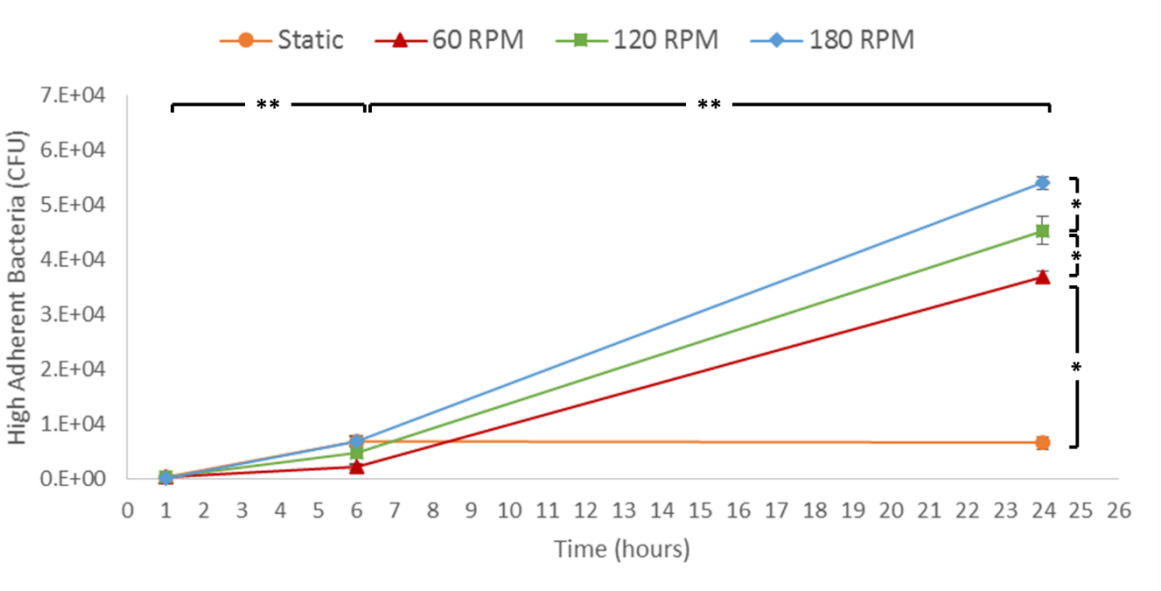

Figure 4.10: CFU counts of bacterial highly adhered to the surface of fixation pins under different shaking frequencies. After 24 hours of incubation levels of bacteria attatchment increased significantly with increasing shaking frequency, indicated by * ($p<0.05$). Bacteria attatchment also increased with increasing incubation time for all samples except the static sample in which bacterial attatchment decreased from 6 to 24 hours, indicated by ** ($p<0.005$). Error bars represent the standard deviation from the mean (n=3).

The shaking frequency and duration of incubation was tested for its effect on the rate of attachment of highly adherent *S. epidermidis* bacteria to the surface of 316L stainless steel external fixation pins. An orbital shaker with an amplitude of 20 mm set at 37 °C was used to generate shaking frequencies of 60 RPM, 120 RPM and 180 RPM which were compared against a static control. After 24 hours of incubation the number of highly adherent bacteria increases with increasing shaking frequency ($p<0.05$). From 1 to 6 hours all samples showed a significant increase in the number of highly adherent bacteria ($p<0.005$). Similarly samples incubated at 60, 120 and 180 RPM all showed a significant increase in bacterial adhesion from 6 hour to 24 hours ($p<0.005$) except the static sample which showed a decrease in bacterial attachment of 2.3 x 10^2 CFU from 6 to 24 hours, however this result was not significant ($p=0.79$)

4.3.4.2 Cell density of bacteria culture

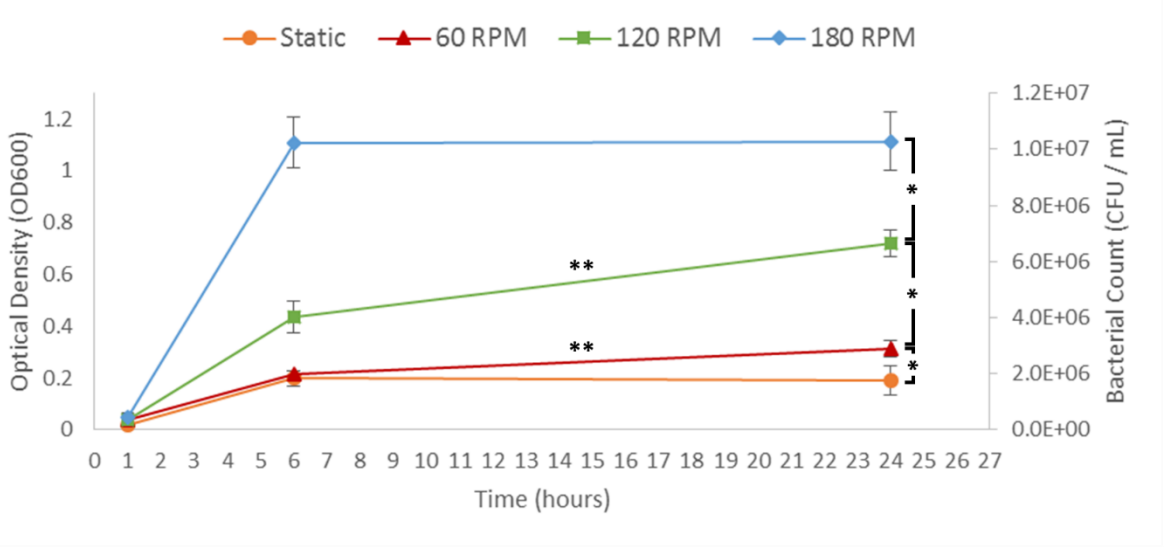

Figure 4.11: Optical density of bacterial broth of which pin was submerged. At 24 hours bacterial concentration of each culture increases with increasing shaking frequency, indicated by * ($p<0.005$). The 60 RPM and 120 RPM showed a significant increase in bacterial attatchment from 6 to 24 hours, indicated by ** ($p<0.05$) while the static and 180 RPM samples showed no significant increase ($p=0.59$ and $p=0.95$ respectively). Secondary axis shows estimated CFU / mL values calculated using the growth rate. Error bars represent the standard deviation from the mean (n=3)

The optical density of the bacterial culture containing the pin samples during the shaking frequency study was measured at 0, 6 and 24 hours in order to determine the concentration of planktonic bacteria in the culture. At 0 hours the cell density of all cultures was 1 x 10^6 CFU / mL as this was the

cell density of the starter cultures used throughout the experiment. Similar to the levels of bacteria attachment *(figure 4.10)* the optical density of each culture at 24 hours increased signficantly with increasing shaking frequency ($p<0.005$). When shaking frequency was increased from static to 60 RPM there was a 65% increasing in optical density, a 130% increase was also observed when shaking frequency was increased from 60 – 120 RPM and a there was a further 55% increase in optical density from 120 – 180 RPM. Unlike in the bacterial attatchment study which showed a significant increase in attatchment was observed from 6 to 24 hours amoung all samples, only the 60 and 120 RPM cultures showed a significant increase in optical density from 6 to 24 hours ($p<0.05$). Interestingly the 24 hour culture increased in density by 95% from 0 to 6 hours but only by 0.5% from 6 to 24 hours. A similar effect was oberved for the static culture whereby a 90% increase in optical density was seen from 0 to 6 hours, but from 6 to 24 hours bacteria density decreased by 5%. However both these results did not show statistical significance ($p=0.95$ and $p=0.83$ respectively).

4.3.4.3 Control study

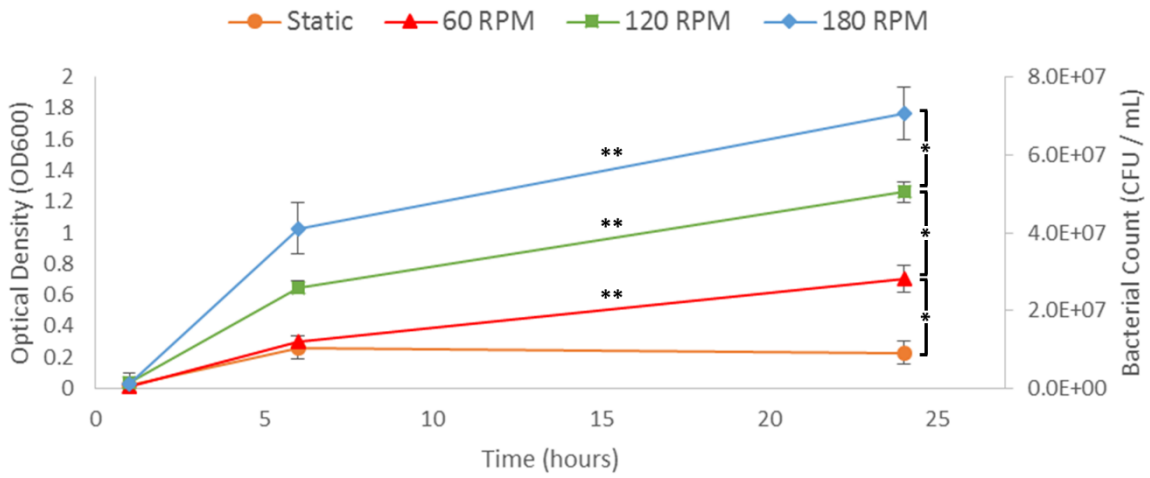

Figure 4.12: Optical density measurements of the control study containing *S. epidermidis* without pin. At 24 hours bacterial concentration of each culture increases with increasing shaking frequency, indicated by * ($p<0.005$). The 60 RPM and 120 RPM and 180 RPM samples showed a significant increase in bacterial attatchment from 6 to 24 hours, indicated by ** ($p<0.05$) Secondary axis shows estimated CFU / mL values calculated using the growth rate. Error bars represent the standard deviation from the mean (n=3)

A control study of *S. epidermidis* cultures in nutrient broth containing no pin samples or pin mount device was conducted and the optical density measured at 0, 6 and 24 hours. The results show that bacterial density of the cultures increased in response to an increased shaking frequency after 24 hour incubation ($p<0.005$) similar to the results observed in *figure 4.11*. Bacterial density significantly increased from 6 to 24 hours for the 60 RPM and 120 RPM and 180 RPM samples ($p<0.05$) and decreased for the static sample ($p=0.61$). In contrast the 180 RPM sample reached a similar optical density to *figure 4.11* of 1.0 OD600 at 6 hours, however this increased by 54% in the control study from 6 – 24 hours ($p<0.05$) which was not seen in *figure 4.11.* It was expected that the control study and the bacterial cultures during the pin shaking study *(figure 4.11)* should have similar optical density measurements, as the only variable between both studies is the presence of the pin and mount device in the culture. However, the optical densities measured during the control study were notably higher that those presented in *figure 4.11*, the cause of this cannot be determined for certain without further investigation, however this may be a result of a negative effect on bacterial viability caused by a possible toxicity of the 316L pin sample or aluminium pin mount device to the bacteria.

4.3.5 Effect of pin movement on bacterial attachment

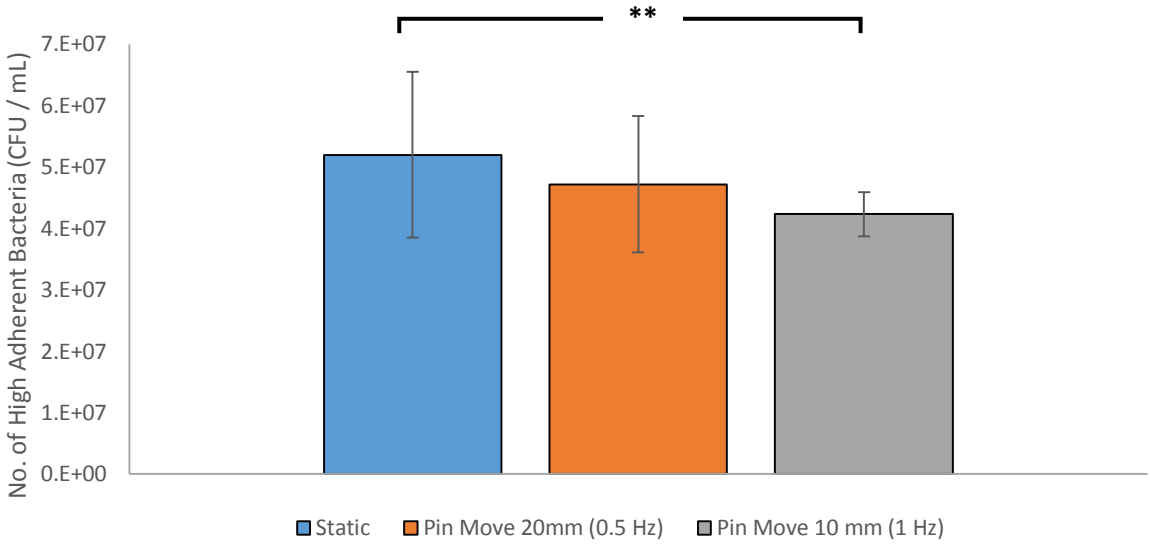

Figure 4.13: Measurement of highly adherent bacteria on the surface of pins at various pin movement magnitudes. Samples that remained static appeared to have the greatest abundance of bacteria with the rate of bacterial adherence decreasing with increasing shaking frequency compared to control (p=0.23 and p=0.37 respectively) *Error bars represent the standard deviation from the mean (n=3 for 0.5 & 1 Hz samples, n=6 for static control)*

The 'pin machine' described in detail in *Chapter 3* was used to apply mechanical movement directly to pins submerged in static bacterial culture, in order to observe the effect pin movement has on the rate of bacterial attachment to the pin surface after 24 hours of static incubation. From *figure 4.13* it appears that the rate of attachment of bacteria decreases with increasing pin movement frequency, as the static sample showed the greatest abundance of highly adherent bacteria, which decreased by an average of 9.3% when pin movement at 0.5 Hz was applied and a further 18.6% from static to 2 Hz pin movement. However only the results for pin movement at 1 Hz showed statistical significance compared to the static samples ($p<0.05$) while the pin movement at 0.5 Hz samples did not ($p=0.23$).

4.3.6 Scanning electron microscopy

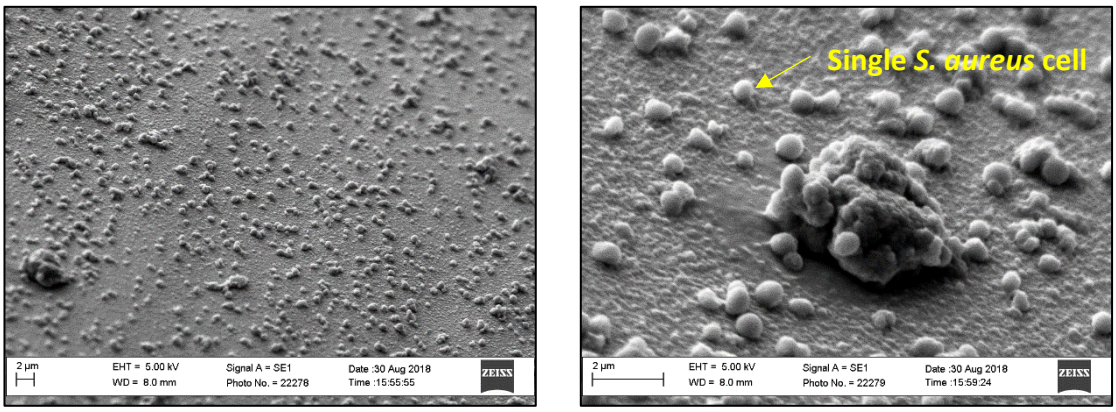

Figure *4.14*: Scanning electron microscope images of *S. aureus* adhered to stainless steel fixation pins

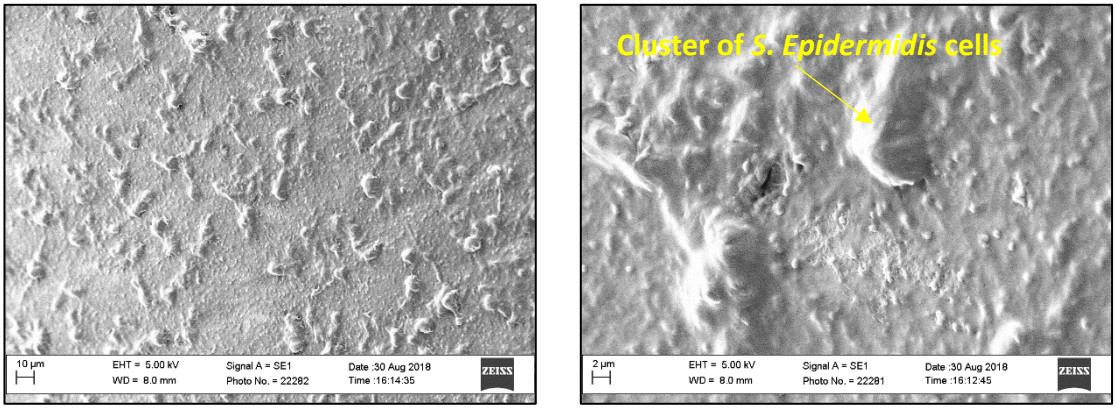

Figure 4.15: Scanning electron microscope images of *S. epidermidis* adhered to stainless steel fixation pins

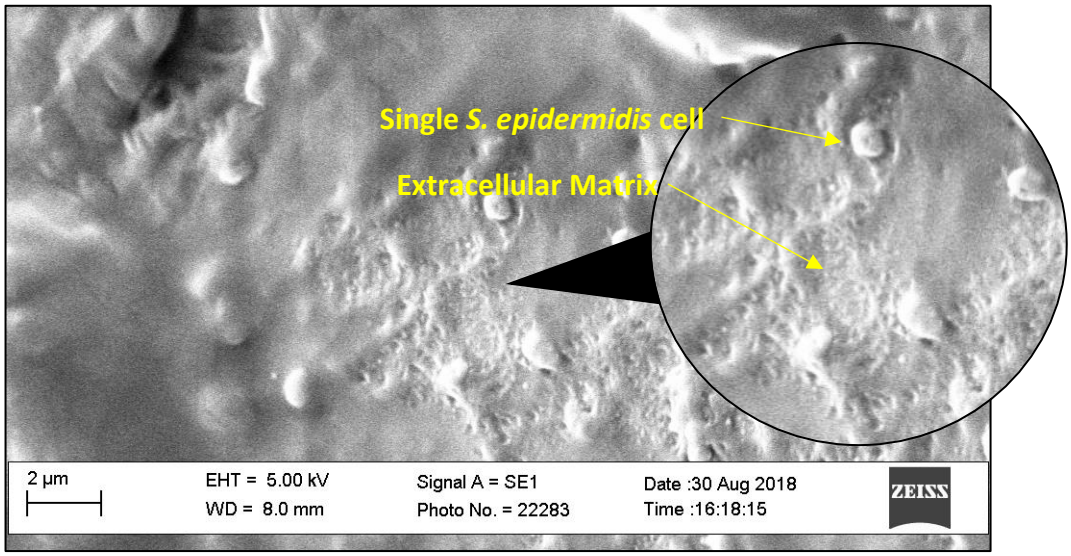

Figure 4.16: Enlarged Image of *S. epidermidis* showing clearly visible extracellular matrix

Scanning electron microscopy (SEM) was performed in order to confirm the formation of *S. epidermidis* biofilm on the surface of the fixation pin after 24 hours incubation. Images of the biofilm were compared against samples colonised by *S. aureus*. The production of extracellular matrix is an important characteristic of biofilms as it provides protection from antibiotics and immune responses. When comparing *figures 4.14* and *figures 4.15* it is clear that *S. aureus* adhere to the pins forming a fairly uniform distribution across the surface with minimal production of ECM. On the other hand *S. epidermidis* form grape like clusters around 10 μm in diameter, contained within a significant production of ECM. This ECM can be seen in more detail in the higher magnification image shown in *figure 4.16*, clearly showing the web like structure of the ECM connecting all cells in the biofilm.

4.4 Discussion

Throughout the literature it is often highlighted by clinicians that excessive movement between the pin and skin across the pin site, correlates to an increase in the rates of pin-site infection (Bibbo *et al*, 2010; Browner *et al*, 2014; Canale *et al*, 2012; Ferreira *et al*, 2012; Holmes *et al*, 2005; Kazmers *et al*, 2016; Santy *et al*, 2009). Previously it has been shown that *P. Aeruginosa* cells create more long lasting adhesion events under greater levels of shear stress, hence we hypothesised that shear forces generated by relative displacement between the pin and skin has a positive influence on the rate of bacterial attachment, leading to a greater rate of bacterial attachment. In order to investigate this hypothesis a study was designed to measure the effect of pin movement on the rate of bacterial adhesion to external fixation pins. As hypothesised an increase in bacterial attachment was observed when shaking frequency was increased ($p<0.05$) however the same effect was not observed we movement was applied directly to the pins.

Currently the majority of studies investigating bacterial adhesion under shear stress utilise micro fluid channels, however these devices are too small to incorporate external fixation pins, and therefore two methods were developed for generating shear force between the bacteria and pin surface. The first method was adapted from Fonseca *et al* method of placing glass beads in culture and generating hydrodynamic shear forces through orbital shaking (Fonseca *et al*, 2007), for our study the glass beads were replaced by the fixation pin sample. This was later developed upon by incorporating the 'Pin Machine' described in *Chapter 3*, to apply movement directly to the pin, allowing for the samples to all remain static during culture.

In order to measure the number of adherent bacteria precisely, it was required that the bacteria must first be dislodged from the surface of the pins so that a CFU count could be performed. Therefore a protocol was designed and optimised which involving washing the pins in PBS to remove low adherent bacteria followed by sonication and vortexing to remove the high adherent bacteria. We believe this protocol to be preferable to other methods due to its strong repeatability between results, while also

being time efficient and fairly inexpensive, making it suitable to replicate in most labs with basic equipment.

When studying the effect of shaking frequency on bacterial adhesion it was found that bacterial adhesion to all pins, except those which were kept static during incubation, increased notably from 6 hours to 24 hours. Out of the 4 shaking frequencies at 20 mm amplitude, the static pin appears to have the greatest number of attached bacteria after 6 hours, however, after 24 hours the static pin shows significantly less attached bacteria compared to the other pins, with 180 RPM showing the highest bacterial growth. These results support our hypothesis that increased shear forces between bacteria and an implant surface leads to a greater biofilm formation on the surface of the pin, however based on the increased CFU count of the bacterial culture it may also be a result of improved circulation of oxygen and nutrients throughout the culture at higher shaking frequencies. During the early stages of bacterial growth, both nutrients and oxygen within the culture are high. As the bacteria proliferate and the concentration of bacteria in the culture increases, nutrients and oxygen in the culture are depleted. After just 6 hours of incubation, the bacteria are still in the logarithmic phase of growth and therefore concentrations are low enough that oxygen and nutrient depletion is negligible. This resulted in the static pin showing a greater number of adhered bacteria as the bacteria don't have to overcome any shear forces generated in the culture though shaking in order to adhere to the pin. After 24 hours however, the bacteria had reached the stationary phase of growth, which indicates that there is enough nutrients and oxygen to maintain existing bacteria but not enough to facilitate proliferation. This is highlighted by the lower optical density value *(figure 4.12)* of the static sample after 24 hours compared to the samples which were shaken. This limitation of oxygen did not happen in those samples which were shaken as shaking a bacterial culture during incubation increases the surface area of culture that is exposed to air, leading to a greater transfer of oxygen into the broth. Maier *et al* demonstrated that at 300 RPM the maximum oxygen transfer ratio (OTR) was 20.5, but when this was halved to 150 RPM the OTR fell to 11 (Maier *et al*, 2001)

Since the optical density of the cultures after 24 hours *(figure 4.11)* correlates closely to the measured number of highly adherent bacteria after 24 hours *(figure 4.12)* it is possible that the increase in number of bacteria adhered to the pin surface when shaking frequency is increased, is simply due to the increase in growth rate at higher shaking frequencies, leading to a greater abundance of bacteria in the culture. This would result in an increase in observed attachment due to the higher frequency of adhesion events occurring, rather than an increase in the percentage of successful adhesion events due to the increased shear forces.

In order to more closely investigate the effect of pin movement on bacterial attachment to external fixation pins, the effect that shaking has on the growth rate of bacteria and therefore the population density of the broth must be eliminated. For this we utilised a pin movement machine described in *chapter 3*. By developing a system that applies various magnitudes and frequencies of movement to the pin while maintaining a static environment for the bacterial broth it can be ensured that the growth rate of each broth remains constant and therefore the effect of pin movement on bacterial attachment can be observed more closely.

By studying two magnitudes of movement, a micro-motion of 10 mm at frequency of 1 Hz to represent the frequency of human gait cycle (Murray *et al*, 1964) and a larger movement of 20 mm at a frequency of 0.5 Hz, and comparing the results against static controls it was found that bacterial adhesion was greatest in the static samples and adhesion decreased with increasing frequency. After performing a one-way analysis of variance, we found no statistical significance between the results meaning we are unable to reject the null hypothesis that there is not significant difference in bacterial adhesion to an external fixation pin when movement is applied to said pin.

However, during the shaking study, the most pronounced increase in bacterial attachment was observed at 180 RPM, which corresponds to a frequency of 3 Hz and a magnitude of 20 mm (radius of orbital shaker), while the maximum magnitude of pin movement during the pin machine study was a displacement of 20 mm at a frequency of 0.5 Hz. Therefore the lack of difference observed when

movement was applied directly to the pin may be due the magnitudes of pin movement not being great enough to produce a significant change in bacteria adhesion. Repeating the study with greater magnitudes of pin movement may result in an increased rate of attachment in response to a increase in pin movement, however the design of the pin machine limited the experiment to study only micro-motions of the pin in the range of 1-20 mm.

Although the results from this study were inconclusive it has provided an insight into the role of movement in external fracture fixation pin-site infections. The lack of clear evidence to support our hypothesis that shear forces, as a result of pin movement, lead to increase bacterial adhesion, highlights the fact that pin-site infection is a complex multifactor problem that is not just a consequence of successful biofilm formation to the pin but combination of bacterial colonisation, wound healing of the skin and mechanics of the pin itself.

Chapter 5: Design and Development of an In vitro Pin-Site Model to Study the Effect of Movement on Pin-Site Wound Healing

5.0 Introduction

Wound healing plays a significant part in the development of healthy pin-site wounds. A review of the literature identified that there is an inverse relationship between wound healing and infection in external fixation (Ferreira *et al*, 2012; Parameswaran *et al*, 2003). If the wound healing process is impaired, wound exposure is prolonged, allowing infectious bacteria a greater opportunity to enter the host and cause infection. However the presence of a fixation pin prevents the wound from fully closing, therefore the aim of wound healing in external fixation is the development of a collagen shell around the pin isolating the pin-site wound from the hosts (Brodbeck *et al*, 2009).

Minimal research has been conducted regarding the process of wound healing in an infected pin-site, however studies that have attempted to tackle this problem are often in vivo studies utilising either clinical or animal models. Although clinical in vivo human skin studies are the most relevant and accurate means of determining the effectiveness of wound therapies, this approach is often impractical due to the intrinsic variations between skin types, such as melanin content, hair follicle density and elasticity, which influence the mechanical and biological physiology of the skin as well as the bacterial skin flora. In order to overcome these challenges several models have been developed for studying wound healing in vitro, the most physiologically accurate of which are human skin equivalent models.

Since the 1970s when keratinocytes were first cultured in the laboratory (Rheinwald *et al*, 1975) there has been great progress into the development of in vitro models of human skin. Skin equivalents were originally designed to provide both dermal and epidermal tissue for grafting onto patients suffering from full-thickness skin loss (Chakrabarty *et al*, 1999), however over the last few decades three-dimensional engineered skin has developed in complexity so that it accurately replicates the biological structure of normal human skin and has therefore been used to study various aspects of skin biology such as skin contraction (Chakrabarty *et al*, 2001; Harrison *et al*, 2006; Ralston *et al*, 1997), skin diseases (Meier *et al*, 2000) and wound healing (Xie *et al*, 2010). Today there are a vast array of human

skin equivalent models available for use in research. The basic models contain either keratinocytes only or incorporate keratinocytes and fibroblasts from both primary (Carlson *et al*, 2008) and immortalised cell lines (Smits *et al*, 2017). However more complex models have been developed such as those with melanocytes incorporated for studying the relationship between skin pigment and UV radiation (Topol *et al*, 1986), endothelial cells incorporated to induce vascularization (Hudon *et al*, 2003), immune cells to study the immune response from UV light (Bechetoille *et al*, 2007) and hair follicles to assess the role of the trans follicular route in percutaneous absorption (Michel *et al*, 1999).

The two main components of a full thickness skin equivalent model are the epidermis and the dermis. The epidermis contains keratinocytes which undergo several morphological and biochemical changes during the culture of the skin equivalent in order to form the basal layer, spinous layer, granular layer and cornified layer. The dermal component of human skin contains mainly fibroblasts contained within collagen and elastin proteins which provides the majority of the mechanical structure to the skin, therefore a scaffold must be used to replicate this 3D structure in vitro. Several methods are available in order to create the dermal component of skin equivalents such as using a de-epidermalised dermis (Chakrabarty *et al*, 1999), whereby the epidermidis is removed from ex vivo skin biopsies and a new epidermis is grown from keratinocytes in vitro. Scaffold substrates such as Alvetex and Mimetex are also available which contain highly porous cross-linked polystyrene, electro spun into a 3D scaffold structure containing pore sizes between 36 - 40 µm allowing cells to grow throughout the scaffold (Hill *et al*, 2015). However the majority of skin equivalents consist of cellular matrices made by incorporating fibroblasts into Type 1 collagen and culturing on transwell membranes where the collagen is allowed to gel.

Although currently no attempt has been made in the direction of developing an in vitro pin-site model for external fixation, several studies have attempted to characterise the skin interface in percutaneous implants such as dental implants, catheters, glucose sensors, intramedullary prosthesis and feeding tubes. Similarly to pin-site wounds, the wounds these devices create are highly susceptible to infection,

often due to micro-trauma that disrupts the interface between the skin and biomaterial, putting the patient at a higher risk (Fleckman *et al*, 2008). The tooth is possibly the most studied percutaneous, biologically anchored implant which has demonstrated that even in a setting of high moisture and microbial contamination, percutaneous dental implants can function effectively and infection free, with survival rates of over 90% at 15 years (Adell *et al*, 1986; Brånemark *et al*, 1982), although this survival rate has yet to be achieved consistently outside of the oral environment. Chai *et al*, developed a novel in vitro three dimensional oral transmucosal model (3D OMM) in order to investigate the implant-soft tissue interface in dental implants (Chai *et al*, 2010). An acellular cadaveric dermis explant was used as a scaffold to culture both oral keratinocytes and human gingival fibroblasts onto the basement membrane of the dermis. Once fully cultured, a 4 mm tissue biopsy punch was used to create a wound in the model to insert a titanium sample. Chai *et al* described the 3D OMM as forming a peri-implant like epithelium attached to the titanium sample similar to the epithelium structure seen in animal models. This research has shown that it is possible to use skin equivalent models to study percutaneous implants and therefore these methods may be translatable to external fixation pins as they exhibit similar wound healing conditions to oral implants. However the study conducted by Chai *et al* does not model the mechanical loading environment experienced by the titanium implant which would be necessary in order to develop a physiologically accurate pin-site model.

There are several methods available for quantitatively measuring the wound healing response of a skin equivalent to a given treatment. Histological analysis can be performed which involves sectioning the tissue into micron thin samples which can then be stained in order to visualise any changes in the cellular structure of the skin equivalent. This method has long been established as a diagnostic approach for many diseases, including vasculitis, kidney disease and transplant rejection as well as its most well-known application in cancer and pre-cancerous lesions (Kallenberg, 2015; Yang *et al*, 2012). Another method involves monitoring cellular events involved in wound healing. Platelets, neutrophils, macrophages, and epidermal cells release inflammatory cytokines, in particular Interleukins 1 alpha and 6 (IL-1α and IL-6) and tumour necrosis factor alpha (TNF-α), are upregulated during the

inflammatory phase in order to act as signalling molecules between cells to initiate various wound healing process such as cellular growth, proliferation, differentiation and reepithelialisation (Werner *et al*, 2003). Therefore measuring the concentration of these cytokines expressed by the skin equivalents under various treatments, using assays such as ELISA and PCR, the effect that the treatment has on wound healing can be analysed.

Cytokine levels of IL-1α, IL-6 and TNF-α have been found to be significantly higher in non-healing wounds compared to that of healing wounds (Lindley *et al*, 2016). Trengrove *et al* found that concentrations of IL-1α were almost 3.5 x greater in non-healing chronic leg ulcers compared to that of healing wounds (Trengove *et al*, 2000). Biedler *et al* also reported similar findings for Il-8 (Beidler *et al*, 2009), yet Beidler stated that the large variation in levels between subjects, possibly due to a variation in immune response and skin physiology, makes it difficult to use as a marker for wound healing in vivo (Gohel *et al*, 2008). However, human skin equivalents are cultured from single donor human epidermal primary cells using identical chemicals, mediums and reagents throughout in order to eliminate the variation between skin types and immune system responses seen in vivo. Therefore cytokines, in particular IL-1α, IL-6 and TNF-α, may be effectively used as markers to assess the quality of wound healing in human skin equivalents when used in conjunction with other biomarker methods such as histological analysis. Several studies have monitored the cytokine levels of skin equivalents, however the outcomes can vary substantially. Reijnders *et al* measured the levels of a multitude of proteins in skin equivalents cultures from both primary and immortalized cell lines and found concentrations of IL-8 to be 78.8 pg / mL and 22.655 pg / mL respectively after 24 hours, however Reijnders reported that levels of TNF-α and IL-1α were undetectable (Reijnders *et al*, 2015). Morgan *et al* conducted a similar study to measure the effect of *Sarcoptes scabiei* mites on skin equivalents in-vitro. After 48 hours levels of IL-1α and IL-8 were observed at 260 pg/ml and 9090 pg/ml respectively in the control sample, which increased to 850 pg / mL and 24,700 pg/ mL in the samples inoculated with scabiei mites. The discontinuity between measured concentrations of cytokines in human skin models means an absolute comparison is not viable, instead relative changes as a result of a given

treatment would provide a more accurate method for quantifying the results. Although extensive work has been done on the development of human skin equivalents and using them as models for studying various pathologies and diseases, it appears that no research has been conducted using skin equivalents to study external fixation pin-site wounds in-vitro where the mechanical loading environment can also be modelled.

5.1 Aims and hypothesis

The primary aim of this chapter was to characterise the role of pin movement in external fixation on the wound healing response of a human skin equivalent. Firstly a human skin full thickness skin equivalent was cultured and validated against native human skin through histological staining to verify the skin equivalents physiological relevance. This model was then used in conjunction with the 'pin machine' described in *chapter 3*, in order to apply mechanical movement to the fixation pin. The effect on the wound healing response was then studied by measuring the secretion of pro-inflammatory cytokines.

The hypotheses for this study are therefore:

1. Pro-inflammatory markers IL-1α, IL-8 and TNF-α will increase from control when a fixation pin is implanted.
2. Pro-inflammatory markers IL-1α, IL-8 and TNF-α will increase when movement is applied to the pin compared to a static pin

5.2 Methods

5.2.1 Cells

For the dermal component, Primary Normal Human Dermal Fibroblasts (HDF) isolated from normal human juvenile foreskin were obtained from (PromoCell, DE. Cat. No 12302). The epidermal component was grown using normal primary human epidermal keratinocytes (NHEK) isolated from single donor juvenile foreskin (PromoCell, DE. Cat #12005). Both cell types were cultured up to a maximum of 15 population doublings as per the manufacturer's recommendations.

5.2.2 Culture mediums

5.2.2.1 Fibroblast growth medium (FGM)

Fibroblasts were cultured in serum-free, low glucose Dulbecco's Modified Eagle Medium (DMEM) (Thermo Fisher Scientific, USA. Cat #11054020) supplemented with 10% (v/v) fetal bovine serum (FBS) (Thermo Fisher Scientific, USA. Cat #16000044), 8mM Hepes (Sigma Aldrich, USA. Cat #83264), 10, 000 U/mL^{-1} penicillin and 10, 000 $\mu g/mL^{-1}$ streptomycin (Thermo Fisher Scientific, USA. Cat #15140122).

5.2.2.2 Keratinocyte growth medium (KGM)

The keratinocytes were cultured in serum-free keratinocyte basal medium (PromoCell, USA. Cat #20011) with additional Growth Medium 2 Supplement Pack (PromoCell, USA. Cat #39011) containing 0.004 mL / mL bovine pituitary extract, 0.125 ng / mL epidermal growth factor, 5 µg / mL Insulin, 0.33 µg / mL hydrocortisone, 0.39 µg / mL epinephrine, 10 µg / mL transferrin and 0.6 mM calcium chloride.

5.2.2.3 O1O medium

O1O medium is an essential component for both the epidermisation and cornification mediums. A mixture of 8.3 g DMEM powder (Sigma Aldrich, USA. Cat #5030) containing no glucose, no l-glutamine, no phenol-red, no sodium pyruvate and no HEPES was dissolved in 1 litre of water. After which 0.1 g magnesium sulphate (Sigma Aldrich, USA. Cat #2643) and 3.7 g sodium bicarbonate was added.

5.2.2.3 Epidermisation medium

O1O medium was mixed with Ham's F12 Nutrient Mix (Sigma Aldrich, USA. Cat #51651) at a ratio of 3:1 (v/v). After which the following supplements were added; 4 mM L-glutamine, 40 µM adenine, 1 µM hydrocortisone, 10 µg transferrin, 10 µg insulin, 20 nM triiodothyronine, 2 nM progesterone and 0.1% FBS (Thermo Fisher Scientific, USA).

5.2.2.4 Cornification medium

O1O medium was mixed with Hams F12 nutrient mix at a ratio of 1:1 (v/v) and the following supplements were added 4 mM L-glutamine, 40 µM adenine, 1 µM hydrocortisone, 10 µg transferrin, 10 µg insulin, 20 nM triiodothyronine, and 2% (v/v) FBS (Thermo Fisher Scientific, USA).

5.2.3 Collagen matrices

5.2.3.1 Acellular matrix

To prepare enough acellular collagen matrix for six 24 mm transwell inserts the following components were mixed in order; 0.6 mL 10x Minimum Essential medium with Earls Salts (MEM) (Sigma Aldrich, USA. Cat #0275), 54 µL 200 mM L-glutamine, 0.68 mL FBS, 187 µL Sodium Bicarbonate (Sigma Aldrich, USA. Cat #6014) and 5 mL of bovine type 1 collagen (Thermo Fisher Scientific, USA. Cat #1064401).

5.2.3.2 Cellular matrix

To prepare enough cellular collagen matrix for a 6-well plate with 24 mm transwell inserts the following components were mixed in order; 1.8 mL 10x MEM with Earls Salts, 163 µL 200 mM L-glutamine, 2.02 mL FBS, 56 µL sodium bicarbonate, 15 mL of bovine type 1 collagen and 1.65 mL of HDF suspended in FGM at a cell density of 3 x 10^5 cells / mL.

5.2.4 Alvetex scaffold skin equivalent model

The following methods describe the development of a skin equivalent model which used an Alvetex scaffold to support dermal fibroblast growth within its structure.

5.2.4.1 Preparing scaffold of cell culture

Before seeding cells onto the scaffold, the scaffold was treated in order to render it hydrophilic. This was done by adding 5 mL of 70 % ethanol to each well until the scaffold was fully immersed. After 5 minutes, the ethanol was aspirated and replaced with 7 mL of PBS for 1 minute. The PBS was then aspirated and again 7 mL of fresh PBS was added to each well. After hydrating the scaffold with ethanol the scaffold was then coated in collagen to allow for the cells to adhere. Bovine Collagen Type II was mixed with cell culture grade water to achieve a final concentration of 0.8 mg / mL (w/v), chilled pipettes were used in order to prevent gelling of the collagen and the collagen was handled on a bed of ice. The PBS was then aspirated from the scaffold and 500 µL of diluted collagen solution was added to each scaffold, at which point the plate lids were replaced and the coated scaffolds left to stand at room temperature for 1 hour. After 1 hour the plates were gently tapped on a workbench to remove excess collagen which was then and aspirated and discarded.

5.2.4.2 Seeding fibroblasts

HDF were grown in FGM so that they achieved 100 % confluency on the day of seeding to the scaffold. At which point the FGM was aspirated from the T75 flask which was then washed with 7 mL of PBS. 7 mL of 0.25 % Trypsin/EDTA (Thermo Fisher Scientific, USA. Cat #25200056) was then added and each flask was returned to the incubator at 37 °C and 5% CO_2 for 5 minutes. Once the cells had released from the bottom of the flask the trypsin was aspirated and added into a 15 mL centrifuge tube. A 7 mL aliquot of fibroblast culture media was added to each flask to collect the remainder of the detached cells and this medium was then added to the centrifuge tube in order to neutralise the trypsin. An aliquot of 20 µL was taken from the cell suspension and added to a 100 µL micro centrifuge tube, to

which 20 µL of trypan blue solution (Thermo Fisher Scientific, USA. Cat #15250061) was added and the solution was titrated to ensure a homogenous solution. A 10 µL aliquot of this solution was then transferred to a haemocytometer and a cell count performed under an optical microscope to determine the concentration of cells in the cell suspension. Once the number of cells in the cell suspension had been calculated the cell suspension was centrifuged for 3 minutes at a relative centrifugal force (RCF) of 220. After which the supernatant was discarded and the cell pellet was re-suspended in with FGM to achieve a cell density of 1 x 10^7 cells / mL. An aliquot of 100 µl (1 million cells) of this fibroblast suspension was then seeded onto each insert and incubated for 1 hour at 37 °C and 5% CO_2. After 1 hour, 6 mL of fibroblast culture medium was added so that the scaffolds were fully immersed. The fibroblasts were then cultured for 1 week replacing the media every other day.

5.2.4.3 Seeding keratinocytes

NHEK were grown in KGM so that they were 90 % confluent on the day of seeded to the scaffold, at which point the NHEK were counted and re-suspended to a concentration of 5 x 10^6 cells / mL, then 100 µl (500,000 cells) were seeded onto each scaffold and incubated for 1 hour at 37 °C and 5% CO_2 to let the NHEK fully adhere. After 1 hour, 6 mL of KGM was added to each well to submerge the scaffold. The KGM media was replaced daily for 3 days after which it was replaced with 4 mL of cornification medium to the outside of the well so that it just touches the bottom of the insert in order to achieve an air liquid interface. The skin models were then maintained at air liquid interface for an additional 2 weeks until fully mature, changing the cornification medium every other day.

5.2.5 Histological analysis of skin equivalent

After two weeks of culture at air liquid interface the skin equivalent models were ready to harvest for histological analysis in order to visualise the cross section of the skin and determine if a physiologically accurate structure of the dermal and epidermal components had developed.

5.2.5.1 Fixing and dehydrating the tissue

First the cornification medium was aspirated from the skin models which was then washed with 5 mL of PBS a total of 3 times. After which the insert was removed from the well and using a surgical scalpel and the polystyrene transwell membrane was carefully separated from the acellular collagen layer. The excised tissue was then placed in a plastic tissue cassette and immersed in 10 % (v/v) formalin (Thermo Fisher Scientific, USA. Cat #5735) for 1 hour. Following this the sample was dehydrated by immersing in ethanol gradations, 70 %, 80 %, 90 %, 95 % and 100 % for 3 minutes each, with the final 100 % ethanol step being repeated. Then sample was then immersed in 100 % xylene twice for 30 minutes.

5.2.5.2 Embedding processed tissue

In order to section the tissue on a microtome it must be embedded in a block of paraffin wax. Firstly an appropriately sized histology mould was selected and filled with liquid paraffin from a wax dispenser. In order to obtain cross sectional sections the tissue was cut into 2 mm wide strips which were then oriented on their side and place into the histology tray containing liquid paraffin after which a plastic tissue cassette was then placed on top of the histology mould and additional paraffin wax was poured onto top. The histology mould was then placed on a bed of ice to cool and solidify. After 24 hours the block was completely solidified and excess wax was trimmed using a surgical scalpel.

5.2.5.3 Sectioning embedded tissue on microtome

In order to observe the tissue under a microscope it must be cut into micrometre thin sections using a microtome. Firstly the paraffin block containing the embedded tissue was placed into the microtome chuck then the blade distance was adjusted until the blade was in close proximity to the block. The block was then adjusted in the chuck using the fine tuning knobs until the block was parallel to the blade to ensure a uniform thickness section. The microtome was then set to 20 µm and the initial paraffin was trimmed away until the tissue became exposed at which point the thickness was reduced to 4 – 5 µm and thin sections were made. Each of these thin sections were carefully placed into a water

bath using forceps and a brush, taking care not to fold the section. After which the sections could be transferred from the water bath to a positively charged glass slide by immersing the slide into the water bath close to the section, angling the slide under the section, and lifting the slide slowly out of the bath so that the section adheres to the slide. At this point the slides were then dried in a slide dryer for several hours.

5.2.5.4 Staining tissue with haematoxylin and eosin

Once the samples had been embedded in paraffin wax then sectioned, the wax was removed from the sections and the sample rehydrated to allow the stain to penetrate the tissue. This was done by placing the slides in a slide rack and immersing them in 100% Xylene for 5 minutes, followed by 100%, 90% and 70% ethanol for 5 minutes each. Once the samples have been rehydrated they were then stained by immersing them in Haematoxylin (Thermo Fisher Scientific, USA. Cat#6766009) for 2 minutes then rinsed in running tap water, followed by Eosin (Thermo Fisher Scientific, USA. Cat #6766009) immersion for 1 minute and again rinsed under running tap water. Finally the samples were dehydrated again by immersing in 70%, 90% and 100% ethanol for 2 minutes each followed by xylene for another 2 minutes after which the slides could be mounted by placing a drop of mounting medium onto the slide and covering with cover glass.

5.2.6 Collagen-based skin equivalent

The following methods describe the development of a skin equivalent model which uses a collagen matrix impregnated with human dermal fibroblasts to similar the dermal component of native skin. Keratinocytes were then seeded onto of the collagen based dermal matrix and differentiated in order to develop a fully keratinized epidermidis *(figure 5.1).*

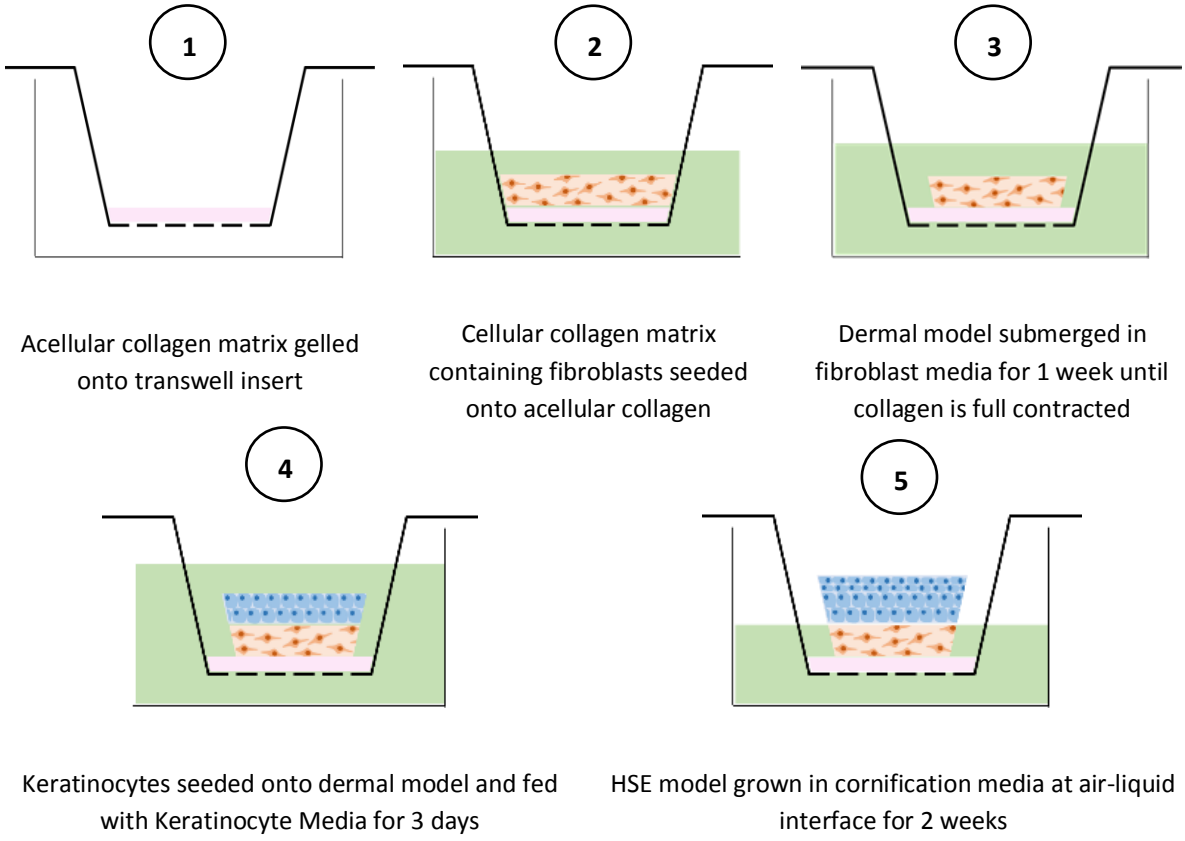

Figure 5.1: Five stages of developing a collagen-based full thickness human skin equivalent model.

5.2.6.1 Aceullar matrix

The dermal component of the skin equivalent model consisted of an acellular layer of collagen, which acted as an attachment substrate for the cellular collagen layer fabricated above it. To prepare the acellular collagen matrix the components listed in *section 5.2.3.1* were combined in order.

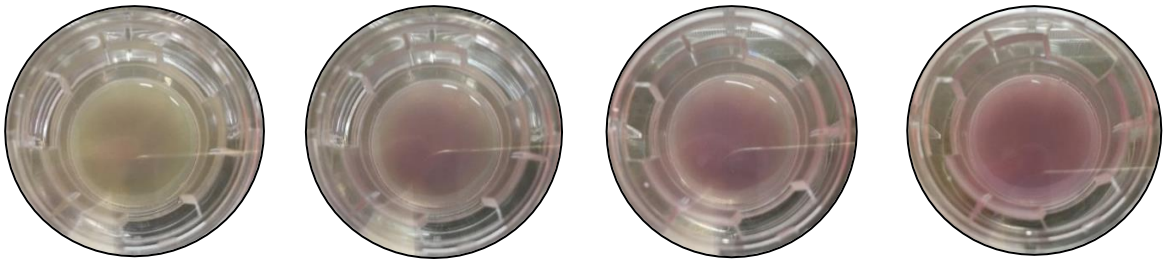

Figure 5.2: Acellular Collagen Layer Colour Change during gelation. - Once the collagen matrix had turned a uniform pink colour it is fully gelled and ready for the cellular matrix to be added

5.2.6.2 Cellular matrix

Once the acellular matrix was fully gelled, the cellular matrix was prepared. The components listed in *section 5.2.3.2* were combined in order again using a bed of ice and chilled pipettes to prevent early gelation. The HDF were trypsinised, counted and re-suspended to a cell density of 3 x 10^5 cells / mL and were added to the mixture last, the mixture was then gently triturated to evenly incorporate the cells, being carefully to avoid creating air bubbles. An aliquot of 3 mL of the cellular matrix was added to each transwell insert, and the 6-well plate was immediately returned to the incubator for 30 – 60 minutes at 37 °C and 5 % CO_2. Once the mixture had completely gelled and turned pink the gels were fed with 4 mL of FGM, adding 3 mL to the outside of the insert and 1 mL directly on-top of the insert. The dermal models were then incubated for 5 - 7 days, replacing the medium every other day. During the first week of culture the gel will contract away from the transwell insert and form a plateau in the centre *(figure 5.3).*

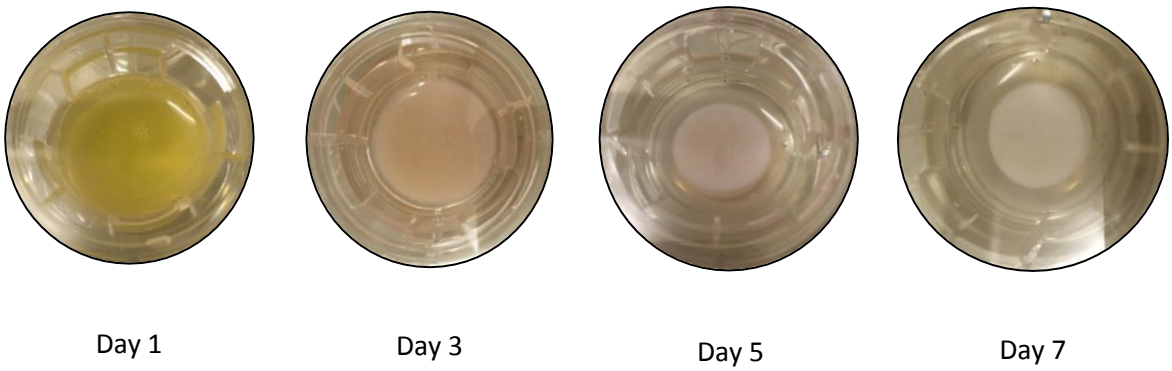

Figure 5.3: Images showing the colour change and contraction of the cellular collagen matrix over 1 week. Once the collagen matrix had fully contracted the epidermal keratinocytes could be seeded

5.2.6.3 Epidermal layer

NHEK were cultured in a T25 flask containing KGM media until 80% confluent, at which point they were trypsinized, ensuring the trypsin was neutralised with Trypsin Neutralising Solution (TNS) (Thermo Fisher Scientific, USA. Cat #002100), counted and re-suspended in KGM to a cell density of 3 x 10^6 cells / mL. An aliquot of 50 µl of the NHEK cell suspension was then transferred onto each transwell insert and left for 15 minutes without moving to allow the cells to attach to the surface of the dermal model. After which the 6-well tray was returned to the incubator for 1 hour at 37 °C and 5% CO_2 without any additional medium, allowing the NHEK to fully adhere in order to prevent the cells from being washed off when adding media. Once the cells had fully adhered 4 mL of KGM was added to the outsides of each well and 1 mL added on top.

As illustrated in *figure 5.4*, skin equivalents were fed every other day with epidermisation medium for 6 days. After day 6 epidermisation medium was aspirated and replaced with 5 mL of cornification medium added to the outside of the well only to achieve an air liquid interface. The air-liquid interface induces differentiation of the NHEK into distinct stratified epidermal layers. The skin models achieved full maturity after culturing for 2 weeks at air liquid interface.

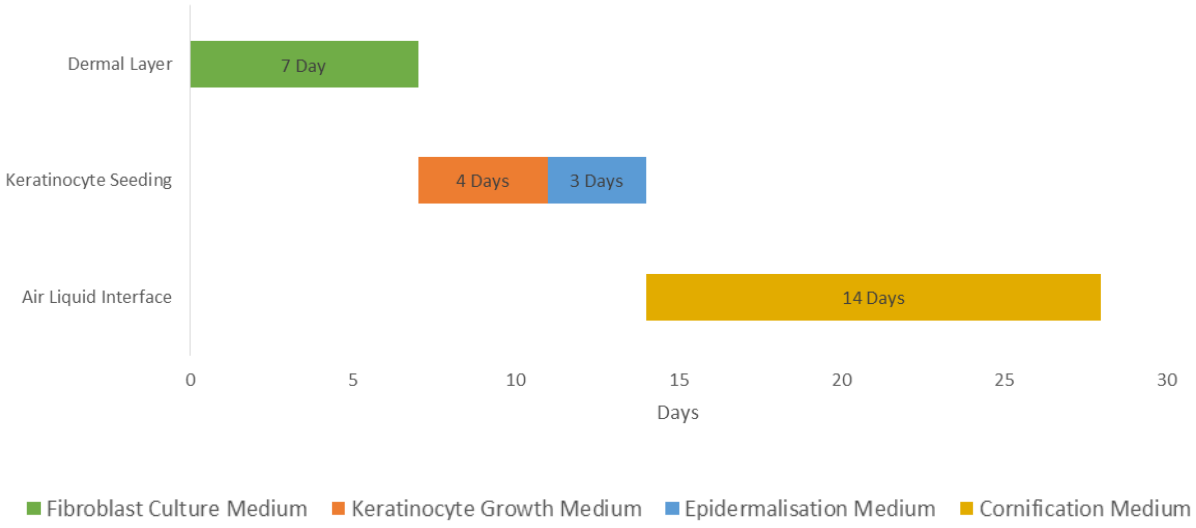

Figure 5.4: Timeline for Culture of Human Skin Equivalent

5.2.7 Pin machine study

In order to investigate the effect that pin movement has on the wound healing properties around the pin-site a human skin equivalent model was used in conjunction with the 'pin machine' described in *chapter 3*. By inserting the skin model into the pin machine and piecing the skin with a 1.8 mm external fixation pin (Orthofix, UK) an in vitro external fixation pin-site model was effectively developed. The design of the pin machine meant a deflection of 20 mm could be applied to the pin which translated to a movement of 1 – 2 mm across the pin-site at a frequency of 0.5 Hz.

5.2.7.1 Pin machine set-up

After 28 days of culture the skin models were fully matured with a fully formed epidermis, at this point the pin movement study was conducted. For each experiment 6 skin models were used, each sample was removed from the 6-well tray and placed into the aluminium wells of the pin machine. For 4 of these skin models a 1 mm surgical needle was used to puncture a hole in the centre, which a fixation wire was then implanted, ensuring it was pushed into the hole at the base of the aluminium well to create an interference fit. Two of this pins were connected to the pin machine to apply a mechanical movement, while two remained static and the unpierced skin models were left as control samples *(figure 5.5).* A displacement of 20 mm was applied to the dynamic pin which translated to a 1 – 2 mm displacement at the pin-site with a frequency of 0.5 Hz. Each aluminium well was filled with 10 mL of cornification media so that an air-liquid interface was achieved and the well was covered with a layer of Opsite (Smith & Nephew, USA) to maintain a sterile environment. Once the aluminium wells had been securely attached to the pin machine and the appropriate fixation wires connected to the pin machine, the linear actuator could be powered up to apply the mechanical movement to the pins and the whole machine was then placed in an incubator at 37 °C and 5% CO_2. After 24 hours the pin machine was removed from the incubator and samples of the media from each well was collected.

This was done by attaching a 2 mL syringe to the stockcock of the aluminium well and turning the stockcock to the open position *(figure 5.6).* The syringe was then pulled to remove 2 mL of media from the well then pushed to return 1 mL of media, ensuring that any cytokines present in the media were thoroughly mixed and a homogenous sample was taken. The remaining 1 mL of media was transferred to a 1 mL Eppendorf tube and frozen at – 80 °C until enzyme-linked immunosorbent assay (ELISA) analysis was conducted. After sampling the media 1 mL of fresh media was added back to the well to maintain the air-liquid interface and the pin machine was returned to the incubator for another 24 hours, at which point samples were taken again from each well, this was repeated 3 times for a total study duration of 72 hours.

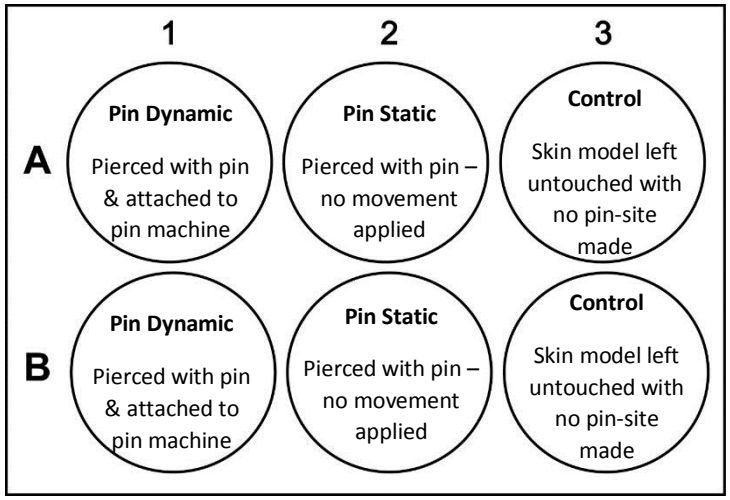

Figure 5.5: Layout of skin equivalent samples for pin machine study. A total of 3 independent variables were tested with replicates requiring a total of 6 skin equivalent models per study.

Figure 5.6: Images of pin machine during incubation and sampling of media from aluminium well. Skin models were placed in the aluminium wells and the skin pieced with a fixation wire. Notice the syringe attachment to the stopcock in order to sample media form below the transwell insert.

5.2.8 Enzyme –linked immunosorbent assay protocol

In order todetect and quantify cytokine production in the human skin equivalent models an enzyme-linked immunosorbent assay (ELISA) was used. Interleukin- 1 alpha (IL-1α), interleukin 8 (IL-8) and Tumor Necrosis Factor Alpha (TNF-α) were selected as the cytokines of interest as existing research has observed higher levels in non-healing wounds compared to healing wounds (Lindley *et al*, 2016) and can therefore be used as a reliable marker for determining the wound healing quality of the samples. Human IL-1 alpha (DuoSet ELISA. Cat #DY200-05), Human IL-8 (DuoSet ELISA. Cat #DY208) and Human TNF-alpha (DuoSet ELISA. Cat #DY210) were purchased from R & D Systems Inc, USA and each assay was performed following the manufactures recommendations.

Firstly for each cytokine measured the capture antibody was reconstituted in PBS to achieve the desired working concentration. A 100 µl aliquot of diluted capture antibody was then added to each well of a 96-well plate which was subsequently covered with parafilm and incubated overnight at room temperature. After incubation the capture antibody was aspirated from each well and each 96-well plate was washed by adding 200 µl of wash buffer (0.05% Tween® 20 in PBS) to each well and then aspirating the PBS a total of 3 times. After washing, the plates were then blocked by adding 200 µl of Reagent diluent (1% (v/v) Bovine Serum Albumin in PBS) to each well and incubating at room

temperature for a minimum of 1 hour. After which the plates were again washed thoroughly three times, using the method described previously. Once the plates had been blocked the standard was added to each well, each ELISA kit contained a recombinant cytokine with a known concentration, this standard was then reconstituted with 0.5 mL of reagent diluent and a two-fold serial dilution was performed for a total of 8 times and each serial dilution was then plated out in duplicates. Due to the low levels of IL-1α and TNF-α produced by skin equivalents reported in the literature and the large amount of media required to achieve air-liquid interface in the aluminium wells of the pin machine, effectively diluting any secretions from the skin equivalent, media samples used during the ELISA assays were not diluted and instead remained neat. After the samples and standards had been aliquoted to each well the plate was covered with a layer of parafilm and incubated at room temperature for 2 hours. Following two hours of incubation the samples and standards were aspirated and the plates were again washed three times in PBS. After which the detection antibody was reconstituted to the required working concentration and 100 µl was added to each well, again covering each plate with parafilm and incubating the plates at room temperature for an additional 2 hours. After 2 hours the plates were again washed 3 times and streptavidin-HRP was reconstituted to the required working concentration and 100 µl was added to each well, the plates were then covered in aluminium foil to avoid contact exposure to light and left at room temperature for 20 minutes. The plates were then washed again three times and the substrate solution was prepared by mixing equal amounts of Color Reagent A and Colour reagent B of which 100 µl was added to each well and again covered with aluminium foil and incubated for 20 minutes at room temperature. Finally the reaction was stopped by adding 50 µl of 2N sulphuric acid to each well, causing the substrate solution to turn from blue to yellow. At this point the absorbance of each well could be measured using a plate reader. The plate reader was programmed to shake the plates in order to ensure thorough mixing of the solutions, then the absorbance was measured at 570 nm and 450 nm, subtracting the former from the latter in order to correct for optical imperfections in the plate. This process was repeated a total of 3 times for each of the three pin machine experiments performing (n=3).

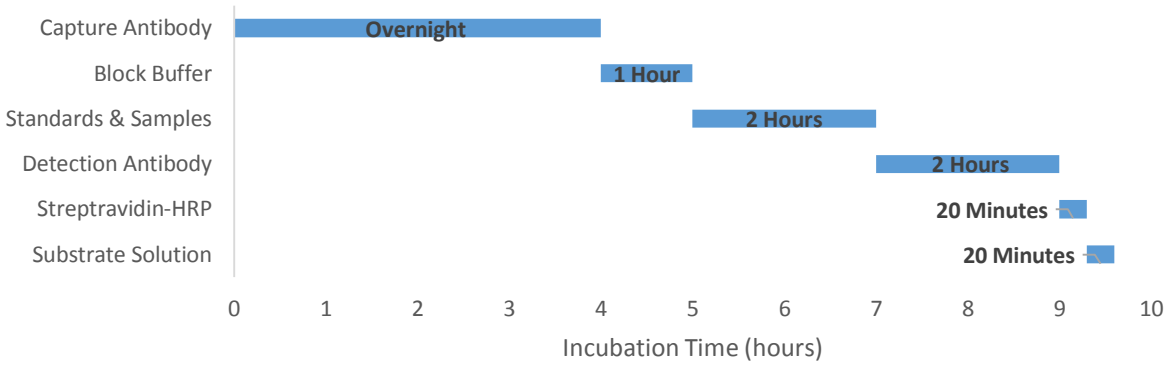

Figure 5.7: Timeline for ELISA assay – ELISA assays can be performed within 6-7 hours after plates have been coated with capture antibody.

5.2.9 Statistical tests

The data collected throughout this study was analysed for statistical significance using a two tailed, unpaired Student's t-test when comparing the difference between two group means. When comparing groups split on two independent variables a two-way analysis of variance was used. A P value of 0.05 was considered statistically significant.

5.3 Results

5.3.1 Histological analysis of dermal equivalent models

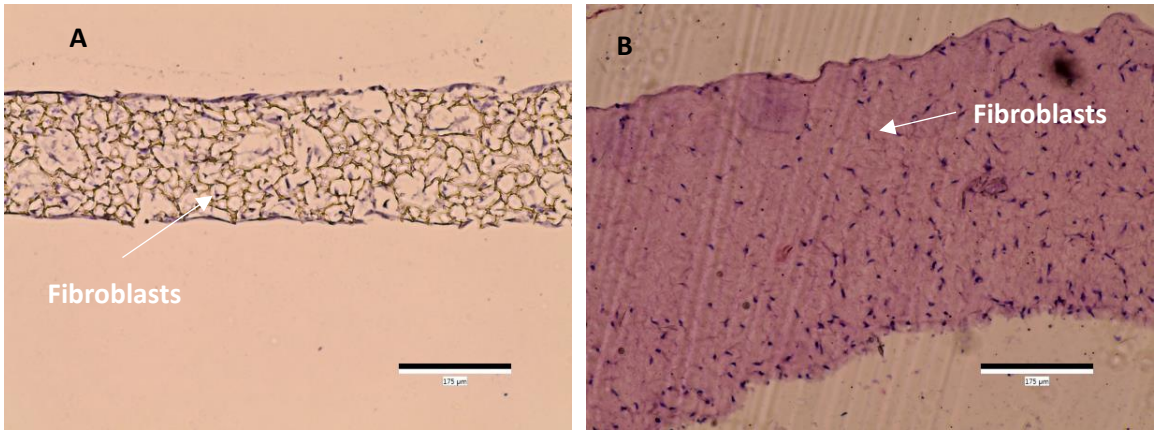

Figure 5.8: Photomicrograph of H&E stained dermal models – Alvetex scaffold containing fibroblasts (purple) can be seen in A. Collagen based dermal model with impregnated fibroblasts can be seen in B.

From the resultant histological images it was realised that the Alvetex scaffold would not provide the thickness required of the human skin equivalent to create a substantial pin-site. Instead, the thickness of the Alvetex dermal equivalent model was in the range of < 1 mm *(Figure 5.8a)* while the thickness of the dermis in vivo is reported as 2.56 ± 0.39 mm (Annaidh *et al*, 2012). *Figure 5.8b* shows a section of the collagen matrix approximately 500 µm thick, as indicated by the scale bar. Although this is significantly less than the reported in vivo dermal thickness of 2.56 ± 0.39 mm the skin equivalents must be fully dehydrated during the histology process, although this didn't have much effect on the polystyrene based Alvetex scaffold, the collagen matrix reduced in thickness considerably compared to the thickness during culture, which was manually measured using Vernier callipers as 1.87 ± 0.21 mm. Therefore the collagen matrix model was adopted for the full thickness skin equivalent as the increased thickness resulted in a more substantial pin tract, which more closely resembled pin-tracts seen in vivo.

5.3.2 Full thickness human skin equivalent

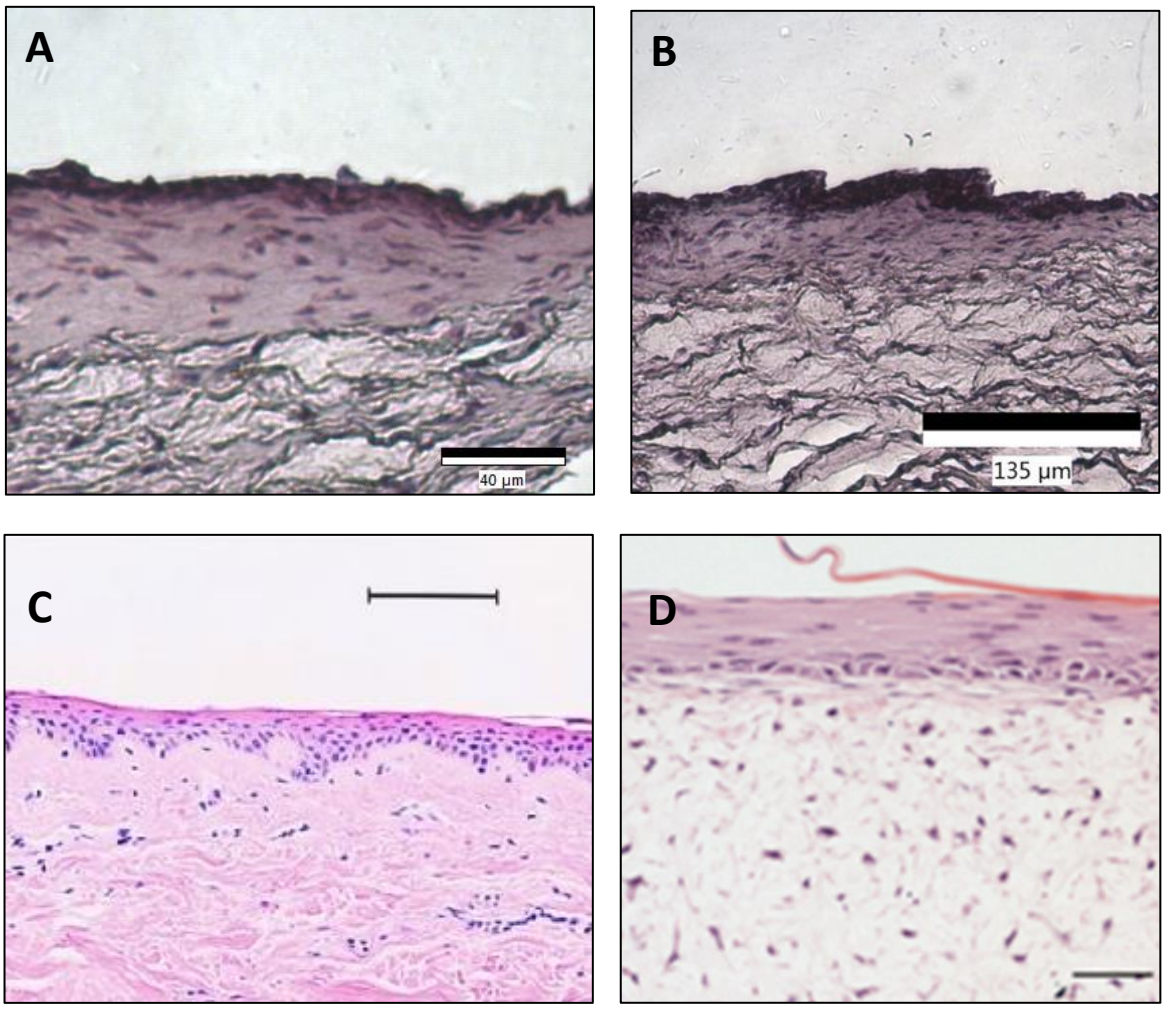

Figure 5.9: Comparison of H&E stained skin equivalents to healthy human skin and Alvetex scaffold based skin equivalent. Images A & B shows 5 µm sections of the collagen based full thickness human skin equivalent stained with H&E. Image C shows H&E stained sections of healthy native skin obtained from abdominoplasty – Scale bar 100 µm (Dabboue *et al*, 2015). Image D shows H&E stained section of skin equivalent developed using Alvetex Scaffold – Scale bar 50 µm (Reprocell ©, USA)

Histological analysis demonstrated that the collagen based skin equivalent retained the morphological characteristics of normal native human skin. *Figure 5.9 A & B* show a section of the skin equivalent stained with haematoxylin and eosin (H&E) which can be compared to the H&E stained section of native human skin (C) (Dabboue et al. 2015). Both the skin equivalent and native skin display a similar cellular structure, consisting of distinct dermal and epidermal layers. The dermal layer consists of long collagen fibres (pink) impregnated by fibroblasts (dark purple / blue) and the epidermal layer showing several layers of keratinocyte cells (dark purple / blue). As a result it can be confirmed that the skin

equivalent accurately simulates the physiology of native human skin and therefore it may be assumed that any subsequent findings obtained from studying these skin equivalents will be similar to those performed on ex vivo skin.

5.3.3 ELISA analysis

5.3.3.1 Standard curves

Figure 5.10 shows the standard curves plotted for each cytokine studied. Each standard concentration was measured in duplicates and the optical density measured, the absorbance at 570 nm was subtracted from the absorbance at 450 nm to correct for any imperfections in the plate. The average absorbance was then plotted against cytokine concentration to find the line of best fit. Since the lines of best fit follow a sigmoidal shape, a four parameter logistic regression model was the used to determine the curve equation, in order to convert between absorbance and cytokine concentration.

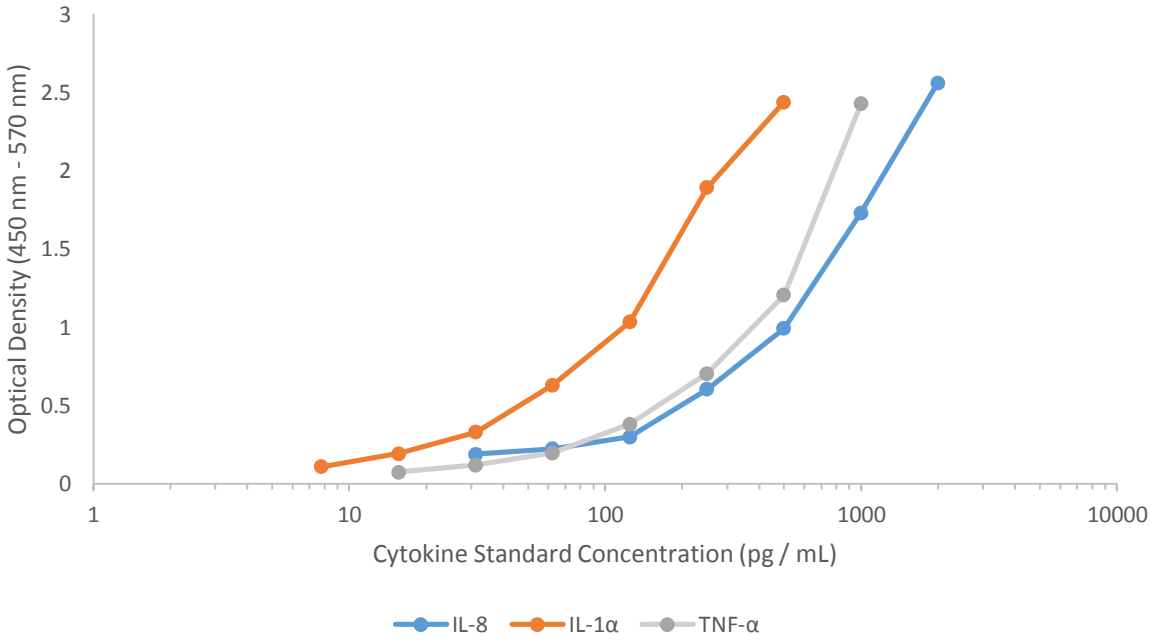

Figure 5.10: Standard curve for IL-8, IL-1α and TNF-α – Standard curves were measured in duplicates in concentrations ranging from 7.8 – 2000 pg/mL

5.3.3.2 Absorbance readings of each ELISA assay

In order observe the change in Il-1α, IL-8 and TNF-α cytokine production by the skin equivalents over 72 hours, media was collected from each sample every 24 hours and ELISA analysis was conducted. *Figure 5.11 – 5.13* presents the absorbance readings of IL-1α, TNF-α and IL-8 for the control, static and dynamic pin samples over the 3 day experiment duration. All variables tested increased in cytokine production from day 1 to day 3, however absorbance levels at day 1 and day 2 were close to or below the detectable limit for all three cytokines measured. On all 3 days the absorbance values indicate that IL-8 concentration increased compared to control when a static pin was implanted into the skin equivalent, the absorbance reading further increased when movement was applied to the pin. This same result was observed for IL-8 on day 3 only, but no such effect was observed for TNF-α.

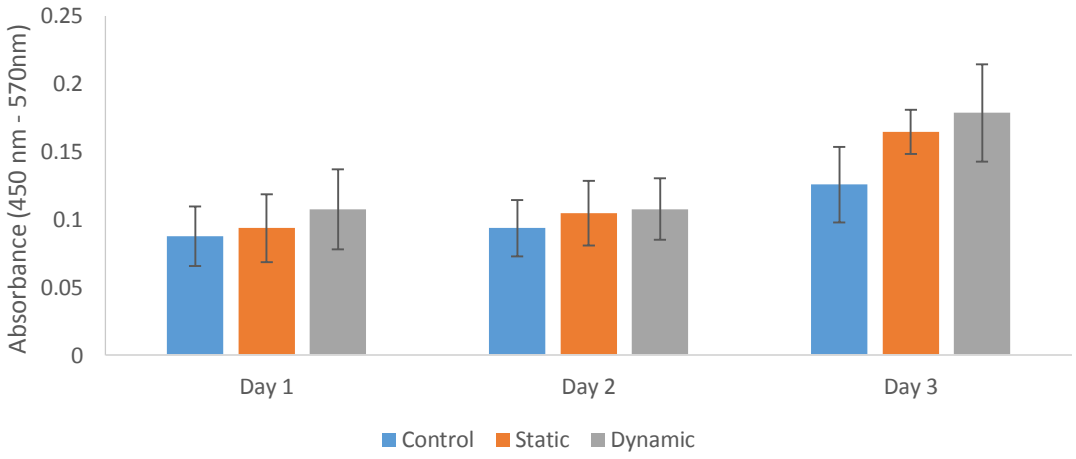

Figure 5.11: Absorbance readings for IL-1α ELISA assay. Error bars represent the standard deviation from the mean (n=3)

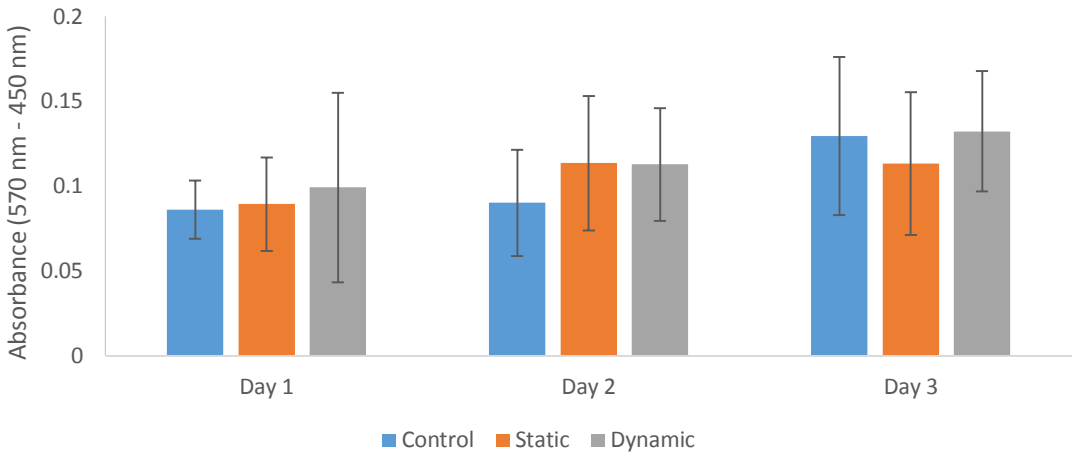

Figure 5.12: Absorbance readings for TNF-α ELISA assay. Error bars represent the standard deviation from the mean (n=3)

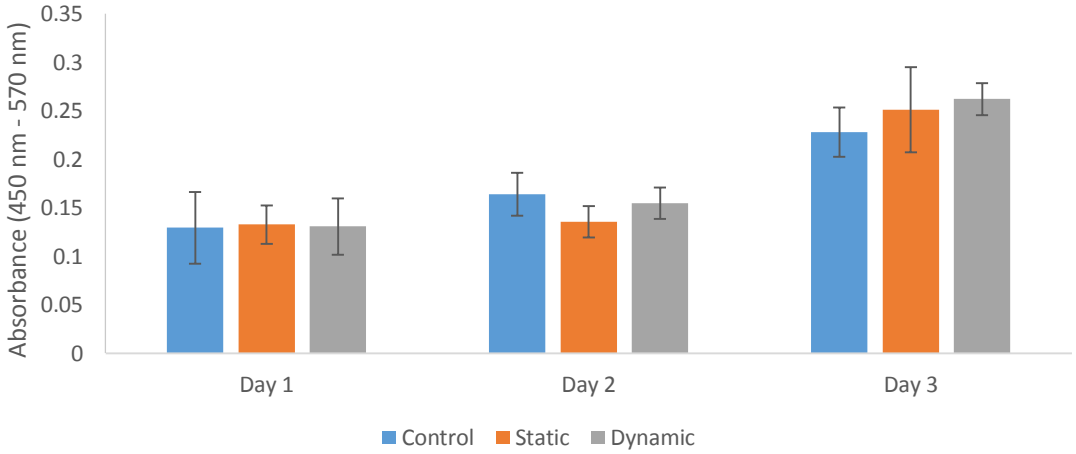

Figure 5.13: Absorbance readings for IL-8 ELISA assay. Error bars represent the standard deviation from the mean (n=3)

5.3.3.3 Cytokine concentration

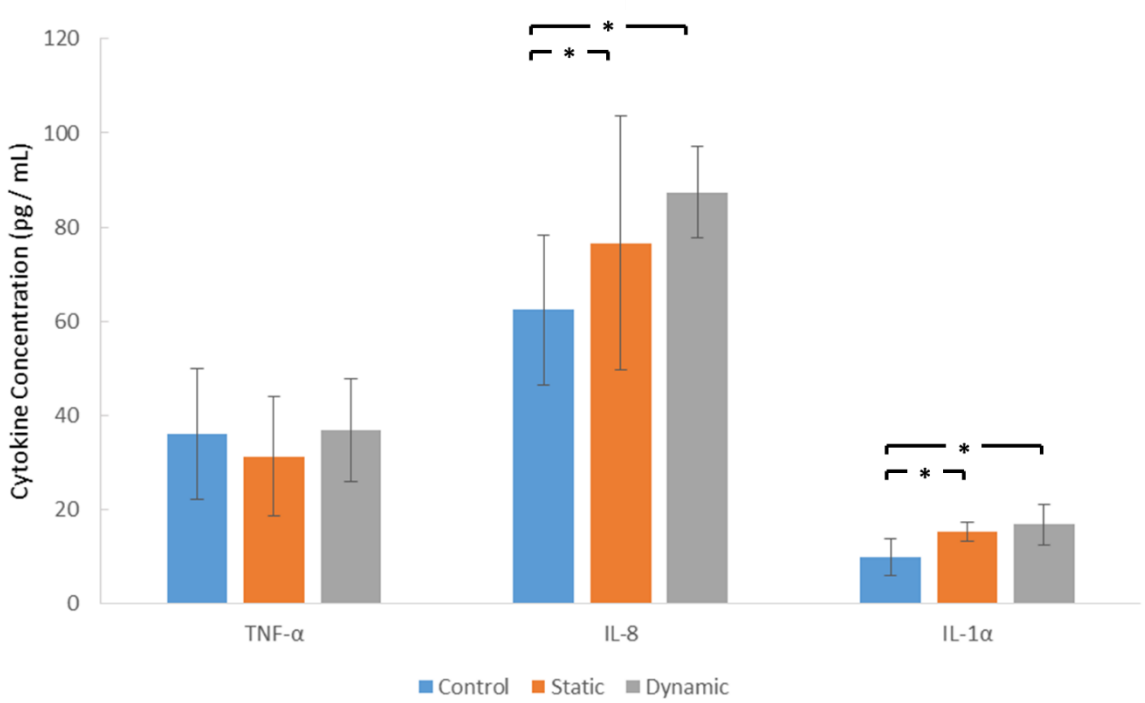

Figure 5.14: Expression of TNF-α, IL-8 and IL-1α on Day 3 - A significant increase in IL-8 and IL-1α expression was observed in both the static and dynamic samples compared to control ($p<0.05$)

Cytokine concentration was calculated from the absorbance values using the standard curves described in *section 5.3.3.1*. Expression of the cytokine IL-8 was significantly greater than the expression of TNF-α and IL-1α for all sample variables ($p<0.001$) while the expression of IL-1α was the lowest among all samples. Production of IL-8 from the skin equivalent models increased on average by 18.6 % when a static pin was introduced ($p<0.05$) and increased further by an average of 12.3 % when movement was applied to the pin ($p<0.05$) compared to control. A similar result was observed for IL-1α where by the concentration increased on average by 35% when a static pin was implanted ($p<0.05$) and a further 10% when movement was applied to the pin ($p<0.05$).

5.4 Discussion

As hypothesised, concentrations of IL-1α showed an increase compared to the control when a static fixation pin was implanted into the skin equivalent, with a further significant increase in the dynamic pin sample ($p < 0.05$). A similar effect was observed for IL-8 only on day 3 ($p < 0.05$) and for TNF-α on day 1 and 2 however no statistical significance was found between these two results. However, for all pro-inflammatory markers measured, concentrations on day 1 and 2 fell below the detection limit of the ELISA. This is most likely due to the large quantity of media required to achieve air-liquid interface in the pin machine during the experiment, meaning any cytokines expressed by the skin equivalents were highly diluted before the media sample was collected. This could be corrected by a re-design of the aluminium wells to reduce the volume required to achieve an air-liquid interface, although this would affect the anatomical accuracy of the pin machine as the wells had been designed so that the distance from the skin surface to the base of the well represents the thickness of soft tissue between the bone and skin interfaces in vivo.

By day 3 expression of all cytokines reached a detectable limit *(figure 5.14)* with the highest concentration seen in IL-8 followed by TNF-α and IL-1α. These results reflect those reported in the literature, Reijnders *et al* conducted ELISA analysis on skin equivalents cultured from both primary and immortalised cell lines after 24 hours of culture and while levels of IL-8 were measured to be 22.65 ± 12.77 pg / mL and 78.80 ± 8.93 pg / mL respectively, no detection of TNF-α and IL-1α was observed (Reijnders *et al*, 2015). Similarly Spiekstra *et al* measured the cytokine levels of ex vivo skin and observed IL-8 and IL-1α levels of 19.64 ± 13.51 and 22 ± 15 respectively, no levels of TNF-α were detected (Spiekstra *et al*, 2007).

From this study we can conclude that the presence of a static pin implanted into the skin equivalent initiates a delayed wound healing response, characterised by the increased production of pro-inflammatory markers which have been shown to be higher in non-healing wounds compared to healing wounds (Trengove *et al*, 2000). The most substantial increase was observed for IL-8, which is

known to influence the wound healing processes of proliferation and migration in keratinocytes, as well as reducing fibroblast associated contraction (Kirker *et al*, 2012), an effect that can be observed in the contraction of the skin equivalent model during the first week of culture *(figure 5.3).*

What is more, the levels of IL-8 and IL-1α increased further in the dynamic sample compared to the static sample ($p<0.05$) indicating that movement of the fixation pin has a negative effect on the wound healing response. Since there is a relationship between pin-site healing and infection, whereby delayed healing leads to an increase risk of infection, it can be said that our results agree with the anecdotal evidence reported throughout the literature that minimising pin movement is a key factor in minimising pin-site infection in external fixation. Although our findings do not offer a solution for reducing the risk of infection by minimising pin-site movement, our in vitro model provides the framework for future studies to investigate the efficacy of pin-site care treatments aimed at minimising pin movement, such as compressive dressings and bungs.

Histological analysis of the skin equivalents verified the development of distinct epidermal and dermal layers, containing primary human dermal fibroblasts and epidermal keratinocytes respectively. Comparison to H&E stained native human skin sections confirmed that our skin equivalent provided a similar cellular structure and is therefore an adequate alternative to ex vivo skin for studying the response of skin to a given treatment. For our application of applying mechanical loading to the skin equivalent and measuring the wound healing response a physiological relevant of the model to in-vivo skin was required in both the biological and mechanical domains. For this reason the Alvetex scaffold was initially adopted for the dermal structure rather than a collagen matrix as the Alvetex scaffold has been measured to have a Young's modulus of 77 kPa (Lai *et al*, 2012) similar to that of skin in vivo (Sanders, 1973). The Alvetex scaffold was seeded with fibroblasts and cultured for 1 week at which point histological analysis was performed. However after this first study it was realised that the Alvetex scaffold will not provide the thickness required of our human skin equivalent to produce a substantial pin-site tract without causing unwanted tearing of the skin equivalent. Instead, the thickness of the

Alvetex dermal equivalent model was in the range of < 1 mm *(figure 5.8)* while the thickness of the dermis in-vivo is reported as 2.56 ± 0.39 mm (Annaidh *et al*, 2012). For this reason we adopted the collagen based skin equivalent model which provided a much thicker sample (1.87 ± 0.21 mm), which if necessary could be further customised by increasing the volume of collagen used during culture.

Throughout the literature many have commented that pin movement is an important factor in determining whether a pin-site will become infected. This has led to a consensus regarding the use of compression dressings and bungs applied to the pin-site in an attempt to minimise this movement. However as of yet no research has been conducted into characterising the role of pin movement and its effect on the development of pin-site infection. This study demonstrates for the first time using a validated in vitro model that there is an effect of mechanical motion to wound healing. Several studies that have investigated pin-site infection, have utilised either clinical or animal models. These studies often fail to produce compelling findings, either due to intrinsic differences among subjects in factors such as skin type and immune response or in the case of clinical pin-site care studies, the high number of variables between care methods makes it difficult to evaluate the efficacy of a given treatment. A novel validated application for human skin equivalents has been presented which investigated the biological response to a mechanical stimuli, the model can therefore be used to investigate various clinical practices such as the use of pressure dressings and alcohol/chlorohexidine solution on the wound healing process.

Chapter 6: The Effect of Biofilm and Planktonic Media on the Wound Healing Properties Human Dermal Fibroblasts

6.0 Introduction

Wound healing of the skin is a complex process involving cellular proliferation, migration and tissue remodelling leading to reestablishment of its primary function. In the case of pin-site wounds the goal of wound healing is to facilitate the growth of a collagen shell around the pin site isolating it from the host. Shortly after wounding fibroblasts migrate into the wound site and proliferate, the repair phase of wound healing. They synthesize growth factors and extracellular matrix (ECM) molecules, mainly collagen and fibronectin which provide structural integrity to the wound and form wound granulation tissue (Clark, 1989).

If a wound becomes infected the wound healing process is delayed, however the mechanisms of delayed wound healing due to biofilms are poorly understood (Zhao *et al*, 2010). Therefore minimising pin-site infection involves not only preventing the colonisation of the pin-site by infectious bacteria but also providing adequate healing of soft tissue around the pin-site. The bacteria most commonly isolated from pin-site wounds differs from those associated with internal implants such as hip replacement prosthesis, as pin-site infections usually originate from commensal bacteria from the skin flora, most commonly *S. epidermidis* and *S. aureus* (Mahan *et al*, 1991). Of these two bacteria, *S. epidermidis* is a greater slime producer, capable of producing extracellular matrix to form biofilms on implant surfaces while *S. aureus* has a much greater virulence due to its ability to produce a wide variety of tissue damaging toxins.

The most commonly used model to study wound healing in vitro is the 2D scratch wound assay. An in vitro scratch assay is a relatively straightforward and economical method for studying cell migration and wound healing. It is also probably the simplest method to study cell migration as it uses common and inexpensive supplies found in most laboratories capable of cell culturing. Most 2D wound healing assays involve 3 basic steps, cell wounding, monitoring the healing process and data acquisition and evaluating the data (Stamm *et al*, 2016). By creating a gap in a confluent monolayer of epithelial cells to represent a wound, the cells on the edge of this gap then begin to migrate in

an attempt to close the gap, mimicking the migration of cells in vivo. Images can be taken at regular intervals either manually or using time-lapse microscopy to perform live-cell imaging during the cell migration study in order to observe the gap closure. These images can then be qualitatively observed or image processing software can be used to measure the rate of cell migration. The difficulty of these models lies in creating constant scratches across the monolayer as migration rate is partially dependant on the gap width, therefore a significant variation in gap width among samples may reduce the reproducibility of the study. There are several 'cell wounding' methods that can be used in order to create a consistent scratch. The most common and simplest method is mechanical wounding of the cells by creating a scratch using a sharp object such as a pipette tip (Liang *et al*, 2007), however other scratching devices are available such as cell scrappers (Doyle *et al*, 2012; Zhang *et al*, 2013), metallic micro-indenters (Topman *et al*, 2012) and toothpicks (Klettner *et al*, 2014). The downside of these scratch methods is due to the difficulty in making consistent scratches with similar width across all samples as well as avoiding damaging the cell culture coatings on the bottom of the cell culture dish (Goetsch *et al*, 2011). Optical wounding via a laser beam can also be used to introduce a wound in a confluent cell monolayer, this offers high reproducibility as well as high throughput, however the equipment required to perform optical wounding is expensive and not commonly found in cell culture labs.

A considerable amount of in vitro studies have been conducted using single species bacteria cultures in planktonic form. However bacteria often exist in poly microbial communities containing anywhere from 2 to 5 different bacteria species (Wolcott *et al*, 2016) which results in significant pathological changes to the bacteria. In the case of external fixation the bacteria may also colonise the surface of the pins forming biofilms, characterised by the production of an ECM encapsulating the bacteria. These biofilms are phenotypically distinct from their planktonic counterparts (Resch *et al*, 2005) and are orders of magnitude more resistant to antibiotics and immune responses than planktonic bacteria due to the difficulty of antibiotics and immune response cells from penetrating the ECM to attack the bacteria forming the first few layers of the biofilm (Stewart *et al*, 2001). Several studies have previously

investigated the effect of biofilm conditioned media (BCM) and planktonic conditioned media (PCM) on wound healing, where the media from biofilm or planktonic cultures was sterile-filtered and added to healthy monolayer cells (scratch assays). Kirker *et al* developed a novel in vitro co-culture model for studying cell migration in the presence of a biofilm *(figure 6.1)* (Kirker *et al*, 2009). Biofilms were grown from methicillin-resistant *Staphylococcus aureus* (MRSA) onto tissue culture inserts which were then placed in a tissue culture plate containing a monolayer of primary human keratinocytes so that the membrane prevented the biofilm and keratinocytes from coming into contact. Kirker found that the biofilm prevented the closure of the scratch, demonstrating that the extracellular by-products released from the biofilm were preventing wound closure and therefore the biofilm itself did not need to be in direct contact to produce the same result.

Secor *et al* went on to analyse the extracellular proteins of *S. aureus* BCM and PCM using mass spectrometry and 1D gel electrophoresis. They found that the total protein concentrations of BCM and PCM were similar, however several glycolytic enzymes were found to be present in PCM and not in BCM. Cytokine production is also significantly different between biofilm and planktonic forms of the same species. Kirker *et al* demonstrated that PCM induced more interleukin-6, interleukin-8, vascular endothelial growth factor, transforming growth factor-β1, heparin-bound epidermal growth factor, matrix metalloproteinase-1, and metalloproteinase-3 production in fibroblasts compared to the BCM. While biofilm-conditioned medium induced more tumor-necrosis factor-α production (Kirker *et al*, 2012). These results show that metabolic processes vary between planktonic and biofilm cultures and that those different metabolic states may have a large impact on the pathology of *S. aureus* on tissue (Secor *et al*, 2011). However to date, there has not been a study on the effect of co-cultured poly microbial communities on wound closure.

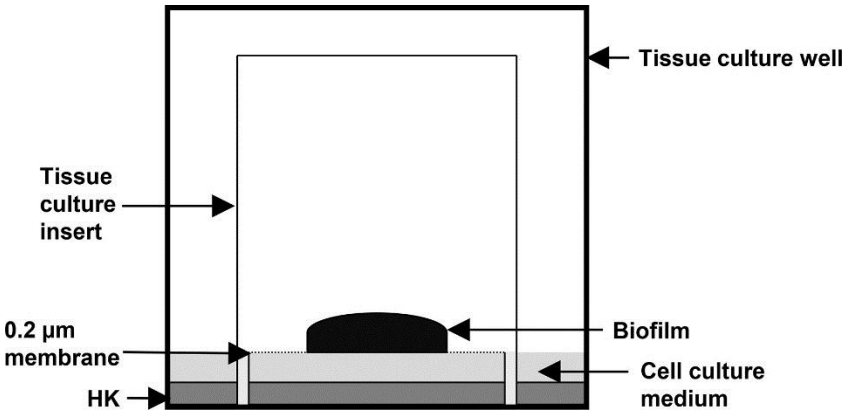

Figure 6.1: Diagram to illustrate the novel method for studying cell migration in the presence of biofilm. Biofilms grown on tissue culture inserts and co-cultured with a human keratinocyte (HK) monolayer grown on the bottom of a well plate (Kirker *et al*, 2012)

6.1 Aims and hypothesis

Since *S. aureus* and *S. epidermidis* are the most commonly isolated bacteria from pin-site wounds the following research aimed to study and compare the effects of these two bacteria in single species and in multi species culture in both biofilm and planktonic states.

The hypothesis for this study were:

1. Biofilm and Planktonic conditioned media will negatively affect the migration rate of fibroblasts compared to control
2. Multi species BCM and PCM will have a greater negative affect on the migration rate of fibroblasts compared to single species equivalents

6.2 Methods

6.2.1 Cell and bacteria species

Primary Normal Human Dermal Fibroblasts (HDF) isolated from normal human juvenile foreskin were (PromoCell USA, Cat #12302) grown in a monolayer. The bacterial species *Staphylococcus epidermidis* RP62A and *Staphylococcus aureus* NCTC 8325 were used throughout this study for the production of the planktonic conditioned media (PCM) and biofilm conditioned media (BCM).

6.2.2 Fibroblast growth medium (FGM)

Fibroblasts were cultured in fibroblast growth medium (FGM) containing serum-free, low glucose Dulbecco's modified Eagle medium (DMEM) (Thermo Fisher Scientific, USA. Cat #11054020) supplemented with 10% (v/v) foetal bovine serum (FBS) (Thermo Fisher Scientific, USA. Cat #16000044), 8mM Hepes (Sigma Aldrich, USA. Cat #83264), 10, 000 U/mL^{-1} penicillin and 10, 000 $\mu g/mL^{-1}$ streptomycin (Thermo Fisher Scientific, USA. Cat #15140122).

6.2.3 Fibroblast culture and scratching monolayer

HDF were cultured in FGM until they reached a cell density of 2 x 10^6 cells / well or 1 x 10^6 cells / well for either 6-well plate or 12-well plate respectively. The well plates were then incubated at 37 °C and 5% CO_2 overnight until they had reached 100% confluency. A 100 µL pipette tip was used to lightly scrape across the surface of each well to create the scratch. The quality of the results obtained from scratch assays lies in the uniformity of the scratch across all samples, therefore a sterile rule was used as a guide when making the scratches in order to produce straight scratches that were centred to the well. After scratching the media was aspirated and each well was washed with 2 mL of PBS a total of 3 times, following which 3 mL of fresh FGM was added.

6.2.4 Bacterial starter culture

Starter cultures were prepared by inoculating 10 mL of nutrient broth (Oxoid Ltd UK. Cat #0003) with 1 single colony of either *S. epidermidis* or *S. aureus*. This inoculum was incubated at 180 revolutions per minute (RPM) for 6 – 12 hours at 37 °C. Following this incubation period the optical density was measured and compared to the standard growth *curve (figure 4.6)* in order to determine the concentration of viable bacteria in each culture and to ensure the culture is in the logarithmic phase of its growth. Once the bacterial suspension had reached the logarithmic phase, the optical density of the culture was measured from which the cell density in CFU / mL could be estimated using *(figure 4.7).*

6.2.5 Biofilm conditioned media (BCM)

A starter culture of *S. aureus* and *S. epidermidis* was cultured for 24 hours from a single colony in nutrient broth. After 24 hours the optical density at 600 nm (OD600) of the starter culture was measured and if necessary diluted to achieve an OD600 of 1.0. An aliquot of 1 mL of this bacterial solution was then seeded onto each membrane of a 6-well plate transwell membranes and incubated at 37 °C for 1 hour. After 1 hour, 1.5 mL of nutrient broth was added to the outside of each transwell and 0.5 mL added gently on top of each membrane and incubated at 37 °C. After 24 hours the media was aspirated and replaced with fresh nutrient broth, this was repeated every 24 hours for 3 days to ensure a mature biofilm had developed. After the 72 hour period, the nutrient broth was aspirated and replaced with 2 mL of antibiotic free FGM containing DMEM, 10% fetal bovine serum and 1% l-glutamine. 1.5 mL of FGM was added to the outside of each well and 0.5 mL on top. Every 24 hours the conditioned FGM was collected and fresh media added to each well. This was repeated for a total of 5 days, so that 60 mL of BCM media has been collected from each 6-well plate. After 5 days of collection, the BCM was pooled together and centrifuged for 10 minutes at 4000 RPM at 37 °C so that the bacteria formed a pellet at the bottom of the universal. The supernatant was then aspirated and filter sterilised using a 0.22 µm filter to obtain sterile BCM. To guarantee sterility, 100 µL of each media

was aliquoted onto nutrient agar and incubated for 24 hours, after which the plates were checked for any bacterial growth. For each repeat of the study (n=2) fresh BCM and PCM media was made for each bacterial species.

6.2.6 Planktonic conditioned media (PCM)

In order to have similar bacterial concentrations of PCM to BCM a starter culture was also grown from a single colony for 24 hours. After 24 hours the optical density was measured and the suspension diluted to achieve an OD600 of 1.0 to match that of the BCM starter culture. An aliquot of 6 mL of starter culture was then added to 12 mL of nutrient broth and after 24 hours the culture was centrifuged for 10 minutes at 4000 RPM and 37 °C to form a cell pellet of which the supernatant was discard. The cell pellet was then re-suspended in 12 ml of nutrient broth and incubated for another 24 hours, this process was repeated a total of 3 times over 72 hours, in order to replicate the 3 days given for the biofilm to form for the BCM. After 3 days of growth in nutrient broth the planktonic bacteria was centrifuged again and the supernatant discard and the pellet was then suspended in antibiotic free FGM. Following this every 24 hours for a total of 5 days the planktonic culture was centrifuged and re-suspended in 12 mL of fresh FGM and the supernatant was collected to later be pooled together and filter sterilised using a 0.22 µm filter to obtain sterile PCM. The sterility was checked by aliquoting 100 µL of each PCM on nutrient agar and incubated for 24 hours to observe if any colonies formed.

6.2.7 Cell IQ scratch assay experimental set-up

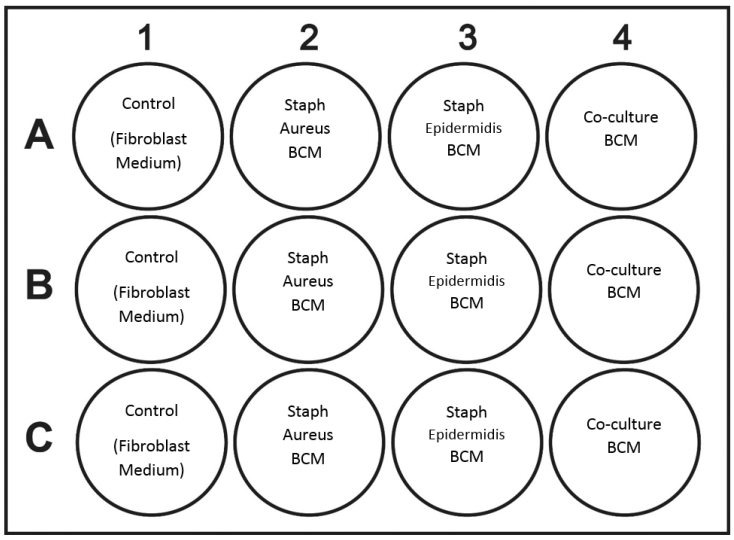

Figure 6.2: Example of 12-well plate layout for Cell-IQ study – Each sample was plated in triplicates with a control containing fibroblasts and fibroblasts growth medium only

For the conditioned media study each variable including the control samples were sampled in triplicates on the same well plate *(figure 6.2).* The plate was then placed into the Cell-IQ incubator and the gas outlet connected to the plate so that the plate remained in an environment of 37 °C and 5% CO_2 throughout the duration of the experiment. Each scratch was then imaged at a minimum of 3 different locations along the scratch, the results of which were averaged to give an average rate of wound closure per well. The average rate of wound closure for each triplicate was also averaged to give a final value of the wound closure for a given variable. The whole study was repeated twice whereby new bacterial cultures and new planktonic and biofilm medias were cultured for each study (n=2). Unfortunately technical issues with the equipment meant we were unable to conduct additional repeats of the experiment.

6.2.8 Image analysis (Cell-IQ analysis)

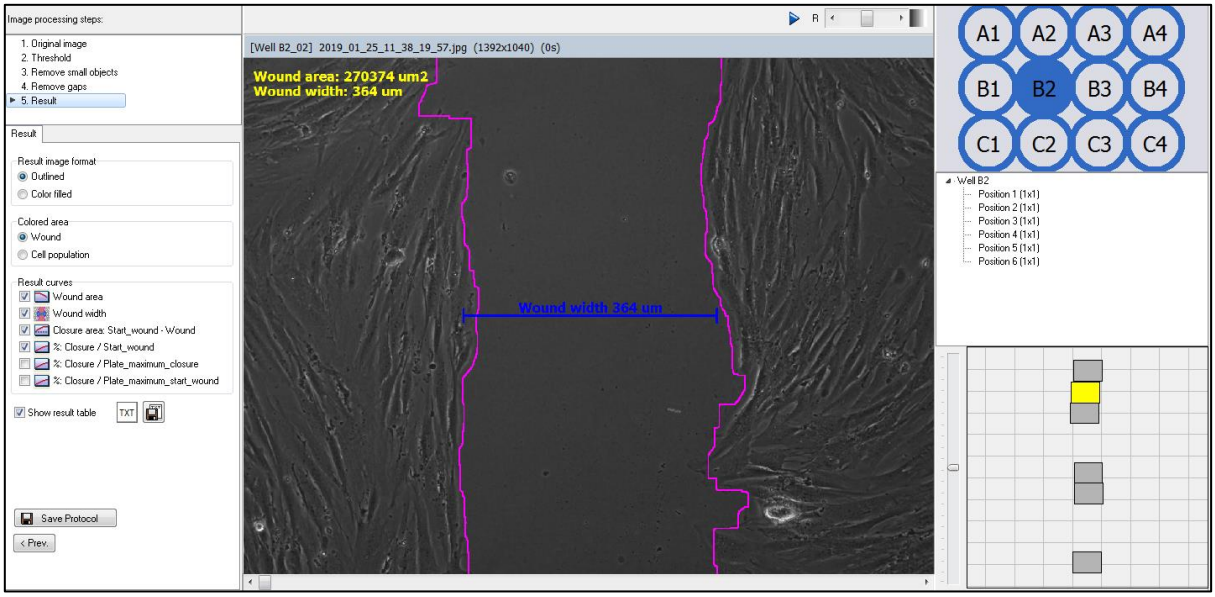

Figure 6.3: Cell IQ analysis software used to analyse the images taken during the conditioned media studies. For each well 3 locations were selected along the scratch (right hand toolbar) which were then averaged to find the average wound closure rate across the entire scratch. Various image processing parameters (left hand toolbar) were adjusted in order to increase the precision in wound edge detection.

The results from the BCM and PCM studies were analysed using the 'Cell-IQ Analyser' software. All images taken during the experiment were uploaded to the software, and the images were then analysed to detect the wound edges *(figure 6.3).* By adjusting various parameters in the left hand panel, the detection accuracy could be improved so that more precise measurements of wound width could be made. Once the parameters had been optimised, the settings were applied to all wells and the measurements of wound width and area were generated for every image over the 72 hour study. The software then presented these measurements in a spreadsheet whereby the wound width for each image location at 30 minute periods over the entire 72 hour experiment are listed. From this spreadsheet the wound width results for each image location from each well could be averaged, and then the triplicates for each variable measured were combined and averaged. This was repeated a total of 2 times on three separate days to achieve n=2 the results of which were again combined and averaged to give the final results for wound closure of each variable presented.

6.2.9 Cell viability assay

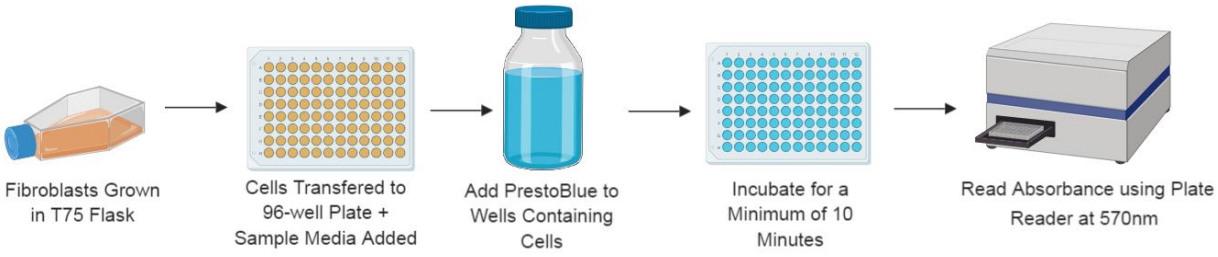

Figure 6.4: Flow chart to describe method for measuring cell viability using Presto Blue

HDF were cultured in T75 flasks then re-suspended in FGM to achieve a cell density of 5 x 10^4 cells / mL. From the cell suspension, 200 µL was aliquoted to 24 wells of a 96 well flat bottom microplate and the plate was incubated overnight at 37 °C and 5% CO_2. After which the media was aspirated from each well and 90 µL of the sample media along with 10 µl of PrestoBlue™ (Thermo Fisher Scientific, USA. Cat #13261) was added to each well as illustrated in *figure 6.4*. Two control samples were used during the cell viability assay in order to establish a baseline absorbance value to compare the absorbance values obtained from the BCM and PCM samples against. The positive control contained HDF cells in antibiotic free FGM, while the negative control contained absolute ethanol as this is known to produce apoptotic cell death. At 1, 6 and 24 hours exposure absorbance readings were taken at 570 nm.

Figure 6.5: Image illustrating the layout of the 96-well plate for studying cell viability. Each sample was plated out in triplicates along with 3 controls. Positive control containined fibroblasts in FGM only, negative control contained fibroblasts in absolute ethanol and an additonal control contanined FGM only with no cells.

6.2.10 Calculating rate of wound closure

One method for comparing the rate of cell migration between treatments groups is to calculate the time for each scratch to reach 50% wound closure. During the first 12 hours of study each scratch closes at a fairly uniform rate, therefore a linear trend line can be plotted and therefore the linear equation of the trend line can be calculated (figure 6.16). The gradient of the trend line represents the rate of wound closure of that sample. Therefore using equation (a), whereby 'Initial Wound Gap' is the wound width at hour 0, and |Gradient| is the absolute value of the gradient of the line.

$$t_{0.5} = \frac{Initial\ Wound\ Gap}{2 \times |Gradient|} \qquad \text{(a)}$$

6.2.11 Statistical Tests

The data collected throughout this study was analysed for statistical significance using a two tailed, unpaired Student's t-test when comparing the difference between two group means. When comparing groups split on two independent variables a two-way analysis of variance was used. A p value of less than 0.05 was considered statistically significant.

6.3 Results

6.3.1 Cell viability

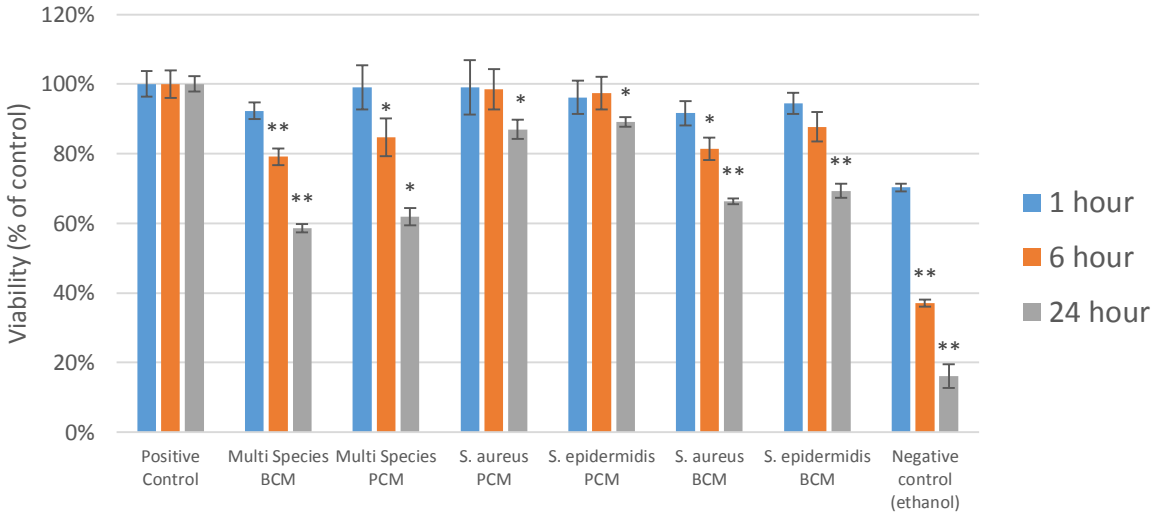

Figure 6.6: Effect of conditioned media on cell viability at 1, 6 and 24 hours. HDF cells were treated with PCM and BCM for up to 24 hours. At 1, 6 and 24 hours post exposure PrestoBlue™ was added and the absorbance measured at 570 nm. Absorbance readings were compared against control to find percentage viability. Only the multi species BCM and PCM and *S. aureus* BCM samples showed a significant reduction in viability from 1 to 6 hours incubation, however all samples showed a significant reduction in viability from 6 to 24 hours. Significant difference of ($p<0.05$) and ($p<0.005$) indicated by * and ** respectively. Error bars represent standard deviation between triplicate samples.

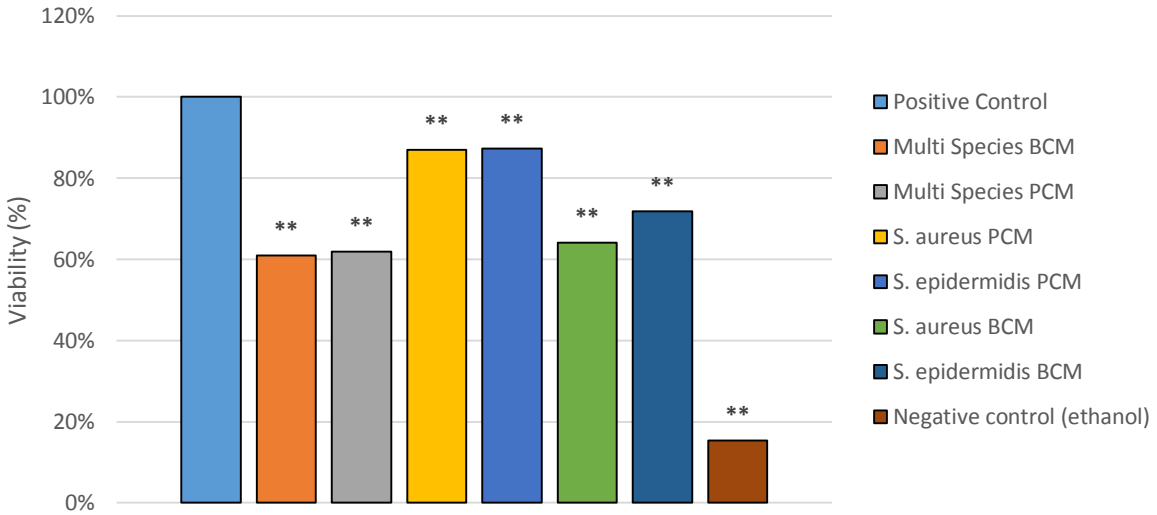

Figure 6.7: Effect of conditioned media on cell viability in-vitro after 24 hours. Absorbance readings were taken for BCM and PCM and compared against control. (*) Indicates significant difference from control group at $p<0.05$. (**) Indicates significant difference from control group at $p<0.005$. Error bars represent standard deviation from the mean at n=3. Control sample contains cells grown in fibroblast culture medium only

The effect of biofilm and planktonic conditioned media on the cell viability of HDF was studied using PrestoBlue™ cell viability assay. Absorbance was read after 1, 6 and 24 hours of exposure to conditioned media and compared against control to determine percentage viability. Cells grown in FGM containing DMEM supplemented with 10 % (v/v) FBS acted as the positive control. Both multi species BCM and PCM as well as single species *S. aureus* BCM showed a significant reduction in viability from 1 to 6 hours of exposure ($p<0.05$), however from 6 to 24 hours this reduction in viability was seen of all samples tested ($p<0.05$). After only 1 hour of exposure to multi species BCM and *S. aureus* BCM there was a significant reduction in cell viability compared with control ($p<0.05$). After 6 hours of exposure multi species PCM and *S. epidermidis* BCM also showed a significant reduction in viability ($p<0.05$) however the single species PCM samples did not. By 24 hours the difference in viability between the groups had increased, both BCM and PCM groups showed a reduction in viability compared to controls ($p<0.05$). However *S. aureus* and *S. epidermidis* BCM showed a significantly greater reduction in viability compared to the PCM equivalent ($p<0.005$) this result was not observed between the multi species BCM and PCM samples *(figure 6.7).* After repeating the experiment for 24 hours exposure only, all samples showed a significant reduction in cell viability compared to control ($p<0.005$). The greatest reduction in viability was observed for the multi species samples which reduced viability by 40% compared to control, although there was no significant difference between the multi species BCM and PCM. The least reduction in viability was observed for the *S. aureus* and *S. epidermidis* PCM samples, although there was no significant difference between the two bacteria species. However there was a difference observed between the *S. aureus* and *S. epidermidis* BCM samples ($p<0.05$) which reduced cell viability on average by 36% and 28% respectively.

6.3.1 Wound Closure Percentage

Figures 6.8 – 6.12 illustrate the change in wound width of each sample over the 70 hour test duration. All samples excluding the multi species BCM achieved 100 % wound closure by 24 – 48 hours. After reaching 100 % wound closure, both BCM collected from single species *S. aureus* and *S. epidermidis* show an increase in wound width after 50 hours. Similarly the multi species BCM showed an initial positive rate of wound closure from 0 to 30 hours up to around 40 % wound closure, after which wound begins to increase *(figure 6.12).* In order to visually illustrate the closure of the scratch, Images of the scratch area for all treatments at 0, 12, 24 and 72 hours can be seen in *table 6.1.*

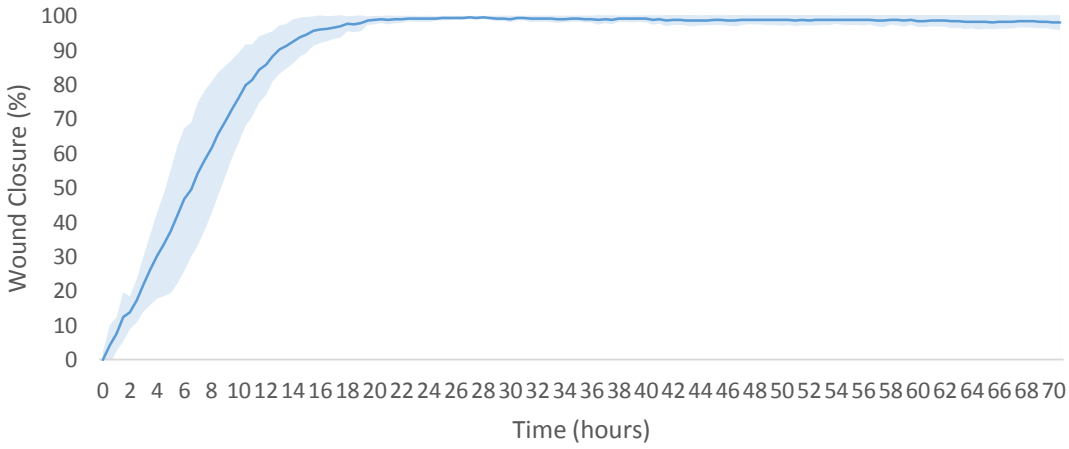

Figure 6.8: Control Sample (Fibroblast media only) - Shading represents standard deviation from the mean (n=6)

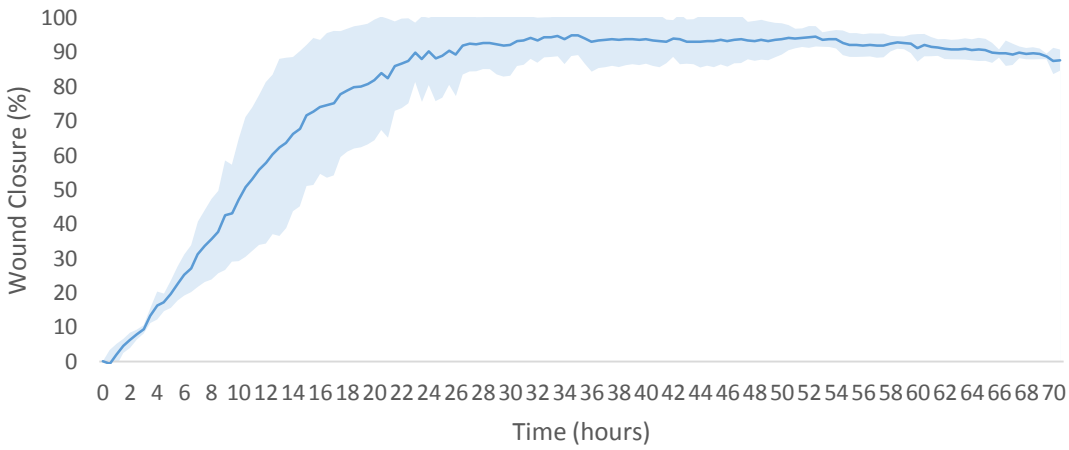

Figure 6.9: Planktonic *S. Epidermidis* conditioned media - Shading represents standard deviation from the mean (n=2)

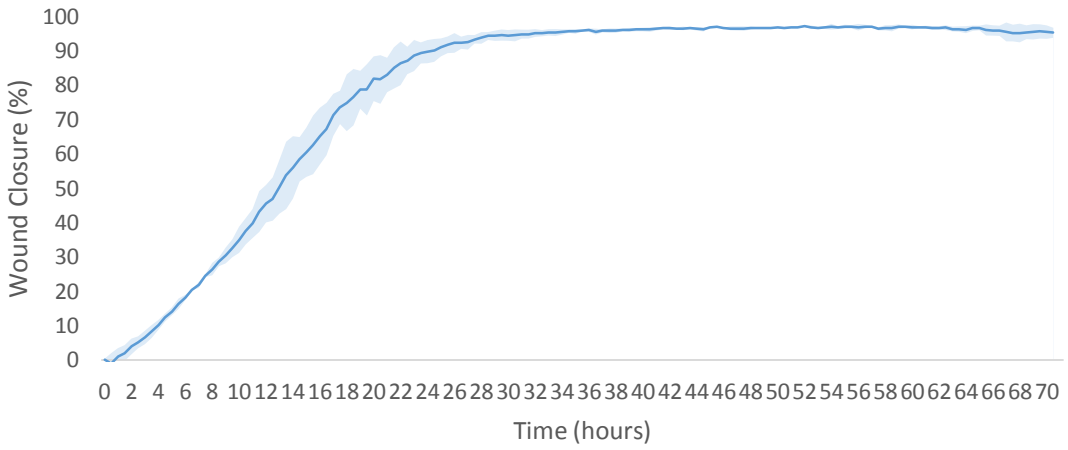

Figure 6.10: Planktonic *S. aureus* conditioned media - Shading represents standard deviation from the mean (n=2)

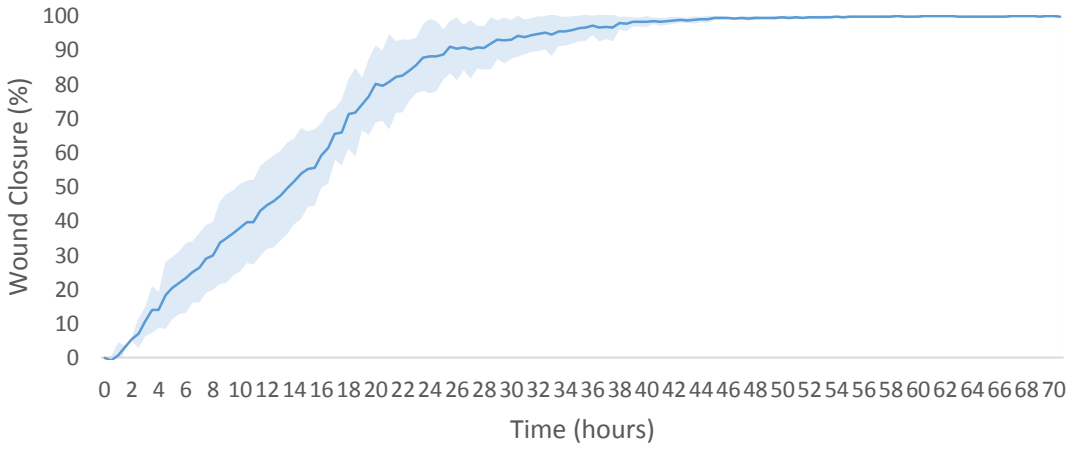

Figure 6.11: Planktonic conditioned media collected from a multi species culture of *S. aureus* and S. *Epidermidis* - Shading represents standard deviation from the mean (n=2)

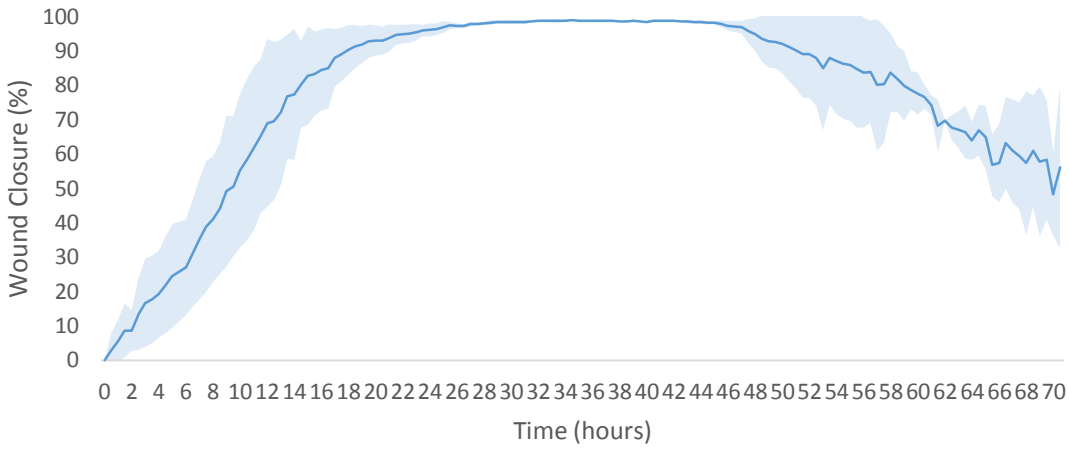

Figure 6.12: *S. aureus* biofilm conditioned media - Shading represents standard deviation from the mean (n=2)

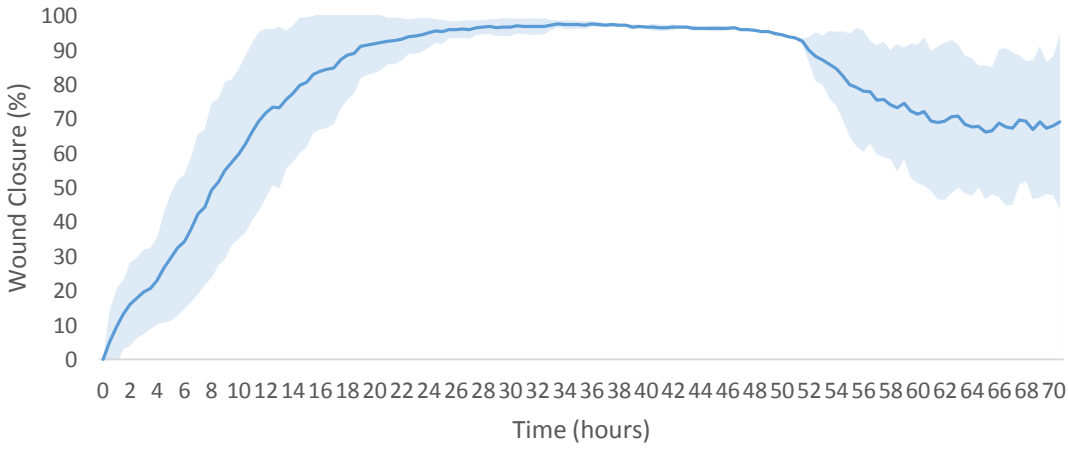

Figure 6.13: *S. Epidermidis* biofilm conditioned media - Shading represents standard deviation from the mean (n=2)

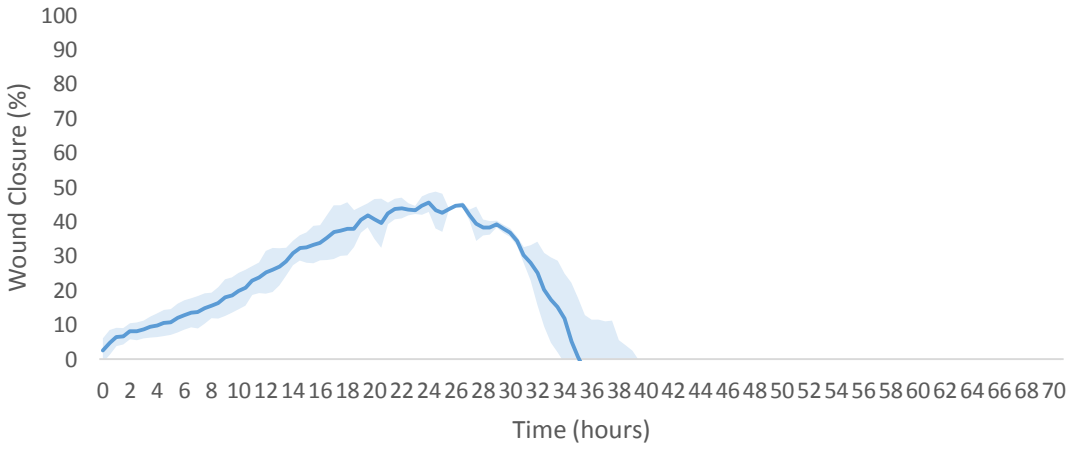

Figure 6.14: Biofilm conditioned media collected from a multi species culture of *S. aureus* and *S. Epidermidis* - Shading represents standard deviation from the mean (n=2)

Table 6.1: Images of scratches for *S. aureus, S. epidermidis* and multi species BCM and PCM – After 24 hours all samples showed near to 100% wound closure excluding the multi species BCM sample of which the gap failed to close for the duration of the study. Both *S. aureus* and *S. epidermidis* PCM show signs of cell detachment after 72 hours incubation except the multi species PCM which appeared to have the least effect on cell migration, with results similar to that of the control (Dotted white lines indicate the initial wound edge at 0 hours)

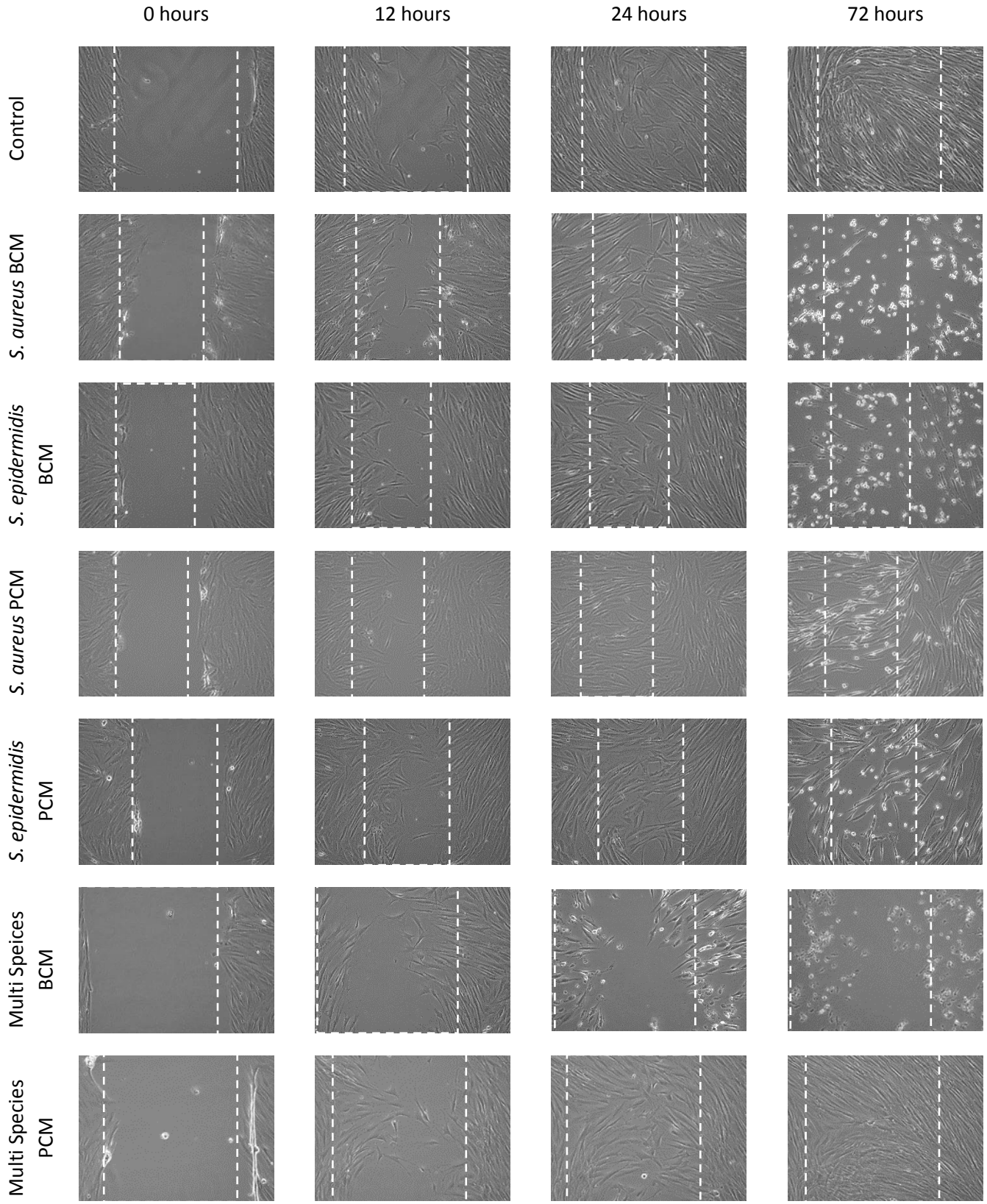

6.3.2 Cell migration velocity

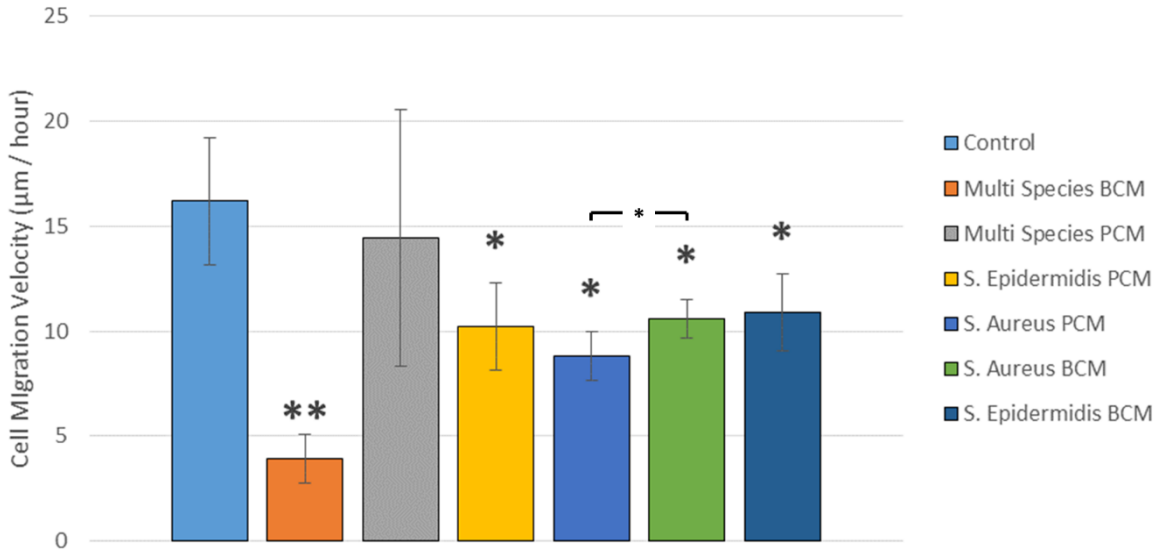

Figure 6.15: Effect of conditioned media on cell migration. The fastest migration rate was observed in the control sample, followed by the multi species PCM sample, however this result was not statistically significant (p=0.59). Both PCM and BCM from single species S. aureus and S. epidermidis had a similar negative effect on cell migration (p<0.05 indicated by *). The greatest negative effect on cell migration was observed in the multi species BCM sample (p<0.005 indicated by **). Error bars represent standard deviation from the mean at n=2, except control at n=6. Control sample contains cells grown in fibroblast culture medium only

All conditioned media samples tested appeared to have a negative effect on migration velocity compared to the control *(figure 6.15)* (p<0.05). The largest reduction in migration velocity was observed for the multi species BCM which reduced migration velocity on average by 75.8% that of control (p<0.005). This effect was not observed in the multi species PCM sample which showed no significant reduction in cell migration velocity (p=0.59). Interestingly the PCM and BCM collected from single species cultures of *S. aureus* and *S. epidermidis* on average showed similar reductions in cell migration velocity of 65 % compared to control, with no significant differences between bacteria grown in biofilm or planktonic state nor between bacterial species.

6.3.3 Time for 50% wound closure

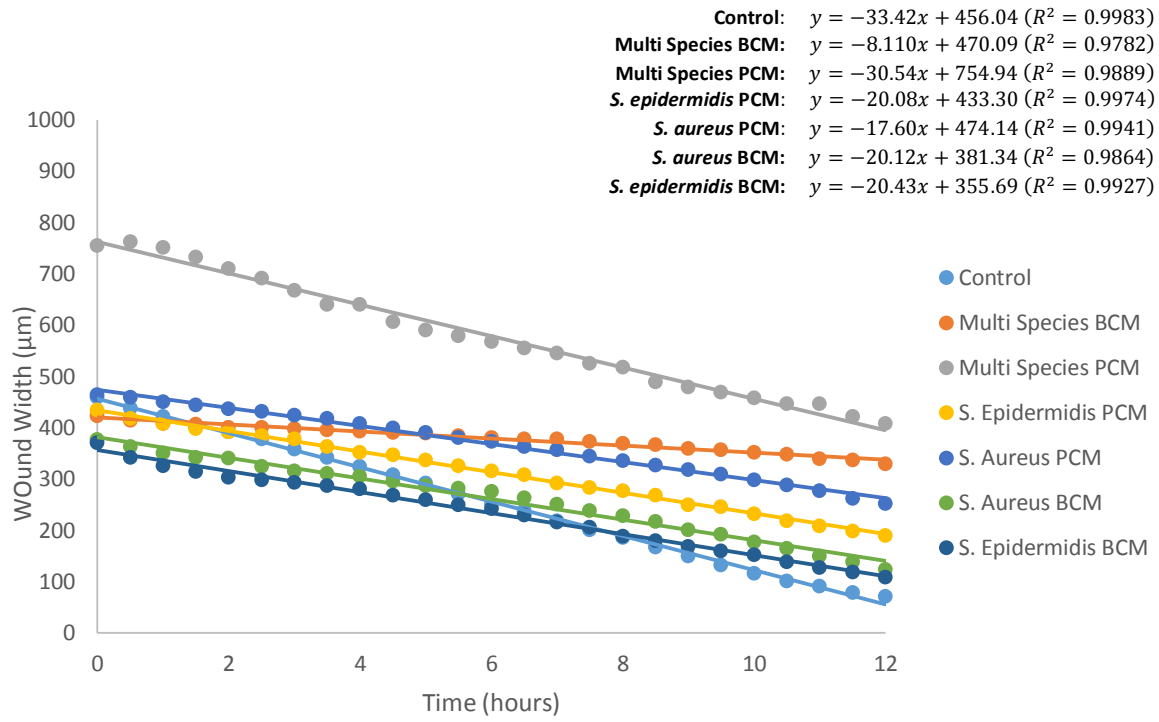

Figure 6.16: Width of wound during first 12 hours of study. Wound width for each treatment from 0 – 12 hour was plotted and the equation of the linear trend line was found

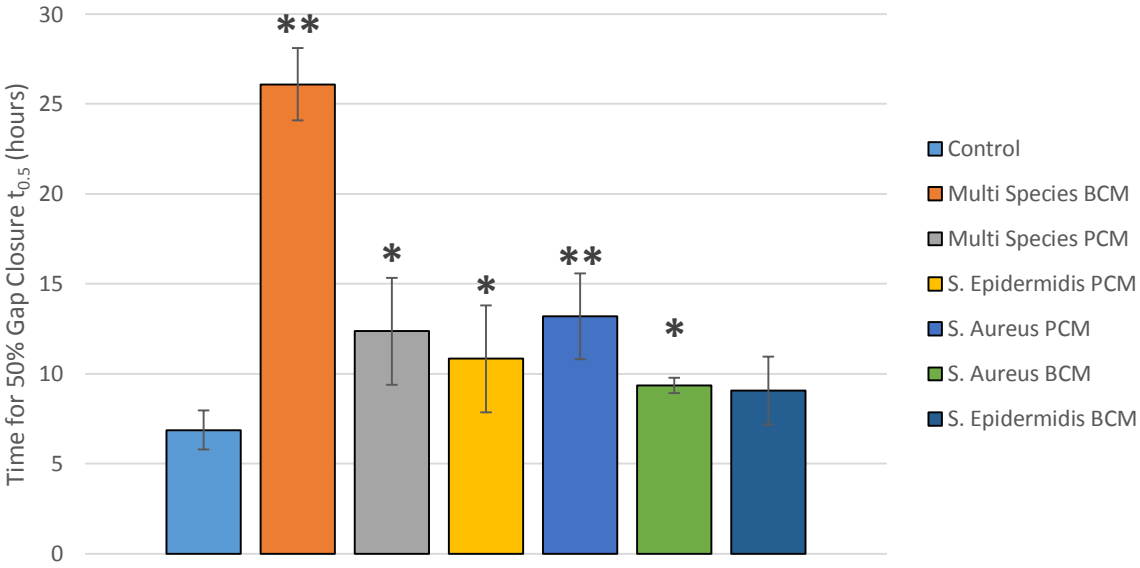

Figure 6.17: Effect of conditioned media on time required to reach 50 % wound closure. Showing significant delay in wound closure compared to control in all but one test (* p<0.05) (** p<0.005). Error bars represent standard deviation from the mean (n = 2, except control where n = 6). Control sample contains cells grown in fibroblast culture medium only.

The time taken for each scratch to reach 50 % closure of the wound width ($t_{0.5}$) was calculated for each conditioned media sample. As expected the 50 % wound closure was achieved in the shortest time by the control sample, requiring an average of 7 hours. The slowest $t_{0.5}$ time was observed in the multi species BCM sample 29.3 hours, an increase of 426 % compared to control, however this value is theoretical based on the cell migration rate during the first 12 hours, as the multi species sample failed to reach 50 % wound closure *(figure 6.16).* Interestingly there was not as dramatic of an increase in $t_{0.5}$ for the multi species PCM media, which only increased by 180 % compared to control ($p<0.05$), however it is important to note that the calculation of $t_{0.5}$ is dependent upon the initial width of the scratch, which was almost double the width of the control in the multi species PCM sample, while the rest of the samples remained fairly consistent. PCM and BCM from single species *S. aureus* and *S. epidermidis* all showed similar increase in $t_{0.5}$ time. *S. aureus* PCM showed the greatest increase of 192 % compared to control ($p<0.005$) while *S. epidermidis* BCM showed an increase of 132 % compared to control, however this result was not significant ($p=0.5$).

6.3.5 Discussion

Biofilm and planktonic conditioned media collected from single species *S. aureus* and *S. epidermidis* cultures as well as multispecies cultures of both organisms were tested for their effect on the rate of cell migration across a scratched monolayer of human dermal fibroblast cells. A study was first conducted to investigate the effect of biofilm and planktonic conditioned media on cell viability. No significant reduction was observed after 1 and 6 hours exposure, however a reduction in cell viability compared to control was observed after 24 hours for all samples ($p<0.05$). Therefore cell migration velocity was calculated during the first 12 hours to minimise the effect that any reduction in cell viability may have on the migration rate.

The greatest negative effect on cell migration was observed for the multi species BCM samples, whereby cell migration fell to 24.2% that of control ($p<0.05$). Multi species BCM also had the largest effect on cell viability compared to control of 40% ($p<0.05$). The same effect on viability was observed for the multi species PCM sample, however no significant effect on migration rate was observed, indicating that biofilms containing both *S. aureus* and *S. epidermidis* may secrete toxins harmful to the wound healing mechanisms of dermal fibroblasts that are not produced by their planktonic equivalent. However, the large error bars and lack of significance of the multispecies PCM sample in *figure 6.15* highlights the uncertainty between data. Conducting more repeats of the experiment would improve the reliability of the results, however this was not possible due to technical difficulties with the equipment.

On the other hand, BCM and PCM collected from single species cultures of *S. aureus* and *S. epidermidis* all showed a significant reduction in both cell viability and migration as compared to control ($p<0.05$). Interestingly no significant difference was seen in both cell viability and migration observed between the PCM and BCM groups ($p>0.1$) suggesting that fibroblasts experience the same outcome when exposed to either planktonic or biofilm for both species (staphylococci): limited migration followed by death.

The time to reach 50 % wound closure ($t_{0.5}$) was also investigated for both BCM and PCM (figure 6.15). Results were similar to that of the cell migration study *(figure 6.15)* with the multispecies BCM sample requiring the longest time to reach 50 % wound closure ($p<0.005$), however this is a theoretical value based on the cell migration rate during the first 12 hours, as the multi species sample failed to reach 50 % wound closure *(figure 6.13).* Interestingly there was not as dramatic of an increase in $t_{0.5}$ for the multi species PCM media, which only increased by 80 % compared to control ($p<0.05$), however it is important to note that the calculation of $t_{0.5}$ is dependent upon the initial width of the scratch which is difficult to maintain constant when using the manual pipette tip scratch method. The initial wound width of the multi species PCM sample was also double that of the control sample, while the rest of the samples remained fairly consistent *(figure 6.16),* which may have had an effect on the observed $t_{0.5}$ value for the multi species PCM.

For all samples excluding multi species BCM, 100% wound closure was achieved by 24 - 48 hours. However after 48 hours all single species BCM samples reported an increase in wound width. It is possible that after 48 hours nutrients within the media had become depleted, resulting the cell death and detachment from the well which was then analysed by the CELL-IQ software as an increase in wound width. This may be a result of the protocol adopted for collection the conditioned media, although care was taken to produce biofilm and planktonic cultures of similar cell density by using starter cultures of the same cell density across as samples, it is difficult to account for the variation in growth rates between biofilm and planktonic cultures. Since an increase in wound width was observed for all cultures which has been attributed to nutrient depletion, it is possible that cell density was higher in the biofilm cultures during the collection of BCM.

Previous studies have examined the effect of PCM and BCM derived from *S. aureus* on keratinocytes and fibroblasts (Kirker *et al*, 2009; Tankersley *et al*, 2014). Using a similar in-vitro scratch assay, both were found to significantly reduce gap closure, as well as reduce viability, which agrees with the results of our study. It was also observed in this study that planktonic Staphylococci grown in multi species

culture significantly influences the rate of wound closure compared to single species cultures. This result has not been previous observed in the literature. In the case of *S. epidermidis*, as well as the multispecies cultures, very little in-vitro research has been conducted into the effects these have on proliferation and migration and certainly warrants further research.

A preliminary study was also carried out to study wound closure when in direct contact with *S. aureus* and *S. epidermidis* (bacterial broth). This was carried out by introducing a Multiplicity of Infection (MOI) ratio of 0 (no bacteria), 1 (1:1 ratio of virions to cells), 5, 10 and 20 to the scratch assays. As expected, the MOI ratio had a negative impact on the migration characteristics of fibroblasts in-vitro and this effect increased with increasing MOI ratio *(Appendicies Section 9.2).* However when the MOI ratio was greater than 1, the bacteria proliferate uncontrollably, releasing waste by-products into the media which causes the media to cloud, making accurate measurements of the wound gap difficult. Additionally as the bacteria proliferate they deplete the media of nutrients, which in turns starves the cells leading to cell death and detachment from the tissue culture well. As a result it is difficult to determine whether our observed reduction in migration rate was due to direct effects of the bacteria on the migration properties of fibroblasts or due to the cell death and detachment. For this reason the study was adapted to investigate biofilm and planktonic conditioned media derived from *S. epidermidis* and *S. aureus* as well as a multi-culture of both species, which have been individually shown to disrupt the normal wound healing processes of cell proliferation and migration in-vitro.

The work presented in this chapter has identified that by-products from *S. aureus* and *S. epidermidis* in multi species culture in either planktonic or biofilm state have a more toxic effect to the wound healing properties of fibroblasts in-vitro compared to mono-bacterial environments. The results achieved from this study have helped develop a fuller understanding of the role bacteria has in wound healing in external fixation, however in order to make the results more clinically relevant to external fixation, the methodology could be developed further in order to create an in-vitro wound healing model which more accurately represents the pin-site scenario in-vivo. Human skin equivalents

consisting of a dermal and epidermal layers are currently the most advanced in-vitro skin model available and have been shown to induce a wound healing response in vivo. Therefore the novel method for studying wound healing proposed by kirker could be adapted for use with skin equivalent models in order to observe the effect of BCM and PCM on the wound healing properties of the skin equivalents.

Chapter 7: Discussion & Summary

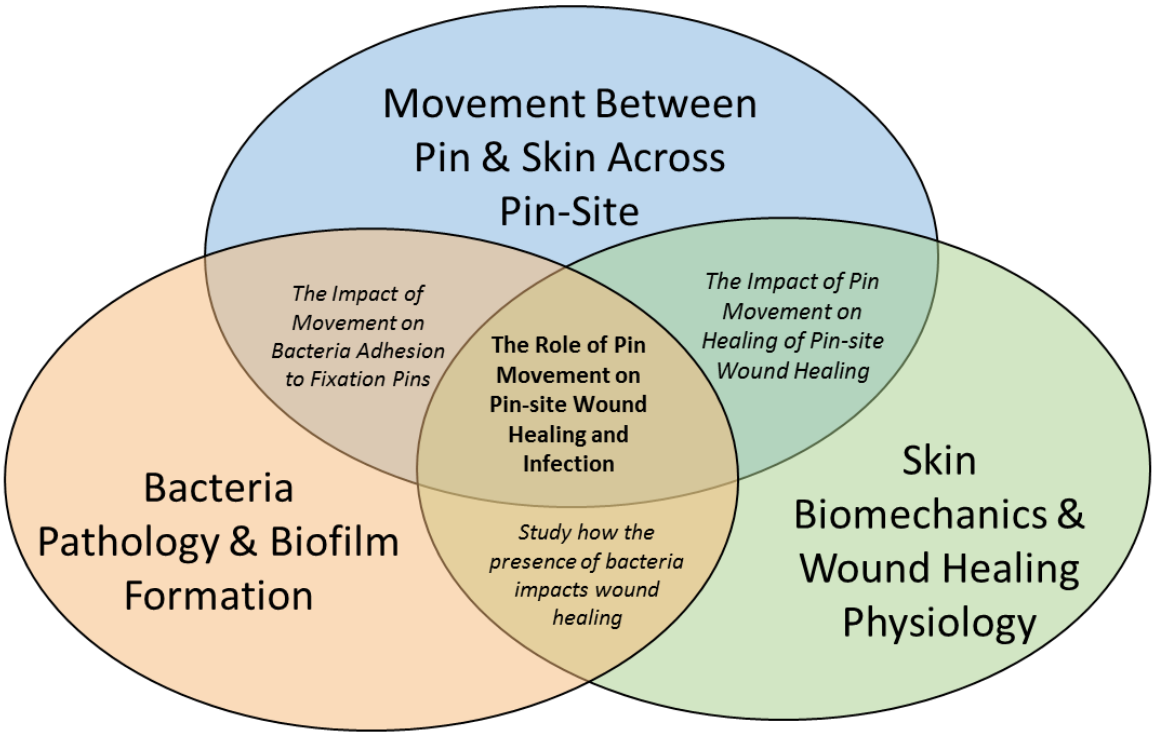

Figure 7.1: Pin movement, bacterial colonisation and biomechanics of the skin were identified as three important mechanisms contributing to pin-site infection. The current thesis describes basic science research to investigate the interactions between each of the mechanisms

External fixation is an essential surgical technique for treating trauma, limb lengthening and deformity correction, however pin-site infection and pin loosening are significant challenges that still need to be overcome. Incidences of pin-site infection reported in the literature range from 4.5 to 100 % (Antoci *et al*, 2008; Garfin *et al*, 1986; Mahan *et al*, 1991; Parameswaran *et al*, 2003) and is considered by clinicians as an inevitable complication when using external fixations.

Although it is clear that pin-site infection is an important issue that needs to be addressed, there is a considerable discontinuity among the reported rates of infection, likely due to a lack of a standardised system for characterising infection (Ferreira *et al*, 2012). The Checketts-Otterburn system is often used for grading infection in order to determine a suitable treatment (De Bastiani *et al*, 2012), however this method relies on visual diagnosis of infection resulting in a discrepancy among clinicians in identifying when an infection has developed.

Tackling the problem of infection in external fixation is not a case of simply reducing bacterial colonisation but also facilitating the healing of skin around the pin-site as the longer the venerable soft tissue is exposed, the greater risk of an infection occurring (Mulder, 2002). In the case of external fixation, the implanted pin prevents the pin-site wound achieving full closure, for this reason the aim of wound healing is the development of a collagen shell surrounding the pin effectively isolating it from the host (Brodbeck *et al*, 2009).

Currently the most frequently used method of treatment for pin-site infections or suspected infection is the administration of systemic antibiotics. Over prescription of these antibiotics has led to an epidemic of antimicrobial resistant bacteria, which cannot be treated with conventional antibiotics. It has been estimated that deaths due to antimicrobial resistance will reach 10 million by 2050 and becoming the number one cause of death globally, costing an estimated 100 trillion USD worldwide (O'Neill, 2017), which would result in a considerable financial burden on the NHS. Additionally systemic antibiotics lead to kidney and liver complications as a result of systemic toxicity, which poses a serious risk to patient health and well-being (Price *et al*, 1996).

At present the most promising method of preventing infection in external fixation, other than pin removal, appears to be through the development of pin coatings. Micro-thin silica sol-gel films, designed to slowly release antibiotics, have been used to coat the surface of external fixation pins and have been shown to inhibit *S. aureus* growth both in vitro and in vivo (Adams *et al*, 2009). While this method is preferable over systemic antibiotics, it does not tackle the problem of antimicrobial resistance. Hydroxyapatite and nitric oxide pin coatings have also been extensively studied, although most of this research has been on improving the pin-bone interface in order to prevent pin loosening, rather than improving the pin-skin interface, where infection first develops. Furthermore, these interventions have not eliminated the infection problem, highlighting a need to understand the pin-site environment more fundamentally.

One mechanism often highlighted in the literature as a potential contributing factor towards pin-site infection is relative movement between the pin and skin. A consensus conducted by the royal school of nursing revealed that the majority of surgeons and clinicians agree that compressive dressings and bungs should be used during pin-site care in an attempt to minimise skin movement around the pins (Timms *et al*, 2013). As of yet no research had been conducted to investigate the relationship of pin movement and infection or the efficacy of these compressive dressings.

Due to the lack of research in this area it was proposed that the aim of this PhD was to characterise the role of pin-movement on the development of infection in external fixation. Three modes of movement were hypothesised, changes in the natural tension of the skin as the patient moves, discrepancies in the movement of the underlying skeletal structure compared to the skin, known as the soft tissue artefact, and mechanical deflections of the pin as a result of the patient walking with the external fixator.

After reviewing these modes of movement it was estimated that pin movement should be in the range of 0.7 – 10.9 mm, based on a systemic review of existing research into the soft tissue artefact *(table 3.1).* It was also decided that the pin movement should be applied at a frequency of 1 Hz, similar to that of a normal adult human gait cycle (Murray *et al*, 1964). From this data a pin machine was designed to generate mechanical movement applied to an external fixation pin, which could be implanted into either a skin equivalent model or a bacterial culture. Since no research had previously been conducted on this subject, a study was designed to investigate the role of movement on the attachment of bacteria to the surface of pins, whereby movement was generated through shaking of the bacterial culture. It was hypothesised that shear forces generated between the bacteria and implant surface positively influence the rate of bacterial attachment, and the forces would be higher when a greater shaking frequency was applied. This has been shown for the adhesion of *Pseudomonas aeruginosa* to glass surfaces which was enhanced by shear stress (Lecuyer *et al*, 2011).

In order to measure the quantity of adhered bacteria to the surface of the fixation pins a protocol was developed and optimised for the removal of both high and low adherent bacteria from the surface of the pin, as an inconsistent method for counting bacteria would result in poor repeatability of the study. After optimising the protocol the effect of incubation shaking frequency on the rate of high adherent bacteria was studied. The results showed that bacterial attachment does in fact increase with shaking frequency, shown in *figure 4.10* ($p<0.05$) supporting the hypothesis. However an increase in bacterial concentration of the culture itself with increasing shaking frequency was also observed, shown in *figure 4.11* ($p<0.05$). Therefore the increase in rate of attachment with increased shaking frequency may have been a consequence of a greater abundance of bacteria in the culture, increasing the possibility of adhesion events occurring as a whole, rather than an alternation in the behaviour of the bacteria (e.g. an increase in the rate of successful adhesion events at higher frequencies). This is also corroborated by the results from our study where the media was kept static and cyclic motion of the pin was applied using our novel pin machine, which showed no significant differences between a static pin and a dynamic pin with movement applied *(figure 4.13)*. Although no significant results were observed, this study highlighted the fact that bacterial adhesion does not appear to be sensitive to a motion amplitude or frequency of 2 - 20 mm and 0.25 - 1 Hz respectively. However further study is needed to address whether there is an effect at higher frequencies that may be experienced e.g. tremor. Additionally the protocol developed for dislodging and counting high and low adherent bacteria may be suitably adopted by other researchers for use in testing the efficacy of various pin materials, implant surfaces or transcutaneous tubes and coatings on their ability to prevent bacterial adhesion.

In order to study the role of pin movement on wound healing in vitro a human skin equivalent model was developed utilising previously established protocols (Carlson *et al*, 2008; Xie *et al*, 2010), which was then implanted with a fixation pin to create a novel in vitro pin-site model. Once the skin model had been established and validated against histological images of native human skin *(figure 5.9),* a study was conducted to investigate the effect of pin movement on the wound healing response of the

skin equivalents. In order to quantify the effect on wound healing, various pro-inflammatory markers, shown to be higher in non-healing wounds compared to healing wounds (Lindley *et al*, 2016), were measured using ELISA.

As hypothesised, an increase in IL-8 and IL-1α was observed when a static pin was implanted in the skin model compared to control *(figure 5.14)* verifying that our model produced physiologically accurate wound healing response ($p<0.05$). When 20 mm of movement was applied to the pin at a frequency of 0.5 Hz we observed a further negative effect on the wound healing response, characterised by the increased production of IL-8 and IL-1α compared to the static pin samples ($p<0.05$). For this reason it was concluded that pin movement has a negative effect on pin-site wound healing. Providing for the first time, evidence that confirms the anecdotal view that minimising pin movement has the potential to improve wound healing around the pin-site and consequently reduce the rate of pin-site infection. As previously mentioned the design of the pin machine meant any pro-inflammatory markers secreted by the skin equivalents were highly diluted, consequently on day 1 and 2, levels of IL-1α, TNF-α and IL-8 were below the detection limit of the assay, however by day 3 marker levels were high enough to accurately be measured.

The final study conducted investigated the impact of bacteria on the wound healing processes of cell migration and proliferation. In the case of medical implant infections, bacteria rarely exist in single species planktonic form (Willems *et al*, 2016) instead the surface of a fixation pin provides an ideal surface for the bacteria to colonise and form biofilms, which improves the bacteria's resistance to antibiotics and immune responses. Additionally bacteria often form multi species communities, often seen in chronic infections, containing anywhere from 2 to 5 difference species (Wolcott *et al*, 2016). Therefore the effect that *S. aureus* and *S. epidermidis*, two of the most commonly isolated bacteria from pin-site wounds, grown as single species and a multi-species culture in both biofilm and planktonic form has on the migration of fibroblasts was investigated. The majority of cell migration studies in the literature have studied the migration effect of keratinocytes in order to simulate

epidermal healing, however since the goal of pin-site healing is the formation of a collagen shell around the pin, a protein that is synthesised mainly by fibroblasts (Narayanan *et al*, 1989), human dermal fibroblasts were selected as the cell of interest. The results revealed that both biofilm and planktonic bacteria have a negative effect on the rate of migration *(figure 6.15)* and viability *(figure 6.7)* of fibroblasts, however there was no significant difference observed between biofilm and planktonic conditioned media. On the other hand it was observed that a planktonic multi-species culture significantly reduced the migration rate of fibroblasts, indicating a possible increased virulence when *S. epidermidis* and *S. aureus* cultured together. Further analysis into the effect of multi species planktonic conditioned media on the production of pro-inflammatory markers by fibroblasts would be beneficial to understanding the mechanisms of the pronounced negative effect on cell migration.

Although this study helped develop a better understanding of the role of bacterial on wound healing, the results could be made more clinically relevant to external fixation by developing the model further. By adapting the protocol for studying cell migration developed by Kirker *et al (figure 6.1)* on keratinocyte monolayers to use with a skin equivalent implanted with a fixation pin, it may be possible to observe the effect of conditioned media on the wound healing around the pin-site.

The research conducted in this doctoral study have led to a better understanding of the role of pin movement in external fixation infection by investigating the interactions between the three mechanisms described: bacterial adhesion, mechanical movement and wound healing *(figure 7.1).* The work presented here indicate that the bacterial cultures studied (*S. epidermidis and S. aureus*) are not sensitive to the mechanical movement ranges studied, however they appear to be more virulent in a planktonic multi-species form. This leads to the conclusion that bacterial wound healing studies should be conducted within a multi-species environment as well as a mono species environment, in order to better model and understand the physiological wound healing environment at the pin site interface. Our work also corroborates the understanding that wound healing is sensitive to pin site movement in a quantitative way.

The next step to further this work would be to study all three mechanisms simultaneously. By combining the methods developed in *chapter 4* to study wound healing of skin equivalents, with the methods in *chapter 6* for developing biofilm and planktonic conditioned media, an in vitro model could be developed which resembles an infected pin-site wound. This in vitro model could then be used to study the efficacy of various pin-site care treatments currently adopted by clinicians, as well as allow for the testing of new treatments for reducing the development of infection and minimising pin movement. Furthermore based on the difference in sensitivities between the bacterial cultures and the human dermal fibroblast cultures to pin motion, the validated models and protocols presented here can be used to investigate the effects of early immobilisation followed by mobilisation post-operatively on developing the fibrous capsule.

Although the aim of this study was to characterise the role of movement on infection in external fixation pins, many other percutaneous implants suffer from the same complications, such as dental implants, catheters and limb prosthesis anchors. Therefore researchers in these fields may also benefits from the results of this study, and the novel in vitro pin-site model and protocols developed may also be adapted to study these applications.

Although the final design of the pin machine managed to satisfy all of the design requirements, several improvement could be made for future studies. The current design could accommodate 4 fixation pins, meaning only four samples could be tested simultaneously. Increasing the number of fixation pin attachments would allow more treatments or a greater number of repeats to be studied at once, which would increase the accuracy and reliability of the results obtained. Additionally when testing skin equivalent samples with the pin machine, 10 mL of media was required to achieve an air-liquid interface, this meant that any by-products produced by the skin equivalent were highly diluted, making them difficult to detect during analysis of the samples. Improving the automation of the system would also greatly benefit the user, by increasing efficiency and allowing for high throughput testing. This could be achieved by developing the microcontroller coding so that the user can input values for

magnitude and frequency of movement, without the need to connect the system to a PC. Additionally a Bluetooth receiver could be included so the user can monitor the progress of each experiment remotely, which would not only help with time management during experiments but also negate the need to open the incubator to check on the status of the experiment, which could potentially introduce contaminates.

7.1 Conclusions

In summary the current thesis employed several novel in vitro models for the study of infection and consequently wound healing, in external fixation pin-sites. Results highlighted that pin-site infection is a multifactor problem involving not only the colonisation of the pin-site by the bacteria itself, but also the ability to achieve adequate wound healing around the pin, which is negatively affected by pin movement. Additionally it was observed that *S. aureus* and *S. epidermidis* grown in a planktonic multi species culture results in an increase negative effect on cell migration compared to the same bacteria in a single species culture, pin pointing a possible synergistic relationship between the two bacteria. The research has confirmed that pin movement is an important factor in maintaining sterile pin-sites however further research is required to evaluate the efficacy of pin movement restriction treatments.

8.0 References

6. Adam, B.Baillie, G. S., & Douglas, L. J. (2002). Mixed species biofilms of Candida albicans and Staphylococcus epidermidis. *J Med Microbiol, 51*(4), 344-349.
7. Adams, C. S.Antoci, V., Jr.Harrison, G.Patal, P.Freeman, T. A.Shapiro, I. M.Parvizi, J.Hickok, N. J.Radin, S., & Ducheyne, P. (2009). Controlled release of vancomycin from thin sol-gel films on implant surfaces successfully controls osteomyelitis. *J Orthop Res, 27*(6), 701-709.
8. Adell, R.Lekholm, U.Rockler, B.Branemark, P. I.Lindhe, J.Eriksson, B., & Sbordone, L. (1986). Marginal tissue reactions at osseointegrated titanium fixtures (I). A 3-year longitudinal prospective study. *Int J Oral Maxillofac Surg, 15*(1), 39-52.
9. Alexander, E. J., & Andriacchi, T. P. (2001). Correcting for deformation in skin-based marker systems. *J Biomech, 34*(3), 355-361.
10. An, Y. H., & Friedman, R. J. (2000). *Handbook of Bacterial Adhesion: Principles, Methods, and Applications*: Humana Press.
11. Anaya, D. A., & Dellinger, E. P. (2006). The obese surgical patient: a susceptible host for infection. *Surg Infect (Larchmt), 7*(5), 473-480.
12. Annaidh, A. N.Bruyère, K.Destrade, M.Gilchrist, M. D., & Otténio, M. (2012). Characterization of the anisotropic mechanical properties of excised human skin. *Journal of the mechanical behavior of biomedical materials, 5*(1), 139-148.
13. Antoci, V.Ono, C. M.Antoci, V., Jr., & Raney, E. M. (2008). Pin-tract infection during limb lengthening using external fixation. *Am J Orthop (Belle Mead NJ), 37*(9), E150-154.
14. Aronson, J., & Harp, j. H. J. (1992). Mechanical Considerations in Using Tensioned Wires in a Transosseous External Fixation System. *Clinical Orthopaedics and Related Research, 280*, 23-29.
15. Babapour, A.Yang, B.Bahang, S., & Cao, W. (2011). Low-temperature sol-gel-derived nanosilver-embedded silane coating as biofilm inhibitor. *Nanotechnology, 22*(15), 155602.
16. Baranoski, S., & Ayello, E. (2008). *Wound Care Essentails: Practice Principles* (Vol. 2). Illinois: Lippincott Williams & Wilkins.
17. Bark, K. Y. J., & University, S. (2009). *Rotational Skin Stretch Feedback: A New Approach to Wearable Haptic Display*: Stanford University.
18. Barraud, N.Hassett, D. J.Hwang, S. H.Rice, S. A.Kjelleberg, S., & Webb, J. S. (2006). Involvement of nitric oxide in biofilm dispersal of Pseudomonas aeruginosa. *J Bacteriol, 188*(21), 7344-7353.
19. Bechetoille, N.Dezutter-Dambuyant, C.Damour, O.André, V.Orly, I., & Perrier, E. (2007). *Effects of Solar Ultraviolet Radiation on Engineered Human Skin Equivalent Containing Both Langerhans Cells and Dermal Dendritic Cells* (Vol. 13).
20. Behrens, F., & Searls, K. (1986). External fixation of the tibia. Basic concepts and prospective evaluation. *Journal of Bone & Joint Surgery, British Volume, 68*(2), 246-254.
21. Beidler, S. K.Douillet, C. D.Berndt, D. F.Keagy, B. A.Rich, P. B., & Marston, W. A. (2009). Inflammatory cytokine levels in chronic venous insufficiency ulcer tissue before and after compression therapy. *J Vasc Surg, 49*(4), 1013-1020.
22. Bibbo, C., & Brueggeman, J. (2010). Prevention and management of complications arising from external fixation pin sites. *J Foot Ankle Surg, 49*(1), 87-92.

23. Bowler, P. G. (2003). The 10(5) bacterial growth guideline: reassessing its clinical relevance in wound healing. *Ostomy Wound Manage, 49*(1), 44-53.

24. Bowler, P. G.Duerden, B. I., & Armstrong, D. G. (2001). Wound microbiology and associated approaches to wound management. *Clin Microbiol Rev, 14*(2), 244-269.

25. Brånemark, P. I., & Albrektsson, T. (1982). Titanium Implants Permanently Penetrating Human Skin. *Scandinavian Journal of Plastic and Reconstructive Surgery, 16*(1), 17-21.

26. Braydich-Stolle, L.Hussain, S.Schlager, J. J., & Hofmann, M. C. (2005). In vitro cytotoxicity of nanoparticles in mammalian germline stem cells. *Toxicological Sciences, 88*(2), 412-419.

27. Brighton, C. T.Wang, W.Seldes, R.Zhang, G., & Pollack, S. R. (2001). Signal transduction in electrically stimulated bone cells. *J Bone Joint Surg Am, 83*(10), 1514-1523.

28. Brodbeck, W. G., & Anderson, J. M. (2009). GIANT CELL FORMATION AND FUNCTION. *Curr Opin Hematol, 16*(1), 53-57.

29. Browner, B. D.Jupiter, J. B.Krettek, C., & Anderson, P. A. (2014). *Skeletal Trauma*: Elsevier Health Sciences.

30. Brözel, V. S.Strydom, G. M., & Cloete, T. E. (1995). A method for the study of de novo protein synthesis in pseudomonas aeruginosa after attachment. *Biofouling, 8*(3), 195-201.

31. Buchholz, H. W., & Engelbrecht, H. (1970). [Depot effects of various antibiotics mixed with Palacos resins]. *Chirurg, 41*(11), 511-515.

32. Calhoun, J. H.Li, F.Bauford, W. L.Lehman, T.Ledbetter, B. R., & Lowery, R. (1992). Rigidity of half-pins for the Ilizarov external fixator. *Bull Hosp Jt Dis, 52*(1), 21-26.

33. Camathias, C.Valderrabano, V., & Oberli, H. (2012). Routine pin tract care in external fixation is unnecessary: A randomised, prospective, blinded controlled study. *Injury, 43*(11), 1969-1973.

34. Canale, S. T., & Beaty, J. H. (2012). *Campbell's Operative Orthopaedics*: Elsevier Health Sciences.

35. Cappello, A.Cappozzo, A.La Palombara, P. F.Lucchetti, L., & Leardini, A. (1997). Multiple anatomical landmark calibration for optimal bone pose estimation. *Human movement science, 16*(2), 259-274.

36. Cappello, A.Stagni, R.Fantozzi, S., & Leardini, A. (2005). Soft tissue artifact compensation in knee kinematics by double anatomical landmark calibration: performance of a novel method during selected motor tasks. *IEEE Trans Biomed Eng, 52*(6), 992-998.

37. Cappozzo, A.Catani, F.Croce, U. D., & Leardini, A. (1995). Position and orientation in space of bones during movement: anatomical frame definition and determination. *Clin Biomech (Bristol, Avon), 10*(4), 171-178.

38. Cappozzo, A.Catani, F.Leardini, A.Benedetti, M. G., & Croce, U. D. (1996). Position and orientation in space of bones during movement: experimental artefacts. *Clin Biomech (Bristol, Avon), 11*(2), 90-100.

39. Carlson, M. W.Alt-Holland, A.Egles, C., & Garlick, J. A. (2008). Three-dimensional tissue models of normal and diseased skin. *Curr Protoc Cell Biol, Chapter 19*, Unit 19.19.

40. Chai, W. L.Moharamzadeh, K.Brook, I. M.Emanuelsson, L.Palmquist, A., & van Noort, R. (2010). Development of a Novel Model for the Investigation of Implant–Soft Tissue Interface. *Journal of Periodontology, 81*(8), 1187-1195.

41. Chakrabarty, K. H.Dawson, R. A.Harris, P.Layton, C.Babu, M.Gould, L.Phillips, J.Leigh, I.Green, C.Freedlander, E., & Mac Neil, S. (1999). Development of autologous human dermal–epidermal

composites based on sterilized human allodermis for clinical use. *British Journal of Dermatology, 141*(5), 811-823.

42. Chakrabarty, K. H.Heaton, M.Dalley, A. J.Dawson, R. A.Freedlander, E.Khaw, P. T., & Mac Neil, S. (2001). KERATINOCYTE-DRIVEN CONTRACTION OF RECONSTRUCTED HUMAN SKIN. *Wound Repair and Regeneration, 9*(2), 95-106.
43. Chaloupka, K.Malam, Y., & Seifalian, A. M. (2010). Nanosilver as a new generation of nanoproduct in biomedical applications. *Trends Biotechnol, 28*(11), 580-588.
44. Charville, G. W.Hetrick, E. M.Geer, C. B., & Schoenfisch, M. H. (2008). Reduced bacterial adhesion to fibrinogen-coated substrates via nitric oxide release. *Biomaterials, 29*(30), 4039-4044.
45. Checketts, R. G.MacEachem, A. G., & Otterbum, M. (2000). Pin Track Infection and the Principles of Pin Site Care. In G. Bastiani, A. G. Apley, & A. Goldberg (Eds.), *Orthofix External Fixation in Trauma and Orthopaedics* (pp. 97-103). London: Springer London.
46. Chehroudi, B., & Brunette, D. M. (2002). Subcutaneous microfabricated surfaces inhibit epithelial recession and promote long-term survival of percutaneous implants. *Biomaterials, 23*(1), 229-237.
47. Christensen, G. D.Baddour, L. M., & Simpson, W. A. (1987). Phenotypic variation of Staphylococcus epidermidis slime production in vitro and in vivo. *Infect Immun, 55*(12), 2870-2877.
48. Churches, A. E.Tanner, K. E., & Harris, J. D. (1985). The Oxford External Fixator: fixator stiffness and the effects of bone pin loosening. *Eng Med, 14*(1), 3-11, 29.
49. Cicchi, R.Kapsokalyvas, D.De Giorgi, V.Maio, V.Van Wiechen, A.Massi, D.Lotti, T., & Pavone, F. S. (2010). Scoring of collagen organization in healthy and diseased human dermis by multiphoton microscopy. *J Biophotonics, 3*(1-2), 34-43.
50. Clark, R. (1989). Wound repair. *Current opinion in cell biology, 1*(5), 1000-1008.
51. Coester, L. M.Nepola, J. V.Allen, J., & Marsh, J. L. (2006). The Effects of Silver Coated External Fixation Pins. *The Iowa Orthopaedic Journal, 26*, 48-53.
52. Cole, G. K.Nigg, B. M.Ronsky, J. L., & Yeadon, M. R. (1993). Application of the joint coordinate system to three-dimensional joint attitude and movement representation: A standardization proposal. *J Biomech Eng, 115*(4 A), 344-349.
53. Collinge, C. A.Goll, G.Seligson, D., & Easley, K. J. (1994). Pin tract infections: silver vs uncoated pins. *Orthopedics, 17*(5), 445-448.
54. Colville, T. P., & Bassert, J. M. (2009). *Clinical Anatomy and Physiology Laboratory Manual for Veterinary Technicians*: Mosby Elsevier.
55. Costerton, J. W.Stewart, P. S., & Greenberg, E. P. (1999). Bacterial biofilms: a common cause of persistent infections. *Science, 284*(5418), 1318-1322.
56. Crossley, K. B.Archer, G.Jefferson, K., & Fowler, V. (2009). *Staphylococci in human disease*: Wiley Online Library.
57. Dabboue, H.Builles, N.Frouin, É.Scott, D.Ramos, J., & Marti-Mestres, G. (2015). *Assessing the Impact of Mechanical Damage on Full-Thickness Porcine and Human Skin Using an In Vitro Approach* (Vol. 2015).
58. Davies, R.Holt, N., & Nayagam, S. (2005). The care of pin sites with external fixation. *J Bone Joint Surg Br, 87*(5), 716-719.

59. De Bastiani, G.Apley, A. G., & Goldberg, A. A. J. (2012). *Orthofix External Fixation in Trauma and Orthopaedics*: Springer London.

60. DeCoster, T. A.Crawford, M. K., & Kraut, M. A. (2004). Safe extracapsular placement of proximal tibia transfixation pins. *J Orthop Trauma, 18*(8 Suppl), S43-47.

61. DeJong, E. S.DeBerardino, T. M.Brooks, D. E.Nelson, B. J.Campbell, A. A.Bottoni, C. R.Pusateri, A. E.Walton, R. S.Guymon, C. H., & McManus, A. T. (2001). Antimicrobial efficacy of external fixator pins coated with a lipid stabilized hydroxyapatite/chlorhexidine complex to prevent pin tract infection in a goat model. *J Trauma, 50*(6), 1008-1014.

62. Del Pozo, J. L.Rouse, M. S.Euba, G.Kang, C.-I.Mandrekar, J. N.Steckelberg, J. M., & Patel, R. (2009). The electricidal effect is active in an experimental model of Staphylococcus epidermidis chronic foreign body osteomyelitis. *Antimicrobial agents and chemotherapy, 53*(10), 4064-4068.

63. Diyana Nordin, N. H.Muthalif, A., & Khusyaie M Razali, M. (2018). *Control of transtibial prosthetic limb with magnetorheological fluid damper by using a fuzzy PID controller* (Vol. 37).

64. Donaldson, F. E.Pankaj, P., & Simpson, A. H. R. W. (2012). Bone properties affect loosening of half-pin external fixators at the pin–bone interface. *Injury, 43*(10), 1764-1770.

65. Dotsch, A.Eckweiler, D.Schniederjans, M.Zimmermann, A.Jensen, V.Scharfe, M.Geffers, R., & Haussler, S. (2012). The Pseudomonas aeruginosa transcriptome in planktonic cultures and static biofilms using RNA sequencing. *PLoS One, 7*(2), e31092.

66. Doyle, W.Shide, E.Thapa, S., & Chandrasekaran, V. (2012). The effects of energy beverages on cultured cells. *Food and Chemical Toxicology, 50*(10), 3759-3768.

67. Dryden, M. S. (2010). Complicated skin and soft tissue infection. *Journal of Antimicrobial Chemotherapy, 65*(suppl 3), iii35-iii44.

68. Duetz, W. A., & Witholt, B. (2001). Effectiveness of orbital shaking for the aeration of suspended bacterial cultures in square-deepwell microtiter plates. *Biochemical Engineering Journal, 7*(2), 113-115.

69. ECDC. (2014). *Antimicrobial Resistance and healthcare-Associated Infections*.

70. Elek, S. D. (1956). Experimental staphylococcal infections in the skin of man. *Ann N Y Acad Sci, 65*(3), 85-90.

71. Ercan, B.Kummer, K. M.Tarquinio, K. M., & Webster, T. J. (2011). Decreased Staphylococcus aureus biofilm growth on anodized nanotubular titanium and the effect of electrical stimulation. *Acta Biomaterialia, 7*(7), 3003-3012.

72. Espaur. (2015). English Surveillance Program for Antimicrobial Utilisation and Resistance 2010 to 2014. *Public Health England*.

73. Ferreira, N., & Marais, L. C. (2012). Prevention and management of external fixator pin track sepsis. *Strategies in Trauma and Limb Reconstruction, 7*(2), 67-72.

74. Finelli, L.Fiore, A.Dhara, R.Brammer, L.Shay, D. K.Kamimoto, L.Fry, A.Hageman, J.Gorwitz, R., & Bresee, J. (2008). Influenza-associated pediatric mortality in the United States: increase of Staphylococcus aureus coinfection. *Pediatrics, 122*(4), 805-811.

75. Finlay, B. (1969). Scanning electron microscopy of the human dermis under uni-axial strain. *Biomed Eng, 4*(7), 322-327.

76. Flanagan, M. (2013). *Wound Healing and Skin Integrity: Principles and Practice*: Wiley.

77. Fleckman, P., & Olerud, J. E. (2008). Models for the histologic study of the skin interface with percutaneous biomaterials. *Biomed Mater, 3*(3), 034006-034006.

78. Fleming, B.Paley, D.Kristiansen, T., & Pope, M. (1989). A biomechanical analysis of the Ilizarov external fixator. *Clinical Orthopaedics and Related Research, 241*, 95-105.

79. Fonseca, A. P., & Sousa, J. C. (2007). Effect of shear stress on growth, adhesion and biofilm formation of Pseudomonas aeruginosa with antibiotic-induced morphological changes. *International Journal of Antimicrobial Agents, 30*(3), 236-241.

80. Fragomen, A. T., & Rozbruch, S. R. (2007). The Mechanics of External Fixation. *HSS Journal, 3*(1), 13-29.

81. Frank, D. N.Feazel, L. M.Bessesen, M. T.Price, C. S.Janoff, E. N., & Pace, N. R. (2010). The human nasal microbiota and Staphylococcus aureus carriage. *PLoS One, 5*(5), e10598.

82. Freinkel, R. K., & Woodley, D. T. (2001). *The Biology of the Skin*: Taylor & Francis.

83. Fuller, J.Liu, L. J.Murphy, M. C., & Mann, R. W. (1997). A comparison of lower-extremity skeletal kinematics measured using skin-and pin-mounted markers. *Human Movement Science, 16*(2-3), 219-242.

84. Gallagher, A.Ní Annaidh, A., & Bruyère, K. (2012). *Dynamic tensile properties of human skin.* Paper presented at the IRCOBI Conference 2012, 12-14 September 2012, Dublin (Ireland).

85. Gao, B., & Zheng, N. (2008). Investigation of soft tissue movement during level walking: Translations and rotations of skin markers. *Journal of Biomechanics, 41*(15), 3189-3195.

86. Garfin, S. R.Botte, M. J., & Waters Nickel, R. L. V. L. (1986). Complications in the use of the halo fixation device. *Journal of Bone and Joint Surgery - Series A, 68*(3), 320-325.

87. Garling, E. H.Kaptein, B. L.Mertens, B.Barendregt, W.Veeger, H. E.Nelissen, R. G., & Valstar, E. R. (2007). Soft-tissue artefact assessment during step-up using fluoroscopy and skin-mounted markers. *J Biomech, 40 Suppl 1*, S18-24.

88. Garrett, T. R.Bhakoo, M., & Zhang, Z. (2008). Bacterial adhesion and biofilms on surfaces. *Progress in Natural Science, 18*(9), 1049-1056.

89. Gasser, B.Boman, B.Wyder, D., & Schneider, E. (1990). Stiffness characteristics of the circular Ilizarov device as opposed to conventional external fixators. *J Biomech Eng, 112*(1), 15-21.

90. Geerligs, M. (2009). Skin layer mechanics.

91. Geesink, R. G. T.De Groot, K., & Klein, C. P. A. T. (1988). Bonding of bone to apatite-coated implants. *Journal of Bone and Joint Surgery - Series B, 70*(1), 17-22.

92. Gessmann, J.Baecker, H.Jettkant, B.Muhr, G., & Seybold, D. (2011). Direct and indirect loading of the Ilizarov external fixator: the effect on the interfragmentary movements and compressive loads. *Strategies in Trauma and Limb Reconstruction, 6*(1), 27-31.

93. Goetsch, K. P., & Niesler, C. U. (2011). Optimization of the scratch assay for in vitro skeletal muscle wound healing analysis. *Anal Biochem, 411*(1), 158-160.

94. Gohel, M. S.Windhaber, R. A.Tarlton, J. F.Whyman, M. R., & Poskitt, K. R. (2008). The relationship between cytokine concentrations and wound healing in chronic venous ulceration. *J Vasc Surg, 48*(5), 1272-1277.

95. Goldman, R. T.Scuderi, G. R., & Insall, J. N. (1996). 2-stage reimplantation for infected total knee replacement. *Clin Orthop Relat Res*(331), 118-124.

96. Goldsmith, L.Katz, S.Gilchrest, B.Paller, A.Leffell, D., & Wolff, K. (2012). *Fitzpatrick's Dermatology in General Medicine, Eighth Edition, 2 Volume set* (Vol. 57 - 91): McGraw-Hill Education.

97. Gollwitzer, H.Ibrahim, K.Meyer, H.Mittelmeier, W.Busch, R., & Stemberger, A. (2003). Antibacterial poly(D,L-lactic acid) coating of medical implants using a biodegradable drug delivery technology. *J Antimicrob Chemother, 51*(3), 585-591.

98. Gristina, A. G. (1987). Biomaterial-centered infection: microbial adhesion versus tissue integration. *Science, 237*(4822), 1588-1595.

99. Gupta, C.Nayak, N.Kalthur, S., & D'Souza, A. (2015). A morphometric study of tibia and its nutrient foramen in South Indian population with its clinical implications. *Saudi Journal of Sports Medicine, 15*(3), 244-248.

100. Gupta, P.Sarkar, S.Das, B.Bhattacharjee, S., & Tribedi, P. (2016). Biofilm, pathogenesis and prevention—a journey to break the wall: a review. *Archives of Microbiology, 198*(1), 1-15.

101. Hall-Stoodley, L.Costerton, J. W., & Stoodley, P. (2004). Bacterial biofilms: from the Natural environment to infectious diseases. *Nat Rev Micro, 2*(2), 95-108.

102. Harper, D.Young, A., & McNaught, C.-E. (2014). The physiology of wound healing. *Surgery (Oxford), 32*(9), 445-450.

103. Harrison, C. A.Gossiel, F.Layton, C. M.Bullock, A. J.Johnson, T.Blumsohn, A., & MacNeil, S. (2006). Use of an in Vitro Model of Tissue-Engineered Skin to Investigate the Mechanism of Skin Graft Contraction. *Tissue Engineering, 12*(11), 3119-3133.

104. Healy, B., & Freedman, A. (2006). Infections. *Bmj, 332*(7545), 838-841.

105. Hendriks, F. M. (2005). *Mechanical Behaviour of Human Epidermal and Dermal Layers in Vivo*: Technische Universiteit Eindhoven.

106. Hermansson, M. (1999). The DLVO theory in microbial adhesion. *Colloids and Surfaces B: Biointerfaces, 14*(1), 105-119.

107. Hess, C. T. (2008). *Skin and Wound Care* (6 ed.). Philadelphia: Lippincott Williams & Wilkins.

108. Hess, C. T. (2013). *Clincal Guide to Skin and Wound Care* (7 ed.). Harrisburg: Lippincott Williams & Wilkins.

109. Hill, D. S.Robinson, N. D. P.Caley, M. P.Chen, M.O'Toole, E. A.Armstrong, J. L.Przyborski, S., & Lovat, P. E. (2015). A Novel Fully Humanized 3D Skin Equivalent to Model Early Melanoma Invasion. *Molecular cancer therapeutics, 14*(11), 2665-2673.

110. Holden, J. P.Orsini, J. A.Siegel, K. L.Kepple, T. M.Gerber, L. H., & Stanhope, S. J. (1997). Surface movement errors in shank kinematics and knee kinetics during gait. *Gait and Posture, 5*(3), 217-227.

111. Holmes, S. B., & Brown, S. J. (2005). Skeletal pin site care: National Association of Orthopaedic Nurses guidelines for orthopaedic nursing. *Orthop Nurs, 24*(2), 99-107.

112. Holt, B.Tripathi, A., & Morgan, J. (2008). Viscoelastic Response of Human Skin to Low Magnitude Physiologically Relevant Shear. *Journal of Biomechanics, 41*(12), 2689-2695.

113. Holt, J.Hertzberg, B.Weinhold, P.Storm, W.Schoenfisch, M., & Dahners, L. (2011). Decreasing bacterial colonization of external fixation pins via nitric oxide release coatings. *J Orthop Trauma, 25*(7), 432-437.

114. Hove, L. M.Furnes, O.Nilsen, P. T.Oulie, H. E.Solheim, E., & Molster, A. O. (1997). Closed reduction and external fixation of unstable fractures of the distal radius. *Scand J Plast Reconstr Surg Hand Surg, 31*(2), 159-164.

115. Hudon, V.Berthod, F.Black, A.Damour, O.Germain, L., & Auger, F. (2003). *A tissue-engineered endothelialized dermis to study the modulation of angiogenic and angiostatic molecules on capillary-like tube formation in vitro* (Vol. 148).

116. Huether, S., & McCance, K. (2012). *Understanding Pathophysiology* (5 ed.). Utah: Elsevier Mosby.

117. Hurlow, J.Couch, K.Laforet, K.Bolton, L.Metcalf, D., & Bowler, P. (2015). Clinical Biofilms: A Challenging Frontier in Wound Care. *Advances in Wound Care, 4*(5), 295-301.

118. Hussain, S. H.Limthongkul, B., & Humphreys, T. R. (2013). The biomechanical properties of the skin. *Dermatol Surg, 39*(2), 193-203.

119. Hutson, J. J., Jr., & Zych, G. A. (1998). Infections in periarticular fractures of the lower extremity treated with tensioned wire hybrid fixators. *J Orthop Trauma, 12*(3), 214-218.

120. Hyldahl, C.Pearson, S.Tepic, S., & Perren, S. M. (1991). Induction and prevention of pin loosening in external fixation: an in vivo study on sheep tibiae. *J Orthop Trauma, 5*(4), 485-492.

121. Ilizarov, G. A. (1992). The Apparatus: Components and Biomechanical Principles of Application *Transosseous Osteosynthesis: Theoretical and Clinical Aspects of the Regeneration and Growth of Tissue* (pp. 63-136). Berlin, Heidelberg: Springer Berlin Heidelberg.

122. Isackson, D.McGill, L. D., & Bachus, K. N. (2011). Percutaneous Implants with Porous Titanium Dermal Barriers: An In Vivo Evaluation of Infection Risk. *Medical engineering & physics, 33*(4), 418-426.

123. Iwase, T.Uehara, Y.Shinji, H.Tajima, A.Seo, H.Takada, K.Agata, T., & Mizunoe, Y. (2010). Staphylococcus epidermidis Esp inhibits Staphylococcus aureus biofilm formation and nasal colonization. *Nature, 465*(7296), 346-349.

124. Jay, S. M.Skokos, E. A.Zeng, J.Knox, K., & Kyriakides, T. R. (2010). Macrophage fusion leading to foreign body giant cell formation persists under phagocytic stimulation by microspheres in in vitro and in vivo in mouse models. *J Biomed Mater Res A, 93*(1), 189-199.

125. Jennison, T.McNally, M., & Pandit, H. (2014). Prevention of infection in external fixator pin sites. *Acta Biomaterialia, 10*(2), 595-603.

126. Jevons, M. P. (1961). “Celbenin” - resistant Staphylococci. *British Medical Journal, 1*(5219), 124-125.

127. Jucker, B. A.Harms, H., & Zehnder, A. J. (1996). Adhesion of the positively charged bacterium Stenotrophomonas (Xanthomonas) maltophilia 70401 to glass and Teflon. *J Bacteriol, 178*(18), 5472-5479.

128. Kallenberg, C. (2015). Pathogenesis and treatment of ANCA-associated vasculitides. *Clin Exp Rheumatol, 33*(4 Suppl 92), S11-S14.

129. Katz, M. H.Alvarez, A. F.Kirsner, R. S.Eaglstein, W. H., & Falanga, V. (1991). Human wound fluid from acute wounds stimulates fibroblast and endothelial cell growth. *J Am Acad Dermatol, 25*(6 Pt 1), 1054-1058.

130. Kazmers, N. H.Fragomen, A. T., & Rozbruch, S. R. (2016). Prevention of pin site infection in external fixation: a review of the literature. *Strategies in Trauma and Limb Reconstruction, 11*(2), 75-85.

131. Keskin, D., & Kiziltunc, A. (2007). Time-dependent changes in serum nitric oxide levels after long bone fracture. *Tohoku J Exp Med, 213*(4), 283-289.

132. Khoury, A. E.Lam, K.Ellis, B., & Costerton, J. W. (1992). Prevention and control of bacterial infections associated with medical devices. *Asaio j, 38*(3), M174-178.

133. Kielty, C. M.Sherratt, M. J., & Shuttleworth, C. A. (2002). Elastic fibres. *J Cell Sci, 115*(Pt 14), 2817-2828.

134. Kirker, K. R.James, G. A.Fleckman, P.Olerud, J. E., & Stewart, P. S. (2012). Differential effects of planktonic and biofilm MRSA on human fibroblasts. *Wound Repair Regen, 20*(2), 253-261.

135. Kirker, K. R.Secor, P. R.James, G. A.Fleckman, P.Olerud, J. E., & Stewart, P. S. (2009). Loss of viability and induction of apoptosis in human keratinocytes exposed to Staphylococcus aureus biofilms in vitro. *Wound Repair and Regeneration, 17*(5), 690-699.

136. Klein, E.Smith, D. L., & Laxminarayan, R. (2007). Hospitalizations and deaths caused by methicillin-resistant Staphylococcus aureus, United States, 1999-2005. *Emerging infectious diseases, 13*(12), 1840-1846.

137. Klettner, A.Tahmaz, N.Dithmer, M.Richert, E., & Roider, J. (2014). Effects of aflibercept on primary RPE cells: toxicity, wound healing, uptake and phagocytosis. *Br J Ophthalmol, 98*(10), 1448-1452.

138. Kloos, W. E., & Musselwhite, M. S. (1975). Distribution and persistence of Staphylococcus and Micrococcus species and other aerobic bacteria on human skin. *Appl Microbiol, 30*(3), 381-385.

139. Kluytmans, J.van Belkum, A., & Verbrugh, H. (1997). Nasal carriage of Staphylococcus aureus: epidemiology, underlying mechanisms, and associated risks. *Clin Microbiol Rev, 10*(3), 505-520.

140. Kobayashi, N.Bauer, T. W.Tuohy, M. J.Fujishiro, T., & Procop, G. W. (2007). Brief ultrasonication improves detection of biofilm-formative bacteria around a metal implant. *Clin Orthop Relat Res, 457*, 210-213.

141. Kofman, K. E.Buckley, T., & McGrouther, D. A. (2012). Complications of transcutaneous metal devices. *European Journal of Plastic Surgery, 35*(9), 673-682.

142. Kummer, F. J. (1990). Technical note: evaluation of new Ilizarov rings. *Bull Hosp Jt Dis Orthop Inst, 50*(1), 88-90.

143. Lafortune, M. A.Cavanagh, P. R.Sommer Iii, H. J., & Kalenak, A. (1992). Three-dimensional kinematics of the human knee during walking. *Journal of Biomechanics, 25*(4), 347-357.

144. Lai, Y., & Kisaalita, W. S. (2012). Performance evaluation of 3D polystyrene 96-well plates with human neural stem cells in a calcium assay. *Journal of laboratory automation, 17*(4), 284-292.

145. Lane, W. A. (1895). Some remarks on the treatment of fractures. *British medical journal, 1*(1790), 861.

146. Leardini, A.Chiari, L.Della Croce, U., & Cappozzo, A. (2005). Human movement analysis using stereophotogrammetry. Part 3. Soft tissue artifact assessment and compensation. *Gait Posture, 21*(2), 212-225.

147. Lecuyer, S.Rusconi, R.Shen, Y.Forsyth, A.Vlamakis, H.Kolter, R., & Stone, H. A. (2011). Shear Stress Increases the Residence Time of Adhesion of Pseudomonas aeruginosa. *Biophysical Journal, 100*(2), 341-350.

148. Lewis, D. D.Bronson, D. G.Samchukov, M. L.Welch, R. D., & Stallings, J. T. (1998). Biomechanics of circular external skeletal fixation. *Vet Surg, 27*(5), 454-464.

149. Liang, C.-C.Park, A. Y., & Guan, J.-L. (2007). In vitro scratch assay: a convenient and inexpensive method for analysis of cell migration in vitro. *Nature Protocols, 2*, 329.

150. Lindley, L. E.Stojadinovic, O.Pastar, I., & Tomic-Canic, M. (2016). Biology and Biomarkers for Wound Healing. *Plast Reconstr Surg, 138*(3 Suppl), 18S-28S.

151. Liu, Y., & Tay, J. H. (2002). The essential role of hydrodynamic shear force in the formation of biofilm and granular sludge. *Water Res, 36*(7), 1653-1665.

152. Llor, C., & Bjerrum, L. (2014). Antimicrobial resistance: risk associated with antibiotic overuse and initiatives to reduce the problem. *Therapeutic Advances in Drug Safety, 5*(6), 229-241.

153. Loot, M. A.Kenter, S. B.Au, F. L.van Galen, W. J.Middelkoop, E.Bos, J. D., & Mekkes, J. R. (2002). Fibroblasts derived from chronic diabetic ulcers differ in their response to stimulation with EGF, IGF-I, bFGF and PDGF-AB compared to controls. *Eur J Cell Biol, 81*(3), 153-160.

154. Lowery, K.Dearden, P.Sherman, K.Mahadevan, V., & Sharma, H. (2015). Cadaveric analysis of capsular attachments of the distal femur related to pin and wire placement. *Injury, 46*(6), 970-974.

155. Mahan, J.Seligson, D.Henry, S. L.Hynes, P., & Dobbins, J. (1991). Factors in pin tract infections. *Orthopedics, 14*(3), 305-308.

156. Mahltig, B.Fiedler, D., & Böttcher, H. (2004). Antimicrobial Sol–Gel Coatings. *Journal of Sol-Gel Science and Technology, 32*(1), 219-222.

157. Maier, U., & Büchs, J. (2001). Characterisation of the gas–liquid mass transfer in shaking bioreactors. *Biochemical Engineering Journal, 7*(2), 99-106.

158. Manal, K.McClay Davis, I.Galinat, B., & Stanhope, S. (2003). The accuracy of estimating proximal tibial translation during natural cadence walking: bone vs. skin mounted targets. *Clin Biomech (Bristol, Avon), 18*(2), 126-131.

159. Manal, K.McClay, I.Stanhope, S.Richards, J., & Galinat, B. (2000). Comparison of surface mounted markers and attachment methods in estimating tibial rotations during walking: An in vivo study. *Gait and Posture, 11*(1), 38-45.

160. Mangram, A. J.Horan, T. C.Pearson, M. L.Silver, L. C., & Jarvis, W. R. (1999). Guideline for Prevention of Surgical Site Infection, 1999. Centers for Disease Control and Prevention (CDC) Hospital Infection Control Practices Advisory Committee. *Am J Infect Control, 27*(2), 97-132; quiz 133-134; discussion 196.

161. Margolis, E.Yates, A., & Levin, B. R. (2010). The ecology of nasal colonization of Streptococcus pneumoniae, Haemophilus influenzae and Staphylococcus aureus: the role of competition and interactions with host's immune response. *BMC Microbiol, 10*, 59.

162. Marić, S., & Vraneš, J. (2007). Characteristics and significance of microbial biofilm formation. *Periodicum Bilogorum, 109*, 115-121.

163. Meier, F.Nesbit, M.Hsu, M. Y.Martin, B.Van Belle, P.Elder, D. E.Schaumburg-Lever, G.Garbe, C.Walz, T. M.Donatien, P.Crombleholme, T. M., & Herlyn, M. (2000). Human melanoma progression in skin reconstructs : biological significance of bFGF. *The American journal of pathology, 156*(1), 193-200.

164. Mendez, M. V.Raffetto, J. D.Phillips, T.Menzoian, J. O., & Park, H. Y. (1999). The proliferative capacity of neonatal skin fibroblasts is reduced after exposure to venous ulcer wound fluid: A potential mechanism for senescence in venous ulcers. *J Vasc Surg, 30*(4), 734-743.

165. Michel, M.L'Heureux, N.Pouliot, R.Xu, W.Auger, F. A., & Germain, L. (1999). Characterization of a new tissue-engineered human skin equivalent with hair. *In Vitro Cell Dev Biol Anim, 35*(6), 318-326.

166. Mims, C. A.Playfair, J. H. L.Roitt, I. M.Wakelin, D., & Williams, R. (1993). *Medical microbiology*: Mosby Europe Limited.

167. Moroni, A.Vannini, F.Mosca, M., & Giannini, S. (2002). State of the art review: techniques to avoid pin loosening and infection in external fixation. *J Orthop Trauma, 16*(3), 189-195.

168. Mulder, M. (2002). *Basic Principles of Wound Care*: Pearson Education South Africa.

169. Murray, M. P.Drought, A. B., & Kory, R. C. (1964). WALKING PATTERNS OF NORMAL MEN. *J Bone Joint Surg Am, 46*, 335-360.

170. Nair, N.Biswas, R.Götz, F., & Biswas, L. (2014). Impact of Staphylococcus aureus on pathogenesis in polymicrobial infections. *Infection and Immunity, 82*(6), 2162-2169.

171. Narayanan, A. S.Page, R. C., & Swanson, J. (1989). Collagen synthesis by human fibroblasts. Regulation by transforming growth factor-beta in the presence of other inflammatory mediators. *The Biochemical journal, 260*(2), 463-469.

172. Nayagam, S. (2007). Safe corridors in external fixation: the lower leg (tibia, fibula, hindfoot and forefoot). *Strategies in Trauma and Limb Reconstruction, 2*(2), 105-110.

173. Nayak, S.Dey, S., & Kundu, S. (2013). *Skin Equivalent Tissue-Engineered Construct: Co-Cultured Fibroblasts/ Keratinocytes on 3D Matrices of Sericin Hope Cocoons* (Vol. 8).

174. Nele, U.Maffulli, N., & Pintore, E. (1994). Biomechanics of radiotransparent circular external fixators. *Clin Orthop Relat Res*(308), 68-72.

175. Nguyen, L. L.Nelson, C. L.Saccente, M.Smeltzer, M. S.Wassell, D. L., & McLaren, S. G. (2002). Detecting bacterial colonization of implanted orthopaedic devices by ultrasonication. *Clinical Orthopaedics and Related Research®, 403*, 29-37.

176. NNIS. (2004). National Nosocomial Infections Surveillance (NNIS) System Report, data summary from January 1992 through June 2004, issued October 2004. *Am J Infect Control, 32*(8), 470-485.

177. O'Neill, J. (2017). UK review on antimicrobial resistance. Antimicrobial resistance: tackling a crisis for the health and wealth of nations, December 2014.

178. Oda, T.Hamasaki, J.Kanda, N., & Mikami, K. (1997). Anaphylactic shock induced by an antiseptic-coated central venous [correction of nervous] catheter. *Anesthesiology, 87*(5), 1242-1244.

179. Olson, M. E.Ruseska, I., & Costerton, J. W. (1988). Colonization of n-butyl-2-cyanoacrylate tissue adhesive by Staphylococcus epidermidis. *J Biomed Mater Res, 22*(6), 485-495.

180. Orgill, D., & Blanco, C. (2009). *Biomaterials for Treating Skin Loss*: Woodhead Publishing.

181. Orgill, D. P. (1983). *The Effects of an Artificial Skin on Scarring and Contraction in Open Wounds*.

182. Otto, M. (2009). Staphylococcus epidermidis--the 'accidental' pathogen. *Nat Rev Microbiol, 7*(8), 555-567.

183. Paley, D.Fleming, B.Catagni, M.Kristiansen, T., & Pope, M. (1990). Mechanical evaluation of external fixators used in limb lengthening. *Clin Orthop Relat Res*(250), 50-57.

184. Parameswaran, A. D.Roberts, C. S.Seligson, D., & Voor, M. (2003). Pin tract infection with contemporary external fixation: how much of a problem? *J Orthop Trauma, 17*(7), 503-507.

185. Park, A.Jeong, H.-H.Lee, J.Kim, K. P., & Lee, C.-S. (2011). Effect of shear stress on the formation of bacterial biofilm in a microfluidic channel. *BioChip Journal, 5*(3), 236.

186. Paulson, D. S. (2014). *Topical Antimicrobials Testing and Evaluation, Second Edition*: CRC Press.

187. Pawlaczyk, M.Lelonkiewicz, M., & Wieczorowski, M. (2013). Age-dependent biomechanical properties of the skin. *Advances in Dermatology and Allergology/Postępy Dermatologii i Alergologii, 30*(5), 302-306.

188. Pendegrass, C. J.Goodship, A. E., & Blunn, G. W. (2006). Development of a soft tissue seal around bone-anchored transcutaneous amputation prostheses. *Biomaterials, 27*(23), 4183-4191.

189. Percival, S. L.Williams, D.Cooper, T., & Randle, J. (2014). *Biofilms in Infection Prevention and Control: A Healthcare Handbook*: Elsevier Science.

190. Peters, A.Galna, B.Sangeux, M.Morris, M., & Baker, R. (2010). Quantification of soft tissue artifact in lower limb human motion analysis: a systematic review. *Gait Posture, 31*(1), 1-8.

191. Pettine, K. A.Chao, E. Y., & Kelly, P. J. (1993). Analysis of the external fixator pin-bone interface. *Clinical Orthopaedics and Related Research*(293), 18-27.

192. Phillip Cochran, M. S. D. V. M. (2010). *Laboratory Manual for Comparative Veterinary Anatomy & Physiology*: Cengage Learning.

193. Picha, G. J., & Drake, R. F. (1996). Pillared-surface microstructure and soft-tissue implants: effect of implant site and fixation. *J Biomed Mater Res, 30*(3), 305-312.

194. Planet, P. J.LaRussa, S. J.Dana, A.Smith, H.Xu, A.Ryan, C.Uhlemann, A.-C.Boundy, S.Goldberg, J.Narechania, A.Kulkarni, R.Ratner, A. J.Geoghegan, J. A.Kolokotronis, S.-O., & Prince, A. (2013). Emergence of the epidemic methicillin-resistant Staphylococcus aureus strain USA300 coincides with horizontal transfer of the arginine catabolic mobile element and speG-mediated adaptations for survival on skin. *mBio, 4*(6), e00889.

195. Potera, C. (1999). Forging a link between biofilms and disease. *Science, 283*(5409), 1837, 1839.

196. Price, J.Tencer, A.Arm, D., & Bohach, G. (1996). Controlled release of antibiotics from coated orthopedic implants. *Journal of Biomedical Materials Research: An Official Journal of The Society for Biomaterials and The Japanese Society for Biomaterials, 30*(3), 281-286.

197. Proksch, E.Brandner, J., & Jensen, J.-M. (2008). The Skin: an indispensable barrier. *Experimental Dermatology*, 1063 - 1072.

198. Qu, H.Knabe, C.Burke, M.Radin, S.Garino, J.Schaer, T., & Ducheyne, P. (2014). Bactericidal micron-thin sol-gel films prevent pin tract and periprosthetic infection. *Mil Med, 179*(8 Suppl), 29-33.

199. Raikar, G.Gregory, J.Ong, J.Lucas, L.Lemons, J.Kawahara, D., & Nakamura, M. (1995). Surface characterization of titanium implants. *Journal of Vacuum Science & Technology A, 13*(5), 2633-2637.

200. Ralston, D. R.Layton, C.Dalley, A. J.Boyce, S. G.Freedlander, E., & MacNeil, S. (1997). Keratinocytes contract human dermal extracellular matrix and reduce soluble fibronectin production by fibroblasts in a skin composite model. *Br J Plast Surg, 50*(6), 408-415.

201. Ramsey, M. M., & Whiteley, M. (2004). Pseudomonas aeruginosa attachment and biofilm development in dynamic environments. *Mol Microbiol, 53*(4), 1075-1087.

202. Ratner, B. D.Hoffman, A. S.Schoen, F. J., & Lemons, J. E. (2012). *Biomaterials Science: An Introduction to Materials in Medicine*: Elsevier Science.

203. Ray, A. J.Pultz, N. J.Bhalla, A.Aron, D. C., & Donskey, C. J. (2003). Coexistence of vancomycin-resistant enterococci and Staphylococcus aureus in the intestinal tracts of hospitalized patients. *Clin Infect Dis, 37*(7), 875-881.

204. Reid, J. S.Van Slyke, M. A.Moulton, M. J., & Mann, T. A. (2001). Safe placement of proximal tibial transfixation wires with respect to intracapsular penetration. *J Orthop Trauma, 15*(1), 10-17.

205. Reijnders, C. M. A.van Lier, A.Roffel, S.Kramer, D.Scheper, R. J., & Gibbs, S. (2015). Development of a Full-Thickness Human Skin Equivalent In Vitro Model Derived from TERT-Immortalized Keratinocytes and Fibroblasts. *Tissue engineering. Part A, 21*(17-18), 2448-2459.

206. Reinschmidt, C.Van Den Bogert, A. J.Nigg, B. M.Lundberg, A., & Murphy, N. (1997). Effect of skin movement on the analysis of skeletal knee joint motion during running. *Journal of Biomechanics, 30*(7), 729-732.

207. Resch, A.Rosenstein, R.Nerz, C., & Gotz, F. (2005). Differential gene expression profiling of Staphylococcus aureus cultivated under biofilm and planktonic conditions. *Appl Environ Microbiol, 71*(5), 2663-2676.

208. Rheinwald, J. G., & Green, H. (1975). Serial cultivation of strains of human epidermal keratinocytes: the formation of keratinizing colonies from single cells. *Cell, 6*(3), 331-343.

209. Richardson, J. B.Kenwright, J., & Cunningham, J. L. (1992). Fracture stiffness measurement in the assessment and management of tibial fractures. *Clinical Biomechanics, 7*(2), 75-79.

210. Romeo, T. (2008). *Bacterial Biofilms*: Springer Berlin Heidelberg.

211. Rosenbach, F. J. (1884). Mikroorganismen bei den Wundinfecktionskrankheiten des Menschen. *JF Bergmann., Wiesbaden*.

212. Saithna, A. (2010). The influence of hydroxyapatite coating of external fixator pins on pin loosening and pin track infection: a systematic review. *Injury, 41*(2), 128-132.

213. Saleh, M., & Scott, B. W. (1992). Pitfalls and complications in leg lengthening: The Sheffield experience. *Seminars in Orthopaedics, 7*(3), 207-222.

214. Sanders, R. (1973). Torsional elasticity of human skin in vivo. *Pflügers Archiv, 342*(3), 255-260.

215. Santy, J.Vincent, M., & Duffield, B. (2009). The principles of caring for patients with Ilizarov external fixation. *Nursing Standard, 23*(26), 50.

216. Santy, J. E.Kamal, J.Abdul-Rashid, A. H., & Ibrahim, S. (2015). The Rubber Stopper: A Simple and Inexpensive Technique to Prevent Pin Tract Infection following Kirschner Wiring of Supracondylar Fractures of Humerus in Children. *Malaysian Orthopaedic Journal, 9*(2), 13-16.

217. Sauer, K.Camper, A. K.Ehrlich, G. D.Costerton, J. W., & Davies, D. G. (2002). Pseudomonas aeruginosa displays multiple phenotypes during development as a biofilm. *J Bacteriol, 184*(4), 1140-1154.

218. Saur, T.Morin, E.Habouzit, F.Bernet, N., & Escudié, R. (2017). Impact of wall shear stress on initial bacterial adhesion in rotating annular reactor. *PLoS One, 12*(2), e0172113-e0172113.

219. Scanlon, V. C., & Sanders, T. (2006). *Essentials of Anatomy and Physiology*: F a Davis Company.

220. Schalamon, J.Petnehazy, T.Ainoedhofer, H.Zwick, E. B.Singer, G., & Hoellwarth, M. E. (2007). Pin tract infection with external fixation of pediatric fractures. *Journal of Pediatric Surgery, 42*(9), 1584-1587.

221. Schwartz, M. H.Trost, J. P., & Wervey, R. A. (2004). Measurement and management of errors in quantitative gait data. *Gait Posture, 20*(2), 196-203.

222. Secor, P. R.James, G. A.Fleckman, P.Olerud, J. E.McInnerney, K., & Stewart, P. S. (2011). Staphylococcus aureus Biofilm and Planktonic cultures differentially impact gene expression,

mapk phosphorylation, and cytokine production in human keratinocytes. *BMC microbiology, 11*(1), 143.

223. Seligson, D.Mauffrey, C., & Roberts, C. S. (2011). *External Fixation in Orthopedic Traumatology*: Springer London.

224. Shah, J. M. Y.Omar, E.Pai, D. R., & Sood, S. (2012). Cellular events and biomarkers of wound healing. *Indian Journal of Plastic Surgery : Official Publication of the Association of Plastic Surgeons of India, 45*(2), 220-228.

225. Shirai, T.Tsuchiya, H.Shimizu, T.Ohtani, K.Zen, Y., & Tomita, K. (2009). Prevention of pin tract infection with titanium-copper alloys. *Journal of Biomedical Materials Research - Part B Applied Biomaterials, 91*(1), 373-380.

226. Silver, F. H.Siperko, L. M., & Seehra, G. P. (2003). Mechanobiology of force transduction in dermal tissue. *Skin Res Technol, 9*(1), 3-23.

227. Singer, A. J., & Clark, R. A. (1999). Cutaneous wound healing. *New England Journal of Medicine, 341*(10), 738-746.

228. Smits, J. P. H.Niehues, H.Rikken, G.van Vlijmen-Willems, I. M. J. J.van de Zande, G. W. H. J. F.Zeeuwen, P. L. J. M.Schalkwijk, J., & van den Bogaard, E. H. (2017). Immortalized N/TERT keratinocytes as an alternative cell source in 3D human epidermal models. *Scientific Reports, 7*(1), 11838.

229. Sommerlad, B. C., & Creasey, J. M. (1978). The stretched scar: a clinical and histological study. *Br J Plast Surg, 31*(1), 34-45.

230. Sontheimer, R. D. (2014). Skin Is Not the Largest Organ. *J Invest Dermatol, 134*(2), 581-582.

231. Spiegelberg, B.Parratt, T.Dheerendra, S. K.Khan, W. S.Jennings, R., & Marsh, D. R. (2010). Ilizarov principles of deformity correction. *The Annals of The Royal College of Surgeons of England, 92*(2), 101-105.

232. Spiekstra, S. W.Breetveld, M.Rustemeyer, T.Scheper, R. J., & Gibbs, S. (2007). Wound-healing factors secreted by epidermal keratinocytes and dermal fibroblasts in skin substitutes. *Wound Repair and Regeneration, 15*(5), 708-717.

233. Stagni, R.Fantozzi, S.Cappello, A., & Leardini, A. (2005). Quantification of soft tissue artefact in motion analysis by combining 3D fluoroscopy and stereophotogrammetry: a study on two subjects. *Clinical Biomechanics, 20*(3), 320-329.

234. Stamm, A.Reimers, K.Strauß, S.Vogt, P.Scheper, T., & Pepelanova, I. (2016). In vitro wound healing assays – state of the art *BioNanoMaterials* (Vol. 17, pp. 79).

235. Stepanovic, S.Vukovic, D.Jezek, P.Pavlovic, M., & Svabic-Vlahovic, M. (2001). Influence of dynamic conditions on biofilm formation by staphylococci. *Eur J Clin Microbiol Infect Dis, 20*(7), 502-504.

236. Stevens, M. A.DeCoster, T. A.Garcia, F., & Sell, J. J. (1995). Septic knee from Ilizarov transfixation tibial pin. *The Iowa Orthopaedic Journal, 15*, 217-220.

237. Stewart, P. S., & Costerton, J. W. (2001). Antibiotic resistance of bacteria in biofilms. *Lancet, 358*(9276), 135-138.

238. Südhoff, I.Van Driessche, S.Laporte, S.de Guise, J. A., & Skalli, W. (2007). Comparing three attachment systems used to determine knee kinematics during gait. *Gait Posture, 25*(4), 533-543.

239. Sussman, C., & Bates-Jensen, B. (2007). *Wound Care - A Collaborative Practice Manual for Health Professionals*. Philadelphia: Lippincott Williams & Wilkins.

240. Sussman, C., & Bates-Jensen, B. M. (2011). *Wound Care: A Collaborative Practice Manual for Health Professionals*: Wolters Kluwer Health/Lippincott Williams & Wilkins.

241. Tankersley, A.Frank, M. B.Bebak, M., & Brennan, R. (2014). Early effects of Staphylococcus aureus biofilm secreted products on inflammatory responses of human epithelial keratinocytes. *J Inflamm (Lond), 11*, 17.

242. Teller, P., & White, T. K. (2009). The Physiology of Wound Healing: Injury Through Maturation. *89*(3).

243. Timms, A.Vincent, M.Santy-Tomlinson, J., & Hertz, K. (2013). A fresh consensus for pin site care in the UK. *International Journal of Orthopaedic and Trauma Nursing, 17*(1), 19-28.

244. Tollefson, D. F.Bandyk, D. F.Kaebnick, H. W.Seabrook, G. R., & Towne, J. B. (1987). Surface biofilm disruption. Enhanced recovery of microorganisms from vascular prostheses. *Arch Surg, 122*(1), 38-43.

245. Topman, G.Sharabani-Yosef, O., & Gefen, A. (2012). A standardized objective method for continuously measuring the kinematics of cultures covering a mechanically damaged site. *Med Eng Phys, 34*(2), 225-232.

246. Topol, B. M.Haimes, H. B.Dubertret, L., & Bell, E. (1986). Transfer of melanosomes in a skin equivalent model in vitro. *J Invest Dermatol, 87*(5), 642-647.

247. Tracy, L. E.Minasian, R. A., & Caterson, E. J. (2016). Extracellular Matrix and Dermal Fibroblast Function in the Healing Wound. *Advances in Wound Care, 5*(3), 119-136.

248. Trampuz, A.Piper, K. E.Jacobson, M. J.Hanssen, A. D.Unni, K. K.Osmon, D. R.Mandrekar, J. N.Cockerill, F. R.Steckelberg, J. M., & Greenleaf, J. F. (2007). Sonication of removed hip and knee prostheses for diagnosis of infection. *New England Journal of Medicine, 357*(7), 654-663.

249. Trampuz, A.Piper, K. E.Jacobson, M. J.Hanssen, A. D.Unni, K. K.Osmon, D. R.Mandrekar, J. N.Cockerill, F. R.Steckelberg, J. M.Greenleaf, J. F., & Patel, R. (2007). Sonication of removed hip and knee prostheses for diagnosis of infection. *N Engl J Med, 357*(7), 654-663.

250. Trengove, N. J.Bielefeldt-Ohmann, H., & Stacey, M. C. (2000). Mitogenic activity and cytokine levels in non-healing and healing chronic leg ulcers. *Wound Repair and Regeneration, 8*(1), 13-25.

251. Tunney, M. M.Patrick, S.Gorman, S. P.Nixon, J. R.Anderson, N.Davis, R. I.Hanna, D., & Ramage, G. (1998). Improved detection of infection in hip replacements: a currently underestimated problem. *J Bone Joint Surg Br, 80*(4), 568-572.

252. Uckay, I.Pittet, D.Vaudaux, P.Sax, H.Lew, D., & Waldvogel, F. (2009). Foreign body infections due to Staphylococcus epidermidis. *Ann Med, 41*(2), 109-119.

253. Ueshima, M.Tanaka, S.Nakamura, S., & Yamashita, K. (2002). Manipulation of bacterial adhesion and proliferation by surface charges of electrically polarized hydroxyapatite. *J Biomed Mater Res, 60*(4), 578-584.

254. van Belkum, A. (2006). Staphylococcal colonization and infection: homeostasis versus disbalance of human (innate) immunity and bacterial virulence. *Curr Opin Infect Dis, 19*(4), 339-344.

255. van de Belt, H.Neut, D.Schenk, W.van Horn, J. R.van Der Mei, H. C., & Busscher, H. J. (2001). Staphylococcus aureus biofilm formation on different gentamicin-loaded polymethylmethacrylate bone cements. *Biomaterials, 22*(12), 1607-1611.

256. Van der Borden, A.Van der Mei, H., & Busscher, H. (2005). Electric block current induced detachment from surgical stainless steel and decreased viability of Staphylococcus epidermidis. *Biomaterials, 26*(33), 6731-6735.

257. van der Borden, A. J.van der Werf, H.van der Mei, H. C., & Busscher, H. J. (2004). Electric Current-Induced Detachment of Staphylococcus epidermidis Biofilms from Surgical Stainless Steel. *Appl Environ Microbiol, 70*(11), 6871-6874.

258. Varki, A. (2009). *Essentials of Glycobiology*: Cold Spring Harbor Laboratory Press.

259. von Recum, A. F. (1984). Applications and failure modes of percutaneous devices: a review. *Journal of Biomedical Materials Research Part A, 18*(4), 323-336.

260. Voos, K.Rosenberg, B.Fagrhi, M., & Seligson, D. (1999). Use of a tobramycin-impregnated polymethylmethacrylate pin sleeve for the prevention of pin-tract infection in goats. *J Orthop Trauma, 13*(2), 98-101.

261. Wassall, M. A.Santin, M.Isalberti, C.Cannas, M., & Denyer, S. P. (1997). Adhesion of bacteria to stainless steel and silver-coated orthopedic external fixation pins. *J Biomed Mater Res, 36*(3), 325-330.

262. Werner, S., & Grose, R. (2003). Regulation of wound healing by growth factors and cytokines. *Physiol Rev, 83*(3), 835-870.

263. Wertheim, H. F.Vos, M. C.Ott, A.van Belkum, A.Voss, A.Kluytmans, J. A.van Keulen, P. H.Vandenbroucke-Grauls, C. M.Meester, M. H., & Verbrugh, H. A. (2004). Risk and outcome of nosocomial Staphylococcus aureus bacteraemia in nasal carriers versus non-carriers. *Lancet, 364*(9435), 703-705.

264. Willems, H. M.Xu, Z., & Peters, B. M. (2016). Polymicrobial Biofilm Studies: From Basic Science to Biofilm Control. *Current oral health reports, 3*(1), 36-44.

265. Wojtowicz, A. M.Oliveira, S.Carlson, M. W.Zawadzka, A.Rousseau, C. F., & Baksh, D. (2014). The importance of both fibroblasts and keratinocytes in a bilayered living cellular construct used in wound healing. *Wound Repair Regen, 22*(2), 246-255.

266. Wolcott, R. D.Hanson, J. D.Rees, E. J.Koenig, L. D.Phillips, C. D.Wolcott, R. A.Cox, S. B., & White, J. S. (2016). Analysis of the chronic wound microbiota of 2,963 patients by 16S rDNA pyrosequencing. *Wound Repair and Regeneration, 24*(1), 163-174.

267. Xie, Y.Rizzi, S. C.Dawson, R.Lynam, E.Richards, S.Leavesley, D. I., & Upton, Z. (2010). Development of a three-dimensional human skin equivalent wound model for investigating novel wound healing therapies. *Tissue Eng Part C Methods, 16*(5), 1111-1123.

268. Xu, F.Lu, T. J., & Seffen, K. A. (2008). Biothermomechanical behavior of skin tissue. *Acta Mechanica Sinica, 24*(1), 1-23.

269. Yang, J., & Schiffer, C. A. (2012). Genetic biomarkers in acute myeloid leukemia: will the promise of improving treatment outcomes be realized? *Expert review of hematology, 5*(4), 395-407.

270. Zalavras, C. G.Patzakis, M. J., & Holtom, P. (2004). Local antibiotic therapy in the treatment of open fractures and osteomyelitis. *Clinical Orthopaedics and Related Research®, 427*, 86-93.

271. Zhang, C.Zhai, W.Xie, Y.Chen, Q.Zhu, W., & Sun, X. (2013). Mesenchymal stem cells derived from breast cancer tissue promote the proliferation and migration of the MCF-7 cell line in vitro. *Oncol Lett, 6*(6), 1577-1582.

272. Zhao, G.Hochwalt, P. C.Usui, M. L.Underwood, R. A.Singh, P. K.James, G. A.Stewart, P. S.Fleckman, P., & Olerud, J. E. (2010). Delayed wound healing in diabetic (db/db) mice with Pseudomonas aeruginosa biofilm challenge: a model for the study of chronic wounds. *Wound Repair Regen, 18*(5), 467-477.

273. Zilberman, M., & Elsner, J. J. (2008). Antibiotic-eluting medical devices for various applications. *J Control Release, 130*(3), 202-215.

9.0 Appendices

9.1 Pin Machine Drawings

9.1.1 Aluminium well

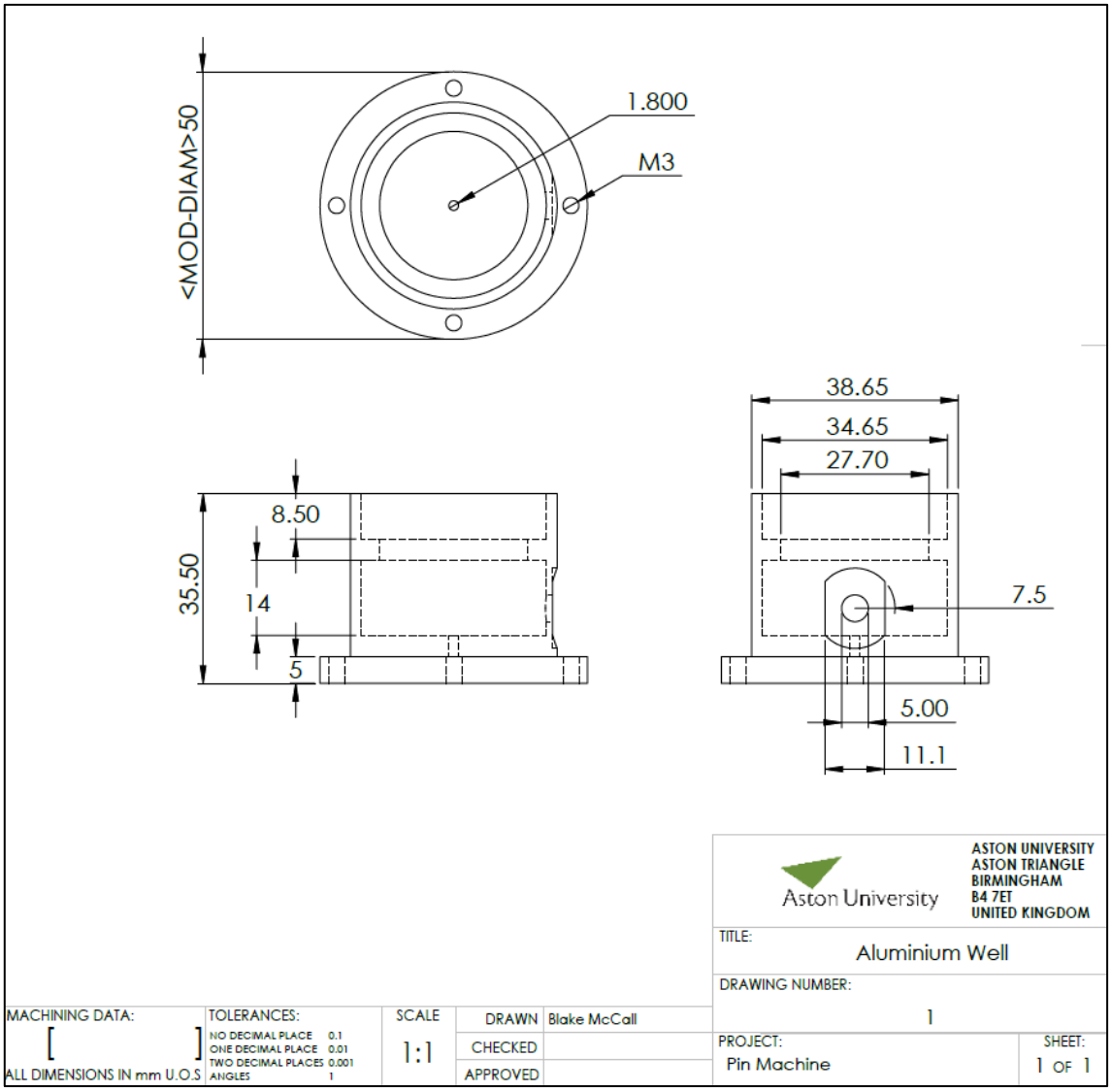

Figure 9.1: Working drawings of the aluminium well design.

9.1.2 Base Plate

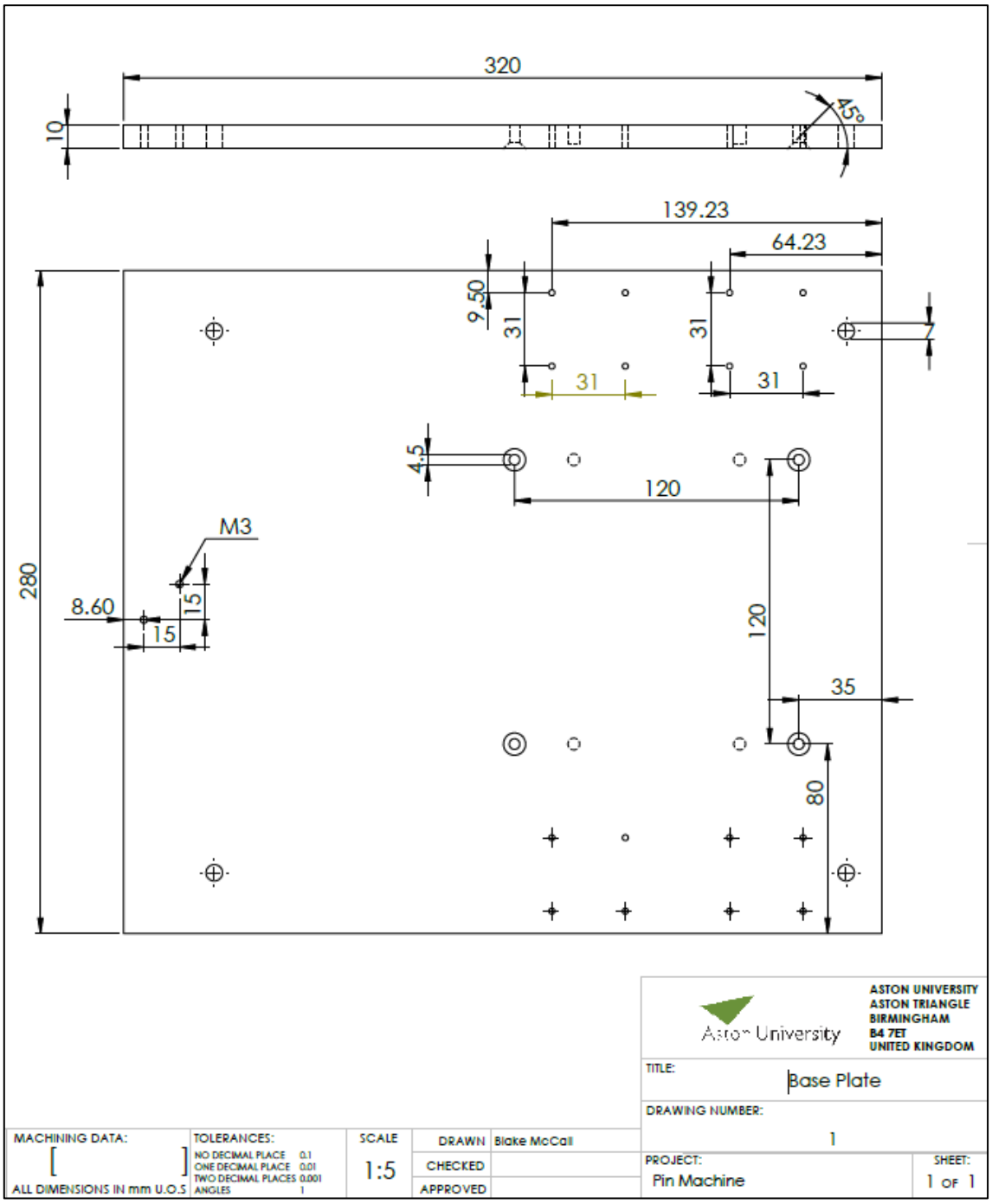

Figure 9.2 Working drawings of the Base Plate of the Pin Machine

9.1.3 Push Plate

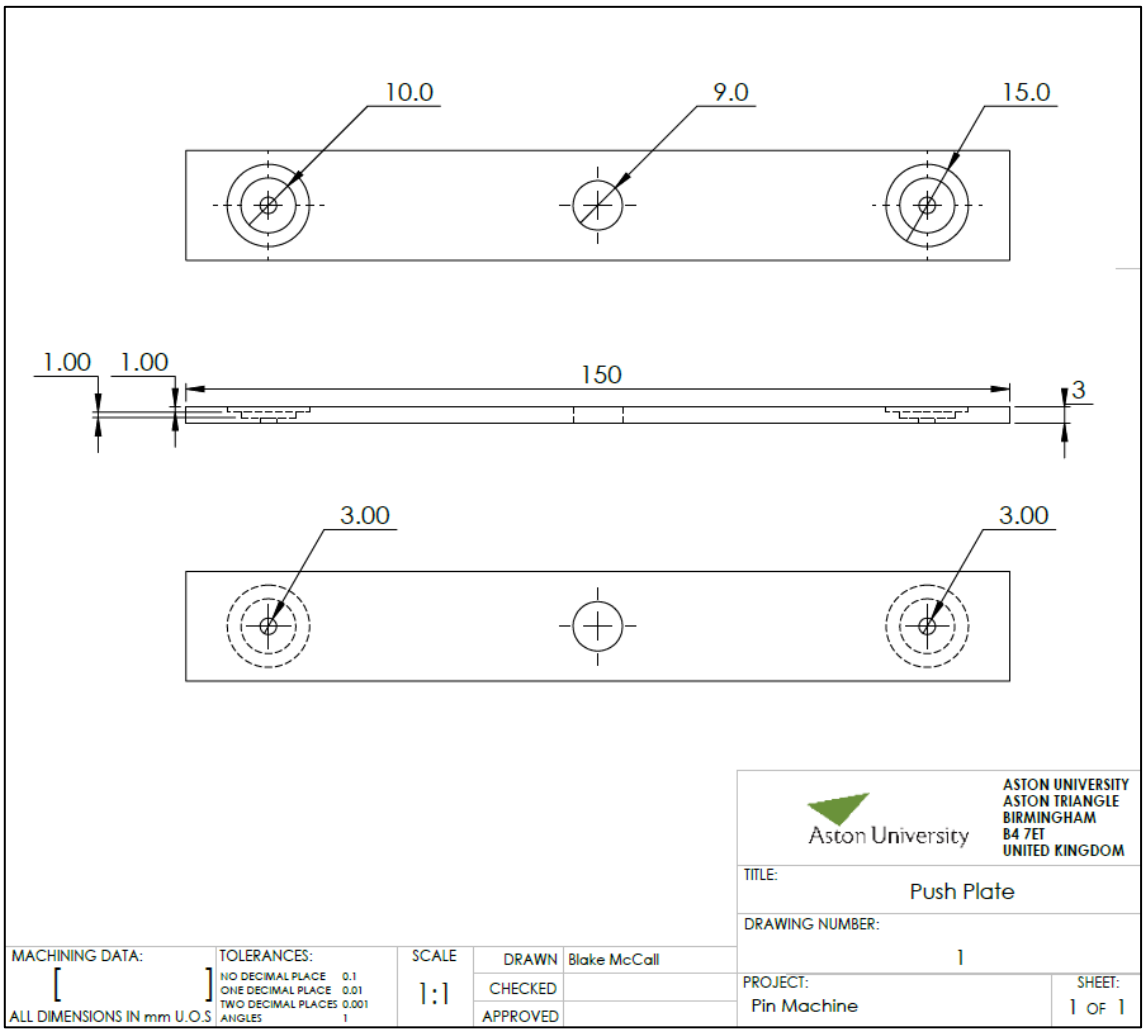

Figure 9.3: Working drawings of the Push Plate Component of the Pin Machine

9.1.4 Arm Shaft

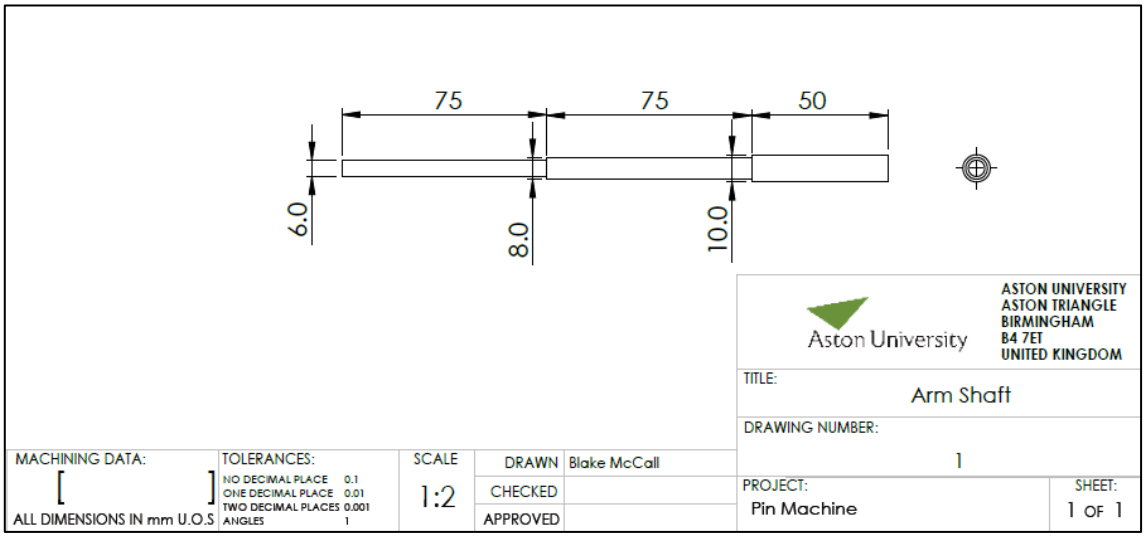

Figure 9.4: Working drawings of the Arm Shaft Component of the Pin Machine

9.1.5 Upright Support

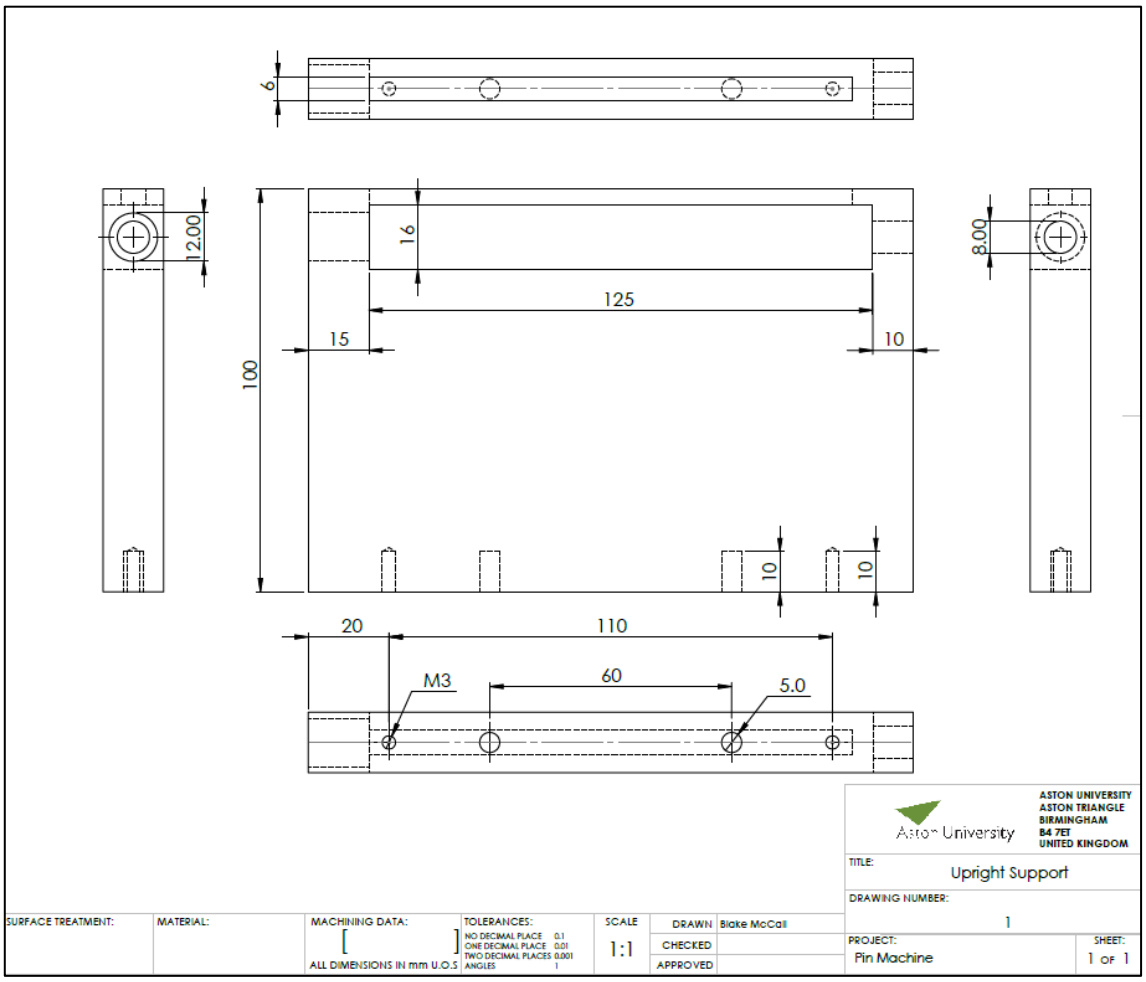

Figure 9.5: Working drawings of the Upright Support Component of the Pin Machine

9.1.6 Arm Bar

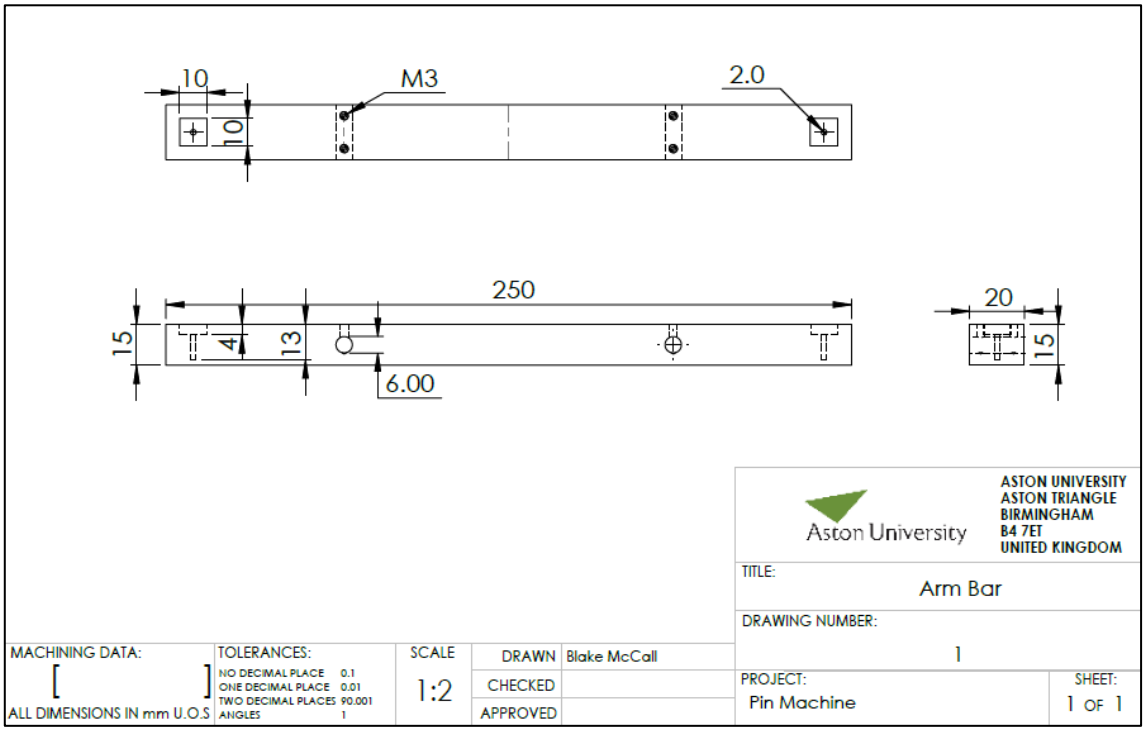

Figure 9.6: Working drawings of the Arm Bar Component of the Pin Machine

9.2 Multiplicity of Infection

9.2.1 Percentage Rate of Gap Closure

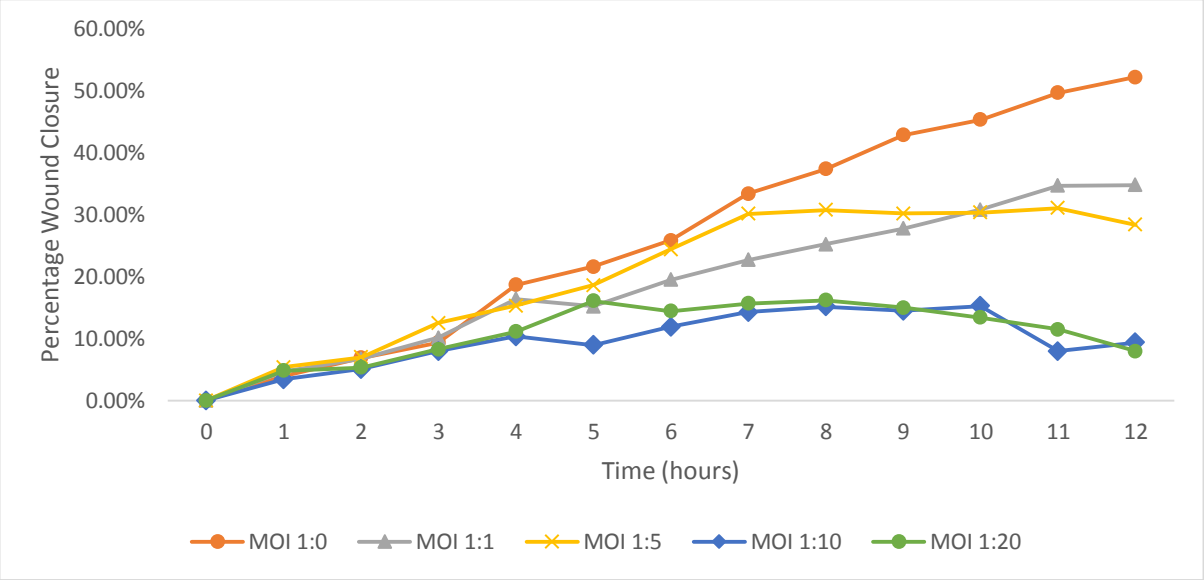

Figure 9.7: Rate of gap closure expressed as a percentage against time for a number of multiplicity of infection ratios. The control sample (MOI 1:0) showed a fairly linear rate of wound closure of the 12 hours. The MOI 1:1 samples showed a similarly linear rate of closure although slower than that of the control sample. For MOI of 1:5 and higher the wound stopped closing at 4-7 hours and began increasing in width, indicating possible cell death and detachment

9.2.2 Change in Wound Width over 12 Hours

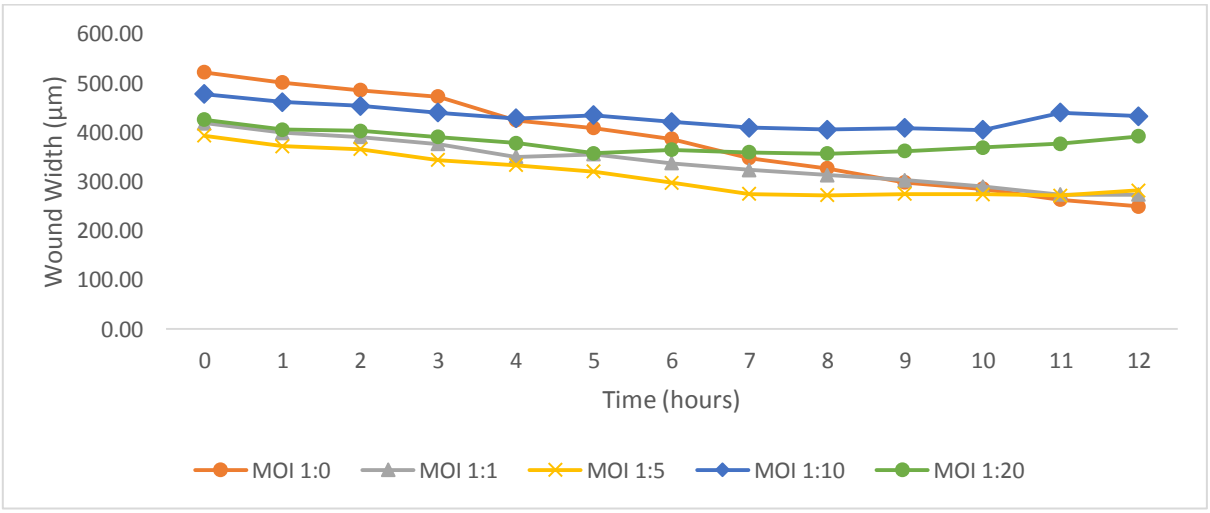

Figure 9.8: Rate of gap closure expressed as a distance against time for a number of multiplicity of infection ratios. All samples except control showed very little reduction in wound width of 12 hours. MOI 1:0 had the narrowest wound width after 12 hours despite having the widest initial wound width at the start of the experiment

9.2.3 Images of Scratch Closure over 24 Hours

Table 9.1: Images of scratches for each MOI ratio at various time points. All but the control sample failed to close the wound gap after 24 hours. MOI 1:1, 1:5 and 1:10 showed cell detachment at 24 hours, 24 hours and 18 hours respectively indicated cell death due to bacterial toxicity. Proliferation of bacteria in the MOI 1:20 sample resulted in the media becoming cloudy by 6 hours and by 12 hours the fibroblasts were difficult to detect even manually, making wound width measurements challenging. (Dotted white lines indicate the initial wound width at hour 0)

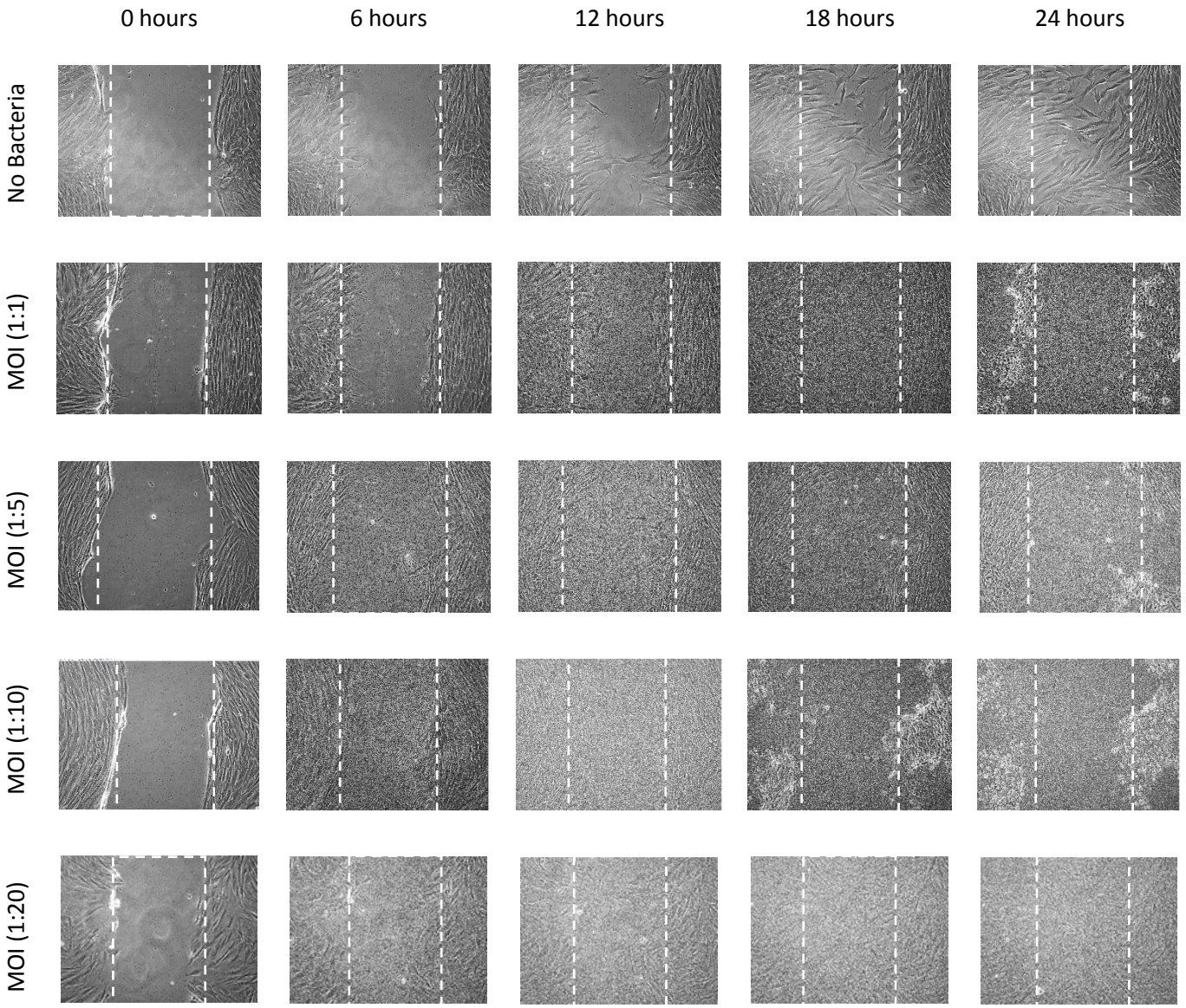

9.2.4 Wound Migration Velocity

Table 9.2: Calculating of cell migration velocity during the first 6 hours of incubation for each MOI ratio. Migration velcoity calculated by measuring the line gradient and deviding the absolute slope value by 2 to account for the wound closing from both sides

Multiplicity of Infection	Equation	|m|	Migration Velocity (µm / hour)
1:0	$y = -23.217x + 550.11$	23.217	11.609
1:1	$y = -13.346x + 428.52$	13.346	6.673
1:5	$y = -15.154x + 406.9$	15.154	7.577
1:10	$y = -8.8593x + 480.63$	8.859	4.430
1:20	$y = -10.875x + 432.63$	10.875	5.438